

SCHOOL OF CHEMISTRY

CARDIFF UNIVERSITY



**Synthesis of novel spirobisfluorenes as
precursors to microporous polymers and
inclusion compounds.**

Thesis submitted for the degree of Doctor of Philosophy by:

Alexander John Tonkins

Supervisor: Neil B. McKeown

2010

UMI Number: U580179

All rights reserved

INFORMATION TO ALL USERS

The quality of this reproduction is dependent upon the quality of the copy submitted.

In the unlikely event that the author did not send a complete manuscript and there are missing pages, these will be noted. Also, if material had to be removed, a note will indicate the deletion.



UMI U580179

Published by ProQuest LLC 2013. Copyright in the Dissertation held by the Author.
Microform Edition © ProQuest LLC.

All rights reserved. This work is protected against
unauthorized copying under Title 17, United States Code.



ProQuest LLC
789 East Eisenhower Parkway
P.O. Box 1346
Ann Arbor, MI 48106-1346

Preface

Declaration

This work has not previously been accepted in substance for any degree and is not concurrently submitted in candidature for any degree.

Signed.......... (candidate)

Date.....25/7/2011.....

STATEMENT 1

This thesis is being submitted in partial fulfilment of the requirements for the degree of Doctor of Philosophy.

Signed.......... (candidate)

Date.....25/7/2011.....

STATEMENT 2

This thesis is the result of my own independent work/investigation, except where otherwise stated. Other sources are acknowledged by explicit references.

Signed.......... (candidate)

Date.....25/7/2011.....

STATEMENT 3

I hereby give consent for my thesis, if accepted, to be available for photocopying and for interlibrary loan, and for the title and summary to be made available to outside organisations.

Signed.......... (candidate)

Date.....25/7/2011.....

Acknowledgments

I would like to thank my supervisor Neil McKeown first and foremost for the constant help and support during my PhD work. I would also like to thank Mariolino Carta, Grazia Bezzu and Dr Kadhum Msayib for their constant support within the laboratory, and from whom I learned so much from in matters relating to chemistry and life in general. I would like to thank my fellow colleagues within the group (Rhys, Jono, James, Rupert, Yulia, Richard and Mathew) for being great people to work with and showing great understanding when necessary. I would also like to thank the stores and office staff who have all helped me on numerous occasions throughout my stay at Cardiff, especially Terrie Dumelow for always going the extra mile to resolve any issues that occurred.

Special appreciation is reserved for Dr Benson Kariuki for his hard work in helping me to collect and refine the crystallographic data in record time. He is a true and consummate professional.

And finally I would like to especially thank Laura. Without her support and understanding, none of this would be possible.

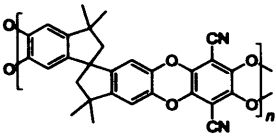
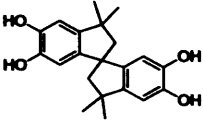
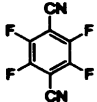
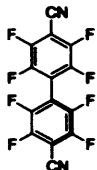
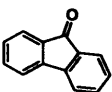
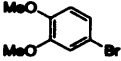
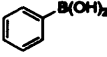
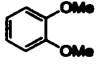
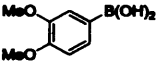
Abbreviations

APCI	Atmospheric pressure chemical ionisation
Å	Angstrom
Aq	Aqueous
Ar	Unspecified aryl substituent
BDBA	1,4-Benzenediboronic acid
BET	Brunauer, Emmett, and Teller
Br	Broad
°C	Degrees centigrade
calc.	Calculated
COD	1,5-Cyclooctadiene
COF	Covalent-Organic-Frameworks
Conc.	Concentrated
DCM	Dichloromethane
DMF	<i>N,N</i> -Dimethylformamide
DMSO	Dimethyl sulphoxide
DSC	Differential scanning calorimetry
EtOAc	Ethyl acetate
EI	Electron Impact
equiv.	Equivalent
ES	Electrospray
Et	Ethyl
G	Grams
GPC	Gel Permeation Chromatography
H	Hour/s
HRMS	High Resolution Mass Spectrometry
Hz	Hertz
IR	Infra Red
IUPAC	International Union of Pure and Applied Chemistry
<i>J</i>	Coupling constant (in Hz)
Lit.	Literature

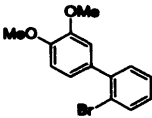
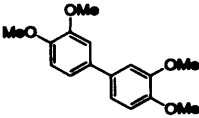
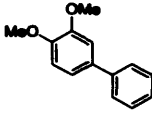
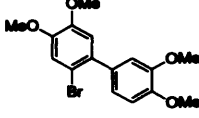
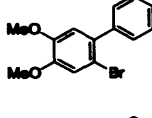
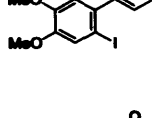
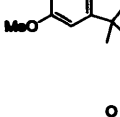
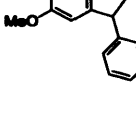
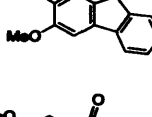
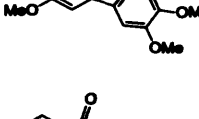
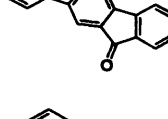
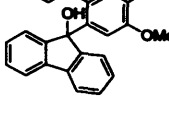
Preface

LRMS	Low Resolution Mass Spectrometry
M	Multiplet
Me	Methyl
min	Minute(s)
mmol	Millimole(s)
M_n	Number-average molecular weight
MOF	Metal Organic Framework
m.p.	Melting point
M_w	Mass-average molecular weight
N°	Number
<i>n</i>-BuLi	<i>n</i> -Butyllithium
nm	nanometer
NMP	<i>n</i> -Methylpyrrolidone
NMR	Nuclear Magnetic Resonance
Oct	<i>n</i> -octane
OFPN	4,4'-Dicyano-2,2',3,3',5,5',6,6'-octafluorobiphenyl
OMIM	Oligomer of intrinsic microporosity
Ph	Phenyl
PIM	Polymers of Intrinsic Microporosity
PPA	Polyphosphoric acid
PTFE	Polytetrafluoroethane
Q	Quartet
r.t.	room temperature
S	Singlet
T	Triplet
<i>t</i>-Bu	Tert-butyl
TFPN	2,3,5,6-Tetrafluoroterephthalonitrile
TGA	Thermo-Gravimetric Analysis
THF	Tetrahydrofuran
TLC	Thin Layer Chromatography
μm	Micrometers

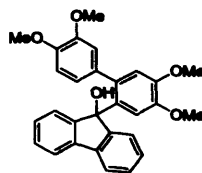
List of recurrent molecules

Name	Structure	N°
PIM-1		PIM-1
4,4',5,5'-Tetrahydroxy-3,3,3',3'-tetramethyl-1,1'-spirobisindane		A1
2,3,5,6-Tetrafluoroterephthalonitrile		TFPN
4,4'-Dicyano-2,2',3,3',5,5',6,6'-octafluorobiphenyl		OFPN
9H-Fluoren-9-one		SM1
4-Bromoveratrole		SM2
Boronic acid		SM3
Veratrole		SM4
3,4-Dimethoxyboronic acid		SM5

Preface

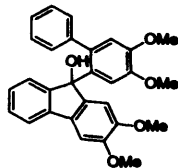
2-Bromo-3',4'-dimethoxy-1,1'-biphenyl		TM1
3,3',4,4'-Tetramethoxybiphenyl		6
3,4-Dimethoxybiphenyl		8
2-Bromo-3',4,4',5-tetramethoxybiphenyl		9
2-Bromo-4,5-dimethoxybiphenyl		10
2-Iodo-4,5-dimethoxybiphenyl		11
5,6-Dimethoxy-3,3-dimethyl-2,3-dihydro-1H-inden-1-one		12
5,6-Dimethoxy-3-phenyl-2,3-dihydro-1H-inden-1-one		13
2,3-Dimethoxy-9H-fluoren-9-one		14
2,3,6,7-Tetramethoxy-9H-fluoren-9-one		15
Indeno[1,2-b]fluorene-6,12-dione		16
9-(4,5-Dimethoxybiphenyl-2-yl)-9H-fluoren-9-ol		17

9-(3',4,4',5-Tetramethoxybiphenyl-2-yl)-9H-fluoren-9-ol



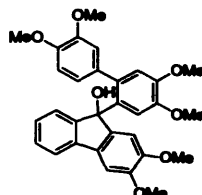
18

9-(4,5-Dimethoxybiphenyl-2-yl)-2,3-dimethoxy-9H-fluoren-9-ol



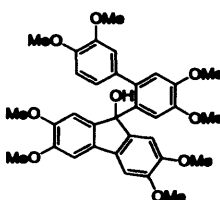
19

(±)2,3-Dimethoxy-9-(3',4,4',5-tetramethoxybiphenyl-2-yl)-9-fluoren-9-ol



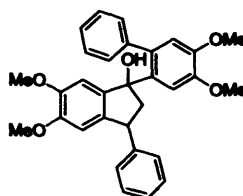
20

2,3,6,7-Tetramethoxy-9-(3',4,4',5-tetramethoxybiphenyl-2-yl)-9H-fluoren-9-ol



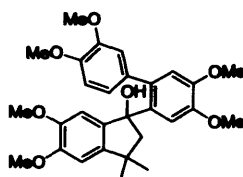
21

1-(4,5-Dimethoxybiphenyl-2-yl)-5,6-dimethoxy-3-phenyl-2,3-dihydro-1H-inden-1-ol



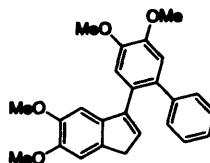
22

5,6-Dimethoxy-3,3-dimethyl-1-(3',4,4',5-tetramethoxybiphenyl-2-yl)-2,3-dihydro-1H-inden-1-ol



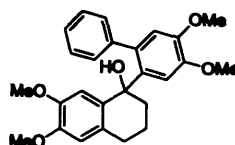
23

3-(4,5-Dimethoxybiphenyl-2-yl)-6,6'-dimethoxy-1H-indene



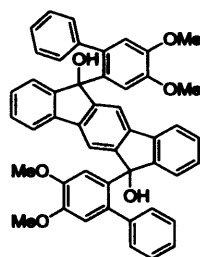
24

1-(4,5-Dimethoxybiphenyl-2-yl)-6,7-dimethoxy-1,2,3,4-tetrahydronaphthalen-1-ol



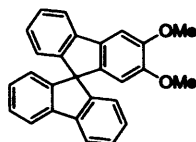
25

6,12-Dihydroxy-6,12-bis(4,5-dimethoxybiphenyl-2-yl)-6,12-dihydroindeno[1,2-b]fluorene



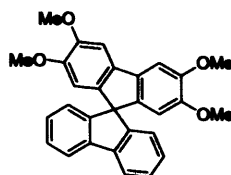
26

2,3-Dimethoxy-9,9'-spirobisfluorene



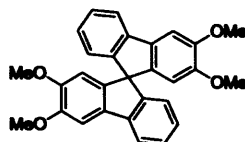
27

2,3,6,7-Tetramethoxy-9,9'-spirobisfluorene



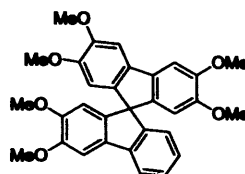
28

2,2',3,3'-Tetramethoxy-9,9'-spirobisfluorene



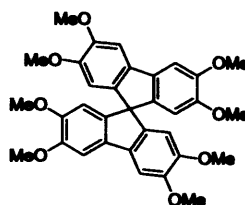
29

2,2',3,3',6,7-Hexamethoxy-9,9'-spirobisfluorene



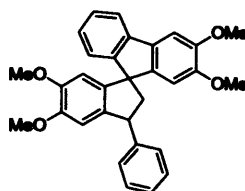
30

2,2',3,3',6,6',7,7'-Octamethoxy-9,9'-spirobisfluorene



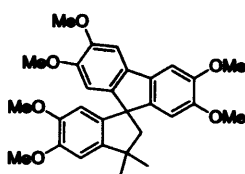
31

2,3,5',6'-Tetramethoxy-3'phenyl-2',3'-dihydrospiro[florene-9,1-indene]



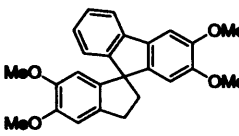
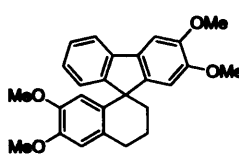
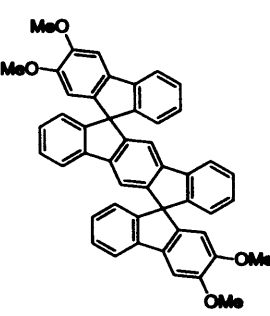
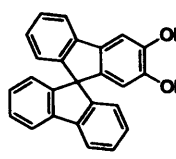
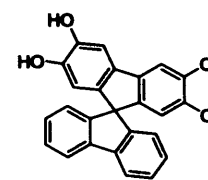
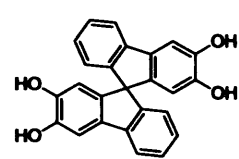
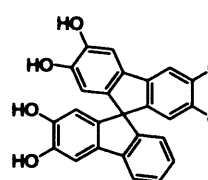
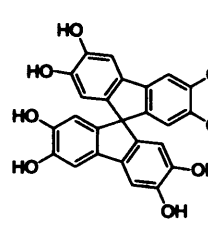
32

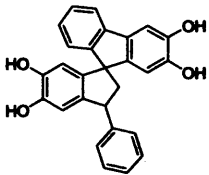
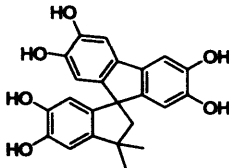
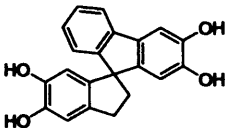
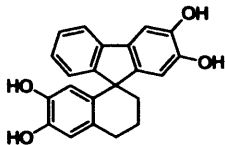
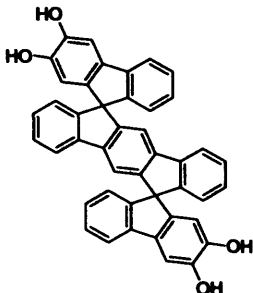
2,3,5',6,6',7-Hexamethoxy-3',3'-dimethyl-2',3'-dihydrospiro[fluorene-9,1'-indene]



33

Preface

2,3,5',6'-Tetramethoxy-2',3'- dihydrospiro[fluorine-9,1'-indene]		34
2,3,6',7'-Tetramethoxy-3',4'-dihydro-2'H- spiro[fluorene-9,1'-naphthalene]		35
2,2'',3,3''-Tetramethoxydispiro[9H-fluorene- 9,6'(12'H)-indeno[1,2-b]fluorine-12',9''- [9H]fluorine]		36
2,3-Tetrahydroxy-9,9'-spirobisfluorene		37
2,3,6,7-Tetrahydroxy-9,9'-spirobisfluorene		38
2,2',3,3'-Tetrahydroxy-9,9'-spirobisfluorene		39
2,2',3,3',6,7-Hexahydroxy-9,9'-spirobisfluorene		40
2,2',3,3',6,6',7,7'-Octahydroxy-9,9'- spirobisfluorene		41

2,3,5',6'-Tetrahydroxy-3'-phenyl-2',3'- dihydrospiro[fluorene-9,1'-indene]		42
2,3,5',6,6',7-Hexahydroxy-3',3'-dimethyl-2',3'- dihydrospiro[fluorene-9,1'-indene]		43
2,3,5',6'-Tetrahydroxy-2',3'- dihydrospiro[fluorene-9,1'-indene]		44
2,3,6',7'-Tetrahydroxy-3',4'-dihydro-2'H- spiro[fluorene-9,1'-naphthalene]		45
2,2'',3,3''-Tetrahydroxydispiro[9H-fluorene- 9,6'(12'H)-indeno[1,2-b]fluorene-12',9''- [9H]fluorene]		46

Abstract

The research described in this thesis was directed towards the synthesis of novel monomers for preparing Polymers of Intrinsic Microporosity (PIMs). Each new monomer contains at least two catechol units fused via a spirobisfluorene centre, which adds a necessary *site of contortion*, and all are compatible with an efficient polymerisation reaction with 2,3,5,6-tetrafluoroterephthalonitrile (TFPN). It was anticipated that the resulting PIMs would possess enhanced properties (e.g. microporosity, solubility, gas permeability etc.) due to the geometry the spirobisfluorene unit.

After an introductory chapter which reviews recent research on the preparation of microporous materials, Chapter 2 is concerned with synthesis of monomeric precursors via the combination of halogenated biphenyls and cyclic ketones via organometallic chemistry. The chemistry was optimised in order to maximise yields of the biphenyl and ketone precursors, the addition reaction and the subsequent cyclization reaction to give the spirocyclic unit.

The third chapter of the thesis reports the synthesis, characterization and physical properties of the polymeric materials obtained from the reaction of the spirocyclic monomers with 2,3,5,6-tetrafluoroterephthalonitrile (TFPN). Network or ladder polymers were obtained depending on the number of catechol pairs on the monomer. The important physical properties of the polymers were assessed such as solubility, microporosity (using nitrogen adsorption), and thermal stability (by Thermo-Gravimetric Analysis - TGA).

Chapter 4 discusses the crystal structures of the monomers and in particular the factors affecting the formation of inclusion compounds (clathrates) and the possible connection between their formation and the presence of microporosity in polymers from which they are derived. The final chapter offers some conclusions and suggests some further work to be raised by the results described in the thesis.

Table of contents

Declaration.....	Error! Bookmark not defined.
Acknowledgments	I
Abbreviations	III
List of recurrent molecules	V
Abstract.....	XII
Table of contents	XIII
Introduction.....	2
1.1 Microporous materials.....	2
1.2 Surface area measurement	3
1.3 Activated carbon	7
1.4 Zeolites	9
1.5 Organic microporous materials	11
1.5.1 Hypercrosslinked polymers	11
1.5.2 Metal Organic Frameworks (MOFs)	14
1.5.3 Covalent Organic Frameworks (COFs)	16
1.5.4 Polymers of Intrinsic Microporosity (PIMs).....	18
1.5.5 Fluorenone based PIMs	20
1.5.6 Polyimide based microporous polymers	21
1.5.7 Triptycene-based PIMs	22
1.6 Inclusion Compounds	24
1.7 Aims of the project	25
Synthesis of monomers	28
2.1 Retrosynthesis of spirobisfluorene monomers	28
2.1.1 Design of route to target compounds	28
2.2 Synthesis of halide-containing intermediates	30
2.2.1 Attempted Suzuki couplings for 1 step halo biphenyl synthesis.....	30
2.2.2 Alternative synthesis of 2-bromo-3',4,4',5-tetramethoxybiphenyl (9)	32

Preface

2.2.3	Synthesis of 2-bromo-4,5-dimethoxybiphenyl (10) and 2-iodo-4,5-dimethoxybiphenyl (11).....	33
2.3	Synthesis of 2,3-dimethoxy-9H-fluoren-9-one (14).	34
2.3.1	Analysis of the synthesis of 2,3-dimethoxy-9H-fluoren-9-one (14)	34
2.3.1	Established routes for the synthesis of 2,3-dimethoxy-9H-fluoren-9-one (14).....	34
2.3.2	Intramolecular Pschörr coupling as a route to 2,3-dimethoxy-9H-fluoren-9-one (14)	37
2.4	Synthesis of 2,3,6,7-tetramethoxy-9H-fluoren-9-one (15)	39
2.4.1	Justification for the synthesis of 2,3,6,7-tetramethoxy-9H-fluoren-9-one (15)	39
2.4.2	Attempted Suzuki couplings	40
2.4.3	Synthesis of 2,3,6,7-tetramethoxy-9H-fluoren-9-one (15) via KMnO ₄ oxidation of 2,3,6,7-tetramethoxy-9H-methylene-9-fluorene	41
2.5	Synthesis of miscellaneous cyclic ketones.	41
2.5.1	Justification for synthesis of various cyclic ketones.	41
2.5.2	Synthesis of 5,6-dimethoxy-3,3-dimethyl-2,3-dihydro-1H-inden-1-one (12)	42
2.5.3	Synthesis of 5,6-dimethoxy-3-phenyl-2,3-dihydro-1H-inden-1-one (13).....	43
2.5.4	Synthesis of indeno[1,2- <i>b</i>]fluorene-6,12-dione (16).....	43
2.6	Precursor synthesis	44
2.6.1	Grignard chemistry	44
2.6.2	Lithium exchange organometallic chemistry	47
2.6.3	Optimisation of organolithium addition.....	48
2.7	Cyclisation of monomer precursors	51
2.7.1	Mechanism of cyclisation	51
2.7.2	Optimization of acid catalysed spiro-centre formation	52
2.7.3	Application of optimized acid cyclisation conditions to produce a range of 9,9'-spirobisfluorenes	53
2.8	Deprotection of monomers via demethylation	55
2.8.1	Discussion of demethylation mechanism.....	55
2.8.2	Protodemethylation reactions to produce monomers	56
Polymer synthesis		59
3.1	Novel 9,9-spirobisfluorene based ladder polymers	59
3.1.1	General procedure for polymerisation and purification	59
3.2	Novel spiro-network polymers.	64

Preface

3.2.1	General procedure for polymerization and purification	64
3.3	Attempted OMIM formation from molecule (37).....	66
Crystallography.....		71
4.1	Analysis of the crystal structures of monomers (37), (39), (40), (41), (44) and (45).	71
4.1.1	Crystal structure of 2,3-Dihydroxy-9,9'-spirobisfluorene (37)	71
4.1.2	Crystal structure of 2,2',3,3'-tetrahydroxy-9,9'-spirobisfluorene (39).....	73
4.1.3	Crystal structure of 2,2',3,3',6,7-hexahydroxy-9,9'-spirobisfluorene (40)	74
4.1.4	Crystal structure of 2,2',3,3',6,6',7,7'-octahydroxy-9,9'-spirobisfluorene (41).	76
4.1.5	Crystal structure of 2,3,5',6'-tetrahydroxy-2',3'-dihydrospiro[fluorene-9,1'-indene] (44).	78
4.1.6	Crystal structure of 2,3,6',7'-tetrahydroxy-3',4'-dihydro-2'H-spiro[fluorene-9,1'-naphthalene] (45).	79
4.1.7	Summary of crystal studies	80
4.2	Summary of crystal data.....	82
Conclusions and future work.....		84
5.1	Conclusions	84
5.2	Future work	84
Experimental		90
6.1	Experimental techniques	90
6.1.1	General remarks	90
6.1.2	InfraRed spectra (IR)	90
6.1.3	Nuclear Magnetic Resonance (NMR).....	90
6.1.4	Mass spectrometry	91
6.1.5	Nitrogen adsorption/desorption	91
6.1.6	Thermo Gravimetric Analysis (TGA).....	91
6.1.7	X-Ray Diffraction (XRD).....	91
6.1.8	MALDI-TOF	91
6.1.9	Elemental analysis	92
6.2	Synthesis.....	922
6.2.1	Dimethyl- <i>p</i> -terphenyl (1).....	92
6.2.2	2,5-Diphenylterephthalic acid (2)	92

Preface

6.2.3	3,4-Dimethoxybenzophenone (3)	93
6.2.4	2-Nitro-4,5-dimethoxybenzophenone (4)	94
6.2.5	2-Amino-4,5-dimethoxybenzophenone (5).....	94
6.2.6	3,3',4,4'-Tetramethoxybiphenyl (6).....	95
6.2.7	9-(Chloromethyl)-2,3,6,7-tetramethoxy-9H-fluorene (7)	95
6.2.8	3,4-Dimethoxybiphenyl (8)	96
6.2.9	2-Bromo-3',4,4',5-tetramethoxybiphenyl (9)	97
6.2.10	2-Bromo-4,5-dimethoxybiphenyl (10).....	98
6.2.11	2-Iodo-4,5-dimethoxybiphenyl (11)	98
6.2.12	5,6-Dimethoxy-3,3-dimethyl-2,3-dihydro-1H-inden-1-one (12)	99
6.2.13	5,6-Dimethoxy-3-phenyl-2,3-dihydro-1H-inden-1-one (13)	99
6.2.14	2,3-Dimethoxy-9H-fluoren-9-one (14)	100
6.2.15	2,3,6,7-Tetramethoxy-9H-fluoren-9-one (15).....	101
6.2.16	Indeno[1,2- <i>b</i>]fluorene-6,12-dione (16).....	101
6.2.17	9-(4,5-Dimethoxybiphenyl-2-yl)-9H-fluoren-9-ol (17)	102
6.2.18	9-(3',4,4',5-Tetramethoxybiphenyl-2-yl)-9H-fluoren-9-ol (18)	103
6.2.19	9-(4,5-Dimethoxybiphenyl-2-yl)-2,3-dimethoxy-9H-fluoren-9-ol (19).....	104
6.2.20	2,3-Dimethoxy-9-(3',4,4',5-tetramethoxybiphenyl-2-yl)-9H-fluoren-9-ol (20)	104
6.2.21	2,3,6,7-Tetramethoxy-9-(3',4,4',5-tetramethoxybiphenyl-2-yl)-9H-fluoren-9-ol (21).....	105
6.2.22	1-(4,5-Dimethoxybiphenyl-2-yl)-5,6-dimethoxy-3-phenyl-2,3-dihydro-1H-inden-1-ol (22).....	106
6.2.23	5,6-Dimethoxy-3,3-dimethyl-1-(3',4,4',5-tetramethoxybiphenyl-2-yl)-2,3-dihydro-1H-inden-1-ol (23)	107
6.2.24	3-(4,5-Dimethoxybiphenyl-2-yl)-6,6'-dimethoxy-1H-indene (24).....	108
6.2.25	1-(4,5-Dimethoxybiphenyl-2-yl)-6,7-dimethoxy-1,2,3,4-tetrahydronaphthalen-1-ol (25)	108
6.2.26	6,12-Dihydroxy-6,12-bis(4,5-dimethoxybiphenyl-2-yl)-6,12-dihydroindeno[1,2- <i>b</i>]fluorene (26)	109
6.2.27	2,3-Dimethoxy-9,9'-spirobisfluorene (27)	110
6.2.28	2,3,6,7-Tetramethoxy-9,9'-spirobisfluorene (28).....	111
6.2.29	2,2',3,3'-Tetramethoxy-9,9'-spirobisfluorene (29).....	111
6.2.30	2,2',3,3',6,7-Hexamethoxy-9,9'-spirobisfluorene (30).....	112
6.2.31	2,2',3,3',6,6',7,7'-Octamethoxy-9,9'-spirobisfluorene (31).....	113

Preface

6.2.32	2,3,5',6'-Tetramethoxy-3'-phenyl-2',3'-dihydrospiro[fluorene-9,1'-indene] (32)	113
6.2.33	2,3,5',6,6',7-Hexamethoxy-3',3'-dimethyl-2',3'-dihydrospiro[fluorene-9,1'-indene] (33)	114
6.2.34	2,3,5',6'-Tetramethoxy-2',3'-dihydrospiro[fluorene-9,1'-indene] (34).....	115
6.2.35	2,3,6',7'-Tetramethoxy-3',4'-dihydro-2' <i>H</i> -spiro[fluorene-9,1'-naphthalene] (35).....	115
6.2.36	2,2'',3,3''-Tetrahydroxydispiro[9 <i>H</i> -fluorene-9,6'(12' <i>H</i>)-indeno[1,2- <i>b</i>]fluorene-12',9''- [9 <i>H</i>]fluorene](36).....	116
6.2.37	2,3-Tetrahydroxy-9,9'-spirobisfluorene (37).....	117
6.2.38	2,3,6,7-Tetrahydroxy-9,9'-spirobisfluorene (38).....	118
6.2.39	2,2',3,3'-Tetrahydroxy-9,9'-spirobisfluorene (39)	118
6.2.40	2,2',3,3',6,7-Hexahydroxy-9,9'-spirobisfluorene (40)	119
6.2.41	2,2',3,3',6,6',7,7'-Octahydroxy-9,9'-spirobisfluorene (41).....	120
6.2.42	2,3,5',6'-Tetrahydroxy-3'-phenyl-2',3'-dihydrospiro[fluorene-9,1'-indene] (42)	120
6.2.43	2,3,5',6,6',7-Hexahydroxy-3',3'-dimethyl-2',3'-dihydrospiro[fluorene-9,1'-indene] (43)	121
6.2.44	2,3,5',6'-Tetrahydroxy-2',3'-dihydrospiro[fluorene-9,1'-indene] (44)	122
6.2.45	2,3,6',7'-Tetrahydroxy-3',4'-dihydro-2' <i>H</i> -spiro[fluorene-9,1'-naphthalene] (45)	122
6.2.46	2,2'',3,3''-Tetrahydroxydispiro[9 <i>H</i> -fluorene-9,6'(12' <i>H</i>)-indeno[1,2- <i>b</i>]fluorene-12',9''- [9 <i>H</i>]fluorene] (46).....	123
6.2.47	OMIM 1 (47)	124
6.2.48	LADDER POLYMER 1 (48).....	125
6.2.49	LADDER POLYMER 2 (49).....	125
6.2.50	LADDER POLYMER 3 (50).....	126
6.2.51	LADDER POLYMER 4 (51).....	127
6.2.52	LADDER POLYMER 5 (52).....	128
6.2.53	NETWORK POLYMER 1 (53).....	129
6.2.54	NETWORK POLYMER 2 (54).....	130
6.2.55	NETWORK POLYMER 3 (55).....	131
6.2.56	NETWORK POLYMER 4 (56).....	132
6.2.57	NETWORK POLYMER 5 (57).....	133
6.2.58	NETWORK POLYMER 6 (58).....	134
Bibliography		136

CHAPTER

1

1.1)	Microporous materials.....	2
1.2)	Surface area measurement.....	3
1.3)	Activated carbon.....	7
1.4)	Zeolites.....	9
1.5)	Organic microporous materials.....	11
1.6)	Clathrate crystals.....	24
1.7)	Aims of the project.....	25

Introduction

1.1 Microporous materials

The study of a material's composition on the atomic scale and how this composition affects their physical properties has been at the cornerstone of modern chemistry and physics for many years. Albert Einstein studied the photoelectric effect^[1] first observed by Heinrich Hertz^[2] and from these studies, technology such as photovoltaic cells was developed. Ernest Rutherford's studies on the scattering of alpha radiation by gold nuclei^[3] led to Niels Bohr's model for the atom^[4], from which the theories behind most of the 20th century's spectroscopic analysis methods are derived^[5]. In a similar vein of thought the postulation and measurement of BET isotherms have given modern scientists an insight into the topography of solid surfaces at the nanometre scale^[6].

The surface geometry of materials can vary wildly on the nanometre scale, from the well defined features of a graphite surface^[7] to the amorphous surface of a solid such as polystyrene^[8] and the nature of the surface define their physical properties, and arise from their molecular structure. In 1959 Richard Feynman gave his seminal lecture "There's Plenty of Room at the Bottom" in which he postulated that direct manipulation of atoms would lead to a more powerful form of synthetic chemistry. Although some of the ideas he envisioned are currently out of reach he was certainly correct that there is plenty of room at the bottom, given that a gram of powdered microporous material can easily contain an area equivalent to that of a tennis court^[9] (approximately 264 m²).

To explain why such small amounts of material can possess such a large surface area we must consider the structure of a material on the nanoscale. A regular smooth surface will have a relatively small surface area, and conversely an irregular and jagged surface will have a relatively large surface area. Inclusion of pores into a surface is known to greatly increase the surface area of the material. The pores of human skin utilise the high surface areas they provide to enable rapid heat loss via the evaporation of sweat^[10].

A pore is loosely defined as a limited space or spatial confinement, and according to the International Union of Pure and Applied Chemistry (IUPAC) can fall into one of three categories^[11]. A channel or pore with a diameter greater than 50 nm is defined as a macropore. Pores with a diameter of between 50 nm and 2 nm are defined as mesopores, but

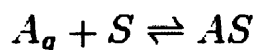
the majority of observed pores fall into the microporous classification, which are defined as pores with a diameter of less than 2 nm.

In recent decades microporous materials have found many applications in an industrial and academic context. Well defined and controlled pore size distribution can lead to materials with highly selective gas separation properties^[12] and materials with high internal volumes can be utilised as gas storage materials^[13]. Of particular interest is the ability to store gasses such as H₂^[14], CH₄^[15], CO₂^[16], and NH₃^[17] for use within the energy generation industry, and adsorption of H₂S^[18], NO_x^[19], and volatile organic compounds (VOCs)^[20] for applications within pollution reduction technologies.

1.2 Surface area measurement

All solid surfaces have a tendency to exhibit some degree of sorption (adsorption and desorption), and observation of the way in which a material exhibits gas sorption will provide extensive information about a solid such as its relative surface area and pore size distribution.

Sorption can occur as chemisorptions in which conventional bonds are formed with the surface^[21] and is typically irreversible, and physisorption in which an association between the gas and the surface is formed via Van der Waal interactions^[22]. As Van der Waal interactions are relatively weak in terms of thermodynamics, physisorption is a reversible process. Physisorption is described mathematically by the Langmuir isotherm and is based on a number of assumptions. The theory postulates that equilibrium is established between gas phase molecules and molecules adsorbed on a surface. As with all chemical equilibria the position of the equilibrium depends on the relative stability of the adsorbed species, the temperature at which the equilibrium is observed, and the pressure exerted by the gas within an equilibrium system^[23]. The Langmuir isotherm can be derived by considering the adsorption as analogous to any other equilibrium process. In this case the equilibrium is established between the numbers of gas phase molecules (A), and the number of adsorption sites (S) on the surface.



Chapter - 1

The direct and inverse rate constants are k and k_{-1} respectively and surface coverage is defined as θ , the fraction of occupied adsorption sites. Hence the equilibrium can be defined by K , where P is the partial pressure of the equilibrium system.

$$K = \frac{k}{k_{-1}} = \frac{\theta}{(1 - \theta)P} \quad \text{or} \quad \theta = \frac{KP}{1 + KP}.$$

For low pressures θ is approximately equal to KP and for high pressures θ is approximately equal to 1.

The Langmuir isotherm is based on several assumptions. Firstly the surface of the adsorbent is uniform and all adsorption sites are equal. Secondly adsorbed molecules do not interact with each other. Thirdly all adsorption occurs via the same mechanism and finally that at maximum adsorption; only a single monolayer will be formed. For most materials the final assumption is usually incorrect and many monolayers are formed consecutively (i.e. gas molecules will be adsorbed on top of an existing monolayer before a vacant site) at maximum adsorption. To counter the flaw in this fourth assumption the BET (Brunauer, Emmett, and Teller) isotherm was developed.

The BET^[24] equation states that:

$$\frac{P}{n(P-P_0)} = \frac{c-1}{cn_m} \left(\frac{P}{P_0} \right) + \frac{1}{cn_m}$$

Where P = the adsorption pressure, P_0 = the saturation pressure, n = the amount of moles of gas adsorbed in terms of moles per gram at a relative pressure P/P_0 , n_m = the monolayer capacity (moles of molecules needed to make a monolayer coverage on the surface of one gram of adsorbent), and c is a constant expressed as

$$c = \exp \left(\frac{E_1 - E_L}{RT} \right)$$

where E_I = the heat of adsorption for the first layer, and E_L = the heat of adsorption for the second and subsequent layers and is equal to the heat of liquefaction, R = The gas constant and T = temperature respectively. By calculating the slope and intercept of a plot of $P/[n(P_0 - P)]$ against (P/P_0) , n_m can be resolved. The specific surface area, S , can then be derived:

$$S = N_A n_m \sigma$$

where N_A is Avagadro's constant and σ is the area covered by the adsorbed molecule. In the case of most BET measurements N_2 is the adsorbed gas and has an area of 16.2 \AA^2 . The specific surface area that can be determined by gas sorption ranges from 0.01 to over 5000 m^2/g . In addition, the determination of pore size and pore size distribution of porous materials can be made from the adsorption/desorption isotherm using an assessment model, based on the shape and structure of the pores. The range of pore sizes that can be measured using gas sorption is a range between a few Ångstroms up to about half a micron. The complete adsorption/desorption analysis is called an adsorption isotherm. To obtain an accurate BET surface area it is necessary to first remove all contaminant gasses adsorbed upon a sample. This is typically achieved by firstly baking the sample within a vacuum oven and then degassing further by purging the sample with an inert gas such as helium, and then further subjecting the sample to a high vacuum at around 120 °C. Controlled doses of an inert gas, such as nitrogen are introduced and the gas is adsorbed, or alternatively, withdrawn and desorbed. The sample material is placed in a vacuum chamber at a constant and very low temperature, usually at the temperature of liquid nitrogen (77K), and subjected to a range of pressures, to generate adsorption and desorption isotherms. For a conventional volumetric analysis, the gas sorption by the material (adsorbent) is determined by the pressure variations on introduction of a known quantity of gas (adsorbate). Knowing the area occupied by one adsorbate molecule, and using the BET isotherm model described previously, the total surface area of the material can be determined.

The IUPAC classification of adsorption isotherms^[11] is illustrated in Fig 1.1 associated with microporous (type I), nonporous or macroporous (types II, III, and VI) or mesoporous (types IV and V) materials.

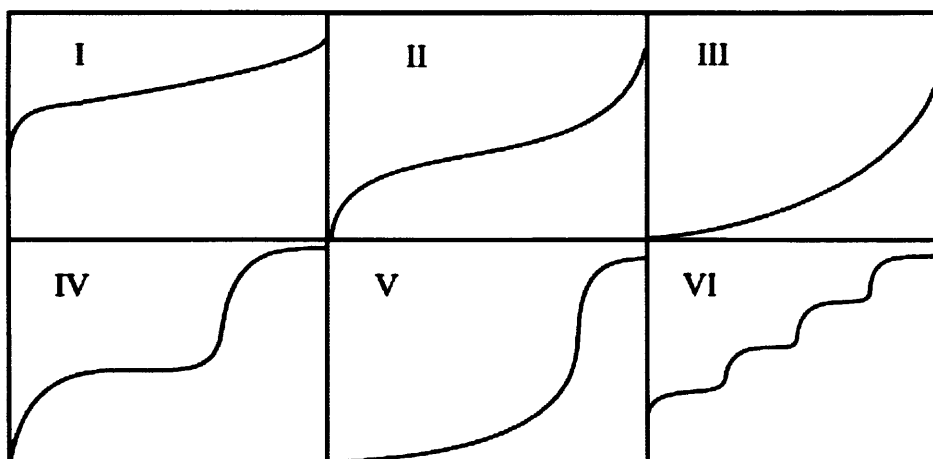


Fig 1.1 Type I is microporous. Type II, III, VI is a material without pores. Type IV, V is mesoporous. Graph axes are typically partial pressure (P/P_0) for the x axis and volume of liquid nitrogen in cubic centilitres adsorbed per gram of material tested (cc/g) for the y axis.

The differences between types II and III isotherms and between types IV and V isotherms arise from the relative strengths of the fluid-solid and fluid-fluid attractive interactions: types II and IV are associated with stronger fluid-solid interactions and types III and V are associated with weaker fluid-solid interactions. Hysteresis loops usually exhibited by types IV and V isotherms are attributed to capillary condensation within the mesopores. The type VI isotherm represents adsorption on nonporous or macroporous solids where stepwise multilayer adsorption occurs. Adsorption by mesopores is dominated by capillary condensation, whereas filling of micropores (type I) is controlled by stronger interactions between the adsorbate molecules and pore walls^[25]. It is worth mentioning that pore width is a well defined criteria but pore shape is often unaddressed. The relationship between pore shape and hysteresis can be intrinsically linked in some circumstances, especially when considering shape selective molecular sieve mechanics.

Studying microporous materials we are, of course, interested in isotherms type I in which at low pressures there can be a great quantity of nitrogen adsorbed for an almost imperceptible increase of P/P_0 ratio. This is the part of the curve which signifies the microporosity of the material (Fig 1.2).

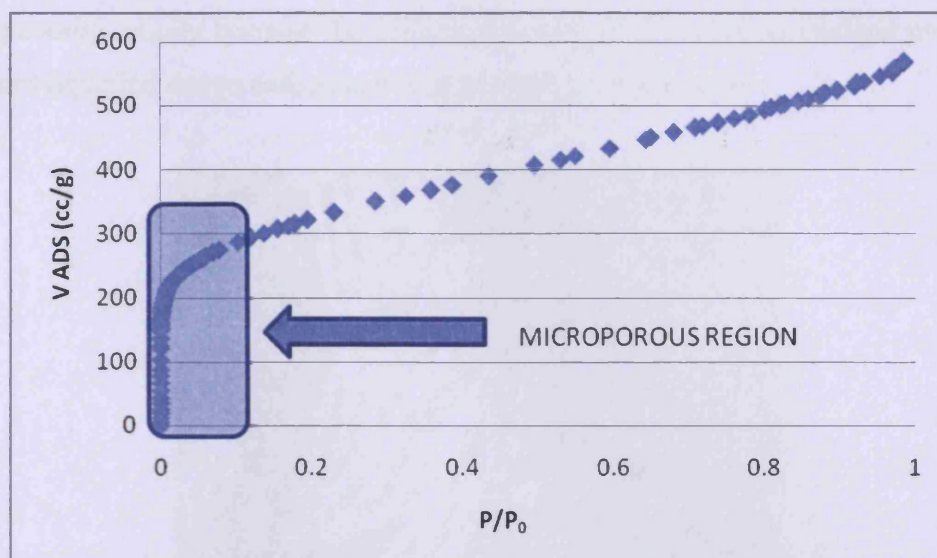


Fig 1.2 Nitrogen adsorption isotherm for a microporous material (volume of liquid nitrogen adsorbed in cubic centiliters per gram against partial pressure)

1.3 Activated carbon

Activated carbon is defined as “the porosity (or space) enclosed by carbon atoms” in the book activated carbon by Henry Marsh and F. Rodríguez-Reinoso^[26]. The classification of materials referred to as activated materials covers a broad range of compounds with many different pore size distributions and the structures that give rise to these pores are by no means uniform. Activated carbons are typically highly adsorbent materials and have a variety of commercial applications. Activated carbons can be engineered to be highly adsorbent of both liquid^[27] and gaseous phases^[28]. Surface areas of between 400 and 2000 m²/g have regularly been reported for these materials^[29], and have been applied to technological fields such as catalysis^[30], filtration^[31], deodorization^[32], and purification^[33]. The specific properties of an activated carbon material are intrinsically linked to both the raw material from which it is derived^[26] and the method used to carbonize the raw material^[34]. Almost any organic material can be carbonized to form some degree of activated carbon but on an industrial scale the starting materials are typically hard woods, coal, or nut shells due to availability and lead to production of activated carbon with well defined pore size distribution. As previously mentioned the term activated carbon refers to a wide variety of materials and for the sake of brevity only a few examples are included. Activated carbon derived from carbonized wood

exhibits porosity largely because the cellular structure of the wood is retained provided the wood is not liquefied due to carbonization at excessive temperatures.

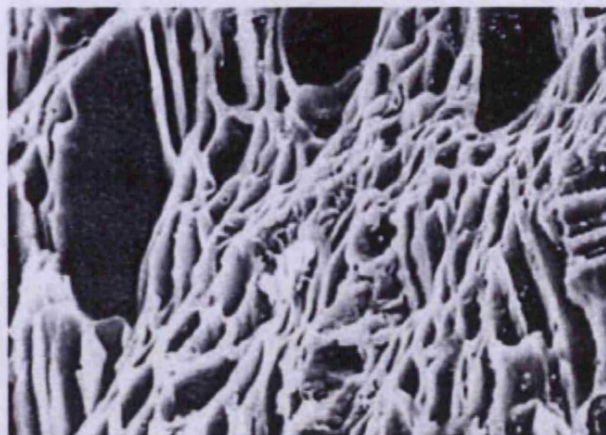


Fig 1.3 SEM picture of the cellular structure of pores present in activated carbon derived from wood (100 x 70 μm)^[26]

Natural coals exhibit some degree of porosity with low grade and anthracites exhibiting high porosity (~ 20% vol), and bituminous coal exhibiting low porosity (~3% vol) although the pore sizes of untreated coal is poorly defined^[26]. By treating coal chemically via phosphoric acid impregnation followed by thermal carbonization at between 400 - 600 °C more regular pores size distribution can be achieved, as well as higher internal volumes^[34].

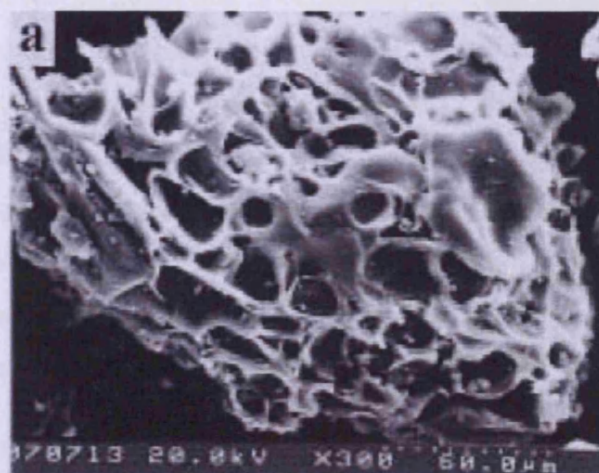


Fig 1.4 SEMs of carbons prepared by chemical activation via phosphoric acid impregnation followed by carbonization at 500 °C for 3 hours^[34]

During the activation process of both wood and coal much of the hydrogen contained in the starting material is removed, resulting in cross linkage of the remaining carbon atoms

into extended graphite fragments. Impurities such as nitrogen and oxygen functional groups are often left on the surface of the activated carbon which in part explains the ability of activated carbons to absorb a wide variety of metallic ions and organic compounds^{[35][36]}.

Although not strictly considered activated carbon compounds, nanotubes are a allotrope of carbon that has received recent attention in regards to microporosity and gas storage^{[28][37]}. Typically the gas adsorption occurs in the pores formed between individual nanotube strands rather than inside the tubes themselves.

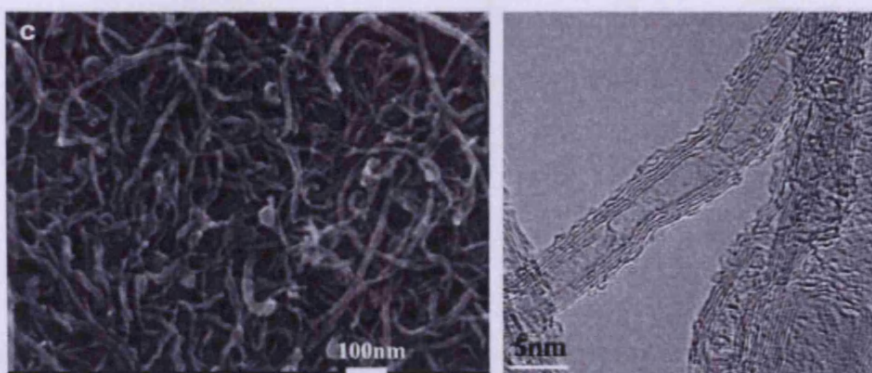


Fig 1.5 FESEM and TEM images of microwave treated multi-walled carbon nanotubes^[37].

1.4 Zeolites

A zeolite is strictly speaking a form of mineral, and was first discovered by mineralogist Axel Fredrik Cronstedt. In 1765 he noted that upon heating the mineral stilbite, a large amount of steam was released from the rock. This indicated that somehow the water was stored within the structure of the mineral but was not strongly bound to the structure. In modern times the various structures of these naturally occurring zeolites are well known^{[38][39][40]} and that the water is stored in the microporous channels created by arrays of hydrated aluminosilicates of alkali and alkaline earth cations. In addition to the naturally occurring zeolites, many man made zeolites have also been synthesised^[41] and find application within fields such as detergents^[42], catalysis^[43], molecular sieves^[44], and oil refining^[45].

Zeolites are inorganic crystalline solids with small pores ranging from 1 – 20 Å diameter running throughout the three dimensional structure of the material. The crystal is built from repeating units of SiO_4 and AlO_4 tetrahedrons.

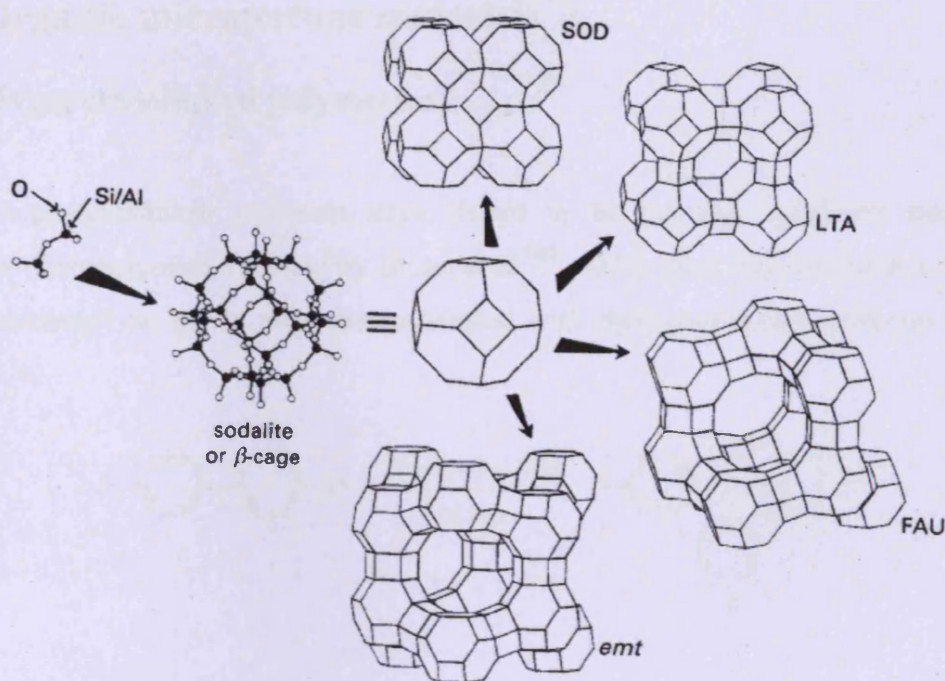


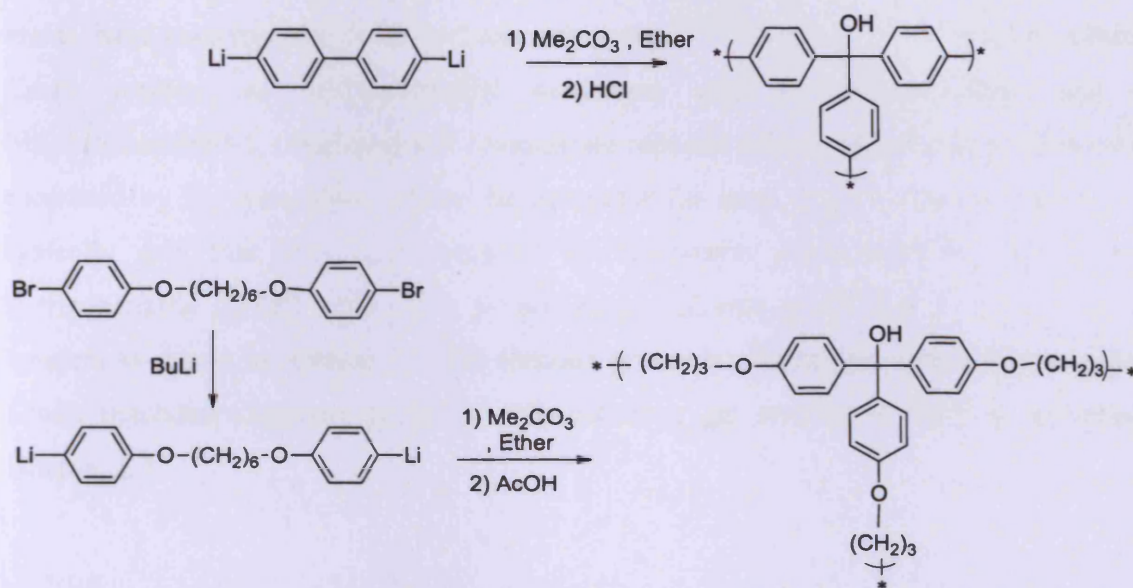
Fig 1.6 Example of various zeolite crystal structures built up from a sodalite unit. (Note the incorporation of voids into the crystal structure)^[44]

The uniform size and shape of the pores created in the zeolite structure as shown in Fig 1.6, are utilised in technology for the separation of mixtures. In contrast to activated carbon the dimensions of the pores are so well defined it is possible to selectively adsorb small molecules from a solution leaving the larger molecules to remain in solution and leading to the term “molecular sieve”^[44]. Molecular sieves are principally used in the oil refining industry for catalytic cracking of long chain hydrocarbons. The purpose of the zeolite is twofold^[45]. Firstly it provides a large surface area upon which the catalyst can be loaded, and secondly the pore sizes will allow hydrocarbons to diffuse through them at different rates depending on the hydrocarbon structure.

1.5 Organic microporous materials

1.5.1 Hypercrosslinked polymers

Several hypercrosslinked polymers have shown to possess significant microporous properties. Two polymers, reported by Urban *et al.*^[46], which were synthesised in a manner so that tri-functional tie points were interconnected with rigid connecting units are shown in Scheme 1.1.



Scheme 1.1. Polyarylcabinols polymers synthesis^[46].

These hypercrosslinked polymers, swell 200-300% in most organic solvents. This behaviour is poorly understood and, since they neither dissolve nor melt, there is very little information available to explain their pore structure and morphology. One explanation, involves the formation of highly crosslinked particles having a high microporosity during the early polymerization stages which give rise to the observed high surface area. The swelling can be explained based on the assumption that micropores are formed full of solvent during polymerization, and contract when the polymer is dried and the solvent removed (Fig 1.7). Since the network structure is rigid, the pores cannot collapse completely, imposing a very high stress on the dry network. To release this stress, the polymers swells, even in thermodynamically poor solvents, in order to regain the conformation that they had during the cross-linking reaction.

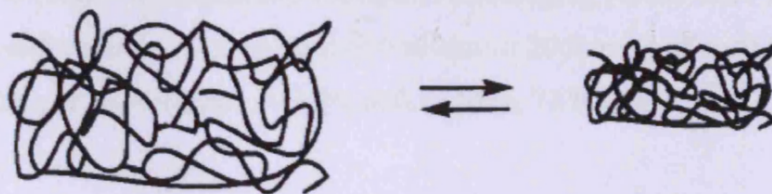
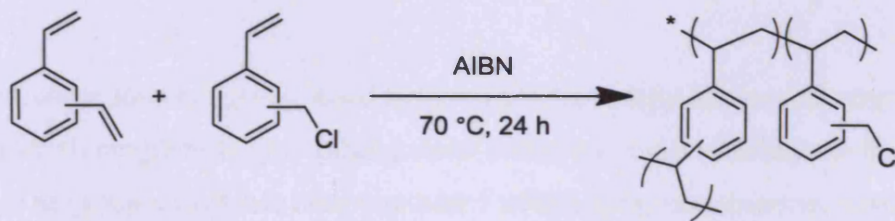
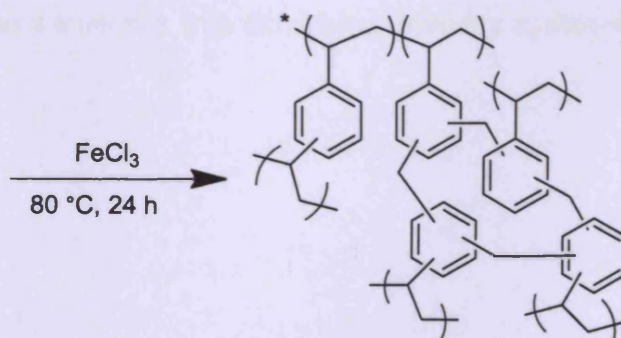


Fig 1.7. Swelling behaviour of polymer with a homogeneous morphology^[46].

In a similar vein, another class of hypercrosslinked polymer, also known as Davankov resins, have been reported by several research groups^{[47][48]}. The resins are based on a Friedel-Crafts reaction of bischloromethyl monomers such as dichloroethylene, and 4,4-bis(chloromethyl)-1,1-biphenyl and demonstrate reported surface areas of up to 1904 m²/g as measured by N₂ adsorption. Often, the precursor for such hypercrosslinked polymers are typically gels that have been prepared by suspension polymerization using 2 wt % divinylbenzene (DVB) with either *p*-vinylbenzyl chloride (pVBC) or a mixture of VBC isomers as shown in Scheme 1.2. The reaction proceeds via multiple intramolecular Friedel-Crafts reactions catalysed by FeCl₃ with precursor gel swollen in DCE as indicated in Scheme 1.3.



Scheme 1.2 Radical initiated synthesis of precursor gel^[47]



Scheme 1.3 Friedel-Crafts cross linking of gel precursor to form Davankov resin^[47].

Adsorption and desorption experiments were carried out to evaluate this hypercrosslinked resin's ability to absorb hydrogen and nitrogen. Encouraging results were obtained showing apparent BET surface areas ranging from 600 to almost 2000 m²/g of surface area and with a maximum loading of H₂ evaluated as 2.2% at 0.12 MPa, 77 K (Fig 1.8)^[48].

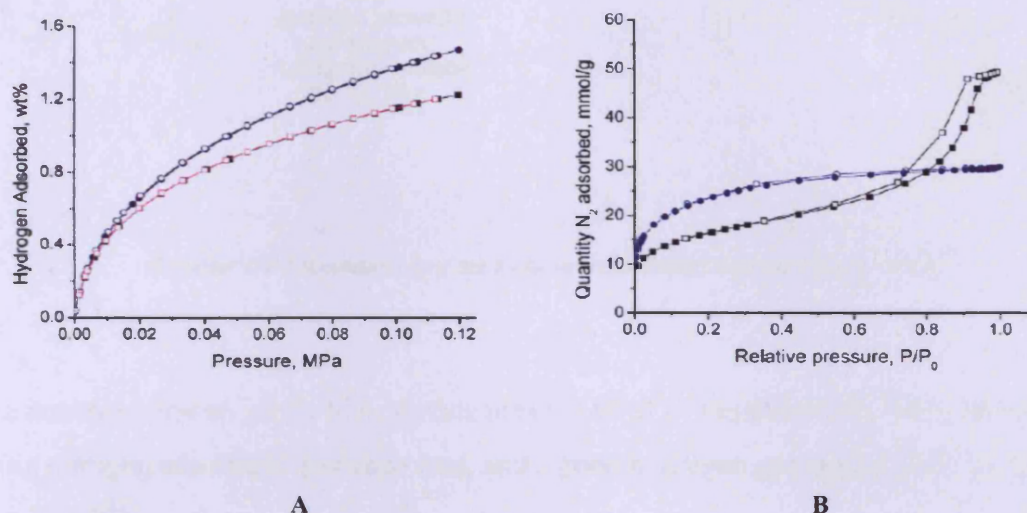
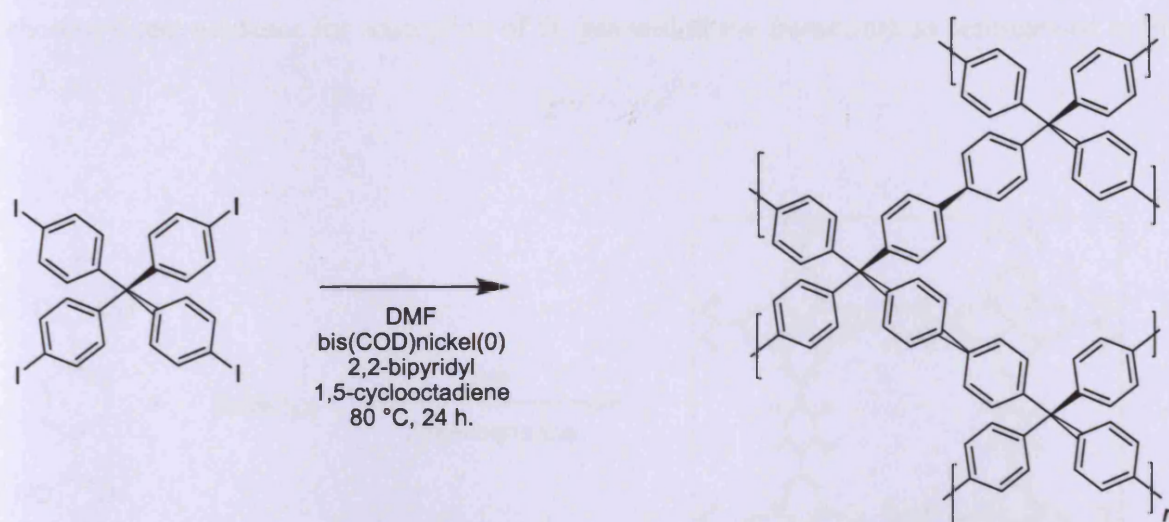


Fig 1.8 Hydrogen adsorption (A) prepared from gel (blue) and macroporous (pink) poly(chloromethylstyreneco-divinylbenzene) and nitrogen adsorption (B) gel (blue) and macroporous (black^[48]).

The Cooper research group based in Liverpool University has recently engaged in an intensive research programme synthesising cross-linked polymers with high surface areas^{[49][50]}. The group's work has been concerned with linking monomers via various cross coupling reactions such as Yamamoto coupling and Songashira-Hagihara palladium coupling. For example, the Yamamoto coupling reaction was used to create a network using tetrakis(4-iodophenyl)methane as a monomer with tetrahedral geometry as shown in Scheme 1.4.



Scheme 1.4 Yamamoto coupling to form cross-linked microporous polymer^[51]

The network showed very a high surface area ($3160 \text{ m}^2\text{g}^{-1}$) calculated by BET methodology using nitrogen adsorption isotherm data, and a good hydrogen gas uptake (2.13 wt %; at 1.13 bar; 77 K)^[51].

1.5.2 Metal Organic Frameworks (MOFs)

Metal Organic frameworks (MOFs) consist of metal clusters linked by polyfunctional organic linkers forming porous three-dimensional networks with large pore volumes and high inner surface areas. They are typically prepared via hydrothermal synthesis. This technique involves dissolving the desired MOF components in a solvent (typically water), sealing the solution in a polytetrafluoroethylene (PTFE) lined autoclave, heating the solution to above 150 °C under high pressure, and allowing the solution to cool very slowly, precipitating MOF crystals^[52]. In contrast to zeolites, MOFs structures can be altered significantly by variation of the organic linker, and in turn a fine control can be exerted over the resulting macro structure in terms of pore volume and diameter. Typically the structure of the resulting framework would collapse into more stable polymorphs when the solvent associated with these frameworks was removed. The first major step in overcoming this problem was reported in 1999 by Yaghi *et al.*^[25]. They reported the metal organic framework, MOF-5, made from hydrothermal synthesis between terephthalic acid and zinc nitrate, which remains crystalline, as evidenced by X-ray single-crystal analyses and stable when fully desolvated and on heating up to 300 °C. A further neutron diffraction study on MOF-5 by Yildirim *et al.*^[53]

showed direct evidence for adsorption of D_2 gas within the framework as summarised in Fig 1.9.

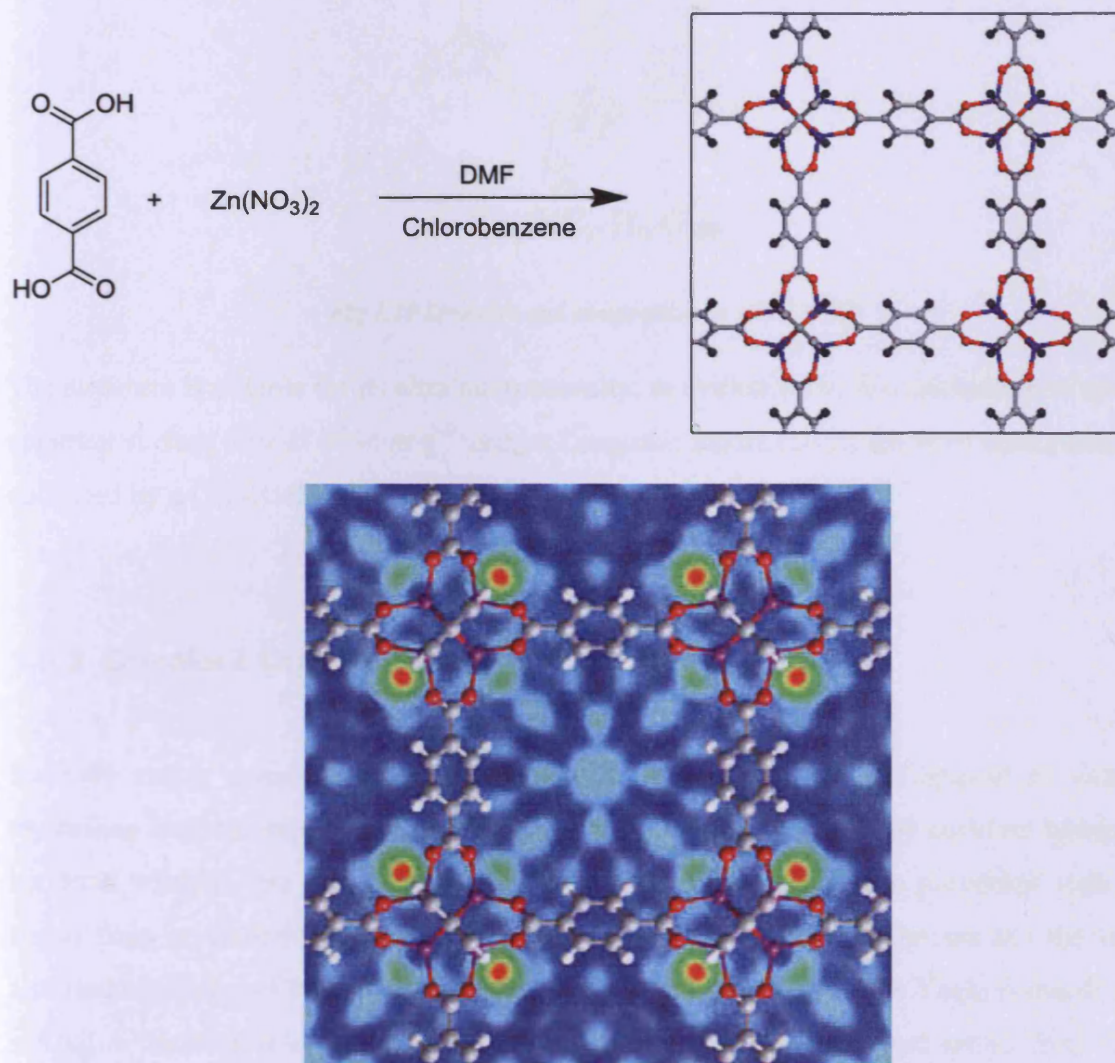


Figure 1.9 Synthesis of MOF-5 and neutron diffraction image showing deuterium (red to green spots) absorbed within the prototypical MOF-5^[53] (Ball and stick model of MOF-5 superimposed)

The next major breakthrough in the field of MOFs was the synthesis of MOF-177^[54]. The synthesis differed from the hydrothermal methodology previously developed by Yaghi et al.^[55] instead using benzenetribenzoic acid and $Zn(OAc)_2 \cdot 2H_2O$ stirred in DMF at 50 °C, and termed solvothermal synthesis, which resulted in the structure shown in Fig 1.10.

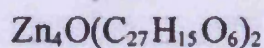
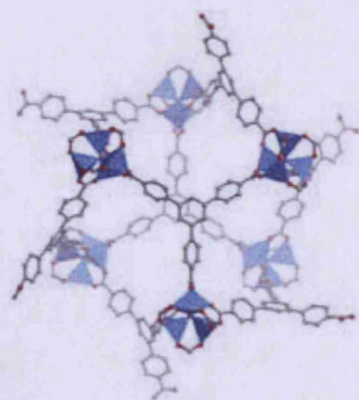


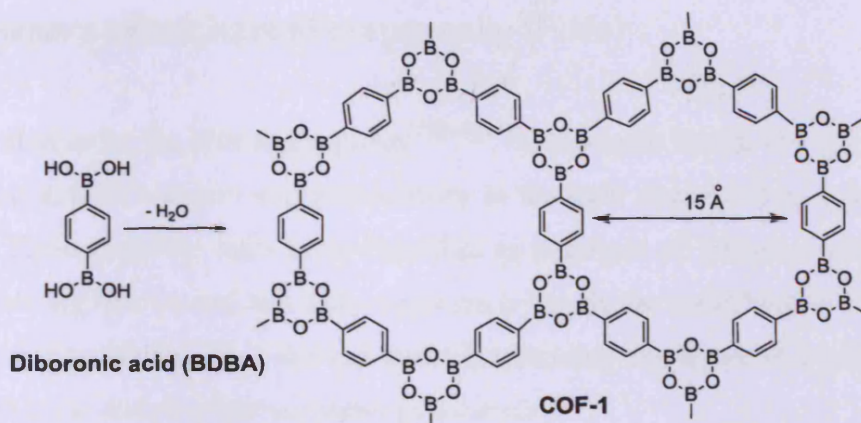
Fig 1.10 Structure and composition of MOF-177^[54]

The structure is notable for its ultra microporosity, as evidenced by the calculation of an apparent surface area of $4944 \text{ m}^2\text{g}^{-1}$ using a Langmuir model calculated from absorption data collected by a Quantachrome Nova surface area analyzer.

1.5.3 Covalent Organic Frameworks (COFs)

Recently much research resources have been directed at the development of extended crystalline arrays composed of small organic building blocks linked by covalent bonds. The accepted wisdom was that microscopic reversibility of crystallization prevented such large arrays from crystallizing and would instead collapse into smaller fragments and the lack of reported structures of this nature was cited as supporting evidence. The Yaghi research group at UCLA decided to challenge this view by choosing to form covalent arrays from simple molecular building blocks functionalized in such a way that they would form strong intermolecular covalent bonds^[56].

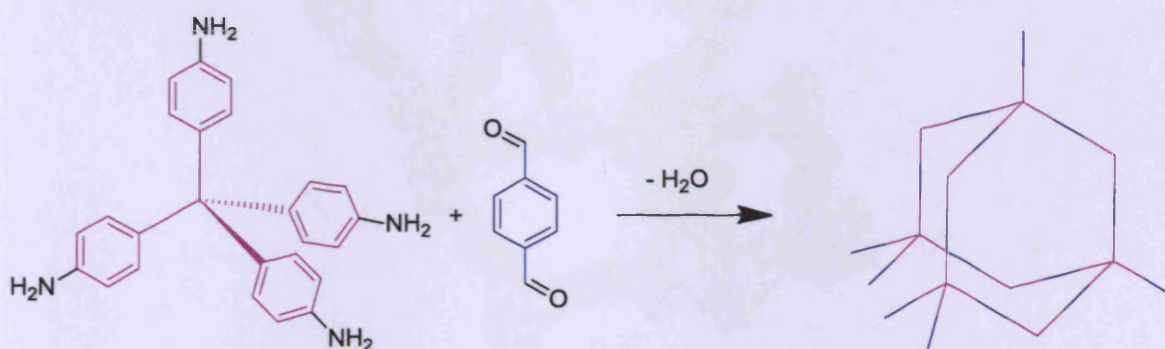
The principle is well illustrated by the example of COF-1^[57] which is formed from the self-condensation of diboronic acid via dehydration caused by mild heating shown in Scheme 1.5. The resulting crystalline array was found to have thermal stabilities in excess of 600°C and exceptionally low density. The microporosity was confirmed by BET analysis, and the isotherm for COF-1 at 77 K indicated an apparent surface area of $711 \text{ m}^2\text{g}^{-1}$.



Scheme 1.5 Self-condensation of DDBA to form COF – 1 crystals^[57].

Other two dimensional frameworks are based upon covalent organic bonding. An example such as the triazine-based frameworks, formed from the trimerization of dicyanobenzene and similar dicyano compounds reacted in molten $ZnCl_2$, also showed microporosity and potential as a catalyst support^[58].

Three dimensional frameworks, often referred to as 2nd generation COFs, have also been reported by Yahgi *et al.*^[59]. A notable example is COF-300 which is based on imine bond-formation chemistry, specifically polymeric condensation of the tetrahedral building block tetra-(4-aminyl)methane with the linear linking unit terephthalaldehyde. The tetrahedral array shown in Scheme 1.6 showed an apparent surface area of $1360 \text{ m}^2 \text{ g}^{-1}$ measured by argon adsorption and calculated using BET isotherm models and has a packing structure similar to that of diamond.



Scheme 1.6 Polyimine condensation to form COF-300^[59].

1.5.4 Polymers of Intrinsic Microporosity (PIMs)

In previous studies by the McKeown group^{[60][14][61]} it has been shown that polymers can be produced that exhibit a degree of microporosity in the bulk material from a wide range of monomers. These materials have been classified as polymers of intrinsic microporosity or PIMs. Considering that the polymerization process is largely the same for each PIM produced to date^[62], it can be assumed that the key factor determining the degree of microporosity in a PIM material is the design of the monomer polymerized.

Intrinsic microporosity is produced from monomers that have two common factors. The monomer must be rigid. This is achieved by designing monomers that contain predominantly sp^2 -hybridized carbons and/or fused cyclic hydrocarbons. The monomers must also contain a site of contortion such as a spiro-centre. The rationale for these structural conditions is that rigidity reduces the degrees of freedom of the polymer chain, and when coupled with the sites of contortion introduced into the polymer chain, produces a polymer chain that cannot pack together efficiently as a bulk material^[63], as illustrated in Fig 1.11. Hence, voids of empty space are introduced into the bulk material. These void spaces are interconnected and thus give rise to the micropores within the bulk material, and ultimately cause the material to adsorb gas via physisorption^[64].

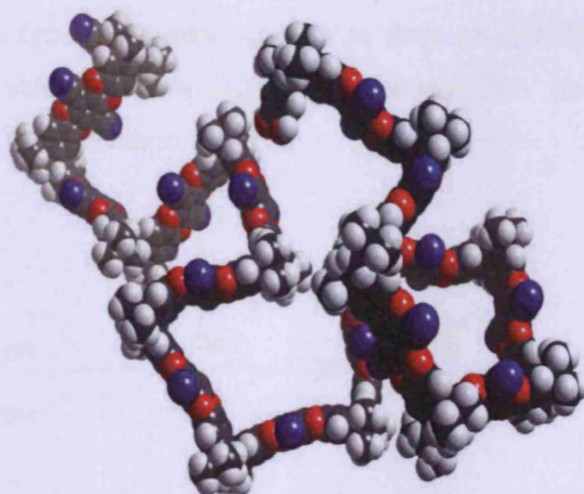


Fig 1.11 Diagram showing contortion of the polymer chain in a PIM resulting in free volume and Microporosity^[65]

After understanding the properties that give rise to microporous polymers, it is then possible to design a wide array of suitable monomers. These monomers fall into two categories as shown in Fig 1.12. A-type monomers that are typically rigid, contain a site of contortion, and also contain catechol aromatic rings. B-type monomers are typically rigid, planar and contain fluoride or chloride on the terminal aromatic rings.

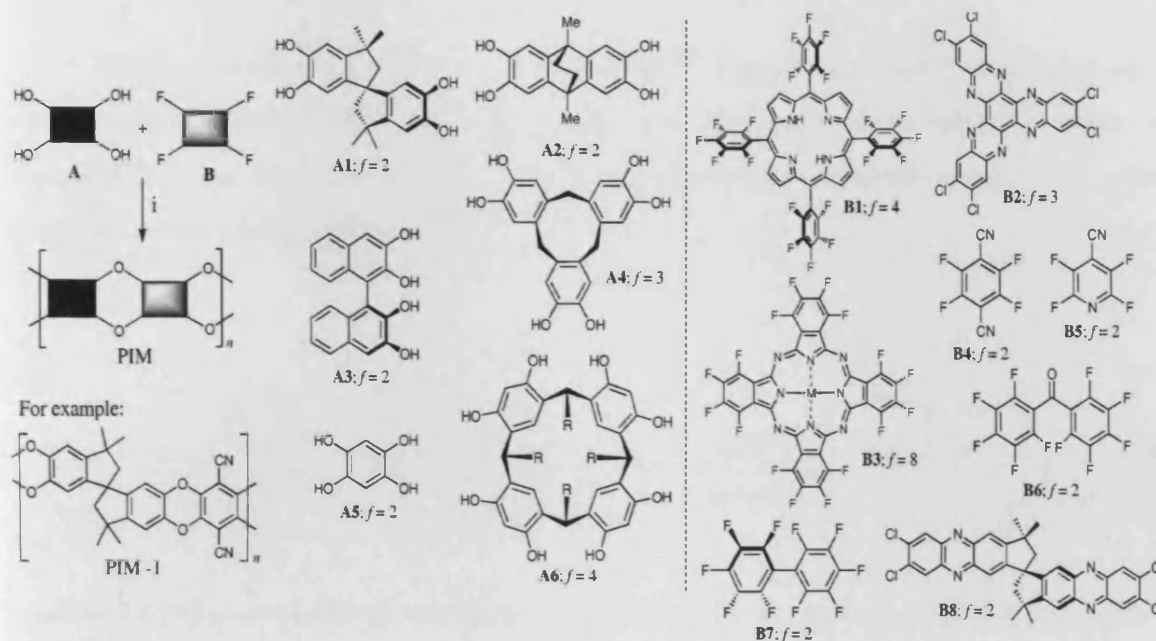
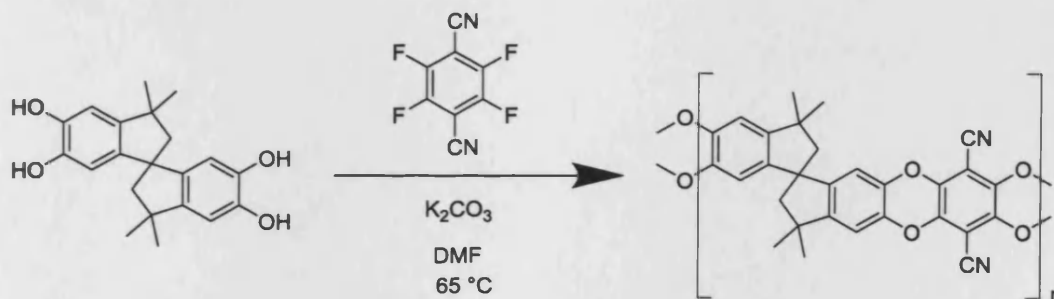


Fig 1.12 Examples of monomers known to produce PIMs^[13]

Polymerizing A and B type monomers together to form an ABAB type chain or network polymer that usually exhibits some degree of microporosity. An example of a typical polymerization (PIM-1) is in Scheme 1.7.

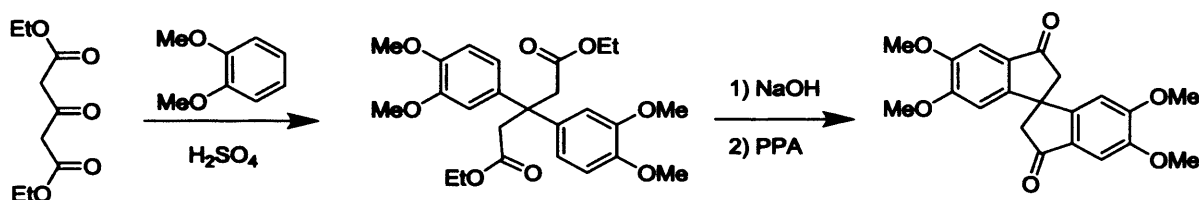


Scheme 1.7 Typical PIM polymerization

Considering that many B-type monomers are readily available, by producing new A-type monomers, a wide range of new microporous materials can be produced relatively rapidly.

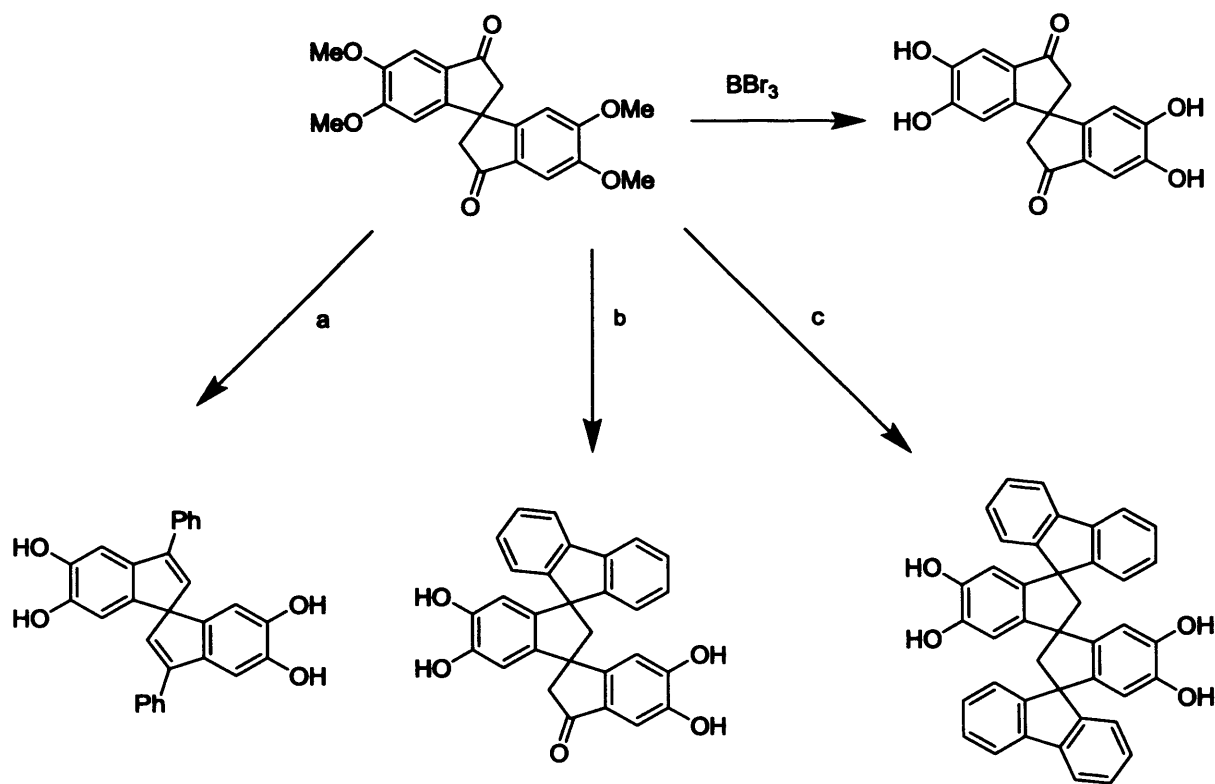
1.5.5 Fluorenone based PIMs

Building on the success of PIM-1, Carta *et al.*^[66] reported a series of monomers which were structural variations on the spirobisindane core. The bulk of the synthesis hinged on preparation of the key intermediate, 5,5',6,6'-tetramethoxytetraphenyl-1,1-spiro-bisindane-3,3-dione, as shown in Scheme 1.8.



Scheme 1.8 Preparation of the key intermediate 5,5',6,6'-tetramethoxytetraphenyl-1,1-spiro-bisindane-3,3-dione.

Having obtained the intermediate, it was possible to prepare 4 different monomers by utilising well established chemistry via reaction with the ketone functional group as shown in Scheme 1.9.



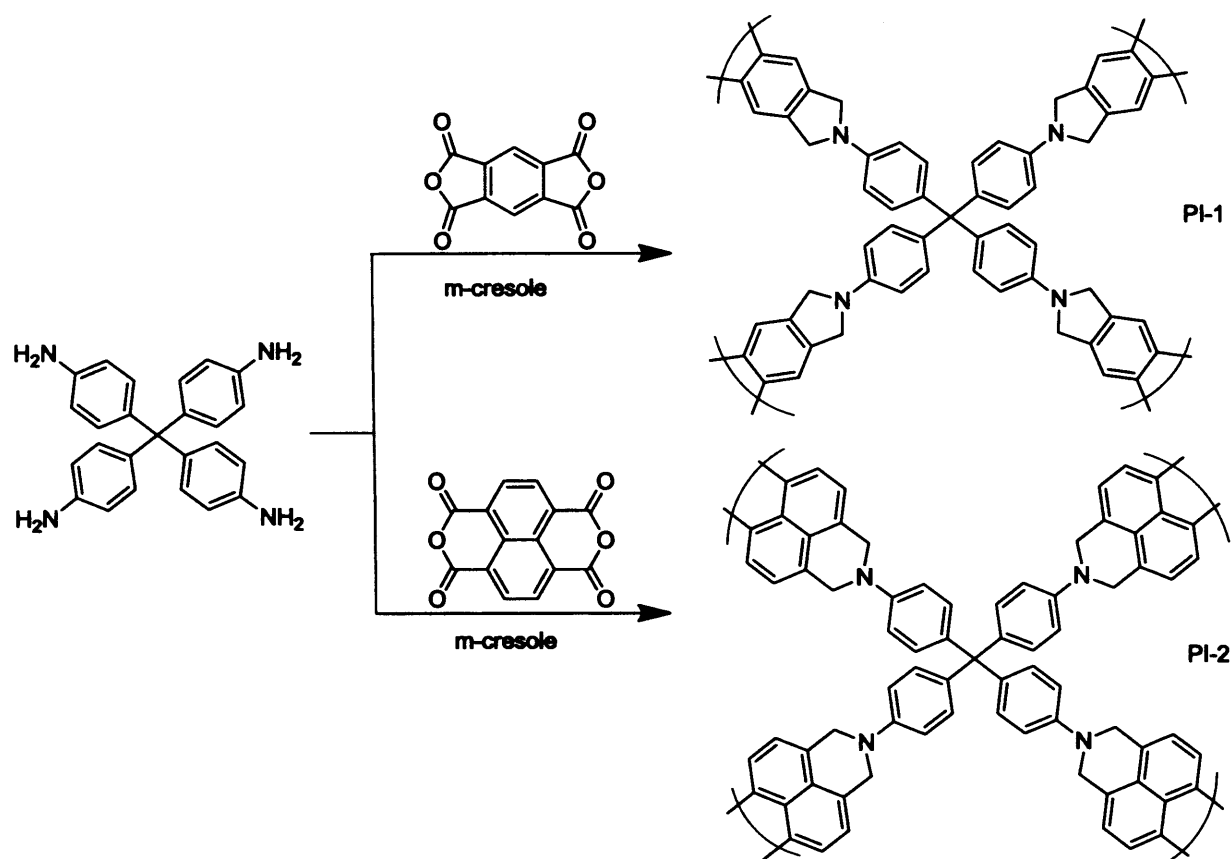
Scheme 1.9 Synthesis of 4 monomers from key spirobisindanedione intermediate. Reagents and conditions. (a) phenyl magnesiumbromide, acid catalysed ring closure, proto demethylation. (b) Single 2-biphenyl magnesium bromide addition, acid cyclization, demethylation. (c) double 2-biphenyl magnesium bromide addition, acid cyclization, protodemethylation.

The monomer derived using route (c) gave a soluble PIM with the highest apparent surface area ($895 \text{ m}^2\text{g}^{-1}$) when polymerized using the same method employed for PIM-1 and, unlike some of the other polymers obtained in this study, was soluble in low boiling point solvents such as THF and CHCl_3 . This study was the first indication that monomers featuring spiro-bisfluorine structures may yield interesting polymers.

1.5.6 Polyimide based microporous polymers

Several other research groups have attempted to produce novel PIM-like materials. Polyimide based polymers have recently been reported which have shown promising initial results^[67]. Using tetrakis(4-aminophenyl)methane, the amino groups were reacted with carboxylic anhydrides such as pyromellitic dianhydride and naphthalenetetracarboxylic anhydride in *m*-

cresol yielding two high surface area polyimides as shown in Scheme 1.10

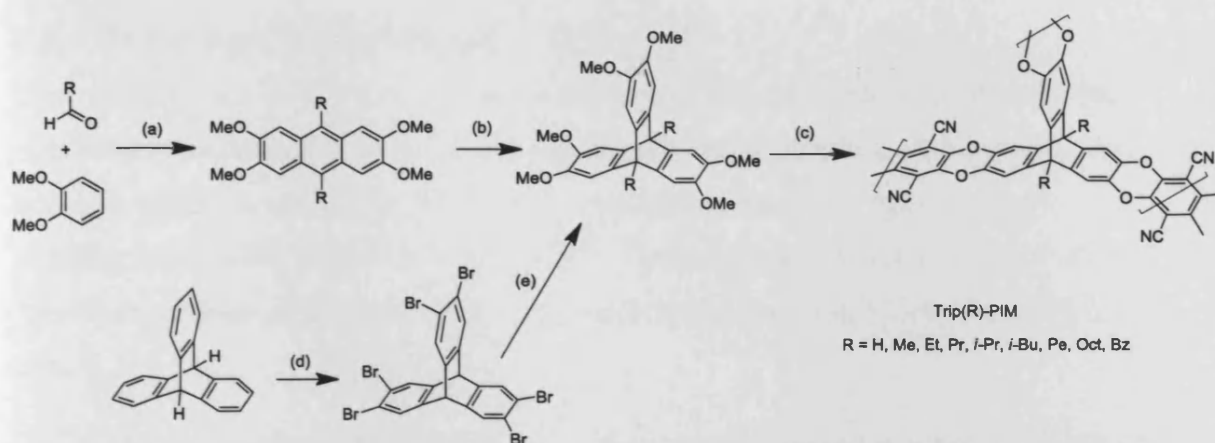


Scheme 1.10. Synthesis of PI-1 and PI-2^[67]

PI-1 demonstrated a high apparent BET surface area of $1407 \text{ m}^2\text{g}^{-1}$, and PI-2 a moderate surface area of $732 \text{ m}^2\text{g}^{-1}$, as measured by nitrogen adsorption. Both polymers showed an average pore size of 6-8 Ångstroms as calculated by the Horvath-Kawazoe method^[67], and thermal stability up to 600°C . PI-1 showed a 0.9% by weight hydrogen gas uptake at -77°C .

1.5.7 Triptycene-based PIMs

Recent research from the McKeown group has shown that triptycenes are excellent building units for producing microporous network polymers^[61]. A series of triptycenes were synthesised with differing R groups attached to the triptycene bridgehead position. The R groups ranged from H, alkyl chains (branched and straight chains), and benzyl substituents. The general synthesis shown in Scheme 1.11 follows a typical method for synthesising triptycenes (anthracene synthesis, followed by Diels-Alder cyclization with benzyne).



Scheme 1.11 Synthesis of triptycene based PIMs. Reactions and conditions: (a) H_2SO_4 , (b) Diels-Alder reaction with benzyne derived from 4,5-dimethoxy-2-aminobenzoic acid, (c) BBr_3 , CH_2Cl_2 , room temperature, 3; 2,3,5,6-tetrafluoroterephthalonitrile (TFPN), DMF, 80°C , 24 h, (d) Br_2 , Fe, CH_2Cl_2 , (e) MeONa, toluene.

The PIMs derived from the triptycene monomers showed a range of apparent surface areas measured by nitrogen adsorption and calculated using a BET isotherm model from $618\text{ m}^2\text{g}^{-1}$ for $\text{R} = \text{Oct}$, to $1760\text{ m}^2\text{g}^{-1}$ for $\text{R} = \text{Me}$. It was speculated that the polymer formed two-dimensional sheets with only loose linking between them, as indicated in Fig 1.12.

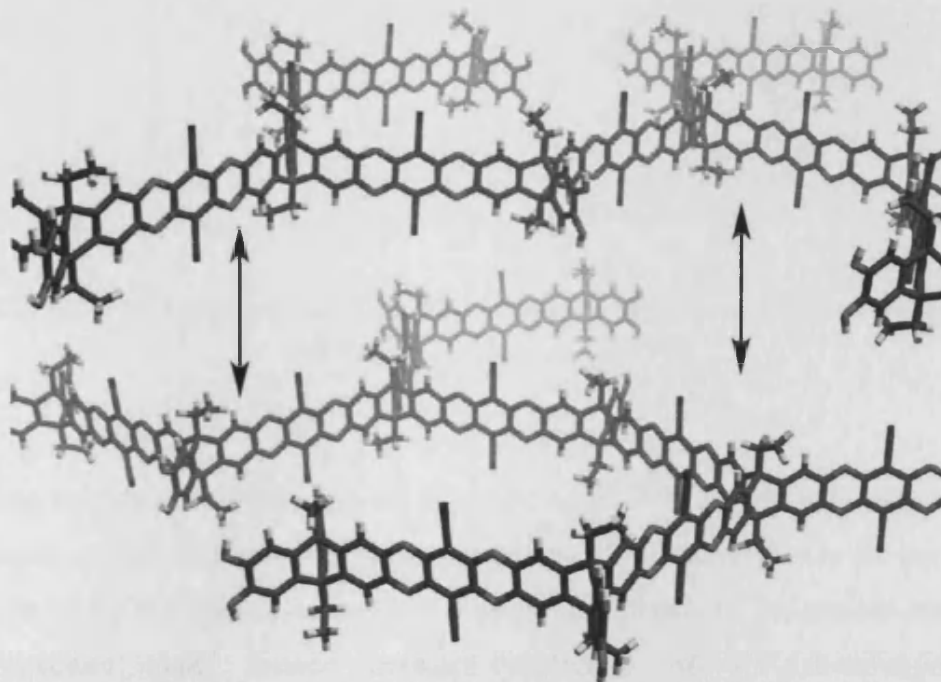


Fig 1.12 Idealised representation of the packing of individual polymer sheets^[61]

1.6 Inclusion Compounds

There is much interest in inclusion compounds (sometimes call clathrates) in which rigid molecules incorporate solvent molecules within their crystal structure. For example, urea inclusion compounds have been extensively studied by a number of research groups including those of Brown and Hollingworth^[68]. The study focused on the inclusion of long chain hydrocarbons inside the hexagonal channels formed in a polymorph of crystallised urea.

The crystallographic study of 5,5',6,6'-tetrahydroxy-3,3',3',3'-tetramethyl-1,1'-spirobisindane (A1) (the catechol from which PIM-1 is derived^[62]), revealed 5,5',6,6'-tetrahydroxy-3,3',3',3'-tetramethyl-1,1'-spirobisindane (A1) to form inclusion compounds within which there is a hydrogen-bonded network of catechols as shown in Fig 1.13^[69].

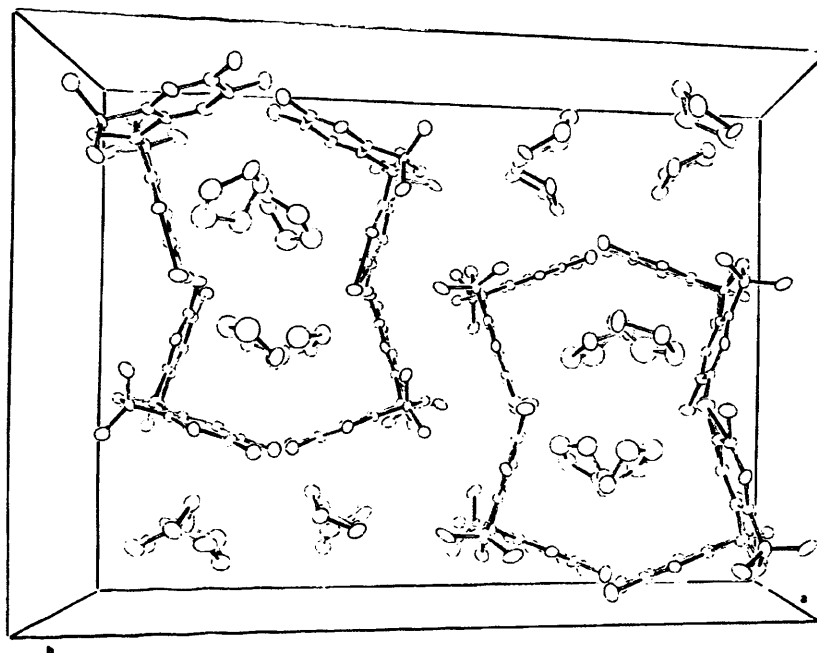


Fig 1.13 Unit cell of 5,5',6,6'-tetrahydroxy-3,3',3',3'-tetramethyl-1,1'-spirobisindane (A1) inclusion compounds with THF as the included solvent^[69].

In an extensive body of research reported by Wuest *et al.*^{[70][71]}, crystals have been engineered to form pores capable of containing a large percentage of solvent relative to the percentage of space taken up by the organic molecule. Of particular interest to the subject matter is the crystal structure motif formed between molecules of 3,3',6,6'-tetrahydroxy-9,9'-spirobifluorene, and between molecules of 2,2',7,7'-tetrasubstituted tetrakis(diaminotriazine).

These molecules demonstrated crystals within which solvent occupied 40% and 60% of the total volume, respectively. These structures are shown in Fig 1.14.

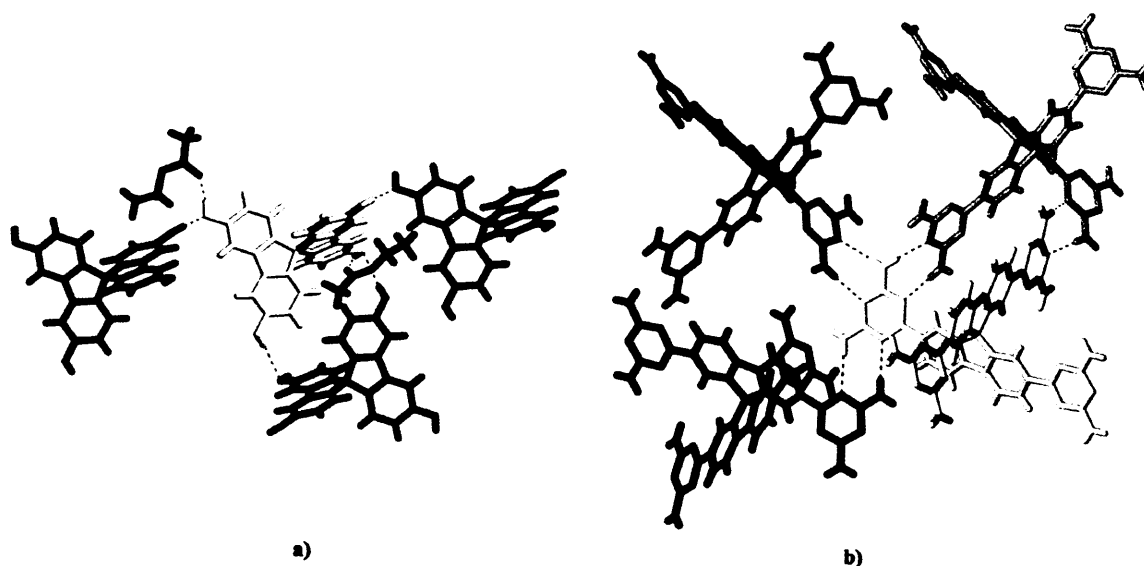


Fig 1.14 Crystal packing motif of a) 3,3',6,6'-tetrahydroxy-9,9'-spirobifluorene hydrogen bound to CH_3COCH_3
b) 2,2',7,7'-tetrasubstituted tetrakis(diaminotriazine) (solvent omitted for clarity)^[71]

1.7 Aims of the project

Following the previous work within the McKeown research group on PIM-1 and the polymers synthesised by Carta^[66] it was speculated that novel polymers based on the spirobisfluorene units would be both microporous and soluble in low boiling point organic solvents. If such polymers could be produced it is possible that membranes could be cast from them, which could find application within gas separation technology.

The compound 2,2',3,3'-tetrahydroxy-9,9'-spirobisfluorene (**39**) was identified as a target monomer early on in the planning of the research project based on its structural similarity to 5,5',6,6'-tetrahydroxy-3,3,3',3'-tetramethyl-2,2',3,3'-tetrahydro-1,1'-spirobisindane (**A1**), (shown in Fig 1.15) the monomer from which PIM-1 is derived. It was hoped that the extended rigid structure of the spirobisfluorene unit would enhance intrinsic microporosity.

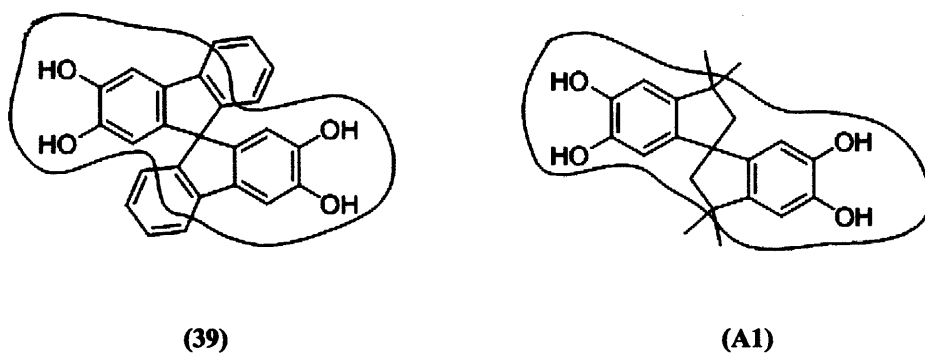
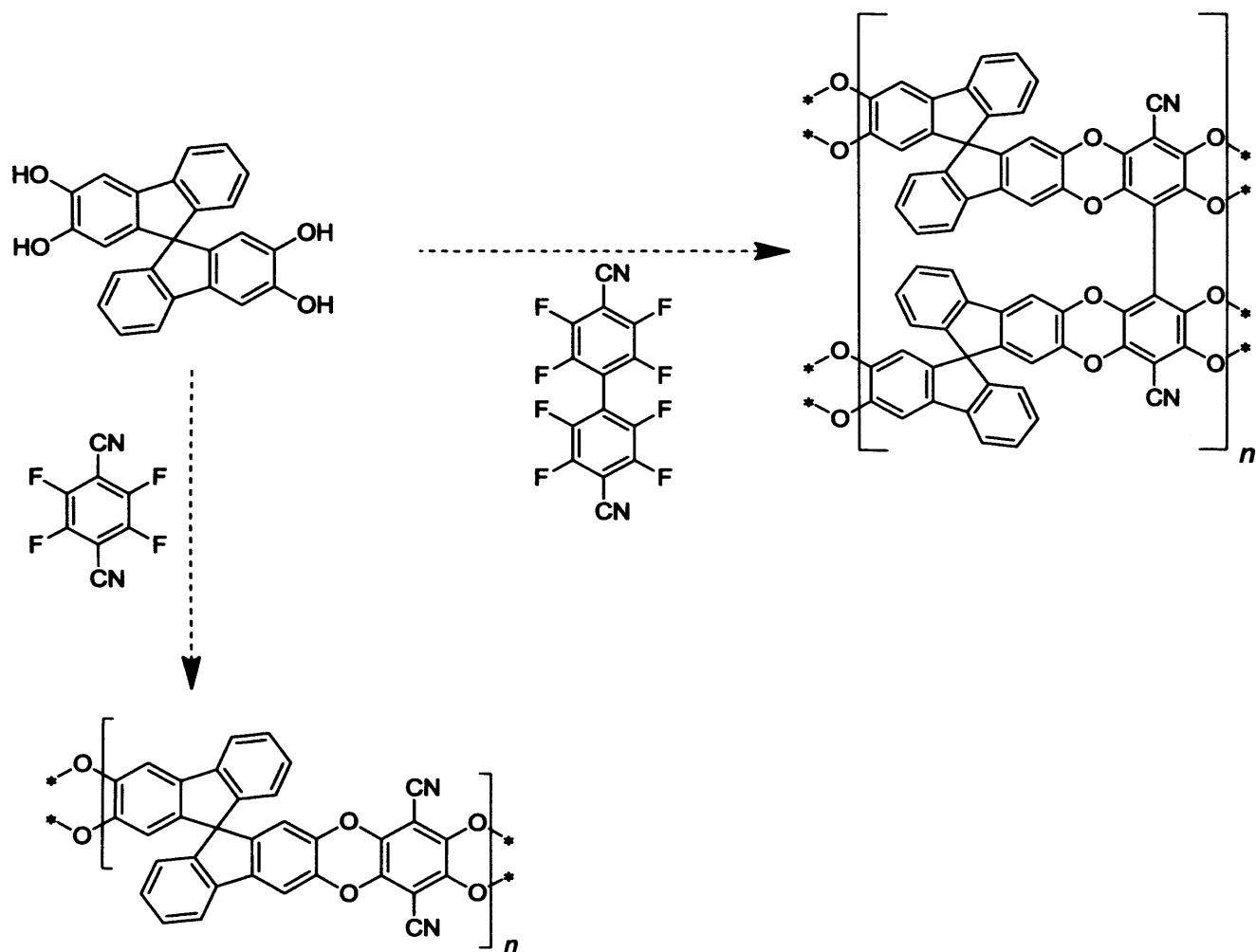


Figure 1.15 Circled area shows the molecular structure shared between the target 2,2',3,3'-tetrahydroxy-9,9'-spirobisfluorene (39) and 4,4',6,6'-tetrahydroxy-3,3,3',3'-tetramethyl-2,2',3,3'-tetrahydro-1,1'-spirobisindane (A1).



Scheme 1.14 Example of producing two polymers from one monomer by altering the fluorine containing monomer.

CHAPTER

2

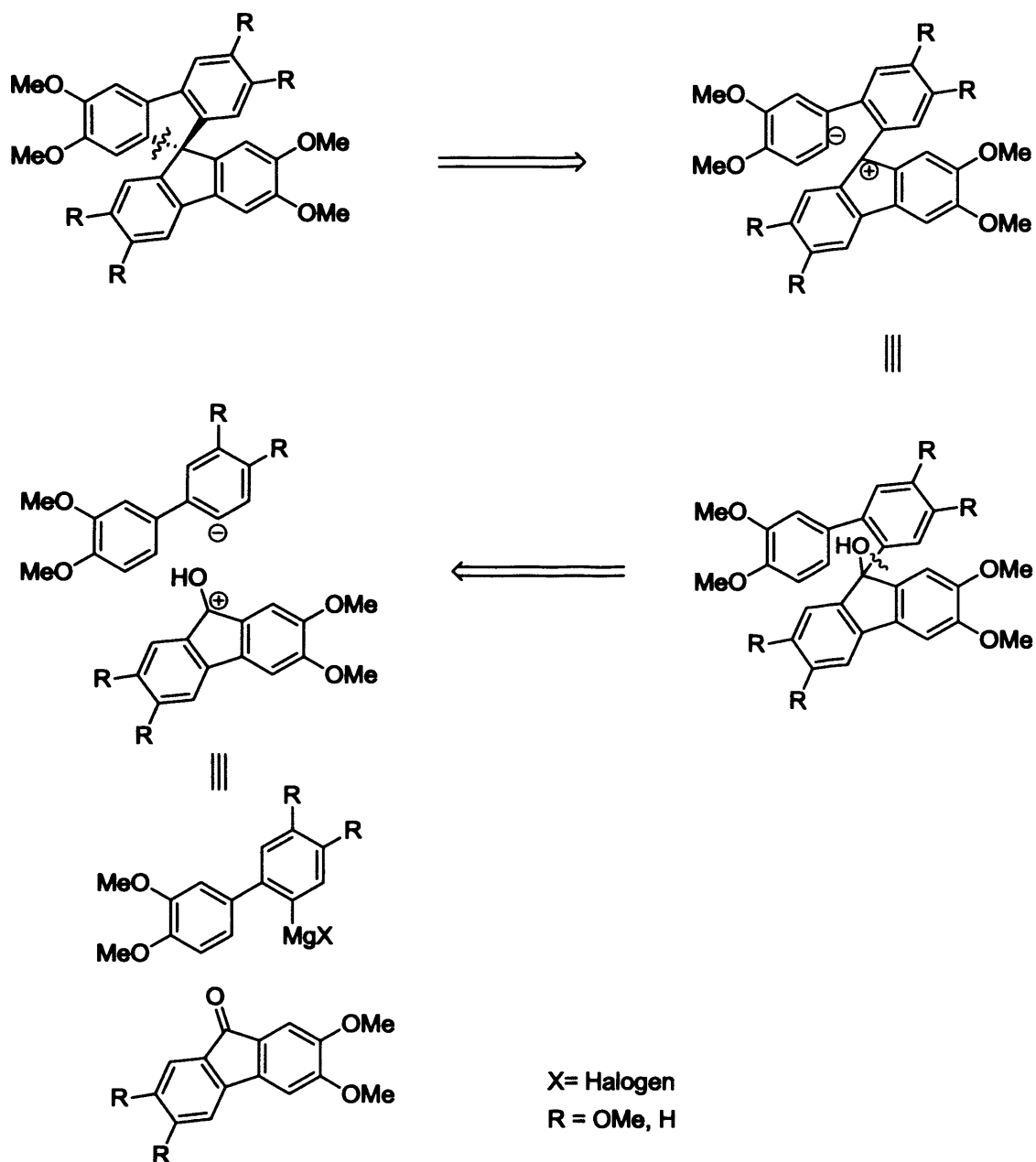
2.1)	Retrosynthesis of spirobisfluorene monomers.....	28
2.2)	Synthesis of halide-containing intermediates.....	30
2.3)	Synthesis of 2,3-dimethoxy-9 <i>H</i> -fluoren-9-one	34
2.4)	Synthesis of 2,3,6,7-tetramethoxy-9 <i>H</i> -fluoren-9-one.....	39
2.5)	Synthesis of miscellaneous cyclic ketones.....	41
2.6)	Precursor synthesis.....	44
2.7)	Cyclization of monomer precursors.....	51
2.8)	Deprotection of monomers via demethylation.....	53

Synthesis of monomers

2.1 Retrosynthesis of spirobisfluorene monomers

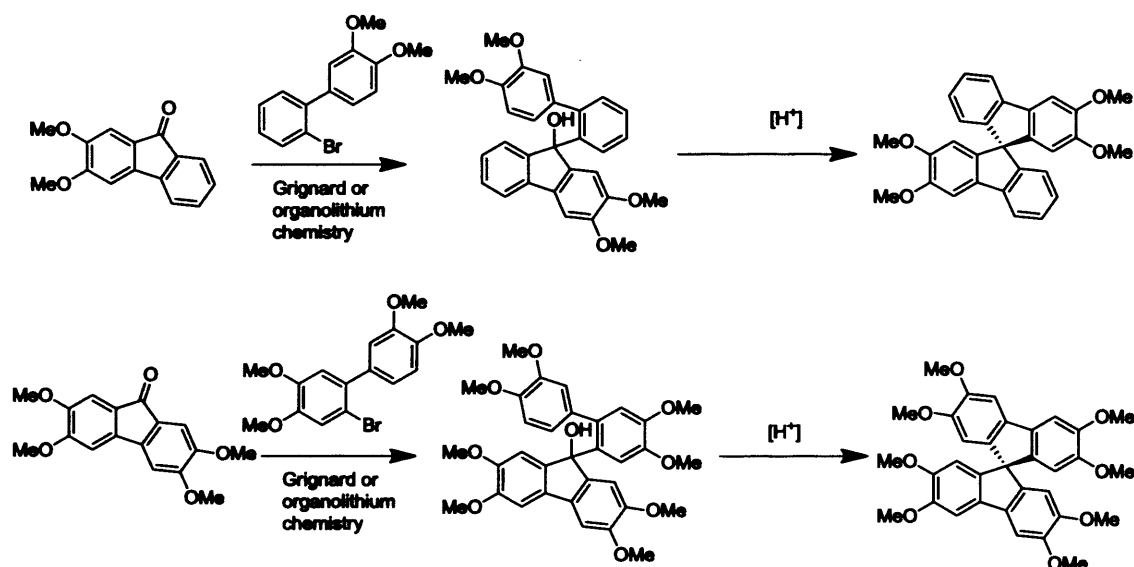
2.1.1 Design of route to target compounds

The first step in synthesizing the target monomers was to perform a retrosynthetic analysis using the disconnection approach as shown in Scheme 2.1



Scheme 2.1 Disconnection approach applied to synthesis of the projects target molecules

Based upon this analysis, the initial route planned to prepare the target monomers discussed in the aims of the project and shown in Scheme 2.2, relied on the synthesis of the aryl halides 2-bromo-3',4,4',5-tetramethoxybiphenyl (**9**) and 2-bromo-3',4'-dimethoxy-1,1'-biphenyl (**TM1**) and then to react these halides as Grignard or organolithium reagents with suitably substituted fluorenes. Only 2-bromo-3',4'-dimethoxy-1,1'-biphenyl (**TM1**) was considered for synthesis at this point as the methoxy group locations on the tertiary alcohol intermediate were speculated to aid the planned acid catalysed cyclization of this precursor to form the spiro-centre of the methyl ether protected monomer. To this end, Suzuki coupling was seen as a viable route to produce both 2-bromo-3',4,4',5-tetramethoxybiphenyl (**9**) and 2-bromo-3',4'-dimethoxy-1,1'-biphenyl (**TM1**).

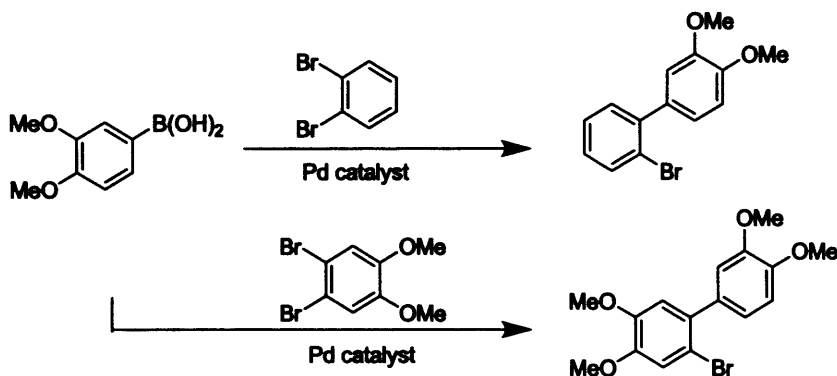


Scheme 2.2 Proposed route for synthesis of initial target methyl-protected monomers.

2.2 Synthesis of halide-containing intermediates.

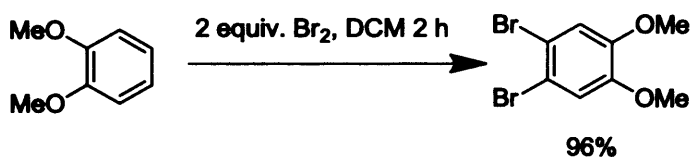
2.2.1 Attempted Suzuki couplings for 1 step halo biphenyl synthesis.

It was speculated that the two desired aryl halides could be synthesised directly via Suzuki couplings between 3,4-dimethoxybenzeneboronic (SM5) acid and 1,2-bromobenzene, or 4,5-dibromoveratrole (SM2) respectively, as shown in Scheme 2.3.



Scheme 2.3 Proposed 1 step Suzuki coupling to target halogenated biphenyls.

The 3,4-dimethoxybenzeneboronic acid (SM5) and 1,2-bromobenzene were commercially available and 4,5-dibromoveratrole was easily synthesised from veratrol (SM4) following the method reported by Song *et al.*^[72] as shown in Scheme 2.4



Scheme 2.4 Double bromination of veratrol (SM4) reported by Song *et al.*^[72]

A systematic study of reaction conditions was carried out in order to optimize the yield of aryl halides from the Suzuki couplings, including the variation of solvents, temperature, palladium catalysts and bases as reported in Table 2.1. Low yields were consistently obtained from these reactions and many side products were also present necessitating purification by flash column chromatography. Analysis of each fraction showed that in all cases aryl halide starting material was recovered as well as the dehalogenated

Chapter - 2

products bromobenzene and 4-bromoveratrole (**SM2**), respectively. 3,4-dimethoxybiphenyl (**8**) and 3,3',4,4'-tetramethoxybiphenyl (**6**) were also recovered in respectable yields (~40%).

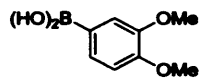
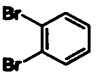
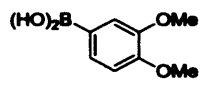
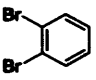
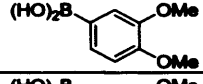
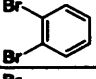
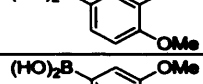
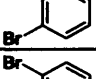
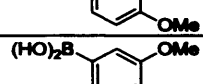
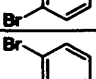
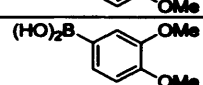
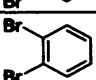
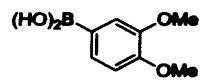
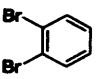
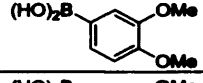
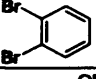
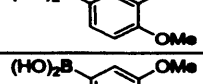
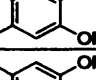
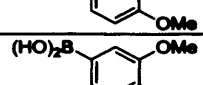
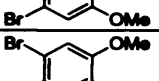
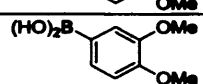
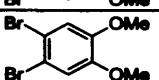
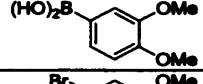
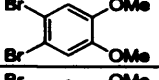
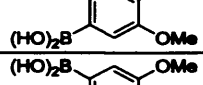
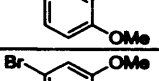
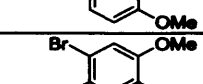
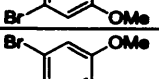
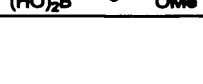
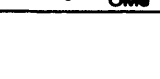
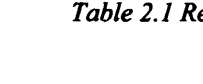
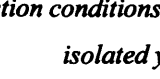


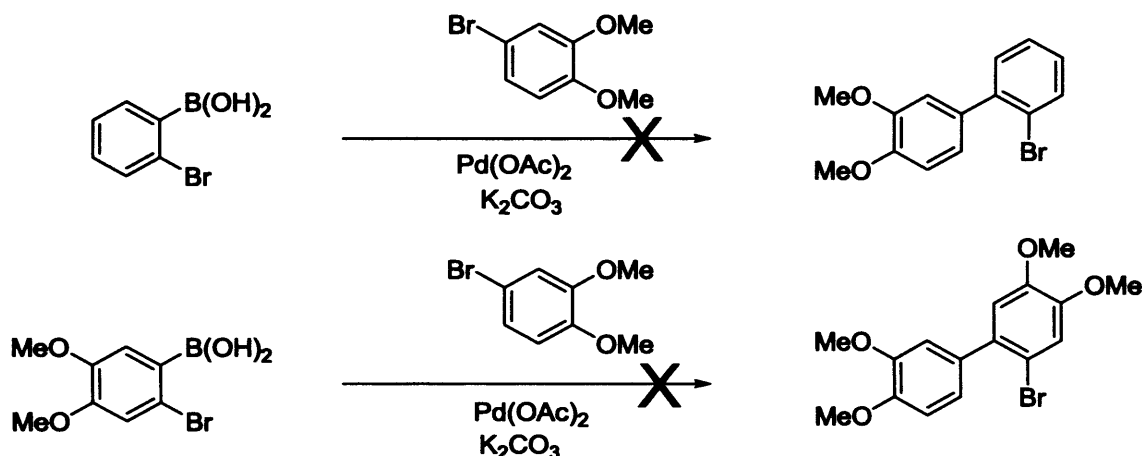
Boronic Acid	Aryl halide	Solvent	Base (5 equiv.)	Temperature	Catalyst	Yield (%) ^a
		DMF	K ₂ CO ₃	65 °C	Pd(PPh ₃) ₄	11
		DMF/H ₂ O (2:1)	K ₂ CO ₃	65 °C	Pd(PPh ₃) ₄	13
		DMF/H ₂ O (2:1)	K ₂ CO ₃	75 °C	Pd(PPh ₃) ₄	9
		DMF/H ₂ O (2:1)	K ₂ CO ₃	55 °C	Pd(PPh ₃) ₄	12
		DMF/H ₂ O (2:1)	K ₂ CO ₃	65 °C	Pd(OAc) ₂	15
		Toluene	K ₂ CO ₃	65 °C	Pd(OAc) ₂	4
		MeOH/H ₂ O (1:1)	K ₂ CO ₃	65 °C	Pd(OAc) ₂	0
		DME	K ₂ CO ₃	65 °C	Pd(OAc) ₂	11
		DMF/H ₂ O (2:1)	Na ₂ CO ₃	65 °C	Pd(OAc) ₂	15
		DMF	K ₂ CO ₃	65 °C	Pd(OAc) ₂	9
		DMF/H ₂ O (2:1)	K ₂ CO ₃	65 °C	Pd(OAc) ₂	11
		DMF/H ₂ O (3:1)	K ₂ CO ₃	65 °C	Pd(OAc) ₂	10
		MeOH/H ₂ O	K ₂ CO ₃	65 °C	Pd(OAc) ₂	0
		DME	K ₂ CO ₃	65 °C	Pd(OAc) ₂	8
		Toluene	K ₂ CO ₃	65 °C	Pd(OAc) ₂	5
		DMF/H ₂ O (2:1)	K ₂ CO ₃	75 °C	Pd(OAc) ₂	10
		DMF/H ₂ O (2:1)	Na ₂ CO ₃	65 °C	Pd(OAc) ₂	11

Table 2.1 Reaction conditions and yields of initial Suzuki couplings [reaction time 24 h]. ^(a) based on isolated yield from flash column chromatography

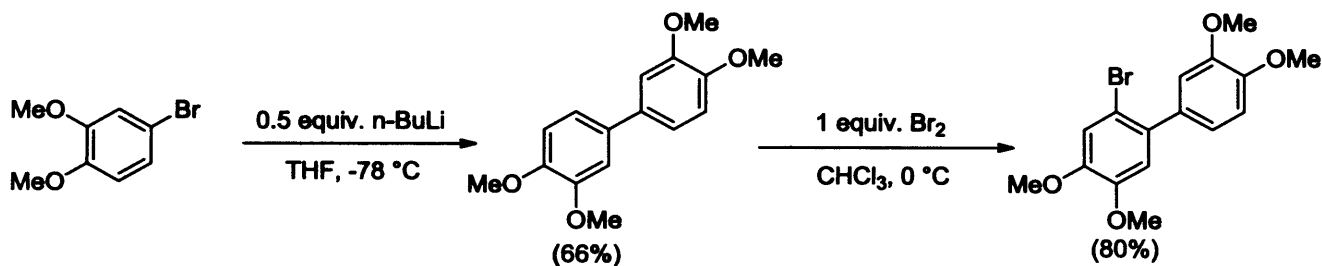
In a final effort to directly synthesize 2-bromo-3',4,4',5-tetramethoxybiphenyl (**9**) and 2-bromo-3',4'-dimethoxy-1,1'-biphenyl (**TM1**), Suzuki couplings between 2-bromoboronic acid and 4-bromoveratrol (**SM2**), and between 2-bromo-4,5-dimethoxyphenylboronic acid and 4-bromoveratrol (**SM2**) were tried but only small amounts of product (< 5%) was obtained from either reaction.



Scheme 2.5 Unviable route to target brominated biphenyls (yields ~ 5% isolated by flash chromatography).

2.2.2 Alternative synthesis of 2-bromo-3',4,4',5-tetramethoxybiphenyl (**9**).

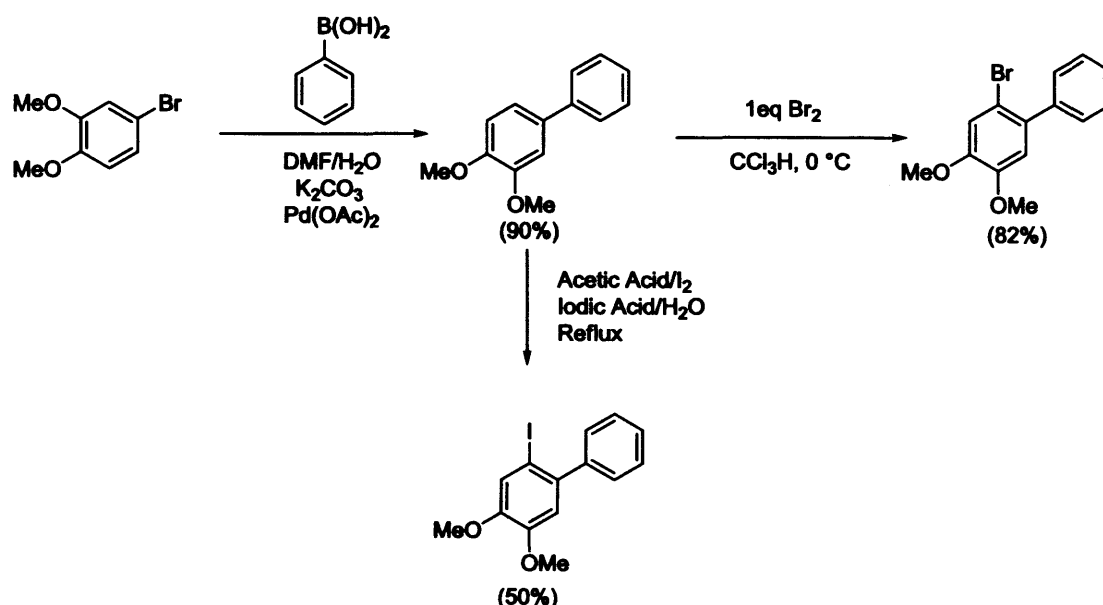
After further inspection of the relevant literature^{[73][74]} several two-step synthetic routes to the brominated biphenyls were identified. Scheme 2.6 shows the route to 2-bromo-3',4,4',5-tetramethoxybiphenyl (**9**), developed by Schulte *et al.*^[75], which ultimately proved successful.



Scheme 2.6 Synthetic route to 2-bromo-3',4,4',5-tetramethoxybiphenyl (**9**) reported by Schulte *et al.*^[75].

2.2.3 Synthesis of 2-bromo-4,5-dimethoxybiphenyl (10) and 2-iodo-4,5-dimethoxybiphenyl (11).

In an effort to make 3,4-dimethoxybiphenyl (8), a number of potential Suzuki couplings were identified^{[76][77]}, however, the preferred conditions were those used by Kang *et al.*^[78] due to their high yield obtained on a large scale, and ease of product purification. A standard bromination was then used to synthesise the target molecule 2-bromo-4,5-dimethoxybiphenyl (10). At this point it was deemed worthwhile to simultaneously synthesis 2-iodo-4,5-dimethoxybiphenyl (11) which was speculated to possibly be better suited to the Grignard/organolithium chemistry that we wished to perform. The synthesis is also included in Scheme 2.7 following the method reported by Blatchley *et al.*^[79]

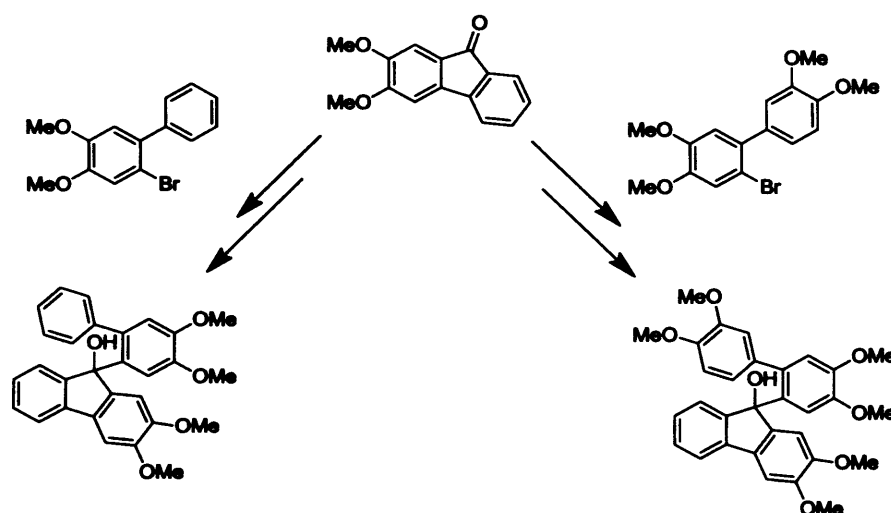


Scheme 2.7 Synthetic route to 2-bromo-4,5'-dimethoxybiphenyl (10) and 2-iodo-4,5-dimethoxybiphenyl (11).

2.3 Synthesis of 2,3-dimethoxy-9H-fluoren-9-one (14).

2.3.1 Analysis of the synthesis of 2,3-dimethoxy-9H-fluoren-9-one (14).

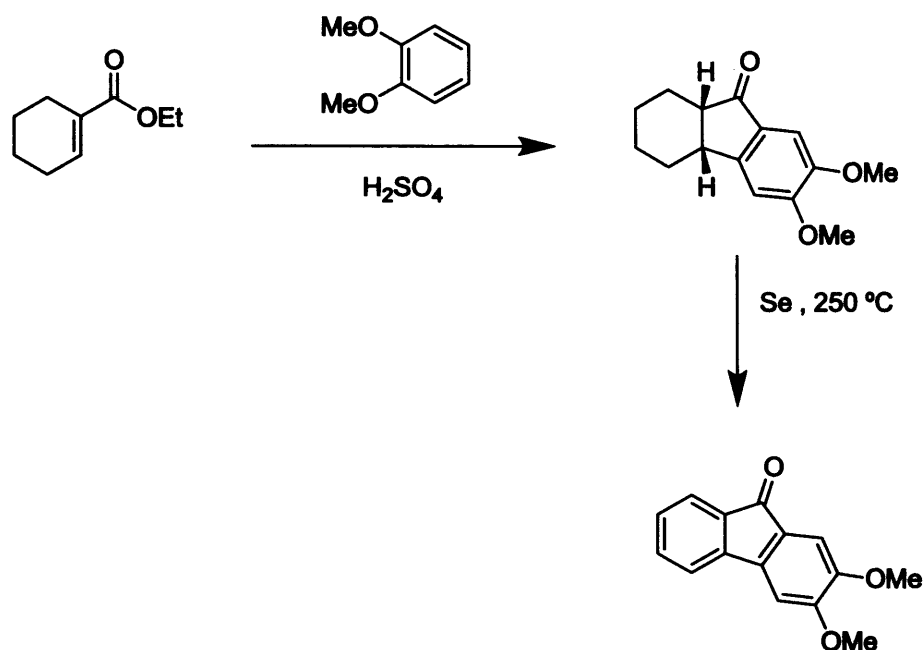
Having produced the relevant halo biaryls in a manner that was easily scaled-up, the next step towards the target synthesis of 2,2',3,3'-tetrahydroxy-9,9'-spirobisfluorene (39) was to find a reliable method of preparing 2,3-dimethoxy-9H-fluoren-9-one (14) on a multi-gram scale. This compound was also of importance as another monomer, 2,2',3,3',6,7-hexahydroxy-9,9'-spirobisfluorene (40) could be synthesised from it as shown in Scheme 2.8



Scheme 2.8 Use of 2,3-dimethoxy-9H-fluoren-9-one (14) to synthesize two monomer precursors.

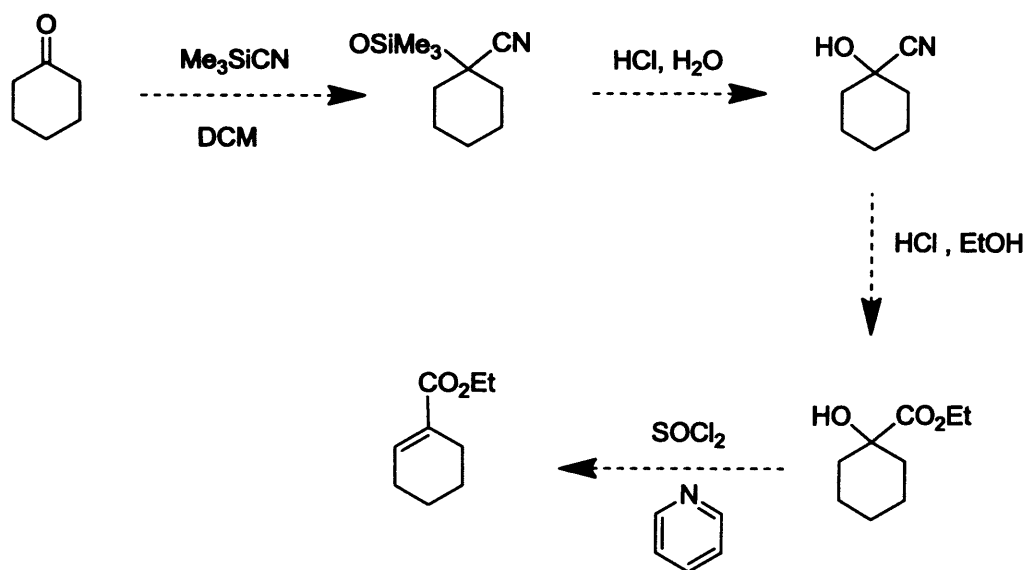
2.3.1 Established routes for the synthesis of 2,3-dimethoxy-9H-fluoren-9-one (14).

Unfortunately, 2,3-dimethoxy-9H-fluoren-9-one (14) is not commercially available so known methods of its synthesis were investigated. Two methods were initially considered. At first the method reported by Ramana and Potnis^[80] as shown in Scheme 2.9 was favoured on the condition that ethyl 1-cyclohexenecarboxylate could be obtained easily.



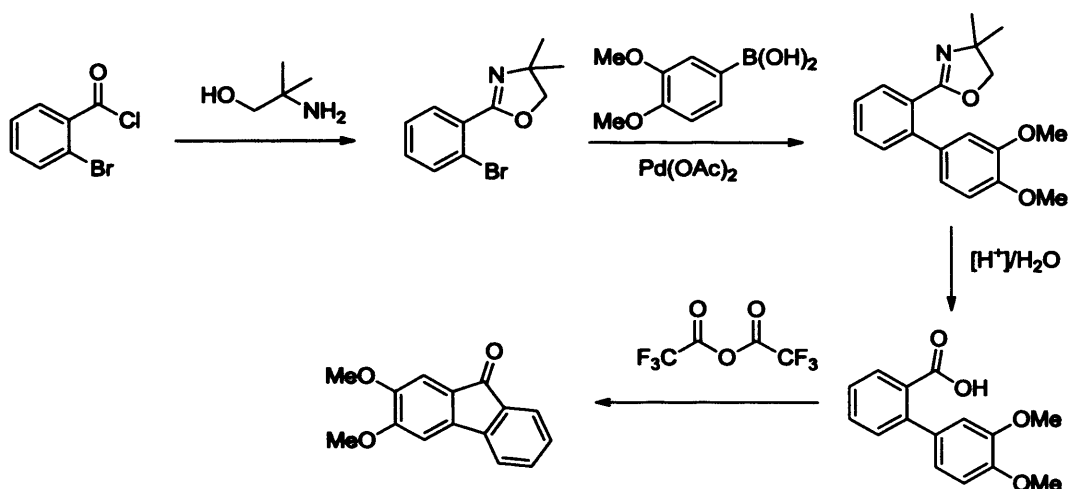
Scheme 2.9 Synthesis of 2,3-dimethoxy-9H-fluoren-9-one (14) reported by Ramana and Potnis^[80]

However ethyl 1-cyclohexenecarboxylate was not trivial to make, requiring either a low yield Birch reduction of ethyl benzoate reported by P. Rabideau *et al.*^[81], or a long-winded trimethylsilyl cyanide addition to cyclohexanone^[82] followed by carboxylation of the nitrile and elimination of the alcohol as shown in Scheme 2.10. The route published by P. Rabideau was strongly considered, but ultimately avoided due to the high toxicity of trimethylsilyl cyanide.



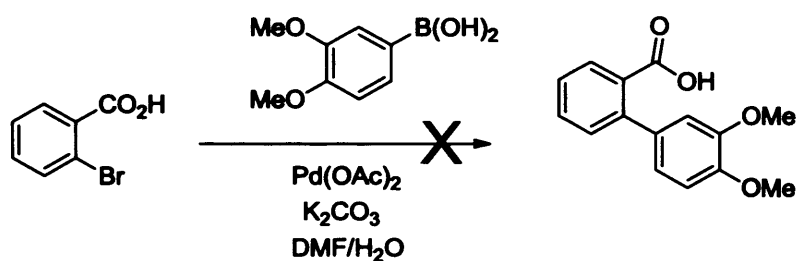
Scheme 2.10 Proposed synthesis of ethyl 1-cyclohexenecarboxylate

The second method shown in Scheme 2.11, reported by Ciske, Fred , Jones, and Winton^[83], was also rather long-winded due to the need for carboxylic acid protection.



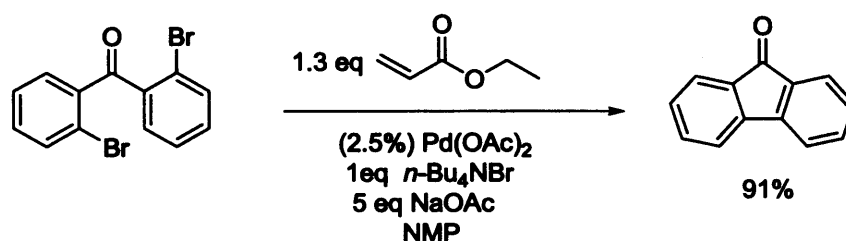
Scheme 2.11 Synthesis of 2,3-dimethoxy-9H-fluoren-9-one (14) reported by Ciske, Fred , Jones, and Winton^[83].

It was noted that due to the need for oxazole protection of the carboxylic acid in the above synthesis, it was unlikely that a direct Suzuki coupling between 3,4-dimethoxyphenylboronic acid (SM5) and 2-bromobenzoic acid would work, but this reaction was still attempted. As expected, the reaction was unsuccessful as shown in Scheme 2.12.



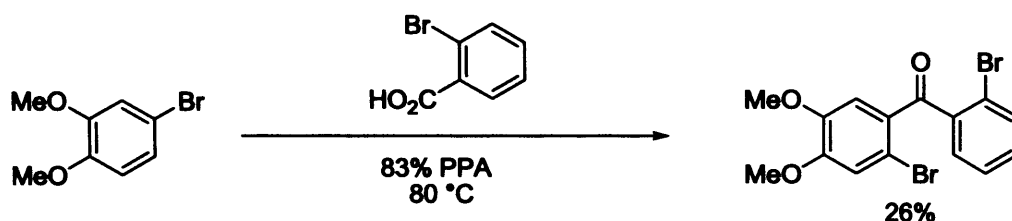
Scheme 2.12 Unsuccessful Suzuki coupling to produce 3',4'-dimethoxybiphenyl-2-carboxylic acid.

A further literature search highlighted a study by Prashad *et al.*^[84] indicated that unintended side reaction of 2,2'-dibromobenzophenone under Heck coupling conditions formed 9H-fluoren-9-one (SM1) in high yield as shown in Scheme 2.13.



Scheme 2.13 Intra-molecular coupling reported by Prashad *et al.*^[84]

It was hypothesised that this reaction could be employed to produce 2,3-dimethoxy-9H-fluoren-9-one (**14**) from 2,2'-dibromo-4,5-dimethoxybenzophenone. On a small scale 2,2'-dibromo-4,5-dimethoxybenzophenone was produced via acid-mediated Friedel-Crafts acylation of 4-bromo-1,2-dimethoxybenzene (SM2) with 2-bromobenzoic acid shown in scheme 2.14.

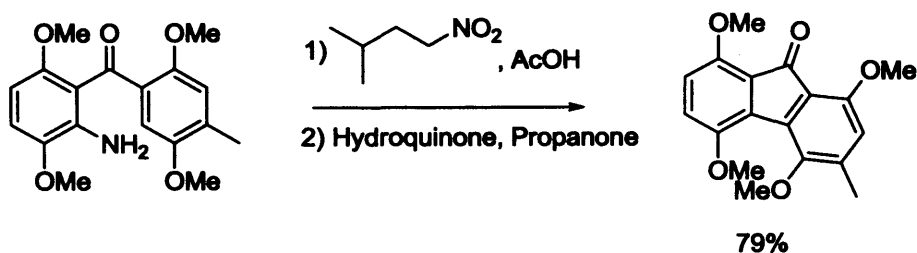


Scheme 2.14 Acid mediated Friedel Crafts acylation of 4-bromo-1,2-dimethoxybenzene (**2**) with 2-bromobenzoic acid.

Using Prashad's method it was possible to obtain a small sample of 2,3-dimethoxy-9H-fluoren-9-one (**14**) for characterization. However the attempt to scale-up the Friedel-Crafts acylation resulted solely in the recovery of starting materials. Unfortunately, despite attempting this reaction with a wide range of temperatures and concentrations of reagents in PPA none provided the benzophenone in a suitable amount.

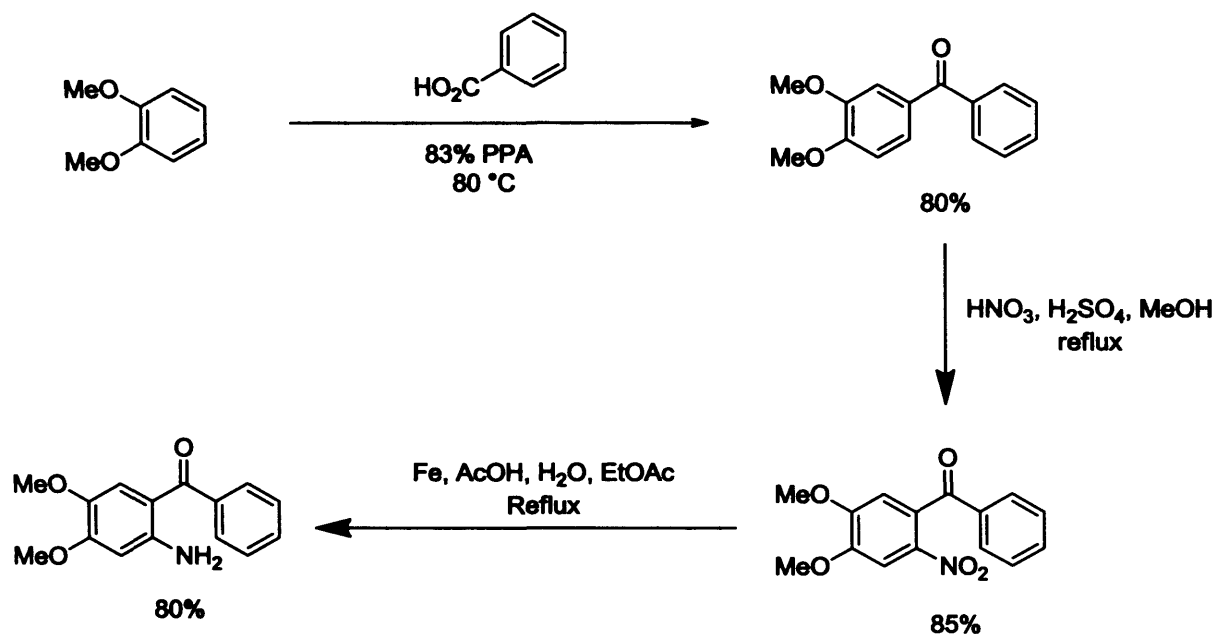
2.3.2 Intramolecular Pschörr coupling as a route to 2,3-dimethoxy-9H-fluoren-9-one (**14**)

Research produced by Saikawa *et al.*^[85] suggested that it may be possible to use an intramolecular Pschörr reaction as shown in Scheme 2.15 to produce 2,3-dimethoxy-9H-fluoren-9-one (**14**) from 2-amino-3,6,2',5'-tetramethoxy-4'-methylbenzophenone, a known compound reported by Butin *et al.*^[86]



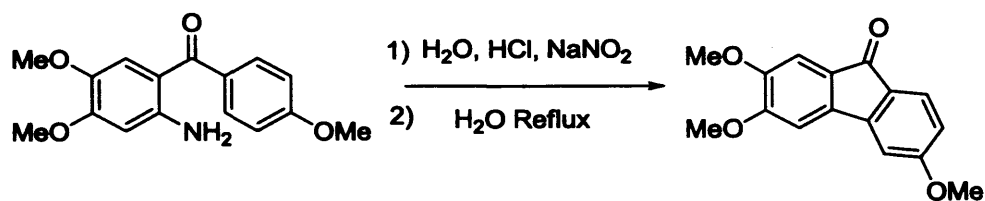
Scheme 2.15 Pschörr coupling employed by Saikawa *et al.*^[85]

The starting material for this synthesis, 3,4-dimethoxybenzophenone, was produced by Friedel-Crafts acylation of veratrol (**SM4**) by benzoic acid in PPA followed by nitration of 3,4-dimethoxybenzophenone, and reduction in acid over iron powder following the method reported by Butin *et al.*^[86] and shown in Scheme 2.16.



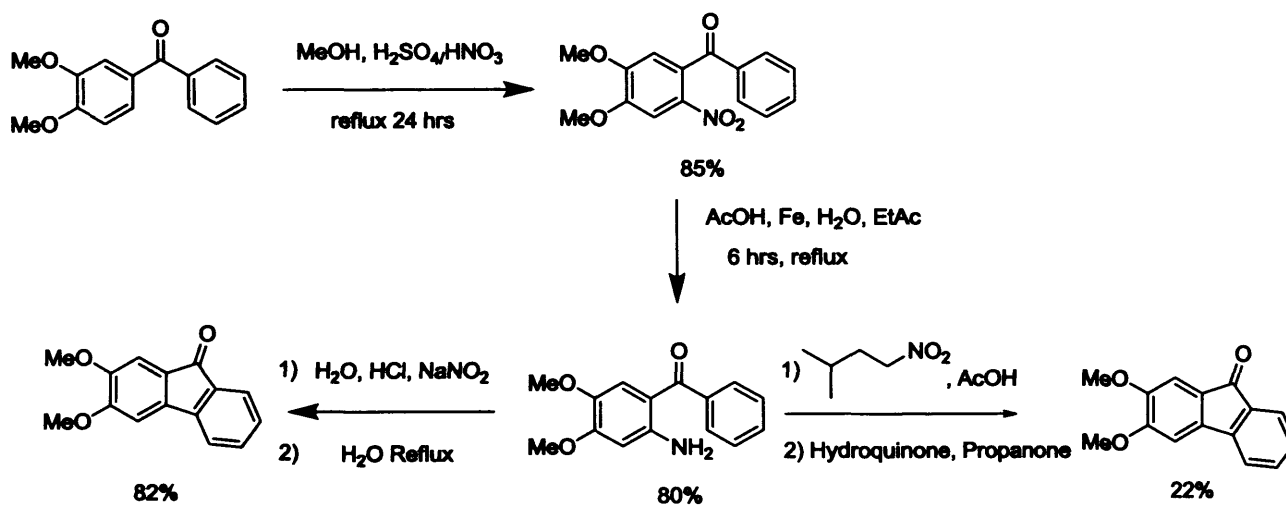
Scheme 2.16 Synthesis of 2-amino-3,4-dimethoxybenzophenone

Having obtained 2-amino-3,4-dimethoxybenzophenone, the Pschörr coupling method reported by Saikawa *et al.*^[85] was attempted and was found to result in a complex mixture from which a 22% yield of 2,3-dimethoxy-9H-fluoren-9-one (**14**) was obtained. It was anticipated that this yield could be improved and further inspection of literature revealed a similar Pschörr coupling reported by Korte *et al.*^[87] which claimed to give a 99% yield as shown in Scheme 2.17.



Scheme 2.17 Pschörr coupling reported by Korte et al.^[87]

By applying Korte's method to 2-amino-3,4-dimethoxybenzophenone, a yield of 82% of 2,3-dimethoxy-9H-fluoren-9-one (**14**) was obtained. A summary of the entire synthesis of 2,3-dimethoxy-9H-fluoren-9-one (**14**) is shown in Scheme 2.18.

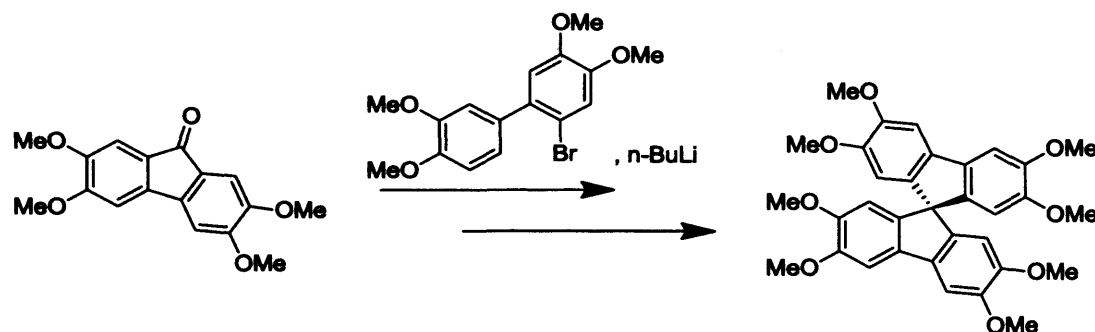


Scheme 2.18 Synthesis of 2,3-dimethoxy-9H-fluoren-9-one (**14**).

2.4 Synthesis of 2,3,6,7-tetramethoxy-9H-fluoren-9-one (**15**).

2.4.1 Justification for the synthesis of 2,3,6,7-tetramethoxy-9H-fluoren-9-one (**15**).

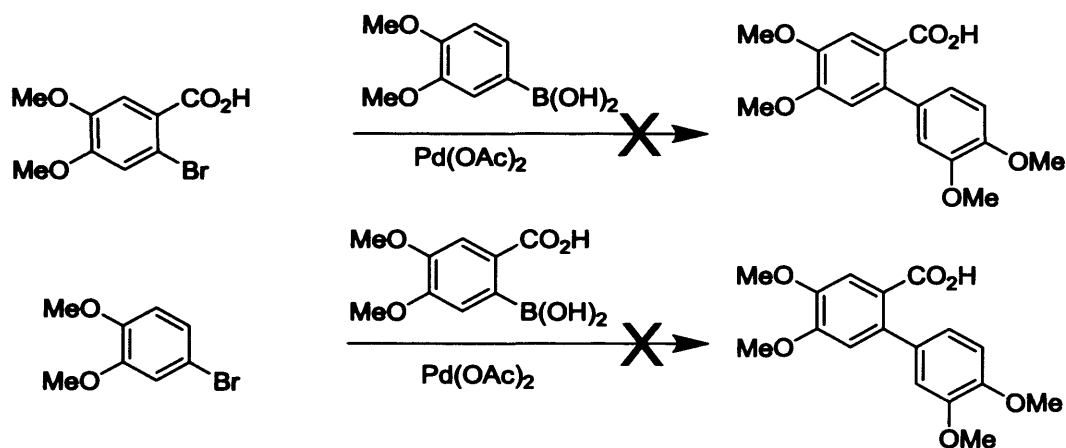
2,3,6,7-tetramethoxy-9H-fluoren-9-one (**15**) was identified as a promising target molecule due to the possibility of synthesising symmetrical monomers that would yield network polymers based around spiro centred molecular geometry as indicated in Scheme 2.19.



Scheme 2.19 Methyl-protected monomer, 2,2'3,3',6,6',7,7'-tetramethoxy-9,9'-spirobisfluorene (31), derived from 2,3,6,7-tetramethoxy-9H-fluoren-9-one (15).

2.4.2 Attempted Suzuki couplings.

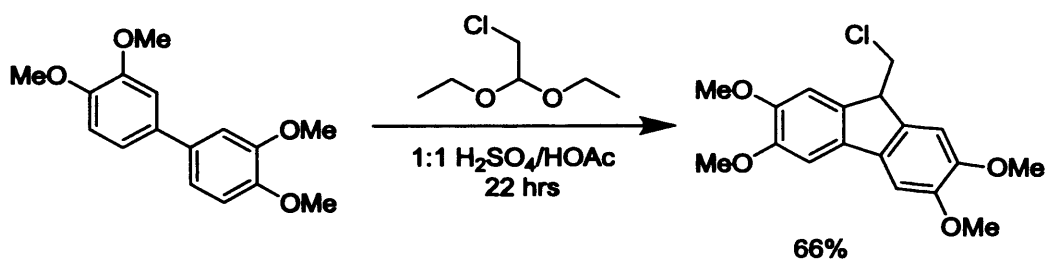
The first attempt at synthesising 2,3,6,7-tetramethoxy-9H-fluoren-9-one (15) was via a Suzuki coupling between 3,4-dimethoxyphenylboronic (5) acid and 2-bromo-4,5-dimethoxybenzoic acid followed by an intramolecular Friedel-Crafts coupling. The first step proved unsuccessful as was the analogous Suzuki coupling between 2-carboxyl-4,5-dimethoxy-boronic acid and 4-bromoveratrole (SM1) as shown in Scheme 2.20.



Scheme 2.20 Unsuccessful Suzuki couplings.

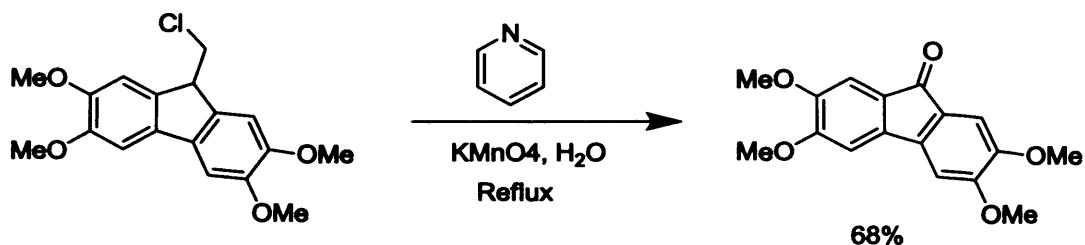
2.4.3 Synthesis of 2,3,6,7-tetramethoxy-9H-fluoren-9-one (15) via KMnO_4 oxidation of 2,3,6,7-tetramethoxy-9-methylene-9H-fluorene.

A facile synthesis of 9-(chloromethyl)-2,3,6,7-tetramethoxy-9-fluorene had been reported by Quelet *et al.*^[88] by reaction of 2-chloro-1,1-diethoxy-ethane and 3,3',4,4'-tetramethoxybiphenyl (**6**) as shown in Scheme 2.21.



Scheme 2.21 9-(chloromethyl)-2,3,6,7-tetramethoxy-9H-fluorene synthesis reported by Quelet *et al.*^[88]

A successful synthesis of 2,3,6,7-tetramethoxy-9H-fluoren-9-one (**15**) was devised using KMnO_4 to oxidise 9-(chloromethyl)-2,3,6,7-tetramethoxy-9H-fluorene with an isolated yield of 68%, as shown in Scheme 2.22.

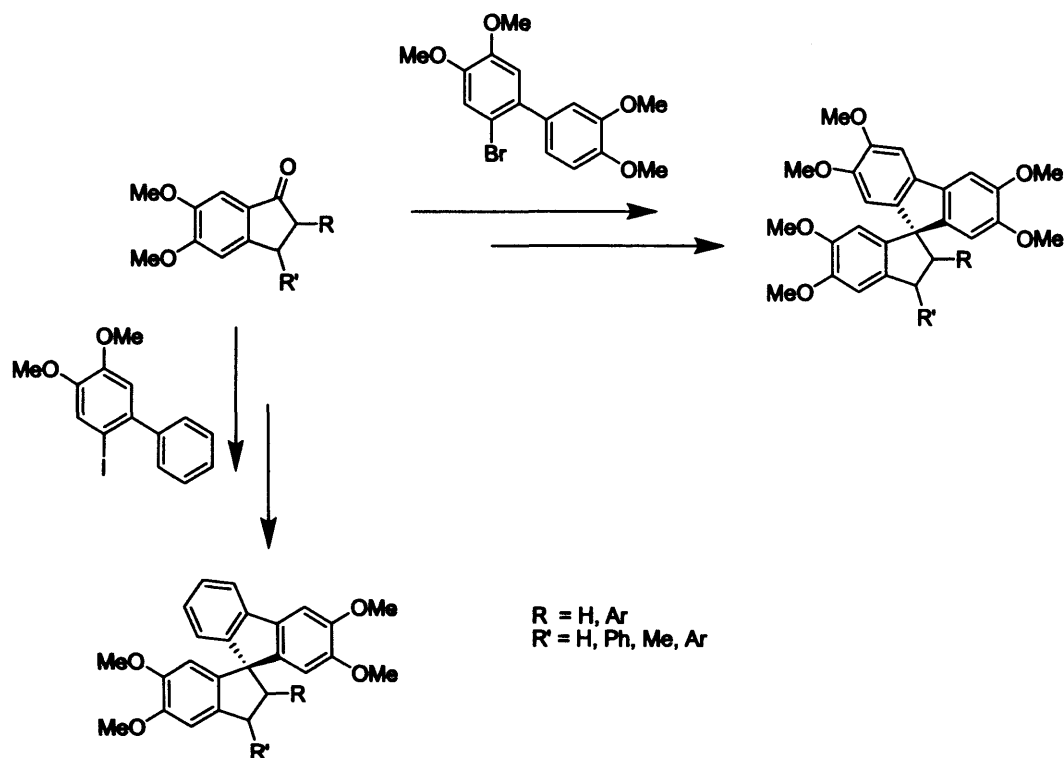


Scheme 2.22 Synthesis of 2,3,6,7-tetramethoxy-9H-fluoren-9-one (**15**)

2.5 Synthesis of miscellaneous cyclic ketones.

2.5.1 Justification for synthesis of various cyclic ketones.

With a reliable synthesis of 2-bromo-4,5-dimethoxybiphenyl (**10**), 2-bromo-3',4,4',5-tetramethoxybiphenyl (**9**) and 2-iodo-4,5-dimethoxybiphenyl (**11**) suitable for multi-gram scale (Sections 2.2.2 & 2.2.3), a number of cyclic ketones could act as precursors to monomers for both ladder and network polymers as shown in Scheme 2.23.

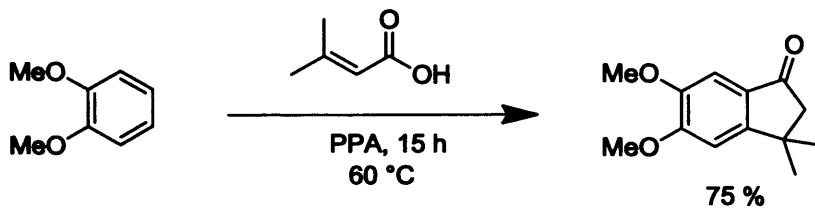


Scheme 2.23 Reaction of a cyclic ketone with either 2-bromo-3',4,4',5-tetramethoxybiphenyl (**9**) or 2-iodo-4,5-dimethoxybiphenyl (**11**) to obtain 2 different methyl protected monomers.

Several cyclic ketones were identified that would be relatively quick to synthesize, and that would potentially produce polymers that would further correlate the relationship between molecular geometry and polymer surface area.

2.5.2 Synthesis of 5,6-dimethoxy-3,3-dimethyl-2,3-dihydro-1H-inden-1-one (**12**).

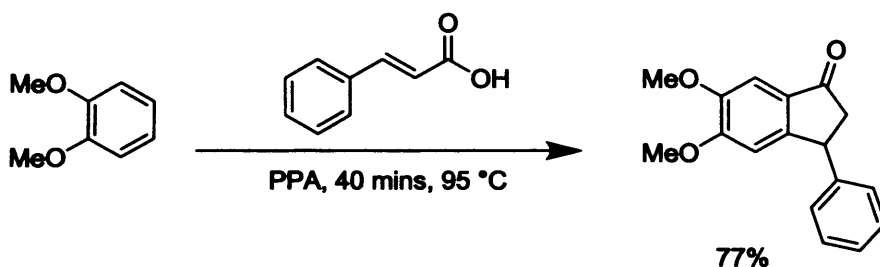
The first cyclic ketone to be prepared for this objective was 5,6-dimethoxy-3,3-dimethyl-2,3-dihydro-1H-inden-1-one (**12**), which can be thought of providing half of the spirobisindane unit used for the synthesis of PIM-1. A one-step synthesis of 5,6-dimethoxy-3,3-dimethyl-2,3-dihydro-1H-inden-1-one (**12**) from a Friedel-Crafts acylation of veratrol (**SM4**) by 3,3-dimethylacrylic acid was reported by Kraft *et al.*^[89] and was easily reproduced (Scheme 2.24).



Scheme 2.24 One-step synthesis of 5,6-dimethoxy-3,3-dimethyl-2,3-dihydro-1H-inden-1-one (12) reported by Kraft *et al*^[89].

2.5.3 Synthesis of 5,6-dimethoxy-3-phenyl-2,3-dihydro-1H-inden-1-one (13)

Using similar chemistry as described in the previous section, Maquardt^[90] reported a one-step synthesis of 5,6-dimethoxy-3-phenyl-2,3-dihydro-1H-inden-1-one (13) from veratrol (SM4) and 3-phenylacrylic acid in PPA as shown in Scheme 2.25 which was reproduced and gave a 77% yield.

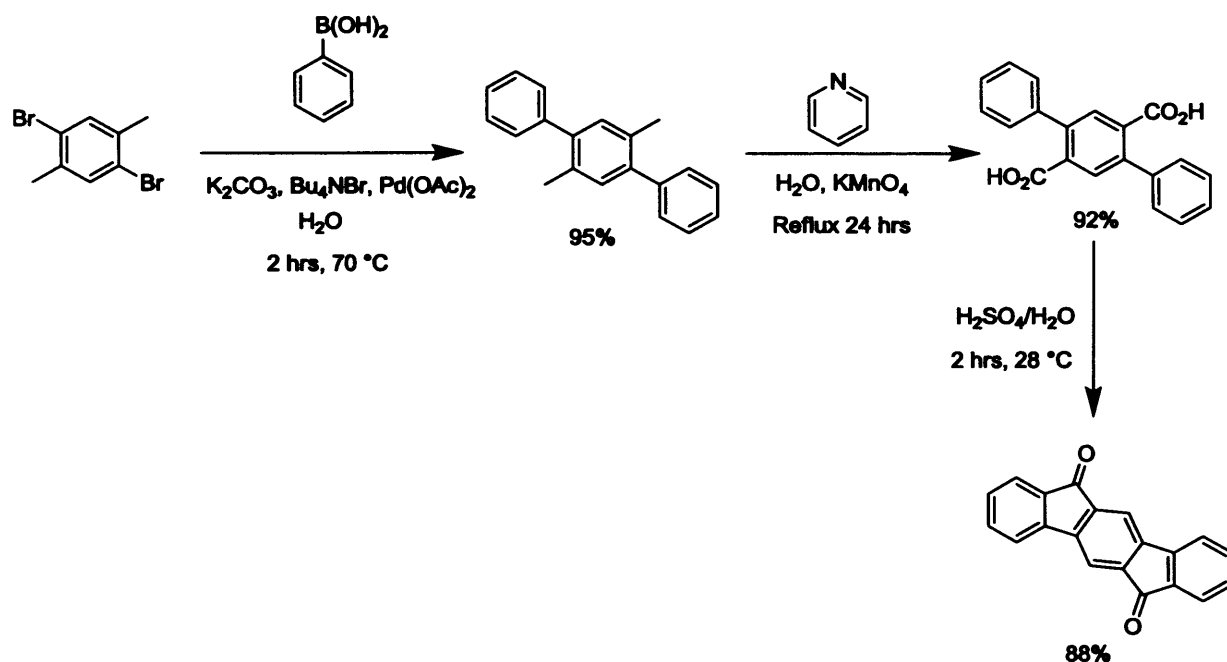


Scheme 2.25 One-step synthesis of 5,6-dimethoxy-3-phenyl-2,3-dihydro-1H-inden-1-one from veratrol as reported by Maquardt^[90].

2.5.4 Synthesis of indeno[1,2-*b*]fluorene-6,12-dione (16).

The final cyclic ketone identified as a target was indeno[1,2-*b*]fluorene-6,12-dione (16) which had previously been synthesised by Hadizad *et al.*^[91]. Although the synthesis involves several steps it was deemed that the time invested to make this dione was worthwhile due to the interesting molecular geometry of the monomers that could be created from it. According to the hypothesis posed in the aims of the project, spiro-centres within a monomer provide sites of contortion within the polymer it produces. The monomer derived from indeno[1,2-*b*]fluorene-6,12-dione (16) contains two distinct sites of contortion and could potentially

produce a highly contorted polymer. The synthesis of indeno[1,2-*b*]fluorene-6,12-dione (**16**) is shown in Scheme 2.26 and was achieved without difficulty.

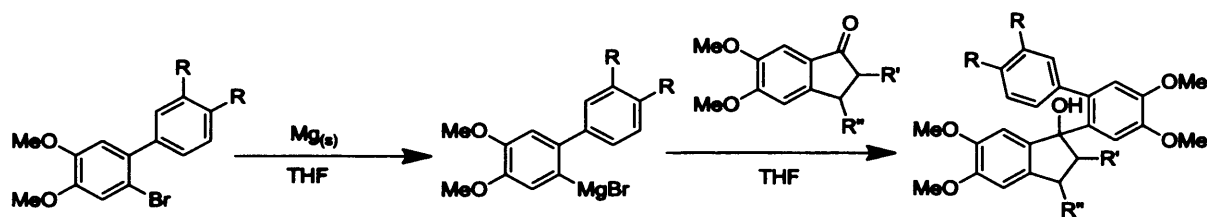


Scheme 2.26 Synthesis of indeno[1,2-*b*]fluorene-6,12-dione (**16**) as reported by Hadizad et al^[91].

2.6 Precursor synthesis

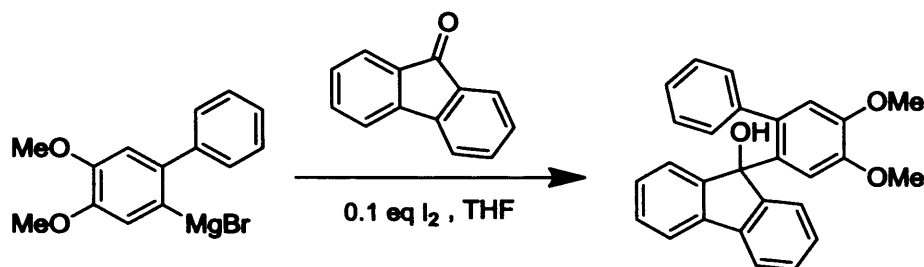
2.6.1 Grignard chemistry

Having optimised the multi-gram synthesis of both 2-bromo-3',4,4',5-tetramethoxybiphenyl (**9**), 2-bromo-4,5-dimethoxybiphenyl (**10**) and a series of cyclic ketone precursors, it was necessary to devise a reliable method of reacting the two components together. The initial strategy for synthesising the desired alcohols was to employ Grignard chemistry as shown in Scheme 2.27.



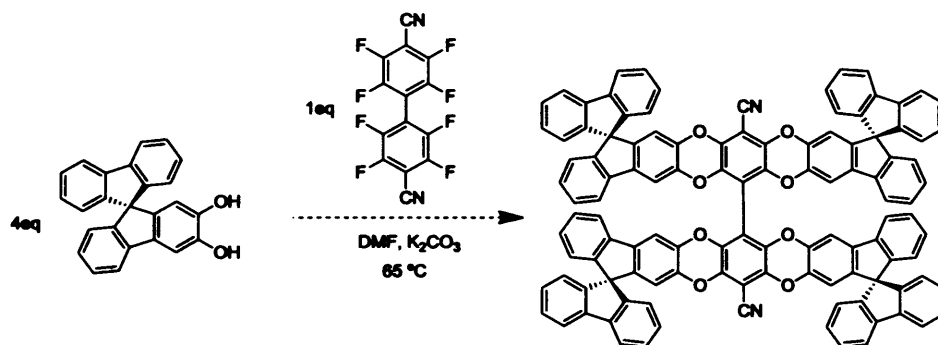
Scheme 2.27 Proposed route to fluoren-9-ols and similar intermediates utilising Grignard chemistry.

In an effort to conserve the limited supply of previously prepared ketones, the optimization of the Grignard reaction was studied using the commercially available 9H-fluoren-9-one (SM1) shown in Scheme 2.28.



Scheme 2.28 Grignard reaction used for optimization of general procedure for 2-bromo-4,5-dimethoxybiphenyl (10) addition.

Although the product of this reaction could not be used to create a polymer due to its functionality of one (i.e. a single catechol unit), this product was still of interest due to the possibility to generate an ‘Organic Molecule of Intrinsic Microporosity’ (OMIM) via reaction with 4,4'-dicyano-2,2',3,3',5,5',6,6'-octafluorobiphenyl (OFPN) as indicated in Scheme 2.29.



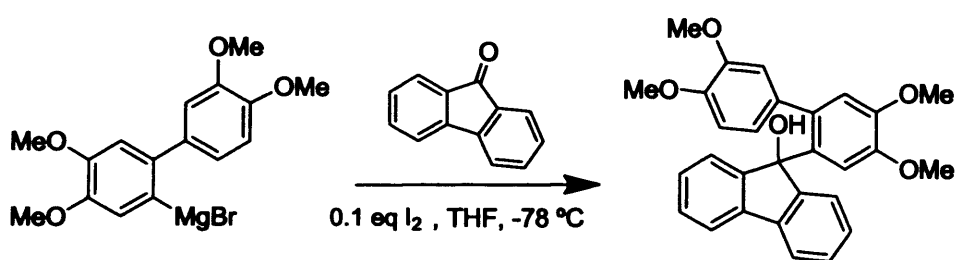
Scheme 2.29 Proposed use of 2,3-dihydroxy-9,9'-spirobisfluorene (37) to form an OMIM.

Initial attempts at the Grignard reaction were largely unsuccessful. Following the reaction over time by TLC showed mainly unreacted starting material and small amounts of debrominated 3,4-dimethoxybiphenyl (8), which would indicate the Grignard reagent had not been successfully formed, even after a 24 h reaction time. Further reactions at elevated temperatures were monitored and showed decreased amounts of desired product which that suggested electron-donating groups para to the bromine substituent cause the Grignard reagent to undergo a competing pseudo Wurtz homocoupling side reaction similar to those utilised by Schulte *et al.*^[75]. In each case, the majority of the mixture was found to be unreacted starting material (~60% recovered). The data collected from these experiments is summarised in Table 2.2.

Time (h)	Mass concentration (g/mL) ^(a)	Temperature (°C)	Yield of 17(%) ^(b)
24	0.05	28	16
12	0.05	35	17
12	0.05	45	12
12	0.05	55	10
12	0.05	66	7
16	0.05	66	6
18	0.05	66	3

Table 2.2 Summary of isolated yields of 9-(4,5-dimethoxybiphenyl-2-yl)-9H-fluoren-9-ol (17) resulting from a Grignard reagent prepared under indicated conditions. Notes ^(a)distilled THF ^(b)yield based on product isolated from flash chromatography.

A similar set of data, shown in Table 2.3, was obtained when the same procedure was performed using 2-bromo-3',4,4',5-tetramethoxybiphenyl (9) as the precursor to the Grignard reagent to form 9-(3',4,4',5-tetramethoxybiphenyl-2-yl)-9H-fluoren-9-ol (18) from 9H-fluoren-9-one (SM1) as shown in Scheme 2.30.



Scheme 2.30 Grignard reaction used for optimization of general procedure for 2-bromo-3',4,4',5-tetramethoxybiphenyl (9) insertion.

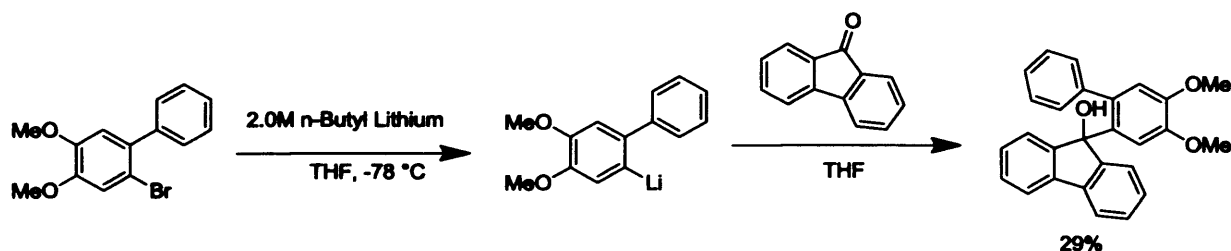
Time (h)	Mass concentration (g/mL) ^(a)	Temperature (°C)	Yield of 18(%) ^(b)
24	0.05	28	21
12	0.05	35	20
12	0.05	55	19
12	0.05	66	17
16	0.05	66	10
18	0.05	66	5

Table 2.3 Summary of isolated yields of 9-(3',4,4',5-tetramethoxybiphenyl-2-yl)-9H-fluoren-9-ol (18) resulting from a Grignard reagent prepared under indicated conditions. Notes: ^(a)distilled THF ^(b)yield based on product isolated from flash chromatography

In the test reactions it was observed that debrominated 3,4-dimethoxybiphenyl **8**), and 2-bromo-4,5-dimethoxybiphenyl (**10**) starting material were recovered from the Grignard reaction involving 2-bromo-4,5-dimethoxybiphenyl (**10**) and similarly, 3,3',4,4'-tetramethoxybiphenyl (**6**) and 2-bromo-3',4,4',5-tetramethoxybiphenyl (**9**) were recovered from the reaction involving 2-bromo-4,5-3',4,4',5-tetramethoxybiphenyl (**9**). This indicated firstly that a side-reaction was occurring causing the bromine to be stripped from the starting material during the Grignard formation, and secondly, that not all the starting material had been reacted. In an attempt to increase the conversion of starting material, the magnesium turnings were heated under a nitrogen atmosphere prior to use and 1,2-dichloroethane was added together with iodine in an effort to remove magnesium oxide coating which limits Grignard formation. After using these measures, no significant increase in yield was observed.

2.6.2 Lithium exchange organometallic chemistry

Due to the low yields obtained from Grignard chemistry, it was desirable to investigate organolithium chemistry as an alternative. The initial test reaction shown in Scheme 2.31 appeared promising so further attempts to refine and optimize the reaction was attempted as shown in Table 2.4.



Scheme 2.31 Initial organolithium reaction used for optimization of general procedure for 2-bromo-4,5-dimethoxybiphenyl (**10**) addition.

Mass concentration (g/mL) ^(a)	Mass concentration(g/mL) ^(b)	Equiv. <i>n</i> -BuLi	Time (h) ^(c)	Yield 17(%) ^(d)
0.05	0.05	1.0	1	19
0.07	0.05	1.0	1	14
0.10	0.05	1.0	1	9
0.05	0.07	1.0	1	18
0.05	0.10	1.0	1	18
0.04	0.05	1.0	1	20
0.04	0.05	1.1	1	21

Table 2.4 Summary of isolated yields of 9-(4,5-dimethoxybiphenyl-2-yl)-9H-fluoren-9-ol (**17**) resulting from an organolithium reagent prepared under indicated conditions. Notes ^(a)conc. 2-bromo-4,5-dimethoxybiphenyl (**10**), ^(b)concentration 9H-fluoren-9-one (**SM1**), ^(c)time from addition of *n*-BuLi to addition of 9H-fluoren-9-one(**SM1**), ^(d)yield based on product isolated from flash chromatography.

2.6.3 Optimisation of organolithium addition

It was noted that 3,4-dimethoxybiphenyl (**8**) was always recovered during the chromatographic purification however no starting material was isolated, indicating that conversion of 2-bromo-4,5-dimethoxybiphenyl (**10**) to organolithium reagent was efficient but that a side reaction producing 3,4-dimethoxybiphenyl (**8**) was still competing with the desired reaction. In an effort to reduce the effect of the competitive side reaction a further optimization study was conducted to investigate the effect of altering the time between addition of *n*-BuLi and addition of 9*H*-fluoren-9-one (**SM1**). Having produced a sizeable quantity of 2-iodo-4,5-dimethoxybiphenyl (**11**), the effects of using this reagent instead of 2-bromo-4,5-dimethoxybiphenyl (**10**) were investigated in the same study, the results of which are given in Table 2.5. It was found that the best results were found for reactions in which the aryl halide and the fluorenone were in solution together and the *n*-BuLi was added to the solution. Presumably, this minimised the time for side-reactions (protonation) to occur.

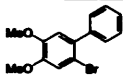
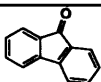
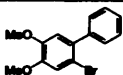
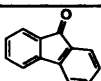
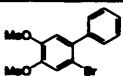
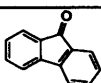
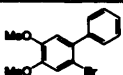
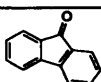
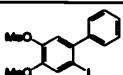
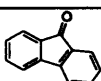
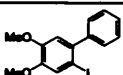
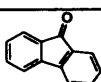
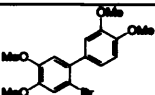
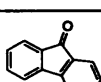
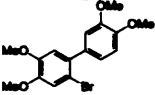
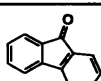
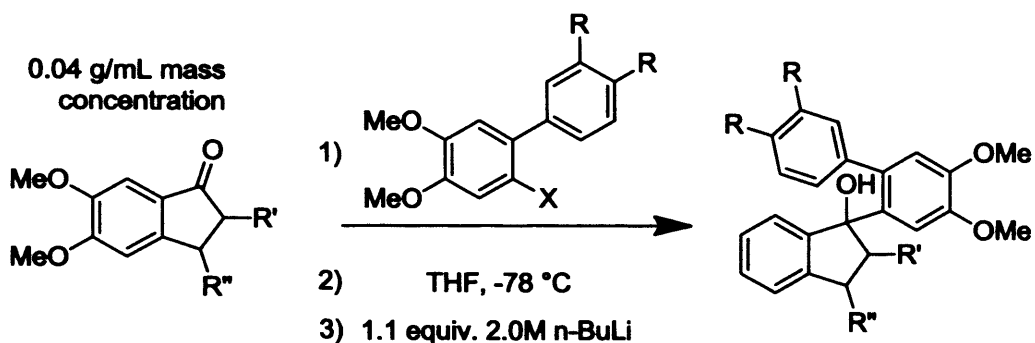
Halo biphenyl	Cyclic ketone	Time(h) ^(a)	Yield(%) ^(b)
		1.0	21
		0.5	23
		0.25	28
		0.0	31
		0.25	34
		0.0	36
		0.25	29
		0.0	38

Table 2.5 The effect of time between additions on halo biaryl insertion yields for various substrates. Notes:

^(a) time from addition of *n*-BuLi to addition of 9*H*-fluoren-9-one (**SM1**). ^(b) yield based on product isolated from flash chromatography

Although dehalogenated biphenyls were still isolated from the reaction mixtures, the yields that were obtained were deemed acceptable enough to risk reacting synthesised cyclic ketones using the optimized conditions indicated in Scheme 2.32.



Scheme 2.32 Optimized general procedure for insertion of halo biaryls into cyclic ketones.

A summary of the yields of the lithium exchange mediated nucleophilic addition of biphenyl on to the cyclic ketones that were synthesised previously, plus two that were purchased, are listed in Table 2.6.

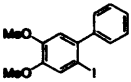
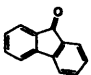
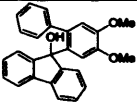
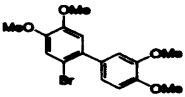
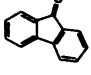
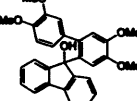
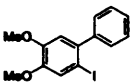
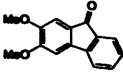
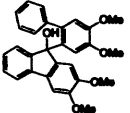
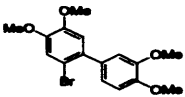
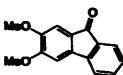
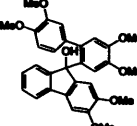
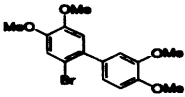
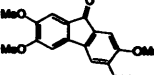
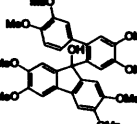
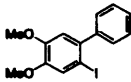
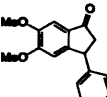
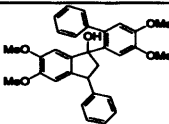
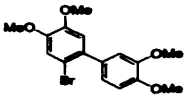
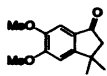
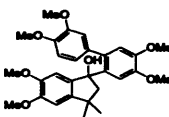
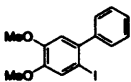
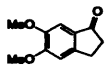
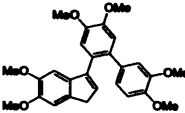
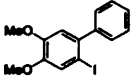
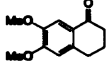
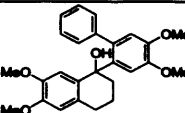
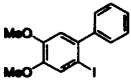
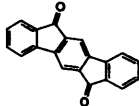
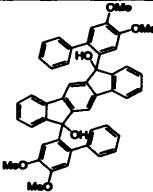
Halo biaryl	Cyclic ketone	Compound Number	Product	Yield (%) ^(a)
		(17)		38
		(18)		40
		(19)		34
		(20)		45
		(21)		42
		(22)		27
		(23)		37
		(24)		27 ^(b)
		(25)		31
		(26)		17 ^(c)

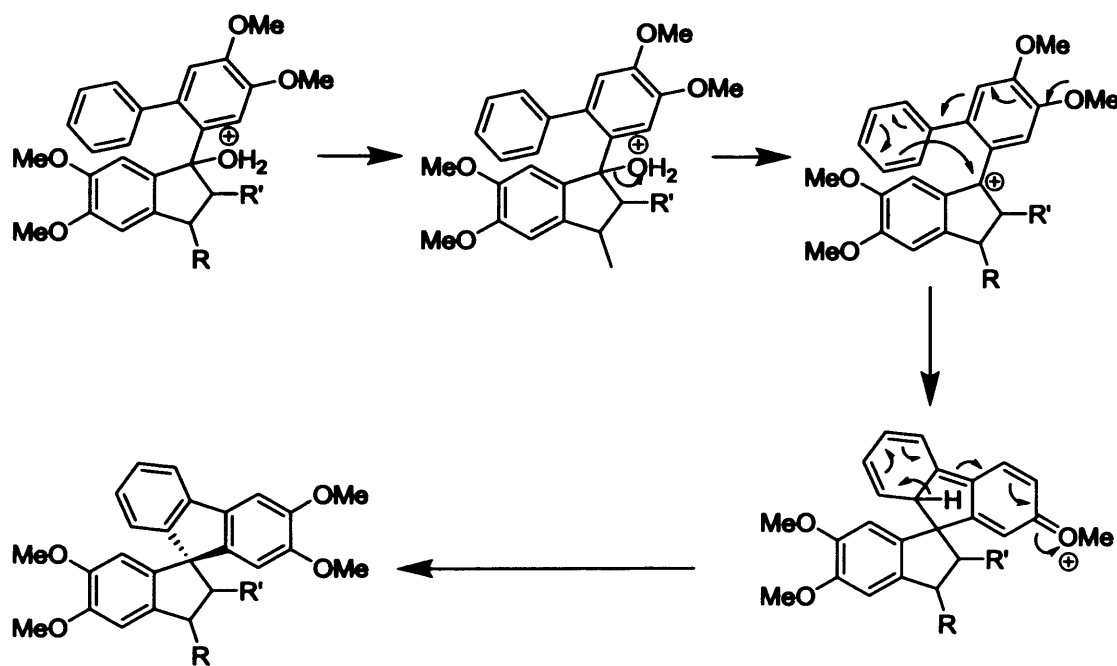
Table 2.6 List of yields obtained for various reactions between combinations of halo biaryls and cyclic ketones.

Notes: ^(a) yield based on product isolated from flash chromatograph ^(b) tertiary alcohol eliminated in situ ^(c) 10% of single addition also isolated

2.7 Cyclisation of monomer precursors

2.7.1 Mechanism of cyclisation

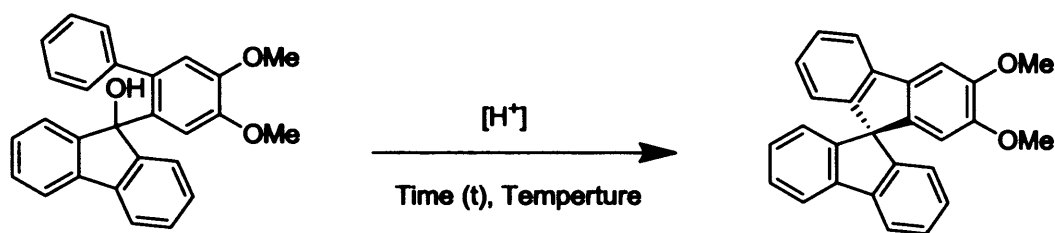
During the planning of the synthesis of the target monomers it was necessary to consider the best way to form the spiro-centre at the core of the monomer. A major factor that contributed to choosing the route that has been discussed above was the geometry of the precursors produced from the reaction between the lithium exchanged halogenated biphenyls (or Grignard derivatives) and a ketone. Since the nucleophilic attack of the ketone is a carbon – carbon bond forming reaction, the resulting product will be a tertiary alcohol. On protonation, the hydroxyl group of the tertiary alcohol is a good leaving group and the tertiary carbocation left behind would be relatively stable. By this reasoning it should be possible to cyclise the precursor to form the desired spiro-centre by an intermolecular Friedel-Craft reaction in which the carbocation performs as the electrophile as illustrated in Scheme 2.33



Scheme 2.33 Mechanism of intramolecular cyclisation routes for formation of the desired 4,4 spiro centre via Friedel-Crafts alkylation.

2.7.2 Optimization of acid catalysed spiro-centre formation

As a result of using the reaction between 2-iodo-4,5-dimethoxybiphenyl (11) and 9H-fluoren-9-one (1) as an optimization study, there was a relative abundance of 9-(4,5-dimethoxybiphenyl-2-yl)-9H-fluoren-9-ol (17) and so it was decided to use this precursor as a reagent for testing the efficiency of different acids in facilitating the desired ring closure as shown in Scheme 2.34.



Scheme 2.34 Proposed variables for optimization of the cyclisation of 9-(4,5-dimethoxybiphenyl-2-yl)-9H-fluoren-9-ol (17).

A range of acids were tried at various temperatures and for various lengths of time in an attempt to optimize the yield of cyclisation of the tertiary alcohol to form the desired spiro-centre. Concentrated sulphuric acid was found to destroy the starting material to the point where only a fraction of the starting material could be recovered. Polyphosphoric acid resulted in a mixture of starting materials and desired product with reasonable yield, but due to the troublesome work up and need for purification, further acid and solvents were investigated. Concentrated HCl initially seemed promising as increasing the reaction time from 1 to 2 hours at 0 °C gave an increase in yield but further increases in reaction time failed to enhance yield. Finally acetic acid was investigated and provided the best results. Raising the temperature to reflux and doubling the reaction time both increased the observed yield to an acceptable 81%. Adding HCl during the reaction provided a further boost in yield to 93% and the product could be used without the need for further purification. The results of the optimization study are summarized in Table 2.7.

Acid ^(a)	Temperature (°C)	Time (hrs) ^(b)	Yield 27(%) ^(c)
H ₂ SO ₄	0	1	0
PPA	60	1	28
PPA	80	1	40
HCl	0	1	37
HCl	0	2	64
HCl	0	3	65
AcOH	0	1	45
AcOH	50	1	68
AcOH	100	2	81
AcOH/HCl (100:1)	100	2	93

Table 2.7 Table of results of the optimization study of the acid catalyzed cyclisation of 9-(4,5-dimethoxybiphenyl-2-yl)-9H-fluoren-9-ol (**17**). Notes: ^(a)Concentrated acid used as a solvent; ^(b)time before reaction was quenched by pouring into ice cold water; ^(c)yield after one recrystallization from ethanol.

It was speculated that an in-situ cyclisation to form the 9,9'-spirobisfluorenes could be incorporated directly into the work-up of the lithium-mediated addition reactions by quenching these reactions with acetic acid. This idea was tried on a small scale reaction between 2-bromo-4,5-dimethoxybiphenyl (**10**) and 9H-fluoren-9-one (**1**), and was indeed somewhat successful, however, it was perceived of little benefit as a chromatographic purification of the product was still required and the tertiary alcohol precursors were all novel and required characterization.

2.7.3 Application of optimized acid cyclisation conditions to produce a range of 9,9'-spirobisfluorenes

Having optimized the conditions for the cyclisation of 9-(4,5-dimethoxybiphenyl-2-yl)-9H-fluoren-9-ol (**17**), these were then applied to the remaining tertiary alcohols with the resulting yields shown in Table 2.8.

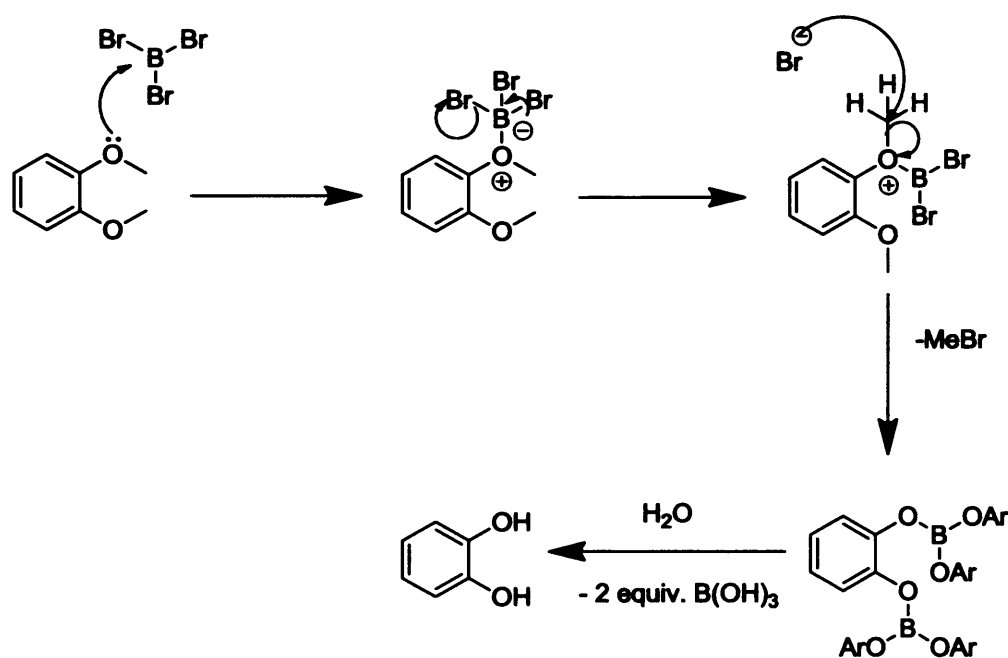
Compound number	Tertiary alcohol	Compound number	9,9'-spirobisfluorene	Yield (%) ^(a)
(17)		(27)		92
(18)		(28)		95
(19)		(29)		91
(20)		(30)		94
(21)		(31)		94
(22)		(32)		89
(23)		(33)		92
(24)		(34)		88
(25)		(35)		89
(26)		(36)		90

Table 2.8 Table showing the yields of the optimized cyclization reaction conditions applied to the remaining tertiary alcohols ^(a)yield after one recrystallization from ethanol.

2.8 Deprotection of monomers via demethylation

2.8.1 Discussion of demethylation mechanism

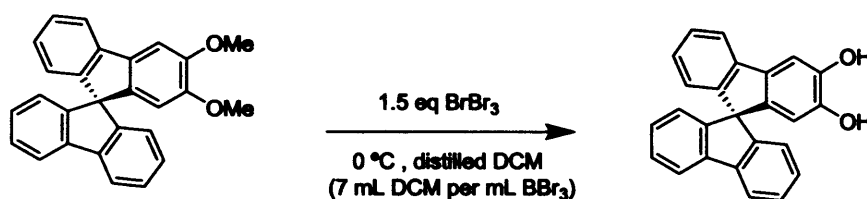
The final step in monomer synthesis was to protodemethylate the spiro-containing compounds. There are many options for methyl-ether cleavage including HBr and AlBr₃ however the favoured method of cleaving aromatic methyl esters is via reaction with boron tribromide as reported by McOmie *et al.*^[92] This reaction has been refined to a high degree and has been used for many similar deprotections within previous and current work within the McKeown group^[62]. The general mechanism of the reaction is shown in Scheme 2.35



Scheme 2.35 Proposed mechanism for protodemethylation of veratrol (SM4).

2.8.2 Protodemethylation reactions to produce monomers

Using standard conditions for BBr_3 , a highly purified sample of 2,3-dimethoxy-9,9'-spirobisfluorene (**27**) was demethylated successfully in good yield as illustrated in Scheme 2.36.



Scheme 2.36 Synthesis of (**37**) via typical demethylation conditions.

Following the successful demethylation of 2,3-dimethoxy-9,9'-spirobisfluorene (**27**), a range of methyl protected spiro compounds (**28** - **36**) were demethylated to give catechol-containing monomers (**38** – **46**) in a similar manner. Thus, 1.5 eq of BBr_3 were used for every pair of aryl methyl ethers present in the spiro compound, and special care was taken to ensure that the methyl protected spiro compounds were thoroughly dried and purified before they were demethylated. For compounds containing aryl methyl-ether pairs connected by π -conjugation even greater care was taken to ensure that the demethylated product was not exposed to unnecessary light, heat or moist air. These steps were taken to ensure that the resulting catechols would not oxidise. No colour changes indicative of oxidation was observed in each case. Each demethylated compound was washed with excess DCM to remove excess reagent and then dried by dissolving in ether and stirring for 1 hour with MgSO_4 . The compounds were dried overnight in a vacuum oven, set below 35 °C to avoid decomposition or oxidation, in preparation for polymerization. The yields of each demethylation are displayed in Table 2.9.

Compound number	Methyl protected spiro compound	Compound number	Product	Equivalents of BBr ₃ used	Yield ^(a)
(27)		(37)		1.5	93
(28)		(38)		3.0	85
(29)		(39)		1.5	88
(30)		(40)		4.5	86
(31)		(41)		6.0	89
(32)		(42)		3.0	88
(33)		(43)		4.5	91
(34)		(44)		3.0	89
(35)		(45)		3.0	92
(36)		(46)		3.0	86

Table 2.9 Yields of protodemethylation of a range of methyl protected spiro compound^(a) Yield based on weight recovered after drying overnight in a vacuum oven at 30°C

CHAPTER

3

3.1)	Novel 9,9-spirobisfluorene monomer based ladder polymers...	59
3.2)	Novel spiro-network polymers.....	64
3.3)	Attempted OMIM formation from molecule.....	66

Polymer synthesis

3.1 Novel 9,9-spirobisfluorene monomer based ladder polymers

3.1.1 General procedure for polymerisation and purification

Having synthesised a range of monomers, they were then reacted with 2,3,5,6-tetrafluoroterephthalonitrile (TFPN) to form polymers, which were subsequently investigated their physical properties in terms of porosity using nitrogen gas adsorption.

The general procedure used for the polymerisations was based upon the optimized synthesis of PIM-1^[93]. Since step-growth polymerisations shows exceptional sensitivity to the molar ratio of the monomers and impurities, rigorous reaction conditions are required. These included the use of anhydrous DMF as solvent, inert nitrogen atmosphere and, importantly, careful measurement of the mass of the two monomers to three decimal places to ensure equimolar amounts, in order not to restrict the mass of the resulting polymer. Using the McKeown group's general procedure for making PIMs, equimolar amounts of the two starting monomers were added to the DMF, the mixture was heated to 65-70 °C and, only when the monomer were completely dissolved, was the K₂CO₃ base added to start the reaction. For a number of the monomers, their complete dissolution in DMF required higher temperatures (e.g. 75-85 °C – see experimental section). The formation of a bright yellow suspension was usually noticed after 15-30 minutes during which time, it was presumed, oligomeric material was formed. The mixture was kept under stirring at constant temperature for 72-96 hours, to hopefully obtain higher mass polymers. Generally, the purification of PIMs, after quenching the reaction with water, depended on the solubility of the product in organic solvents. The ladder polymers proved to be only soluble in DMSO, conc H₂SO₄ and veratrole and it proved difficult to use conventional reprecipitation methods to remove more soluble lower mass material. Each polymerization reaction was quenched in water and the majority of the precipitate was dissolved in acetone. The acetone was removed by rotary evaporation and the resulting solid residue was refluxed in methanol for four hours. The undissolved material was then filtered and dried at 120 °C overnight in a vacuum oven. After drying, the polymers were no longer soluble in acetone, THF, or CHCl₃ but were soluble in DMSO and H₂SO₄ (see Table 3.1), which indicated that the material had not become cross-linked during the drying procedure. ¹H NMR analysis of the polymers dissolved in deuterated DMSO (in which they were all fully soluble) showed a significant broadening of the peaks as

compared to the respective monomer (Fig. 3.1), which is an indication that the polymerisation had been successful in that high mass polymer was

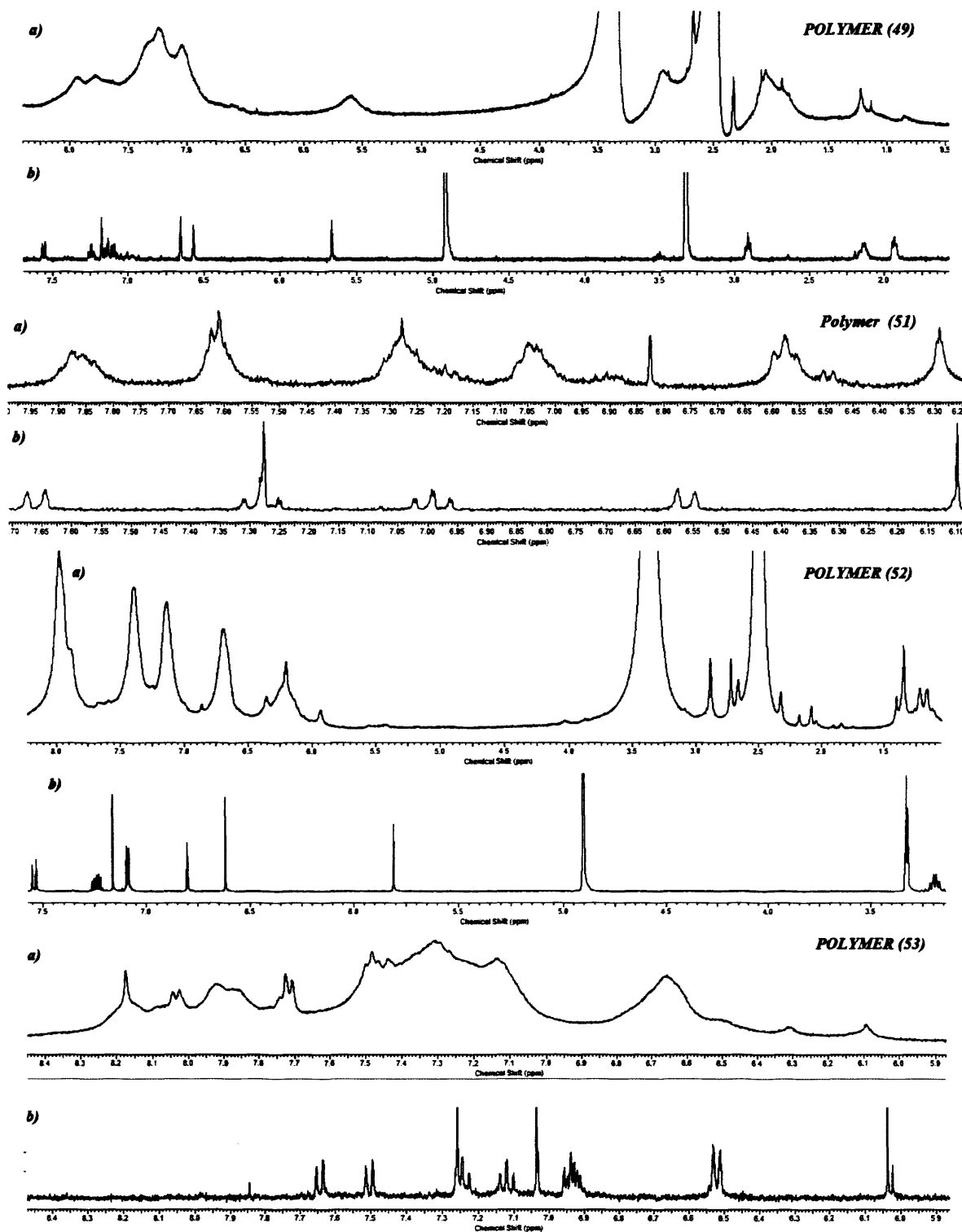


Fig 3.1 Comparison of a) polymer ^1H NMR in $\text{DMSO}-d_6$ and b) monomer ^1H NMR in $\text{MeOH}-d_4$ for indicated ladder polymers.

obtained. IR confirmed the presence of a nitrile peak. GPC analysis was not possible due to poor solubility in suitable solvents. In each case MALDI-MS analysis of the material was attempted but no high mass material was detected. For each polymer, nitrogen adsorption analysis of the dried material indicated a surprisingly lack of any microporosity (e.g. BET surface area in the range $0\text{--}20\text{ m}^2/\text{g}^{-1}$) with the shape of the nitrogen adsorption isotherm indicating that the materials were non-porous solids (Fig. 3.2). Polymer (51) showed an unusual nitrogen adsorption isotherm (Fig. 3.2) with significant and rapid N_2 adsorption at high relative pressure ($P/P_0 > 0.90$), which might indicate that swelling of the polymer allows access to otherwise hidden pores. A pore volume of $0.24\text{ cm}^3/\text{g}$ can be calculated from the uptake at $P/P_0 = 0.98$.

Solvent	Insoluble	Partial solubility ^(a)	Soluble
conc. H_2SO_4	-	-	x
hexane	x	-	-
CHCl_3	x	-	-
THF	-	x	-
methanol	-	x	-
acetone	-	x	-
DMSO	-	-	x
anisole	-	x	-
veratrole	-	-	x
toluene	x	-	-
quinoline	-	-	x

Table 3.1 Solubility study of the polymer derived from 2,2',3,3'-tetrahydroxy-9,9'-spirobisfluorene and TFPN (x indicates positive result). Note: ^(a)partial solubility indicated by uptake of yellow colour into solution but majority of material remains undissolved

The polymerization of 2,2',3,3'-tetrahydroxy-9,9'-spirobisfluorene (39) was repeated three times and no significant difference in the resulting polymeric material was observed indicating that the reaction was repeatable. It is reasonable to assume the same is true for the other monomers but this assertion could not be confirmed due to limited amounts of monomeric material availability.

Chapter - 3

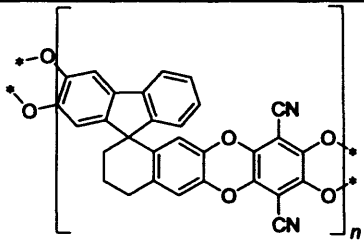
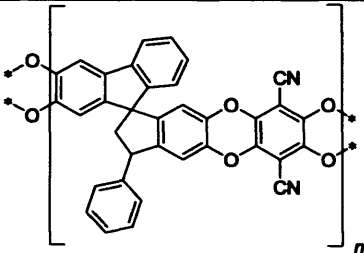
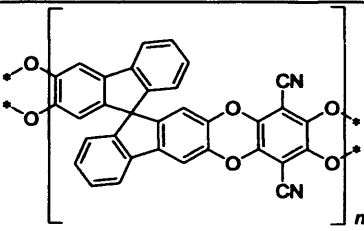
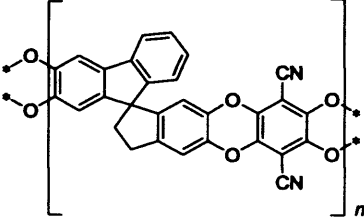
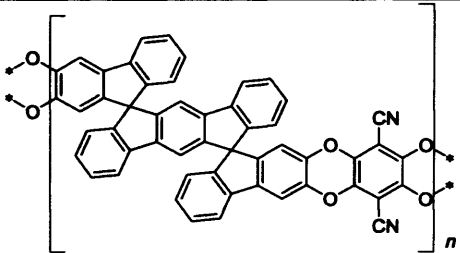
Monomer N°	Fluorine monomer	Polymer	Polymer N°	Yield (%)	Surface area (m ² /g)
45	TFPN		48	82	0
42	TFPN		49	73	0
39	TFPN		50	87	0
44	TFPN		51	86	20
46	TFPN		52	79	0

Table 3.2 Summary of ladder polymerization results

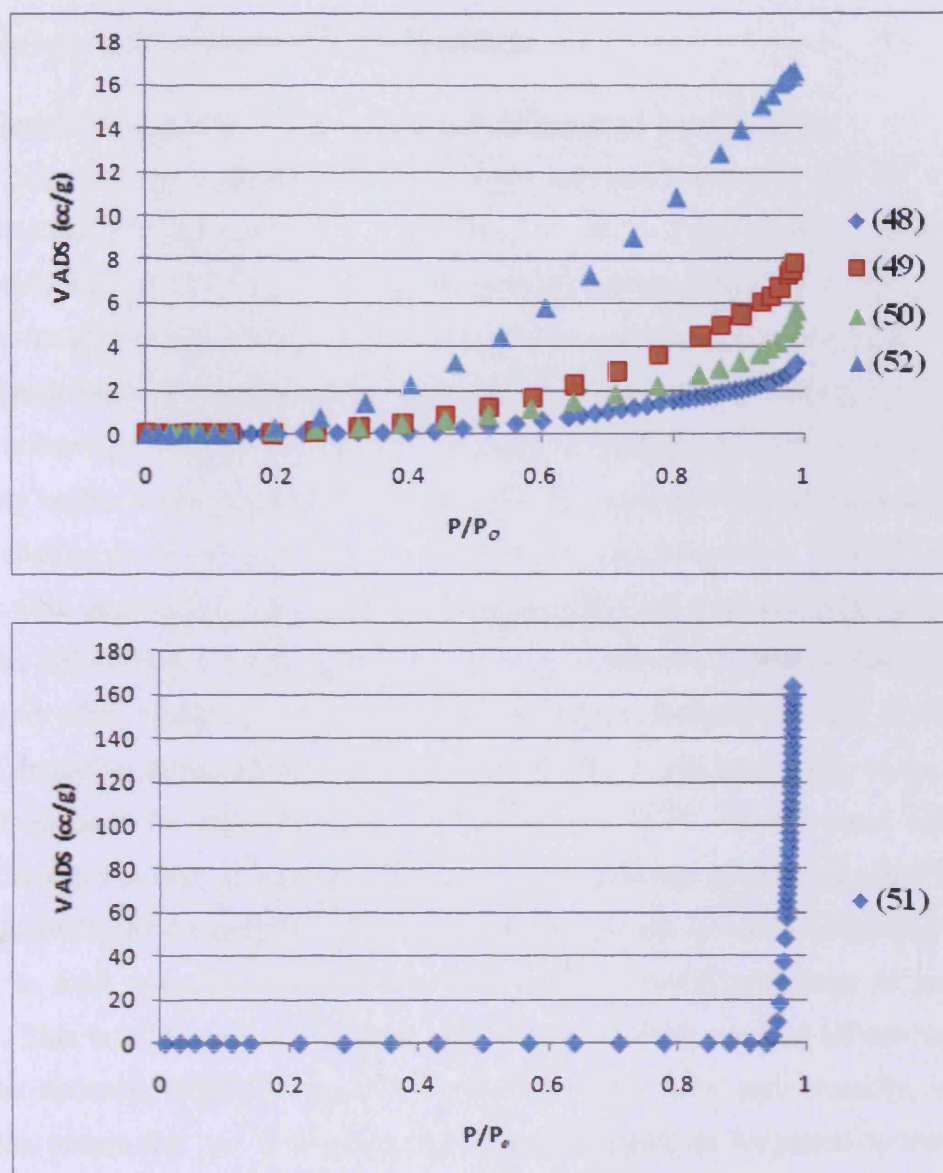


Figure 3.2. Collated isotherm data collected for the range of ladder polymers obtained in this study.

3.2 Novel spiro-network polymers.

3.2.1 General procedure for polymerization and purification

Network polymers were prepared by reacting the catechol monomers **38** - **41** with either 2,3,5,6-tetrafluoroterephthalonitrile (TFPN) or 4,4'-dicyano-2,2',3,3',5,5',6,6'-octafluorobiphenyl (OFPN) (Table 3.3). The polymerization method for producing network polymers was slightly modified from that optimised for the preparation of PIM-1. The PIM-1 method limits reaction temperature to between 65–70 °C so as to minimise cross-linking, which is promoted by higher temperatures. In order to facilitate efficient network formation, the slightly higher temperature of 80 °C was used. The concentration of reagents in DMF is lowered slightly to 30 mL/g so as to prevent instant gel formation. After 24 hours, the reactions were quenched in water and the resulting solids collected and refluxed for 4 hours in acetone, chloroform, and methanol, sequentially, to remove soluble oligomers, included solvent and other impurities. All resulting solids were insoluble in hot H₂SO₄, which indicated extensive network formation had occurred. Due to the insolubility of the networks, the usual methods for characterizing soluble polymers (GPC, NMR) could not be used, however, it was possible, in each case, to obtain an IR spectrum by forming a mull with nujol oil, which confirmed the presence of nitrile functional groups, as well as obtaining elemental analysis. In each case, the elemental analysis shows a lower percentage of carbon than expected. This is presumed to be due to two factors. Firstly, trapped solvent or moisture within the network, which is apparent from TGA (Fig. 3.3), and secondly, incomplete combustion occurs due to a high degree of carbon formation as suggested by the relatively low loss of mass at high temperature in the TGA (e.g. ~30% at 1000 °C).

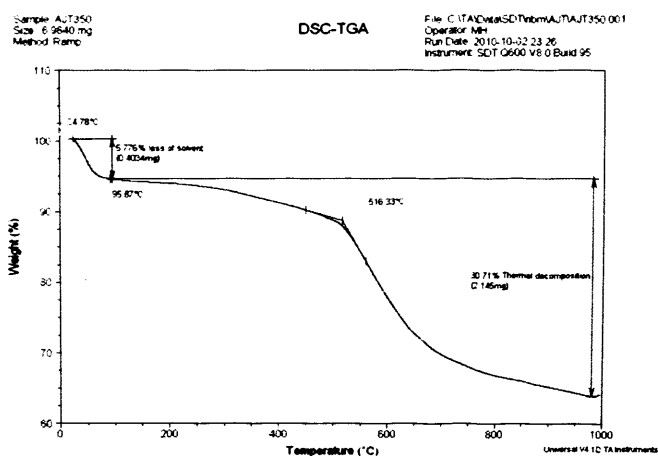


Fig 3.3 Example of a typical TGA analysis using polymer (60) as an example

Chapter - 3

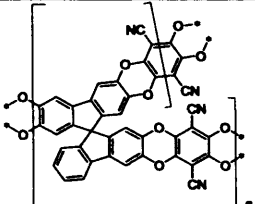
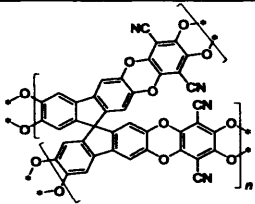
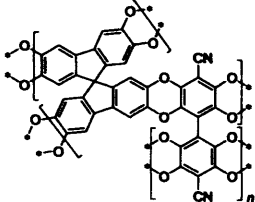
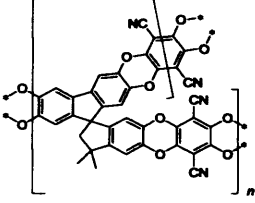
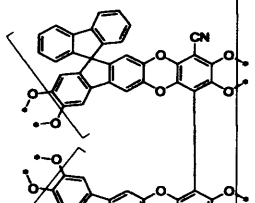
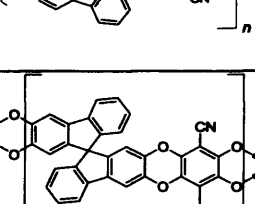
Monomer N°	Fluorine monomer	Polymer	Polymer N°	Yield (%)	Surface area (m ² /g)
40	TFPN		53	92	1048
41	TFPN		54	90	550
41	OFPN		55	91	1084
43	TFPN		56	93	1054
38	OFPN		57	83	593
39	OFPN		58	76	20

Table 3.3 Summary of network polymerization results

With the exception of Polymer **59**, for which there is no satisfactory explanation, nitrogen adsorption analysis (Fig. 3.4; Table 3.3) on the network polymers **54** - **58** all show evidence of significant microporosity with apparent BET surface area in the range 593-1048 m²/g, and pore volumes in the range 0.32 - 0.75 cm³/g, as estimated by the nitrogen uptake at $P/P_0 = 0.98$. All isotherms demonstrate a shape typical for a PIM-like microporous material. The network polymers have similar isotherms to the previously reported polymer derived from 5,5',6,6'-tetrahydroxy-3,3,3',3'-tetramethyl-1,1'-spirobisindane (**A1**) and 4,4'-dicyano-2,2',3,3',5,5',6,6'-octafluorobiphenyl (**OFPN**), which is also shown for comparison (**KJM**).

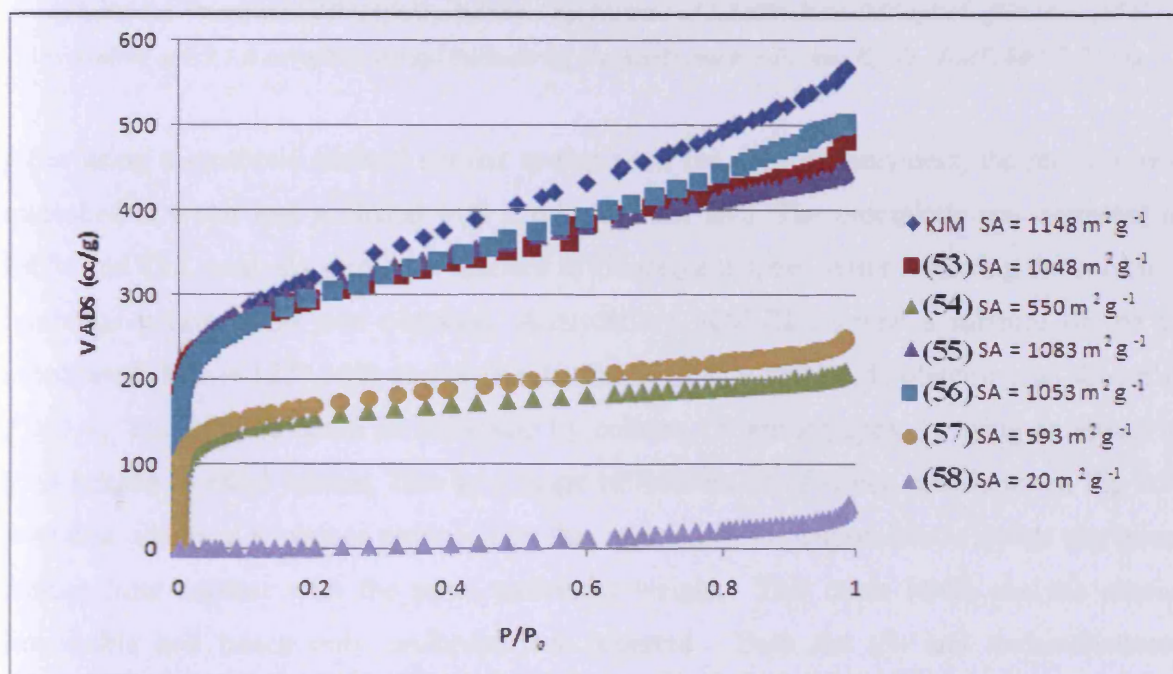
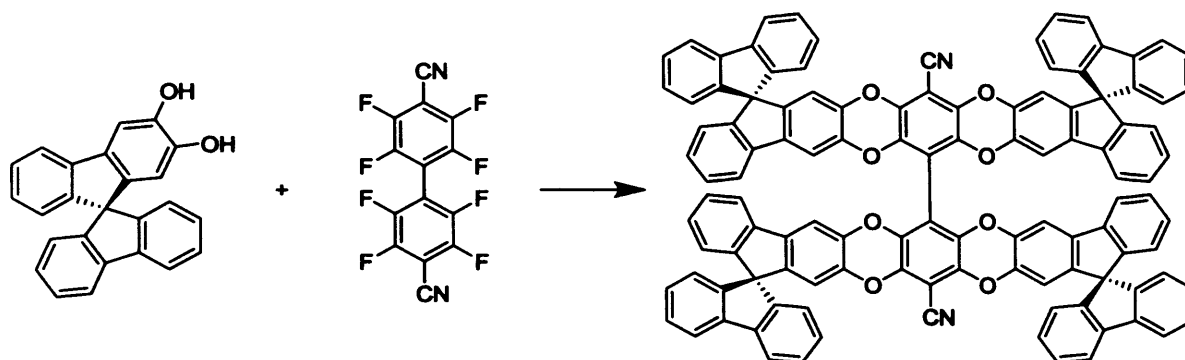


Fig 3.4 Comparison of reported network polymers with network polymer KJM derived from 5,5',6,6'-tetrahydroxy-3,3,3',3'-tetramethyl-1,1'-spirobisindane (**A1**) and 4,4'-dicyano-2,2',3,3',5,5',6,6'-octafluorobiphenyl (**OFPN**)

3.3 Attempted OMIM formation from molecule (37).

It was not possible to produce a polymer from 2,3-dihydroxy-9,9'-spirobisfluorene (**37**) as the compound has a functionality of only one (i.e. only one catechol group), and therefore reaction with 2,3,5,6-tetrafluoroterephthalonitrile (**TFPN**) was likely to yield only a dimer. However, it was suggested that an oligomer produced from reaction of 4 equivalents of 2,3-dihydroxy-9,9'-spirobisfluorene (**37**) with 1 equivalent of 4,4'-dicyano-2,2',3,3',5,5',6,6'-octafluorobiphenyl (**OFPN**) could possibly possess microporosity, and may belong to a class of compounds known as Oligomeric Molecules of Intrinsic Microporosity or OMIMs, which are currently being studied by other members of the McKeown group.



Scheme 3.1 Attempted OMIM synthesis from 4 equivalents of 2,3-dihydroxy-9,9'-spirobisfluorene and 1 equivalent of 2,3,5,6-tetrafluoroterephthalonitrile. Reagents and conditions: K_2CO_3 , DMF, 80 °C, 24 hrs.

After using a synthetic method similar to that used for network polymers, the reaction was quenched in water and acidified with 2 mL of 2.0M HCl. The precipitate was extracted in DCM and TLC analysis showed a mixture of fluorescent spots. After removing the solvent a luminous yellow solid was obtained. Analysis by MALDI showed a mixture of the tri substituted ($M_w = 1273.308$) and tetra substituted ($M_w = 1582.414$) oligomers as shown in Fig 3.4. The mixture could be separated by column chromatography by using an eluant of 95:5 hexane to ethyl acetate. Due to a range of isomers (2 of which are shown in Fig 3.5) with near-identical R_f values produced by this reaction it was impossible to isolate any given isomer from another with the same molecular weight. This made NMR analysis almost impossible and hence only multiplets are reported. Both the tri- and tetra-substituted oligomer were tested for microporosity via nitrogen adsorption in the same manner as was used previously for the polymers but unfortunately neither exhibited any characteristics of a microporous material.

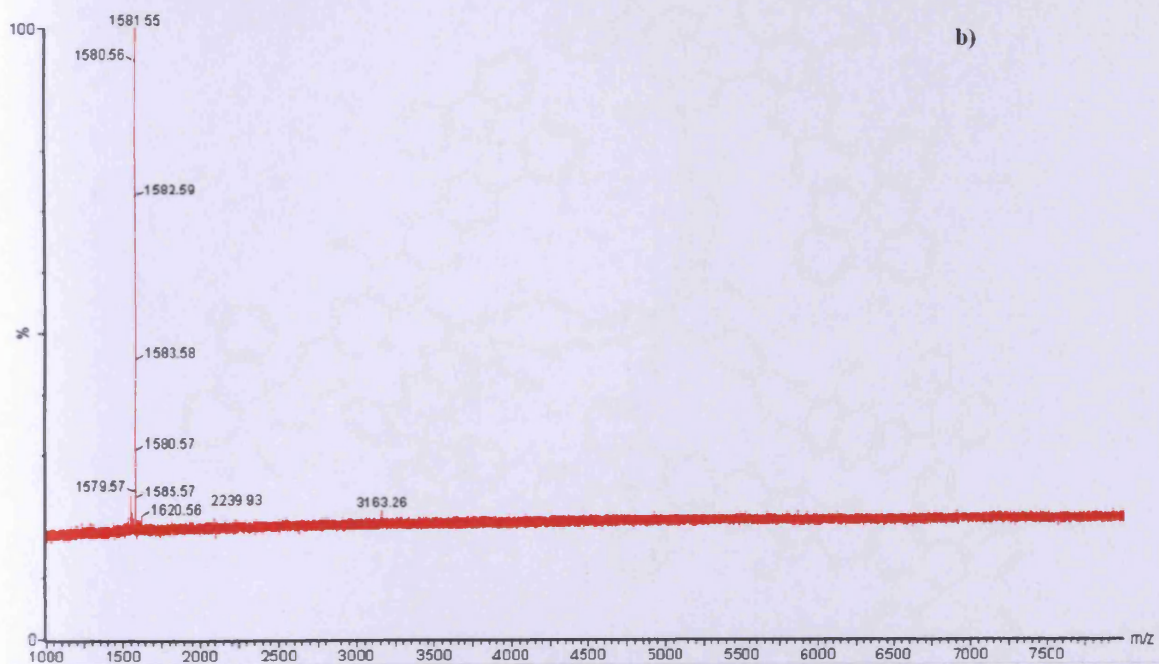
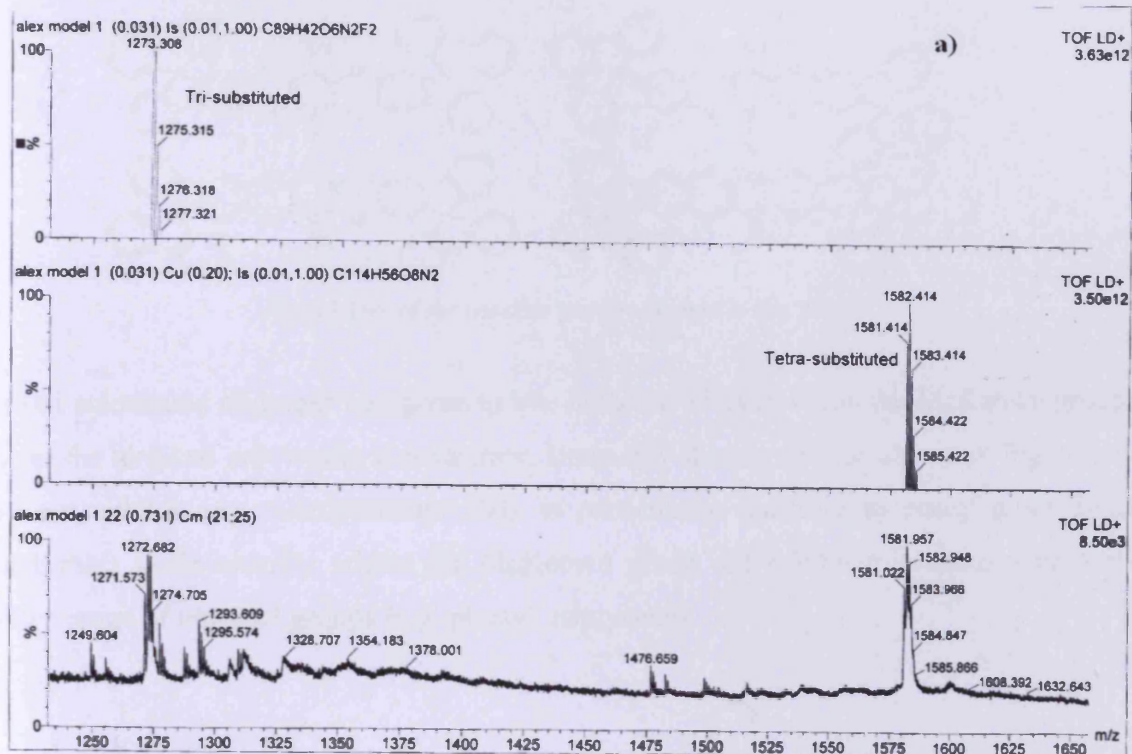


Fig 3.4 MALDI showing a) both tetra and tri substituted oligomer and b) purified tetrasubstituted oligomer

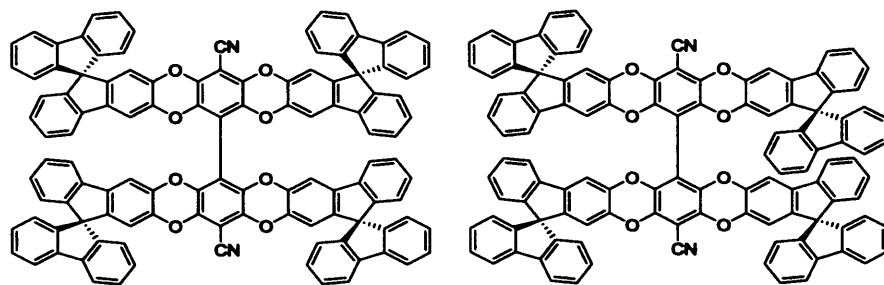


Fig 3.5 Two of the possible isomers present in the 'OMIM'

The tri-substituted oligomer was given to Mr. Jonathan Walker within the McKeown group to use as the terminal unit within a dendrimer. Unusually this dendrimer, shown in Fig 3.6, also did not exhibit any microporosity. This is particularly puzzling as many other similar dendrimers made recently within the McKeown group did exhibit microporous properties with a range of terminal groups (e.g. phenyl, triptycene).

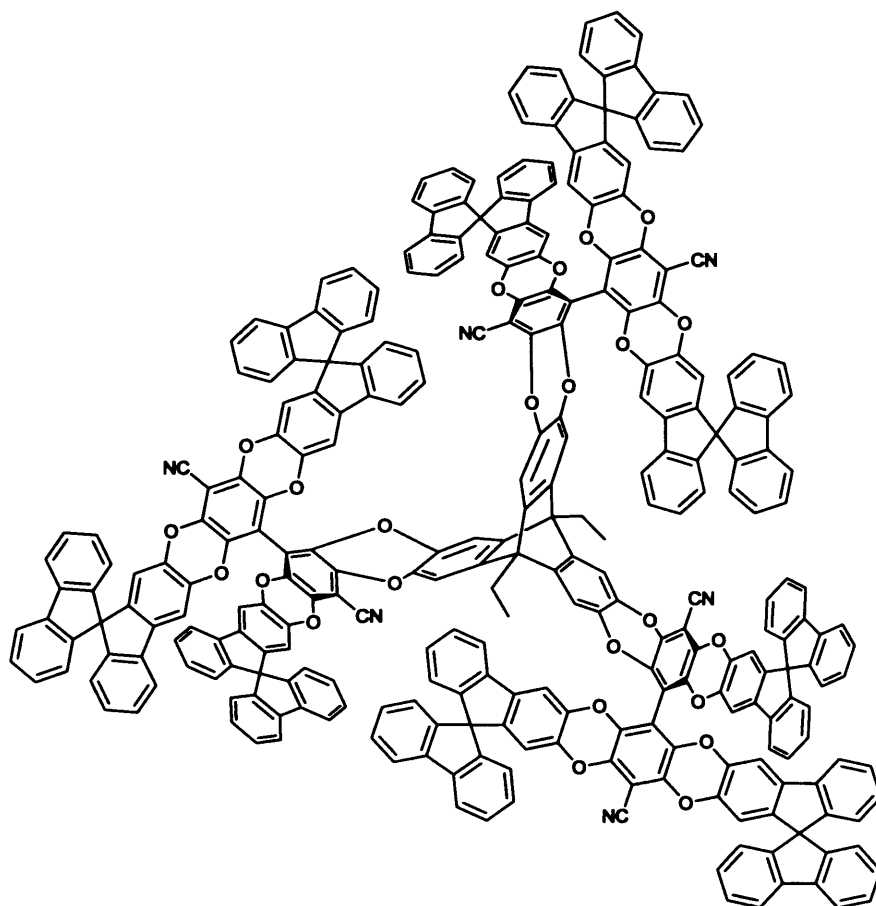


Fig 3.6 Dendrimer synthesised from tri substituted oligomer.

CHAPTER

4

4.1) Analysis of the crystal structures of monomers	71
4.2) Summary of crystal data.....	82

Crystallography

4.1 Analysis of the crystal structures of monomers 37, 39, 40, 41, 44 and 45.

All credit for collection and mathematical analysis of the data goes to Dr Benson Kariuki and Dr Grazia Bezzu.

In an attempt to understand any geometrical differences between the catechol-based monomers used in the formation of the different polymers described above, It was decided to grow crystals suitable for single crystal XRD analysis. In addition, the cruciform shape of the 9,9'-spirobisfluorene unit is thought to disfavour close packing in the crystal phase as shown by the work of Wuest and co-workers^{[70][71]}, therefore the crystals formed by monomers 37 - 46 may provide interesting packing behaviour of significance within the active research area of 'crystal engineering'.

In general, crystals derived from catechol-containing compounds, tend to form with extended H-bonded frameworks that often include solvent molecules (i.e. they form inclusion compounds or clathrates)^[69]. These properties can lead to difficulties in the growth of the crystal and a more difficult crystallographic solution, however in spite of these potential problems, it was thought desirable to perform a systematic structural analysis of the catechol-based monomers.

4.1.1 Crystal structure of 2,3-dihydroxy-9,9'-spirobisfluorene (37)

A clathrate of the 2,3-dihydroxy-9,9'-spirobisfluorene (37) monomer was crystallized by slow diffusion of hexane into an ethyl acetate solution. The crystal was monoclinic with space group *C2/c* and cell parameters [$a = 11.4117(4)$, $b = 13.9975(5)$, $c = 28.7524(11)$ Å, $\alpha = \gamma = 90$, $\beta = 90.556(2)$; cell volume = 4582.56 Å³]. It contained eight molecules per unit cell with one molecule of included ethyl acetate per spirobisfluorene unit. The molecular structure is shown in Fig 4.1 in which the central carbon atom that constitutes the spiro centre of the spirobisfluorene molecule is clear.

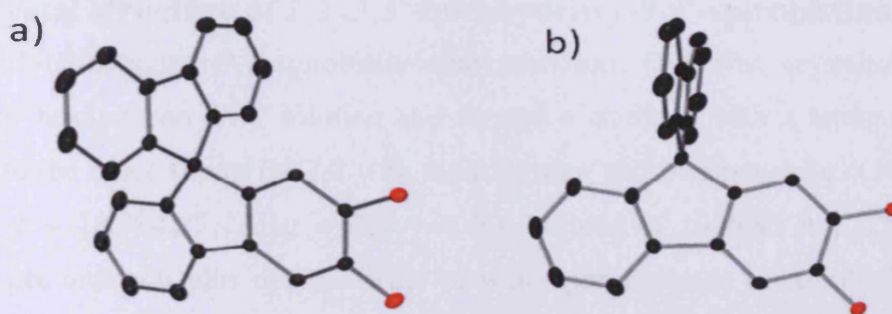


Fig 4.1 ORTEP projections of the molecular structure of 2,3-dihydroxy-9,9'-spirobisfluorene (37).

The molecules form a discrete assembly *via* mutual hydrogen bonding between the catechol moieties of adjacent monomers and further hydrogen bonding with the included ethyl acetate, as shown in Fig 4.2.

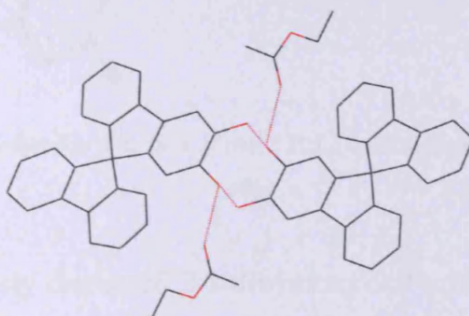


Fig 4.2. Hydrogen bonding of the 2,3-dihydroxy-9,9'-spirobisfluorene monomer (37).

Looking closely at the packing, we find that the spirobisfluorene molecules are linked by the hydrogen bonding on one side, and on the other by a short interaction shown in Fig 4.3 (3.7 Å), which could be evidence of π - π interactions^[94]. Therefore, the packing of the hydrocarbon portion of the spirobisfluorene is relatively space-efficient, despite the presence of the spiro-centre.

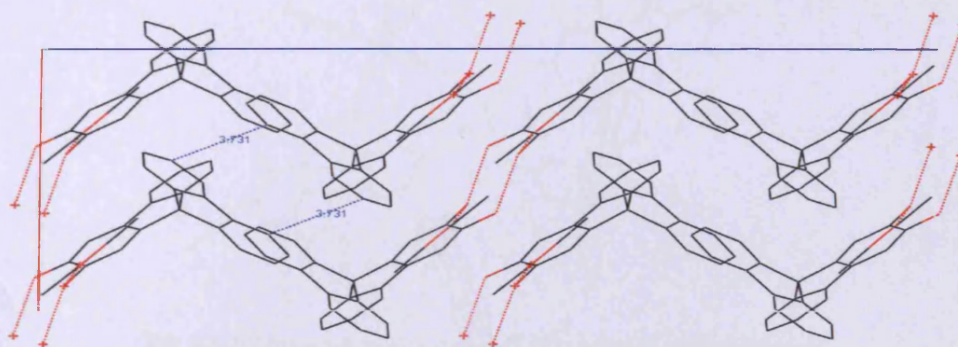


Fig 4.3 Packing of the 2,3-dihydroxy-9,9'-spirobisfluorene monomer viewed along the crystal b axis

4.1.2 Crystal structure of 2,2',3,3'-tetrahydroxy-9,9'-spirobisfluorene (39)

The 2,2',3,3'-tetrahydroxy-9,9'-spirobisfluorene monomer (**39**) was crystallized by slow diffusion of hexane into THF solution and formed a clathrate with a tetragonal unit cell belonging to the space group $P4_12_12$ with the following cell parameters [$a = 10.075(4)$, $b = 10.075(4)$, $c = 18.7841(7)$ Å; $\alpha = \beta = \gamma = 90$; volume of 1906.86 Å³]. There are four molecules per unit cell plus one molecule of water per molecule of spirobisfluorene. The molecular structure derived from the crystal analysis is shown in Fig 4.4.

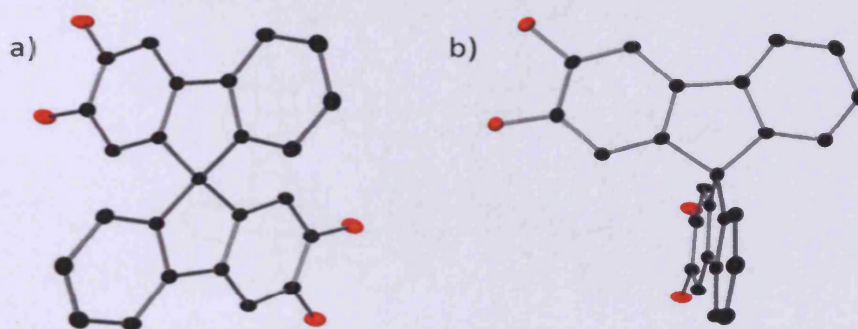


Fig 4.4 ORTEP projections of molecular structure of the 2,2',3,3'-tetrahydroxy-9,9'-spirobisfluorene monomer (**39**).

Compared with the previously discussed 2,3-dihydroxy-9,9'-spirobisfluorene monomer (**37**), it is possible to notice an enhancement in the symmetry in the molecule, which is reflected in the packing arrangement within the crystal. The molecules of included water play an important role in the packing of the crystal with each water molecule being hydrogen bonded to four molecules of spirobisfluorene in a tetrahedral motif (Fig 4.5). Both enantiomers are used to build the structure and alternate with each other.

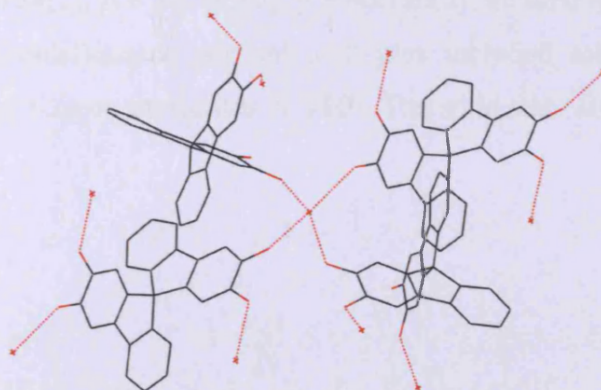


Fig 4.5 Hydrogen bonding around (**39**) included water molecule.

Looking at the packing along the c axis it is possible to see that this interaction with the included water seems to create narrow hydrophilic channels through the crystal (Fig 4.6).

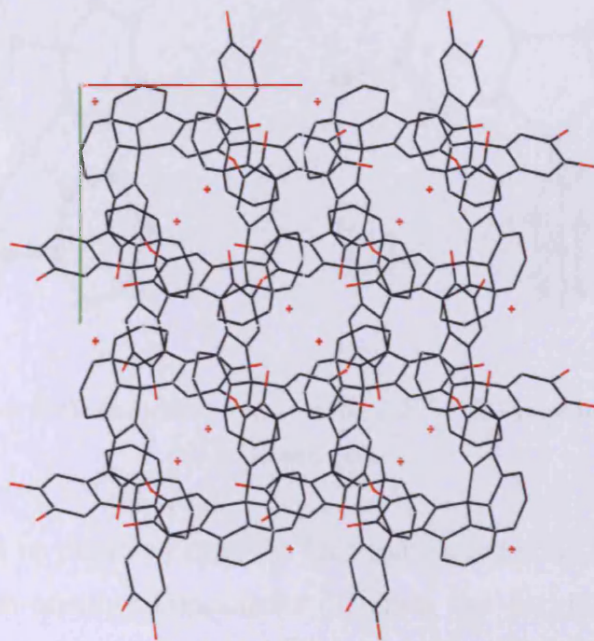


Fig 4.6 Packing of the 2,2',3,3'-dihydroxy-9,9'-spirobisfluorene monomer(40) along c axis.

4.1.3 Crystal structure of 2,2',3,3',6,7-hexahydroxy-9,9'-spirobisfluorene

Crystals for the 2,2',3,3',6,7-hexahydroxy-9,9'-spirobisfluorene monomer (**40**) were obtained by slow diffusion of hexane into THF solution. They are clathrates with triclinic unit cell belonging to the space group $P-1$ with cell parameters of [$a = 10.7693(3)$, $b = 18.4510(6)$, $c = 19.3503(6)$ Å; $\alpha = 83.138(2)$, $\beta = 84.762(2)$, $\gamma = 80.120(2)$; volume = 3750.97 Å³]. There are four molecules of spirobisfluorene per unit cell plus included solvent comprised of two molecules of water and sixteen molecules of THF. The solid state structure of this monomer is shown in Fig 4.7.

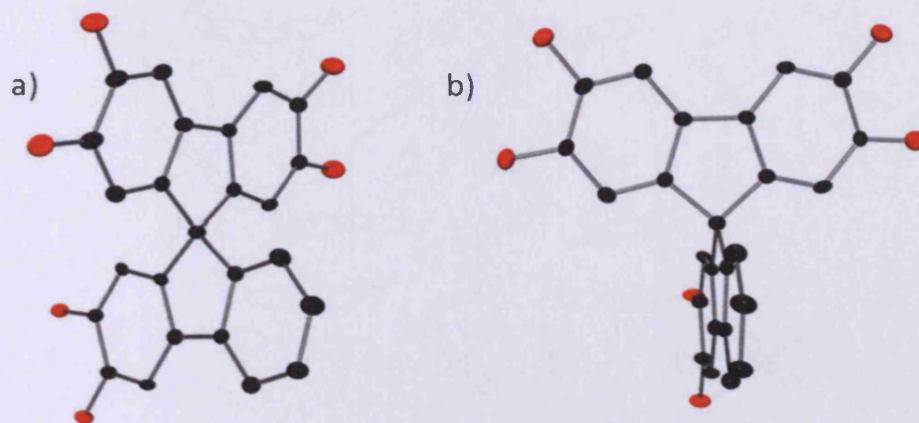


Fig 4.7 ORTEP projections of the molecular structure of the 2,2',3,3',6,7-hexahydroxy-9,9'-spirobisfluorene monomer (**40**).

In this crystal, as could be expected from the increasing number of hydroxyl groups present in the molecule, the H-bonding interactions dominate the packing. A very complicated pattern of different hydrogen-bonds is formed. For example, viewed along the *b* axis (Fig 4.8 a) a helical arrangement is apparent in which two different catechol moieties, one that belongs to the unsymmetrical fluorene unit and one that belongs to the other fluorene, link via H-bonding.

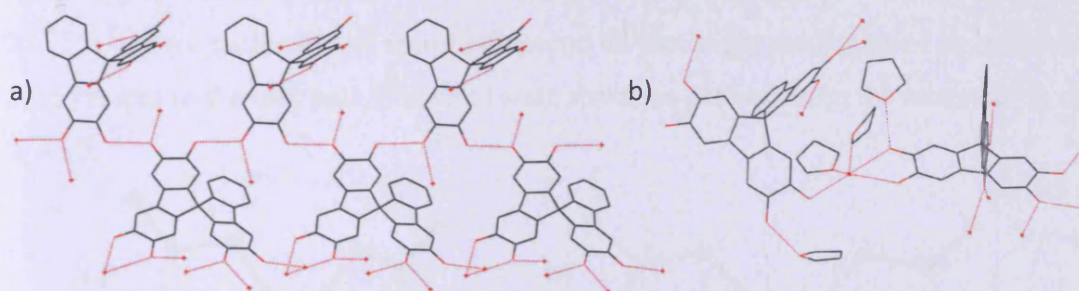


Fig 4.8 a) Hydrogen bonding, view along *b* axis and b) hydrogen bonding around the included water in the 2,2',3,3',6,7-hexahydroxy-9,9'-spirobisfluorene monomer (**40**).

Another system of hydrogen bonds present in the crystal arrangement recalls the one found in the 2,2',3,3'-tetrahydroxy-9,9'-spirobisfluorene monomer (**40**). The included water plays a very important role by linking two catechols unit and two THF molecules. Each catechol is further involved in hydrogen bonding with another THF molecule (Fig 4.8 b). Looking at the packing it is possible to appreciate the impressive amount of space occupied by the solvent which is distributed in a series of different channels which run along the *a*-axis direction (Fig.4.9).

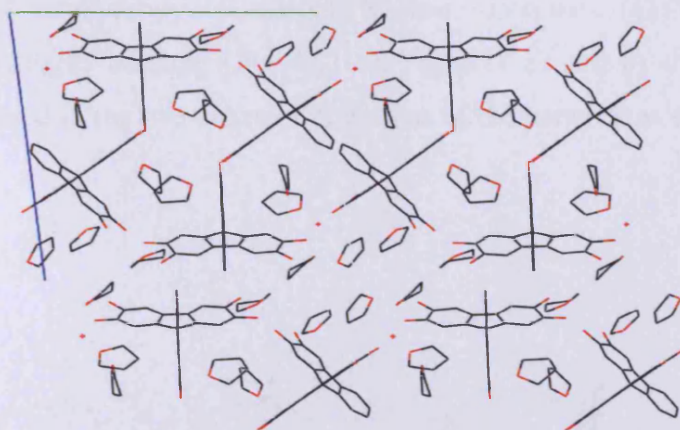


Fig 4.9 Packing of the 2,2',3,3',6,7-hexahydroxy-9,9'-spirobisfluorene monomer (**40**) viewed long a axis showing the included THF molecules.

4.1.4 Crystal structure of 2,2',3,3',6,6',7,7'-octahydroxy-9,9'-spirobisfluorene (**41**).

Crystals for the 2,2',3,3',6,6',7,7'-octahydroxy-9,9'-spirobisfluorene monomer (**41**) were grown by slow diffusion of hexane into diethyl ether solution. They are clathrates with a triclinic unit cell belonging to the space group *P*-1 with a cell parameters [$a = 11.5238(4)$, $b = 11.6296(3)$, $c = 18.4134(6)$ Å; $\alpha = 103.558(2)$ $\beta = 96.643(2)$ $\gamma = 115.090(2)$; volume = 2106.75 Å³]. Two molecules of spirobisfluorene **41** plus eight molecules of included diethyl ether are present in the unit cell. The solid state structure derived from the monomer is shown in Fig 4.10.

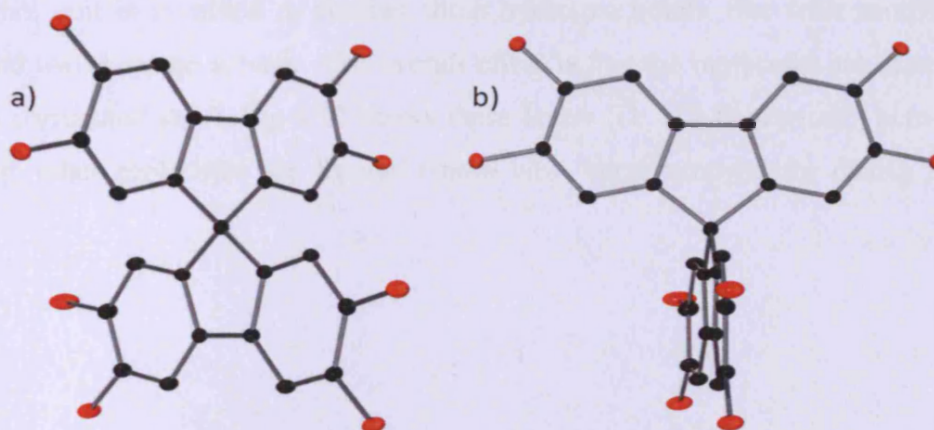


Fig 4.10 ORTEP projections of the molecular structure of the 2,2',3,3',6,6',7,7'-octahydroxy-9,9'-spirobisfluorene monomer (**41**).

The 2,2',3,3',6,6',7,7'-octahydroxy-9,9'-spirobisfluorene molecules (**41**) form an extended network through hydrogen bonding (Fig 4.11 c). Fig 4.11 a) and b) show the patterns of hydrogen bonds formed in the two different directions of the network as seen along the *b* and *a* axes respectively.

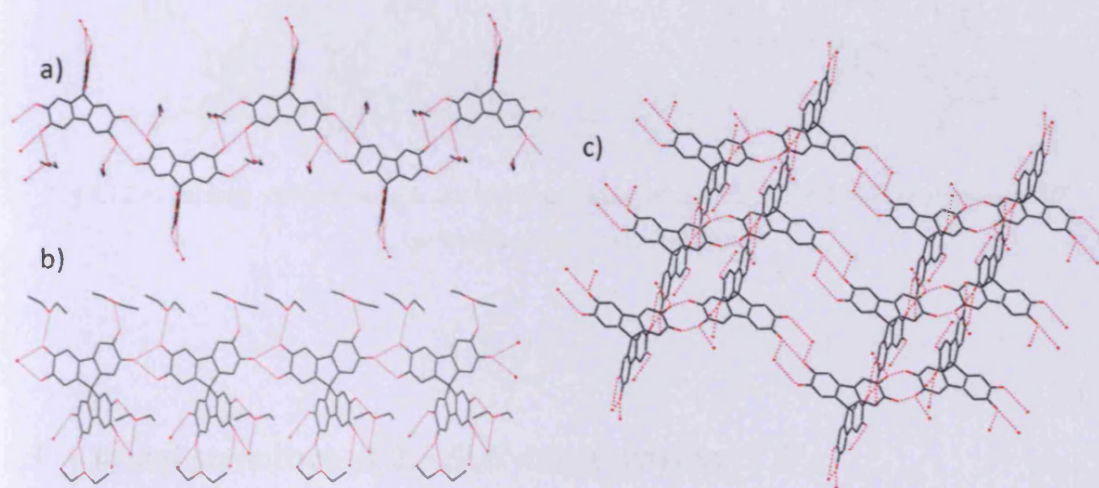


Fig 4.11 a) Hydrogen bonding, viewed along *b*-axis and b) along *a* axis; c) network formed by the H-bonding for the 2,2',3,3',6,6',7,7'-octahydroxy-9,9'-spirobisfluorene monomer (**41**).

Focussing on Fig 4.12 a) it can be seen that that one catechol moiety on one side of the molecule forms two hydrogen bonds with the catechol of the neighbouring spirobisfluorene **41** and two further H-bonds with included diethyl ether. On the opposite side of the molecule the catechol unit is involved in another three hydrogen bonds, one with another catechol moiety and two with the solvent. The overall effect is that the molecules are linked together to form a corrugated sheet. Fig 4.12 shows these layers (i.e. a 2-D network), between which the diethyl ether molecules are located (these have been removed for clarity from these pictures).

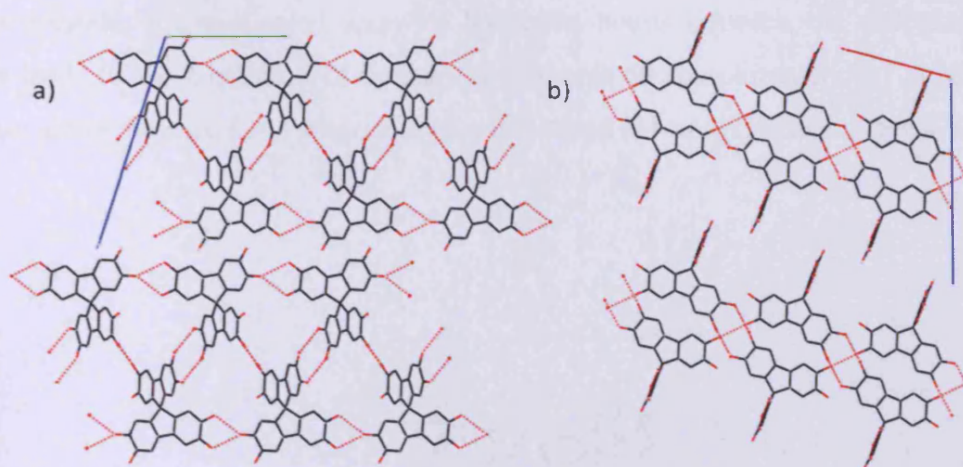


Fig 4.12 a) packing viewed along b and b) along a axes for the 2,2',3,3',6,6',7,7'-octahydroxy-9,9'-spirobisfluorene monomer (**41**).

4.1.5 Crystal structure of 2,3,5',6'-tetrahydroxy-2',3'-dihydrospiro[fluorene-9,1'-indene] (**44**).

The 2,3,5',6'-tetrahydroxy-2',3'-dihydrospiro[fluorene-9,1'-indene] monomer (**44**) was crystallized by slow diffusion of hexane into diethyl ether solution and forms a clathrate with a hexagonal unit cell belonging to the space group $P6_1$ with a cell parameter [$a = 16.8770(11)$, $b = 16.8770(14)$, $c = 11.3790(9)$ Å; $\alpha = \beta = 90$, $\gamma = 120$; volume = 2806.89 Å³]. There are six molecules of monomer per unit cell together with some delocalised solvent, which could not be well-defined. The molecular structure derived from the first monomer is shown in Fig 4.13.

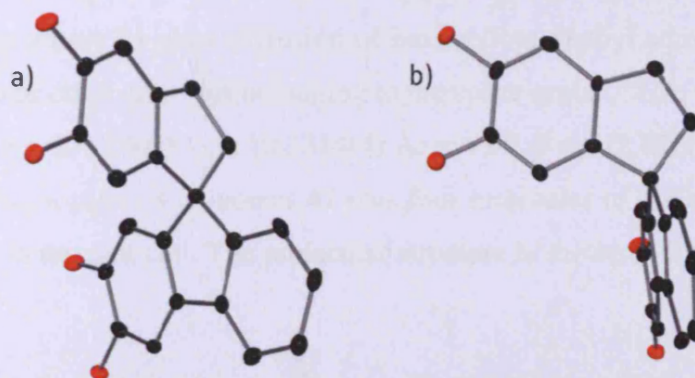


Fig 4.13 ORTEP projections of the molecular structure of 2,3,5',6'-tetrahydroxy-2',3'-dihydrospiro[fluorene-9,1'-indene] monomer (**44**).

In these crystals, a complicated array of hydrogen bonds between the different catechol moieties leads to the formation of hexagonal channels of approximately 8.7 Å in diameter which run along the *c* axis and where the poorly defined solvent is included (Fig 4.14).

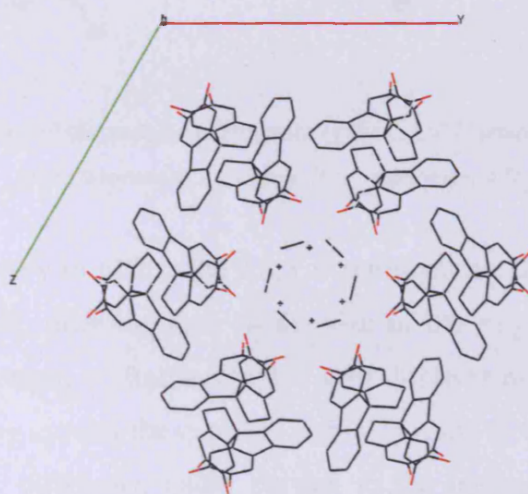


Fig 4.14 View of hexagonal channels along *c*-axis for 2,3,5',6'-tetrahydroxy-2',3'-dihydrospiro[fluorene-9,1'-indene] monomer (**44**) crystals.

4.1.6 Crystal structure of 2,3,6',7'-tetrahydroxy-3',4'-dihydro-2'H-spiro[fluorene-9,1'-naphthalene] (**45**).

Crystals of the 2,3,6',7'-tetrahydroxy-3',4'-dihydro-2'H-spiro[fluorene-9,1'-naphthalene] monomer (**45**) were grown by slow diffusion of hexane into diethyl ether solution. They are clathrates with a monoclinic unit cell belonging to the space group *P21/c* with cell parameters of [$a = 8.4384(3)$, $b = 27.7052(13)$, $c = 10.3314(4)$ Å; $\alpha = 90$, $\beta = 112.216(2)$ $\gamma = 90$; volume = 2236.05 Å³]. Four molecules of monomer **47** plus four molecules of diethyl ether as included solvent are present in the unit cell. The molecular structure is shown in Fig 4.15.

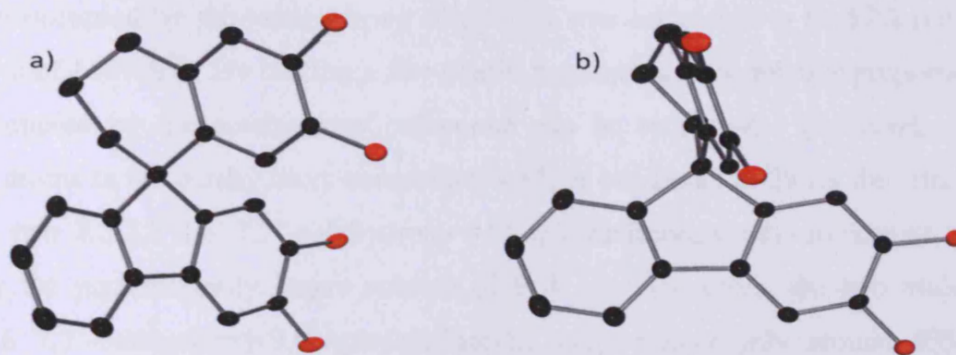


Fig 4.15 ORTEP projections of the molecular structure of the 2,3,6',7'-tetrahydroxy-3',4'-dihydro-2'H-spiro[fluorene-9,1'-naphthalene] monomer (45).

This monomer, although very similar to the 2,3,5',6'-tetrahydroxy-2',3'-dihydrospiro[fluorene-9,1'-indene] monomer (44), differing only in the size of the ring that completes the spiro-centre opposite to the fluorene, crystallises with a very different packing arrangement. In this case the hydrogen bonding around the catechol moieties leads to the formation of helices as shown in Fig 4.16. This difference could be due to the increased flexibility of the six-membered ring with consequent loss of symmetry.

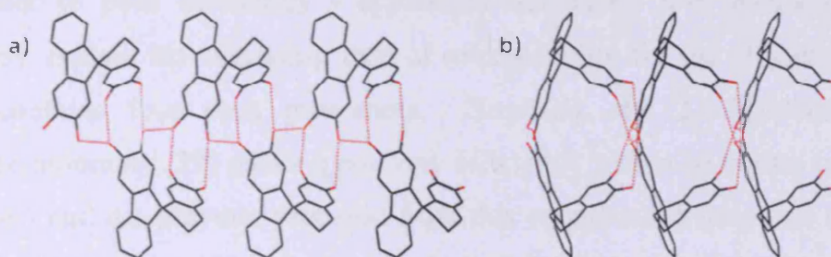


Fig 4.16 View of "helices" along a and c axes for the 2,3,6',7'-tetrahydroxy-3',4'-dihydro-2'H-spiro[fluorene-9,1'-naphthalene] monomer (45).

4.1.7 Summary of crystal studies

It is of particular interest to compare the proportion of the crystal occupied by the host framework of 2,2',3,3',6,6',7,7'-octahydroxy-9,9'-spirobisfluorene (41) with that of the related 3,3',6,6'-tetrahydroxy-9,9'-spirobisfluorene reported by Wuest and co-workers^[71]. The unit cells of both crystals contain two spirobisfluorene hosts with the former possessing 8 molecules of diethyl ether and the latter four molecules of ethyl acetate. The proportion of

the crystal occupied by the tetrahydroxy compound was calculated to be 57% (i.e. 803 Å³ from a total of 1409 Å³). By making a few simple assumptions, the relative proportion of the crystal occupied by the octahydroxy compound can be estimated. The number of non-hydrogen atoms in the octahydroxy compound is 33, as compared to 29 for the tetrahydroxy, therefore, two 2,2',3,3',6,6',7,7'-octahydroxy-9,9'-spirobisfluorene (**41**) molecules are likely to occupy the proportionally larger volume of 914 Å³. Therefore, the two molecules of 2,2',3,3',6,6',7,7'-octahydroxy-9,9'-spirobisfluorene (**41**) occupy only around 43% of the volume of the crystal unit cell ($V = 2106 \text{ Å}^3$). Independent calculations using CrystalMaker software (8.1) confirm that the solvent accessible void space is 58%. Only a few simple organic compounds occupy such a small proportion of their crystals, For example, the solvent accessible volume within the crystals of 2,2',3,3',6,6',7,7'-octahydroxy-9,9'-spirobisfluorene (**41**) exceeds even that of the much-studied urea clathrates (50%)^[71].

It would be misguided to draw any firm conclusions relating to the amorphous packing of the polymers described in Chapter 3 from the above crystal structures of their monomer precursors, nevertheless, some striking correlations can be made. The 2,3-dihydroxy-9,9'-spirobisfluorene monomer (**37**) contains only a small amount of included solvent (ratio of 2,3-dihydroxy-9,9'-spirobisfluorene:ethylacetate = 1:1) and the hydrocarbon portions of the monomer appear to pack efficiently - apparently helped by π - π interactions. Similar interactions may explain the surprising lack of microporosity for the oligomeric compound (**48**), which contains four such monomers. Similarly, the 2,2',3,3'-tetrahydroxy-9,9'-spirobisfluorene monomer (**39**) packs space very efficiently within its crystal (with the aid of water molecules) and the polymer prepared from this compound displays no microporosity. In contrast, large amounts of solvent are included within the crystals of monomers 2,2',3,3',6,6',7,7'-octahydroxy-9,9'-spirobisfluorene monomer (**40**) and 2,2',3,3',6,6',7,7'-octahydroxy-9,9'-spirobisfluorene (**41**) and the polymers derived from these monomers are highly microporous. Therefore, it could be argued that the H-bonding systems within these monomer crystals provide a non-covalent analogy to the covalent framework of the related polymer that they are used to prepare. Although the long-range order found in the crystals will be absent in the amorphous polymers, the local structure, based on similar intermolecular interactions, could be related. This hypothesis could be tested further by considering the clathrate-forming ability of other catechol-containing monomers and relating this to their utility in PIM formation. As a final observation it should be noted that the successful PIM monomers 5,5',6,6'-tetrahydroxy-3,3',3',3'-tetramethyl-1,1'-spirobisindane (**A1**)^[69] and

2,3,6,7,2,13-hexahydroxy-9,10-diethyltritycene both form clathrate crystals with large amounts of included solvent. [B.S. Ghanem and N. B. McKeown, personal communication]

4.2 Summary of crystal data

A summary of the collected data from single crystal XRD measurements is presented in Table 4.1.

Monomer	Solvent of crystallization	Symmetry/ Space group	Cell dimensions	Cell angles	Z
2,3-dihydroxy-9,9'- spirobisfluorene (37)	EtOAc/Hexane	Monoclinic <i>C2/c</i>	$a = 11.4117(4)$ $b = 13.9975(5)$ $c = 28.7524(11)$	$\alpha = 90$ $\beta = 90.556(2)$ $\gamma = 90$	8
2,2',3,3'-tetrahydroxy-9,9'- spirobisfluorene (39)	THF/Hexane	Tetragonal <i>P4₁2₁2</i>	$a = 10.075(4)$ $b = 10.075(4)$ $c = 18.7841(7)$	$\alpha = \beta = \gamma = 90$	4
2,2',3,3',6,7-hexahydroxy- 9,9'-spirobisfluorene (40)	THF/Hexane	Triclinic <i>P-1</i>	$a = 10.7693(3)$ $b = 18.4510(6)$ $c = 19.3503(6)$	$\alpha = 83.138(2)$ $\beta = 84.762(2)$ $\gamma = 80.120(2)$	4
2,2',3,3',6,6',7,7'- octahydroxy-9,9'- spirobisfluorene (41)	EtO ₂ /Hexane	Triclinic <i>P-1</i>	$a = 10.7693(3)$ $b = 18.4510(6)$ $c = 19.3503(6)$	$\alpha = 83.138(2)$ $\beta = 84.762(2)$ $\gamma = 80.120(2)$	4
2,3,5',6'-tetrahydroxy-2',3'- dihydrospiro[fluorene-9,1'- indene] (44)	EtO ₂ /Hexane	Hexagonal <i>P6₁</i>	$a = 16.877(11)$ $b = 16.877(14)$ $c = 11.379(9)$	$\alpha = 90$ $\beta = 90$ $\gamma = 120$	6
2,3,6',7'-tetrahydroxy-3',4'- dihydro-2'H-spiro[fluorene- 9,1'-naphthalene] (45)	EtO ₂ /Hexane	Monoclinic <i>P2₁/c</i>	$a = 8.4384(3)$ $b = 27.7052(13)$ $c = 10.3314(4)$	$\alpha = 90$ $\beta = 112.216(2)$ $\gamma = 90$	4

Table 4.1 Summary of the collected crystallographic data reported in section 5.1

CHAPTER

5

5.1) Conclusions.....	84
5.2) Future work.....	84

Conclusions and future work

5.1 Conclusions

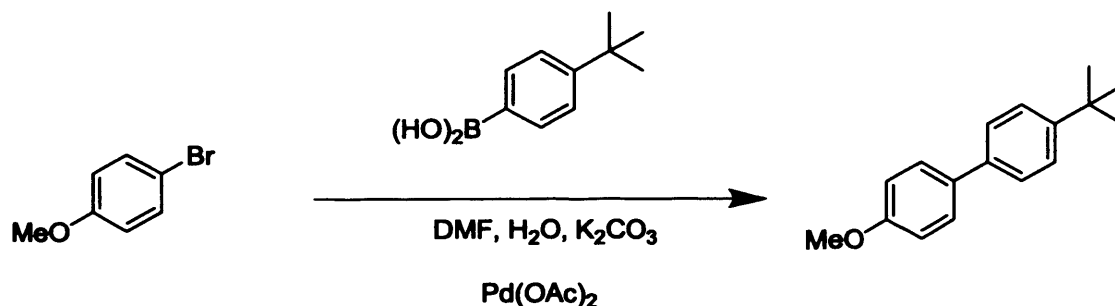
Chapter 2 described the strategy has been developed for the construction of novel spirobisfluorene-based monomers for making Polymers of Intrinsic Microporosity (PIMs). These monomers were subsequently polymerised, as described in Chapter 3, to give a range of network and ladder polymers, the former of which possess microporosity as expected, whereas surprisingly, the latter do not. Although not proven by GPC analysis, due to their lack of solubility in a suitable solvent, their insolubility in common organic solvents gives a strong indication that the ladder polymers are of reasonably large molecular mass. Had only oligomers been formed it is likely that they would be soluble in solvents such as THF or CHCl_3 . The solubility of the ladder polymers in higher-boiling solvents such as DMSO, veratrole and quinoline suggests that the polymers have packed together in a dense arrangement of polymer chains, perhaps mediated by strong π - π interactions, which highly polar or aromatic solvents are able to disrupt. This dense packing, which also seems apparent in the tetrameric spirobisfluorene (**39**), is clearly incompatible with microporosity. The elucidation of the crystal structures sheds some light on the close-packing interactions of spirobisfluorene in the solid state. In contrast, the network polymers showed more promise in regards to microporous behaviour by providing materials with apparent BET surface areas in the range $500\text{-}1000\text{ m}^2\text{ g}^{-1}$. It would appear that the covalent network polymer structure disrupts the intermolecular interactions of the spirobisfluorene units and provides a more open structure.

5.2 Future work

The most pressing issue to be resolved with regards to the synthetic study, described in this thesis, is the estimation of the molecular mass of the ladder polymers. Gel Permeation Chromatography (GPC) is often the most convenient method of determining the average molecular mass of a polymer. However, this method relies of the polymer being soluble in a convenient solvent. Unfortunately, the GPC system of the McKeown group is not compatible with DMSO – the solvent, which is best for the ladder polymers. It is planned to have the

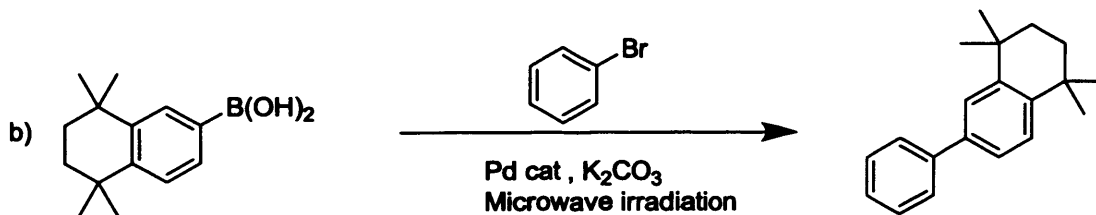
analysis done at a specialist laboratory such as a Smithers RAPRA lab. Analysis using viscometry would also be useful.

The synthetic chemistry used to form spirobisfluorene-based monomers could be applied to create a variety of interesting monomers. Based on the conclusion that the dense packing of the spirobisfluorene-based ladder polymers prevents the polymers from exhibiting microporous behaviour, it would be of interest to alter the structure of the monomers in order to prohibit the close interactions of the type observed in the crystal structures of the monomers that were highlighted in Chapter 4. It is anticipated that this could be achieved by two methods. Firstly, by attaching bulky substituents such as *t*-butyl groups onto the spirobisfluorene unit or, secondly, by attaching similar groups onto the fluorinated monomer. The former could be achieved by adapting the chemistry developed during the course of this study. The report by Kang *et al.*^[78], from which the method of producing 3,4-dimethoxybiphenyl (7) was taken, also included a Suzuki coupling between 4-bromoanisole and 4-*t*-butylphenylboronic acid (Scheme 5.1). Using this method it should be possible to perform an analogous reaction utilising 3,4-bromoveratrole, from which could be made 3,3'-di-*t*-butyl-6,6',7,7'-tetrahydroxy-9,9-spirobisfluorene following the same procedures as described in Chapter 2.

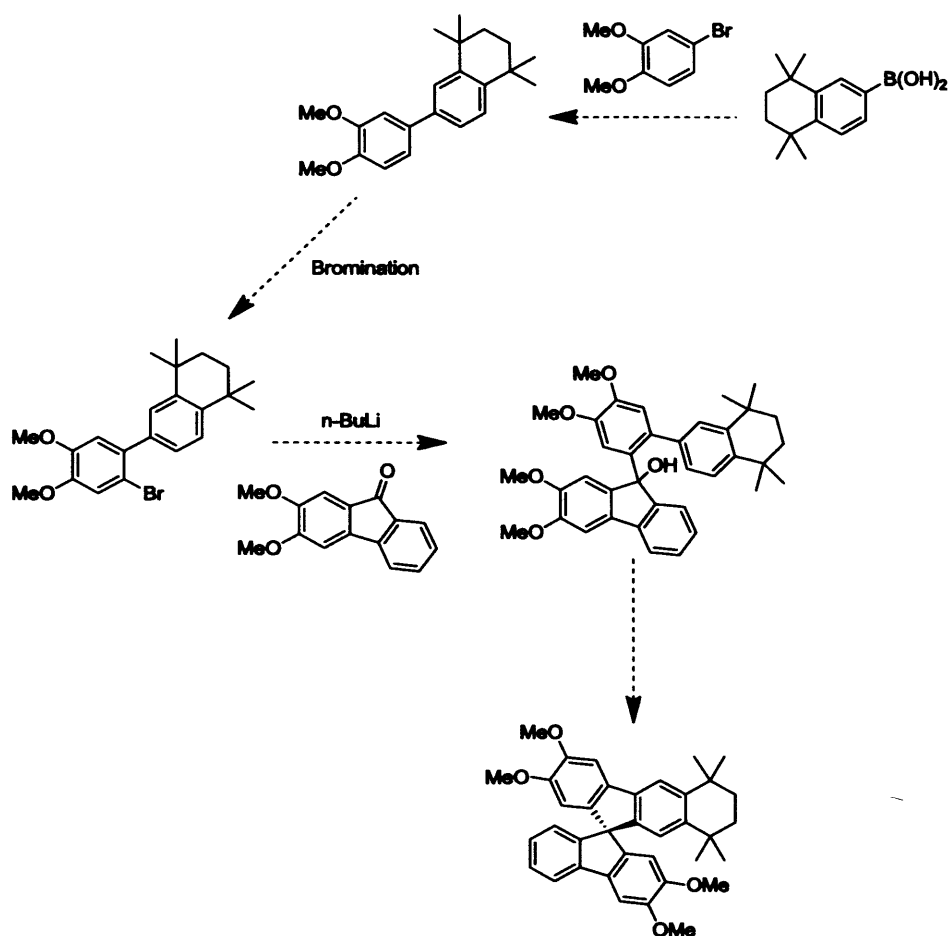


Scheme 5.1 Suzuki coupling reported by Kang *et al.*^[78]

Similarly, the 1,2,3,4-tetrahydro-1,1,4,4-tetramethyl naphthalene ring could be attached to a biphenyl to further increase the bulkiness of the resulting monomer following literature methods reported by Guilhemat *et al.*^[95] as shown in Scheme 5.2.

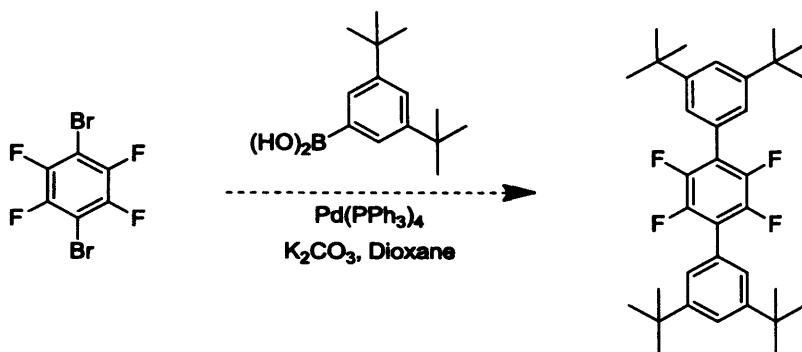


Scheme 5.2 1,2,3,4-tetrahydro-1,1,4,4-tetramethyl-6-phenyl-naphthalene synthesis reported by Guilhemat *et al.*^[95]



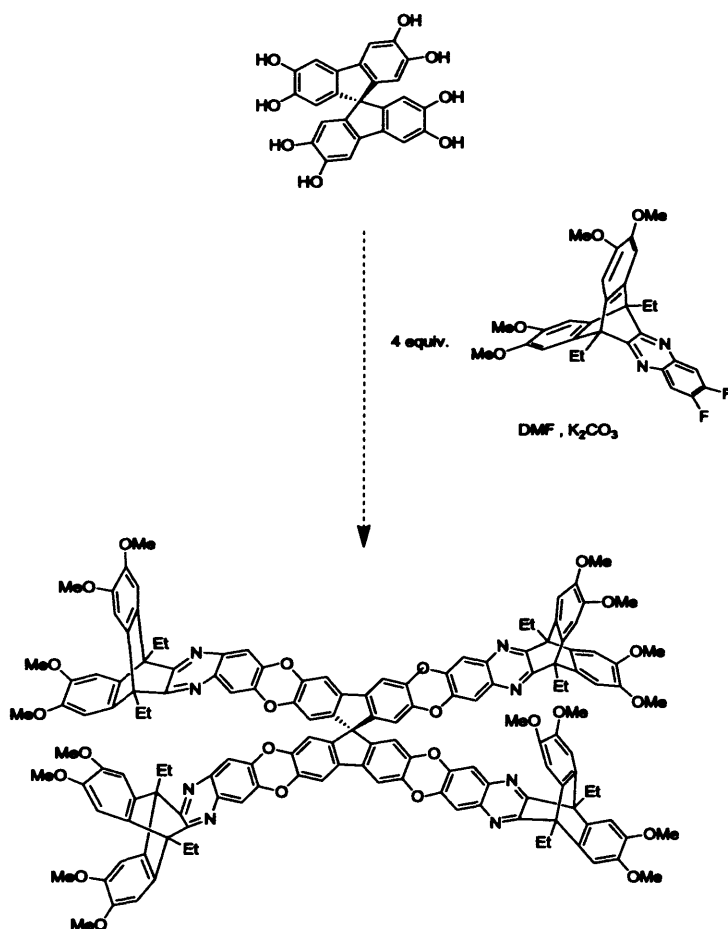
Scheme 5.3 Possible modifications to 2,2',3,3'-tetramethoxy-9,9'-spirobisfluorene to increase bulkiness and reduced π - π interactions between polymer chains.

A universal approach to decreasing the packing efficiency of the ladder polymers would be the utilization of fluorine-containing monomers that contain bulky groups, which could be synthesised using similar chemistry to that recently reported by Lin *et al.*^[96] and shown in Scheme 5.4. The reactivity of this monomer would be reduced as compared to that of 2,3,5,6-tetrafluoroterephthalonitrile (TFPN), however, it may be reactive enough to allow polymer formation from catechol-based monomers.



Scheme 5.4 Synthesis of bulky fluorine based monomer based on work reported by Lin et al.^[96]

Following the success of the 2,2',3,3',6,6',7,7'-octahydroxy-9,9'-spirobisfluorene (**41**) in producing microporous polymers, and its interesting crystal motif revealed by the crystallography study in Chapter 4, it would seem reasonable to further explore the potential of this monomer as a building unit for microporous materials. This could include its use as a core for possible OMIMs and dendrimers such as the trypticene-based OMIM shown in Fig 5.1.



Scheme 5.5 Proposed OMIM derived from 2,2',3,3',6,6',7,7'-octahydroxy-9,9'-spirobisfluorene as the core unit.

During the course of the viva process the issue of diastereoisomer generation was raised in regards to 1-(4,5-dimethoxybiphenyl-2-yl)-5,6-dimethoxy-3-phenyl-2,3-dihydro-1*H*-inden-1-ol (22) and 6,12-dihydroxy-6,12-bis(4,5-dimethoxybiphenyl-2-yl)-6,12-dihydroindeno[1,2-*b*]fluorene (26) was raised. Due to an oversight only one diastereoisomer from each reaction was collected from flash chromatography and reported. At this point in the project it was not feasible to return to the lab to identify exactly which diastereoisomer was obtained via a polarimetry analysis. It would therefore be beneficial to repeat the synthesis of 1-(4,5-dimethoxybiphenyl-2-yl)-5,6-dimethoxy-3-phenyl-2,3-dihydro-1*H*-inden-1-ol (22) and 6,12-dihydroxy-6,12-bis(4,5-dimethoxybiphenyl-2-yl)-6,12-dihydroindeno[1,2-*b*]fluorene (26) and collect both diastereoisomers. Having collected both diastereoisomers, a study could be conducted with regards to the effect of generating a polymer from monomers derived from each diastereoisomer on polymer performance. Subsequently these results could be compared to the results obtained from analysis of a polymer formed from a monomer which was been derived from the cyclization of a 50:50 mixture of both diastereoisomers. Depending on the results this line of enquiry could generate important information pertaining to the effect of stereochemistry within a monomer on the physical properties of the bulk polymer from which it is derived.

CHAPTER

6

6.1) Experimental techniques.....	90
6.2) Synthesis.....	92

Experimental

6.1 Experimental techniques

6.1.1 General remarks

Commercially available reagents were used without further purification. Anhydrous dichloromethane was obtained by distillation over calcium hydride under nitrogen atmosphere. Dry tetrahydrofuran was obtained by pre-drying commercially available tetrahydrofuran over sodium in presence of sodium benzophenone as indicator. Anhydrous *N,N*-dimethylformamide was bought from Aldrich. All reactions using air/moisture sensitive reagents were performed in oven-dried or flame-dried apparatus, under a nitrogen atmosphere. TLC analysis refers to analytical thin layer chromatography, using aluminum-backed plates coated with Merck Kieselgel 60 GF₂₅₄. Product spots were viewed either by UV fluorescence, or by staining with a solution of Cerium Sulfate in aqueous H₂SO₄. Flash chromatography was performed on silica gel 60A (35-70 micron) chromatography grade (Fisher Scientific). Under vacuum refers to evaporation at reduced pressure using a rotary evaporator and diaphragm pump, followed by the removal of trace volatiles using a vacuum oven. Melting points were recorded using a Gallenkamp Melting Point Apparatus and are uncorrected.

6.1.2 InfraRed spectra (IR)

Infrared spectra were recorded in the range 4000-600 cm⁻¹ using a Perkin-Elmer 1600 series FTIR instrument either as a thin film or as a nujol mull between sodium chloride plates. All absorptions are quoted in cm⁻¹.

6.1.3 Nuclear Magnetic Resonance (NMR)

¹H NMR spectra were recorded in CDCl₃ (unless otherwise stated) using an Avance Bruker DPX 400 instrument (400 MHz) or an Avance Bruker DPX 500 (500 MHz), with ¹³C NMR spectra recorded at 100 MHz or 125 MHz respectively. Chemical shifts (δ_H and δ_C) were recorded in parts per million (ppm) from tetramethylsilane (or chloroform) and are corrected

to 0.00 (TMS) and 7.26 (CHCl₃) for ¹H NMR and 77.00 (CHCl₃), centre line, for ¹³C NMR. The abbreviations s, d, t, q, m and br. denote singlet, doublet, triplet, quartet, multiplet and broadened resonances; all coupling constants were recorded in hertz (Hz).

6.1.4 Mass spectrometry

Low-resolution mass spectrometric data were determined using a Fisons VG Platform II quadrupole instrument using electrospray ionisation (ES) unless otherwise stated.

High-resolution mass spectrometric data were obtained in electrospray (ES) mode unless otherwise reported, on a Waters Q-TOF micromass spectrometer.

6.1.5 Nitrogen adsorption/desorption

Low-temperature (77 K) N₂ adsorption/desorption measurements of PIM powders were made using a Coulter SA3100. Samples were degassed for 800 min at 120 °C under high vacuum prior to analysis.

6.1.6 Thermo Gravimetric Analysis (TGA)

The TGA was performed using the device Thermal Analysis SDT Q600 at a heating rate of 20 °C/min from room temperature to 1000 °C.

6.1.7 X-Ray Diffraction (XRD)

X-Ray measurements were made in Cardiff using a Bruker-Nonius Kappa CCD area-detector diffractometer equipped with an Oxford Cryostream low temperature cooling device operating at 150(2) K ($\lambda = 0.71073 \text{ \AA}$).

6.1.8 MALDI-TOF

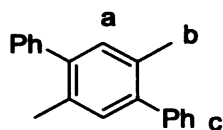
MALDI-TOF analyses were performed with a Waters MALDI Micro MX spectrometer.

6.1.9 Elemental analysis

Elemental analyses were obtained using a Carlo Erba Instruments CHNS-O EA 108 elemental analyzer.

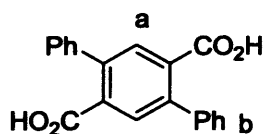
6.2 Synthesis

6.2.1 Dimethyl-*p*-terphenyl (1)



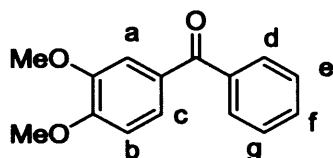
A flask was flushed with nitrogen and charged with 2,5-dibromo-*p*-xylene (1.08 g, 4.1 mmol), phenylboronic acid (1.00 g, 8.2 mmol) (**SM1**), Pd(OAc)₂ (1.7 mg, 0.2 mol%), potassium carbonate (2.62 g, 18.95 mmol), and butyl ammonium bromide (2.43 g, 7.58 mmol). Water (8.3 mL), degassed via nitrogen bubbling, was added and the suspension was stirred for half an hour. The mixture was heated to 70 °C and stirred for 2 h under nitrogen, cooled, diluted with water (20 mL), and extracted with toluene (5 x 10 mL). The combined organic extracts were dried over magnesium sulphate and the solvent was removed under reduced pressure, yielding 0.93 g of dimethyl-*p*-terphenyl (**1**) as a white powder (95% yield); m.p. = 181 – 182 °C (lit.^[91]; m.p. = 182 -184 °C); ¹H NMR (400 MHz, CDCl₃): δ_H 7.45-7.32 (m, 10H, H_c), 7.15 (s, 2H, H_a), 2.35 (s, 6H, H_b). LRMS (EI): m/z (%): 258 (M⁺); in accordance with literature data^[91].

6.2.2 2,5-Diphenylterephthalic acid (2)



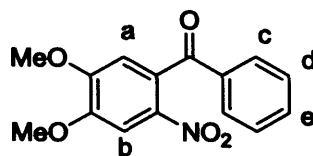
A sample of dimethyl-*p*-terphenyl (1.50 g, 4.71 mmol) (**1**) was dissolved in pyridine (19 mL) and water (1.8 mL) containing potassium permanganate (2.30 g). The mixture was refluxed and potassium permanganate (1.00 g) in water (3.0 mL) was added every half an hour for 2 h. After 5 h, water (40 mL) was added and the reaction was refluxed overnight. The mixture was filtered hot and washed with boiling water (100 mL), concentrated and acidified with 2M HCl (50 mL). 2,5-Diphenylterephthalic acid (**2**) was collected via filtration and dried in a vacuum oven at 80 °C. (1.38 g, 92% yield); m.p. = 288 – 290 °C (lit.^[91]; m.p. = 291 °C); ¹H NMR (400 MHz, DMSO-*d*₆): δ_H 7.73 (s, 2H, H_a), 7.52-7.41 (m, 10H, H_b); LRMS (EI): *m/z* (%): 318 (M⁺); in accordance with literature data^[91].

6.2.3 3,4-Dimethoxybenzophenone (**3**)



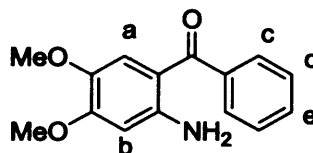
Benzoic acid (14.90 g, 121.97 mmol) was dissolved in a minimum amount of DCM (15 mL). The solution was diluted with veratrole (16.39 mL, 128.07 mmol) (**SM4**) and PPA (85 g) added. The mixture was refluxed at 85 °C for 24 h while stirring. The reaction was quenched in ice-cold water (300 mL) and stirred at 80 °C for a further 2 h. The precipitate was filtered and washed with water (3 x 150 mL). The precipitate was crystallised from ethanol and dried in a vacuum oven at 80 °C overnight. Light yellow crystals of 3,4-dimethoxybenzophenone (**3**) were obtained (23.64 g, 80% yield); m.p. = 93 - 95 °C (lit.^[97]; m.p. = 94 - 96 °C); IR (film)/cm⁻¹: 3000, 2940, 2840, 1660, 1580, 1480, 1320, 1250, 1180, 1030, 964, 814, 770, 690; ¹H NMR (400 MHz, CDCl₃) δ_H : 7.76 (dd, J_{de} = 8.3 Hz, J_{df} = 1.4 Hz, 2H, H_d), 7.57 (ddt, J_{ef} = 8.3 Hz, J_{fg} = 6.6 Hz, J_{df} = 1.4 Hz, 1H, H_f), 7.52-7.44 (m, 2 H, H_e, H_g), 7.50 (d, J_{ac} = 1.8 Hz, 1 H, H_a), 7.38 (dd, J_{bc} = 8.4 Hz, J_{ac} = 1.8 Hz, 1 H, H_c), 6.89 (d, J_{bc} = 8.4 Hz, 1H, H_b), 3.96 (s, 3H, OMe), 3.94 (s, 3H, OMe); ¹³C NMR (100 MHz, CDCl₃) δ_C : 195.6 (C=O), 153.0, 149.0, 138.3, 131.9, 130.2, 129.7, 128.2, 125.5, 112.1, 109.7 (Aryl), 56.1, 56.0 (OMe); LRMS (EI): *m/z*: 242 (M⁺, 100%).

6.2.4 2-Nitro-4,5-dimethoxybenzophenone (4)



A sample of 3,4-dimethoxybenzophenone (10.44 g, 43.08 mmol) (3) was dissolved in the minimum amount of methanol (25 mL). A 1:1 mixture of conc. nitric acid: conc. sulphuric acid (120 mL) was added to the solution and was refluxed for 48 h. The reaction was quenched in ice-cold water and stirred for 1 h. The precipitated was filtered with water (3 x 150 mL) and recrystallized from ethanol. Yellow crystals of 2-nitro-4,5-dimethoxybenzophenone (4) were obtained. (10.52 g, 85% yield); m.p. = 136 - 137 °C (lit.^[86]; m.p. = 136 -138 °C); IR (film)/cm⁻¹: 1671, 1576, 1519, 1447, 1390, 1334, 1290, 1225, 1180, 1064, 994, 875, 833, 790, 758, 720, 689, 633, 616; ¹H NMR (400 MHz, CDCl₃) δ_H 7.77–7.74 (m 2H, H_c), 7.74 (s, 1H, H_b), 7.60–7.55 (m, 1H, H_c), 7.47–7.42 (m, 2H, H_d), 6.87 (s, 1H, H_a), 4.04 (s, 3H, OMe), 3.97 (s, 3H, OMe); ¹³C NMR (100 MHz, CDCl₃) δ_C : 193.4 (C=O), 154.0, 149.6, 139.4, 136.1, 133.7, 130.4, 129.0, 128.8, 109.9, 106.9 (Aryl), 56.7, 56.6 (OMe); LRMS (EI): *m/z*: 287 (M⁺, 100%).

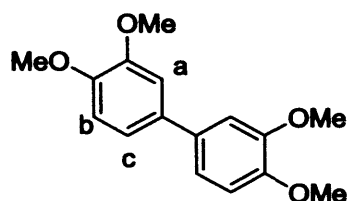
6.2.5 2-Amino-4,5-dimethoxybenzophenone (5)



A mixture of 2-nitro-4,5-dimethoxybenzophenone (10.00 g, 34.81 mmol) (4), iron powder (18.00 g), AcOH (65 mL), water (90 mL), and ethyl acetate (18 mL) was refluxed for 6 h. The reaction mixture was neutralised with NaHCO₃ until pH = 7. The residue was filtered and washed with ethyl acetate (3 x 150 mL). The aqueous solution was extracted with ethyl acetate (5 x 50 mL) and the combined organic extracts were washed with brine. The organic extract was dried over MgSO₄ and purified by flash chromatography using a 3:7 ethyl acetate to hexane elutant. Luminous yellow crystals of 2-amino-4,5-dimethoxybenzophenone (5) were obtained as (7.17 g, 80% yield); m.p. 78–80 °C (lit.^[86]; m.p. = 78-80 °C); IR (film)/cm⁻¹: 3426, 3314, 1627, 1588, 1530, 1510, 1461, 1446, 1396, 1320, 1249, 1126, 832, 699; ¹H NMR (400 MHz, CDCl₃) δ_H 7.63–7.61 (m, 2H, H_c), 7.53–7.43 (m, 3H, H_d, H_e), 6.94 (s, 1H,

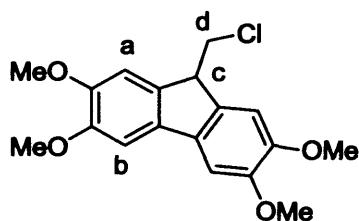
H_a), 6.22 (br s, 2H, NH₂), 6.21 (s, 1H, H_b), 3.91 (s, 3H, OMe), 3.66 (s, 3H, OMe); ¹³C NMR (125 MHz, CDCl₃): δ_C 197.7 (C=O), 155.8, 148.8, 141.1, 141, 131.0, 129.1, 128.5, 116.9, 110.4, 99.7 (Aryl), 56.9, 56.3 (OMe); LRMS (EI): *m/z*: 257 (M⁺, 100%).

6.2.6 3,3',4,4'-Tetramethoxybiphenyl (6)



A sample of 4-bromoveratrole (25.00 g, 115.18 mmol) (SM2), and distilled THF (40 mL) were added to a flame dried flask under nitrogen atmosphere. *n*-Butyl lithium (2.5M, 23.00 mL, 57.59 mmol) was added drop wise to the mixture at -78 °C. The temperature was maintained for 2 h, and then subsequently allowed to reach room temperature and stirred overnight. The resulting yellow suspension was concentrated under vacuum and crystallised from ethanol to give 3,3',4,4'-tetramethoxybiphenyl (6) (10.42 g, 66% yield); m.p. = 129-131 °C (lit.^[98]; m.p. = 130-132 °C); IR (film)/cm⁻¹: 3100, 3094, 3022, 3002, 2990, 2913, 2821, 1606, 1595, 1502, 1445, 1438, 1398, 1250, 1208, 1181, 1133, 1048, 1010, 981, 870, 801, 755, 620; ¹H NMR (500 MHz, CDCl₃): δ_H 7.11 (dd, *J*_{bc} = 7.6 Hz, *J*_{ac} = 1.4 Hz, 2H, H_c), 7.07 (d, *J*_{ac} = 1.4 Hz, 2H, H_a), 6.95 (d, *J*_{bc} = 7.6 Hz, 2H, H_b) 3.98 (s, 3H, OMe), 3.96 (s, 3H, OMe); ¹³C NMR (125 MHz, CDCl₃): δ_C 149.2, 148.4, 134.3, 119.2, 111.6, 110.5 (all aryl), 56.1, 56.0 (OMe). LRMS (EI): *m/z*: 274 (M⁺, 100 %).

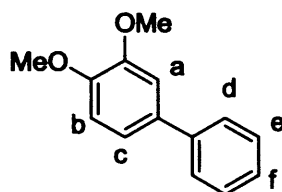
6.2.7 9-(Chloromethyl)-2,3,6,7-tetramethoxy-9H-fluorene (7)



3,3',4,4'-Tetramethoxybiphenyl (1.03 g, 3.97 mmol) (6) was dissolved in glacial acetic acid (20 mL) and cooled in an ice bath. Chloroacetaldehyde diethyl ester (0.61 g, 3.97 mmol) was added to the mixture and stirred for half an hour. A 1:1 (by volume) mixture of conc. sulphuric acid and glacial acetic acid (20 mL) was added drop wise so that the temperature of

the mixture was maintained within a 5-10 °C range for approx. 2 h. The mixture was then stirred at room temperature for 20 h. The mixture was diluted in ice cold water (150 mL) and extracted with ethyl acetate (3 x 20 mL). The organic phase was dried over magnesium sulphate, filtered, and concentrated on a rotary evaporator. The crude grey powder obtained was the crystallised from ethanol to give 9-(chloromethyl)-2,3,6,7-tetramethoxy-9H-fluorene (**7**) (0.88 g, 66% yield) as light yellow granular crystals; m.p = 204–206 °C (lit.^[88]; m.p. = 205–206 °C); IR (film)/cm⁻¹: 3071, 2997, 2952, 2836, 1606, 1505, 1470, 4788. 1441, 1415, 1319, 1302, 1280, 1258, 1228, 1213, 1201, 1178, 1147, 1135, 1117, 1035, 1017, 968, 877, 862, 834, 797, 777, 669; ¹H NMR (500 MHz, CDCl₃): δ_H 7.15 (s, 2H, H_b), 7.08 (s, 2H, H_a), 4.00 (t, J_{cd} = 3.5 Hz, 1H, H_c), 3.92 (s, 3H, OMe), 3.88 (s, 3H, OMe) 3.78 (d, J_{cd} = 3.5 Hz, 2H, H_d); ¹³C NMR (125 MHz, CDCl₃): δ_C 149.6, 148.1, 136.6, 134.2, 108.5, 102.4 (all aryl), 56.3, 56.2 (OMe), 49.0, 47.6 (Alkyl); LRMS (EI): m/z : 334 (M⁺, 100 %).

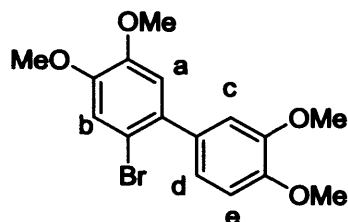
6.2.8 3,4-Dimethoxybiphenyl (**8**)



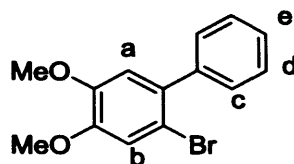
4-Bromo-1,2-dimethoxybenzene (15.00 g, 69.11, mmol) (**SM2**) and phenylboronic acid (8.43 g, 69.11 mmol) (**SM1**) were dissolved in a 1:2 mixture of water (25 mL) and DMF (50 mL) that was previously degassed by nitrogen bubbling. Na₂CO₃ (36.62 g, 345.55 mmol) was added followed by Pd(OAc)₂ (0.5% mol, 0.078 g) and the mixture was stirred for 24 h at room temperature. The reaction was quenched with HCl (50 mL, 2.0M) and extracted with ethyl acetate (3 x 20 mL). The organic extracts were filtered through celite filter aid and dried over MgSO₄ and reduced in volume under rotary evaporation. The oily residue was dissolved in a minimum amount ethanol and diluted with water until a white precipitate began to appear. The solution was warmed until the white precipitate dissolved and the solution was allowed to evaporate overnight. White crystals of 3,4-dimethoxybiphenyl (**8**) as were obtained (13.33 g, 90% yield); m.p. = 68-70 °C (lit.^[78]; m.p. = 68-71 °C); IR (film)/cm⁻¹: 3064, 2837, 1606, 1574, 1522, 1443, 1408, 1325; ¹H NMR (400 MHz, CDCl₃): δ_H : 7.55 (m, 2H, H_d), 7.42 (t, J_{ef} = 7.2 Hz, 2H, H_e), 7.33 (m, 1H, H_f), 7.16-7.10 (m, 2H, H_a, H_c), 6.94 (d, J_{bc} = 8.1 Hz, 1H, H_b), 3.95 (s, 3H, OMe), 3.92 (s, 3H, OMe); ¹³C NMR (100 MHz, CDCl₃):

δ_C 149.1, 148.6, 141.0, 134.2, 126.8, 128.7, 119.4, 111.5, 110.5 (Aryl), 55.9 (OMe); LRMS (EI): m/z : 214 (M^+ , 100%).

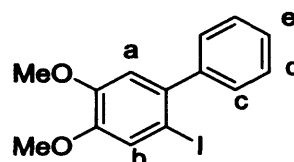
6.2.9 2-Bromo-3',4,4',5-tetramethoxybiphenyl (9)



A sample of 3,3',4,4'-tetramethoxybiphenyl (2.00 g, 7.29 mmol) (6) was dissolved in chloroform (10 mL) and cooled to 0 °C. Bromine (1.17 g, 7.29 mmol) dissolved in chloroform (20 mL) was added drop wise over 1 h and allowed to react for 4 h in total. The reaction was quenched with saturated sodium thiosulphate and stirred for a further hour. The organic layer was collected, dried over magnesium sulphate and reduced in volume under vacuum. The resulting brown viscous liquid was dissolved in ethanol and diluted in water (3:1 ethanol to water) and allowed to evaporate overnight. The resulting precipitate was collected and dried under vacuum to give 2-bromo-3',4,4',5-tetramethoxybiphenyl (9) (2.06 g, 80% yield); mp = 82-84°C (lit.^[99]; m.p. = 84-85 °C); IR (film)/cm⁻¹: 3059, 2964, 2938, 2910, 2838, 1603, 1519, 1505, 1489, 1441, 1379, 1208, 1020, 860, 770, 704; ¹H NMR (400 MHz, CDCl₃): δ_H 7.12 (s, 1H, H_b), 6.98 (dd, J_{de} = 7.6 Hz, J_{dc} = 1.4 Hz, 1H, H_d), 6.95 (d, J_{de} = 7.6 Hz, 1H, H_e), 6.94 (d, J_{dc} = 1.4 Hz, 1H, H_c) 6.88 (s, 1H, H_a), 3.98 (s, 3H, OMe), 3.97 (s, 3H, OMe), 3.96 (s, 3H, OMe), 3.90 (s, 3H, OMe); ¹³C NMR (125 MHz, CDCl₃): δ_C 148.6, 148.4, 148.3, 148.3, 134.6, 133.9, 121.7, 115.8, 114.0, 113.1, 112.7, 110.7 (all aryl), 56.3, 56.1, 56.0, 55.9 (OMe); LRMS (EI): m/z : 352 (⁷⁹Br M^+ , 35%) 354 (⁸¹Br M^+ , 35%).

6.2.10 2-Bromo-4,5-dimethoxybiphenyl (10)

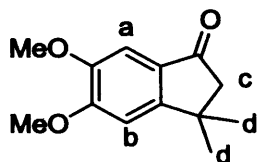
To a solution of 3,4-dimethoxybiphenyl (9.30 g, 43.5 mmol) (**8**) in CHCl_3 (150 mL) bromine (7.60 g, 47.9 mmol) was added drop-wise with stirring at 0 °C. The reaction was stirred for 24 h at room temperature, and then washed with an aqueous solution of sodium thiosulfate to eliminate excess of bromine. The organic layer was dried over magnesium sulfate, filtered and the solvent evaporated under vacuum. The crude compound was reprecipitated as a white solid (10.40 g, 82% yield) with MeOH from DCM; m.p. = 110 - 112 °C; IR (film)/ cm^{-1} 3059, 2964, 2938, 2910, 2838, 1603, 1519, 1505, 1489, 1441, 1379, 1208, 1020, 860, 770, 704; ^1H NMR (400 MHz; CDCl_3) δ_{H} 7.42 (m, 5H, H_{c} , H_{d} , H_{e}), 7.13 (s, 1H, H_{b}), 6.84 (s, 1H, H_{a}), 3.92 (s, 3H, OMe), 3.87 (s, 3H, OMe); ^{13}C NMR (100 MHz; CDCl_3) δ_{C} 148.7, 148.2, 141.0, 134.7, 129.5, 127.9, 127.4, 115.7, 113.8, 112.4 (Aryl), 56.2, 56.0 (OMe); LRMS, (EI^+), m/z : 292.01 ($^{79}\text{Br M}^+$, 35%), 294.01 ($^{81}\text{Br M}^+$, 35%).

6.2.11 2-Iodo-4,5-dimethoxybiphenyl (11)

A sample of 3,4-dimethoxybiphenyl (10.00 g, 46.67 mmol) (**8**), and iodine (5.92 g, 23.33 mmol) were dissolved in AcOH (120 mL) and refluxed. After 0.25 h of reflux, iodic acid (2.05 g, 11.67 mmol) dissolved in water (11.5 mL) was added drop-wise. The reaction was stirred under reflux for 5 h and quenched by addition of saturated sodium thiosulphate. The solution was cooled to 0 °C for 12 h and then filtered. The precipitate was recrystallised twice from ethanol to give 2-iodo-4,5-dimethoxybiphenyl (**11**) as pale yellow crystals (7.94 g, 50% yield); m.p. = 107-108 °C (lit.^[100]; m.p. = 107-108.5 °C); IR (film)/ cm^{-1} : 3061, 3055, 3011, 3000, 2943, 2935, 2905, 2836, 1594, 1561, 1505, 1486, 1463, 1438, 1374, 1325, 1254, 1237, 1207, 1172, 1073, 1030, 915, 891, 859, 786, 763, 732, 702, 629, 611; ^1H NMR δ_{H} 7.69 (s,

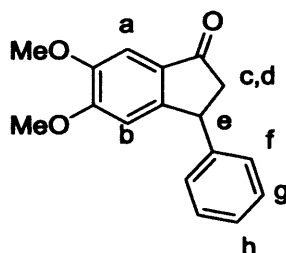
^1H , H_b), 7.28-7.40 (m, 5H, H_c , H_d , H_e), 7.05 (s, 1H, H_a), 3.92 (s, 3H, OMe), 3.90(s, 3H, OMe); ^{13}C NMR (100 MHz, CDCl_3) δ_{C} : 149.1, 148.7, 144.2, 139.3, 129.5, 128.0, 127.5, 121.7, 86.3 (Aryl), 56.2, 56.0 (OMe); LRMS, (EI^+), m/z : 340 (M^+ , 100%).

6.2.12 5,6-Dimethoxy-3,3-dimethyl-2,3-dihydro-1H-inden-1-one (12)



A mixture of veratrol (5.18 g, 37.5 mmol) (SM4) and 4,4-dimethyl-3-butanoic acid (6.42 g, 56.25 mmol) in 83% PPA (55 mL) was stirred at 60 °C for 15 h. The mixture was then poured into an ice/water mixture (1:1 125 mL) and stirred for half an hour. The product was extracted with diethyl ether (3 x 50 mL). The combined organic washings were washed with 2 M Sodium hydroxide (2 x 25 mL), water (25 mL) and brine (12.5 mL). The organic phase was dried over magnesium sulphate, reduced in volume under vacuum, resulting in viscous yellow oil. 5,6-Dimethoxy-3,3-dimethyl-2,3-dihydro-1H-inden-1-one (**12**) were obtained as yellow crystals via flash chromatography (elutants: dichloromethane followed by ethyl acetate) (6.22 g, 75% yield); m.p. = 68-69 °C (lit.^[101]; m.p. = 69-71 °C); IR (film)/ cm^{-1} : 3008, 2989, 2848, 2810, 1725, 1498, 1397, 1300, 1275, 1201, 1110, 1080, 1021, 858; ^1H NMR (500 MHz, CDCl_3): δ_{H} 7.05 (s, 1H, H_a), 6.79 (s, 1H, H_b), 3.92 (s, 3H, OMe), 3.82 (s, 3H, OMe), 2.50 (s, 2H, H_c), 1.33 (s, 6H, H_d); ^{13}C NMR (125 MHz, CDCl_3): δ_{C} 204.3 (C=O), 159.2, 155.7, 149.2, 128.2, 104.4, 103.9 (aryl), 56.2, 56.1 (OMe), 53.0 (CH_2), 38.2 (R_4C), 29.4 (2 x Me); LRMS, (EI^+), m/z : 220 (M^+ , 100%).

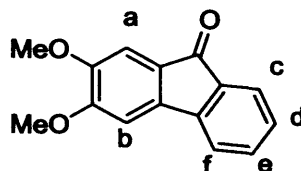
6.2.13 5,6-Dimethoxy-3-phenyl-2,3-dihydro-1H-inden-1-one (13)



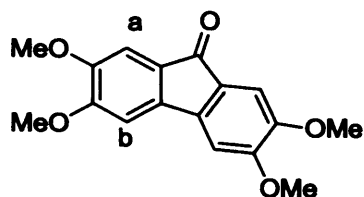
A solution of veratrol (12.31 g, 89.09 mmol) (SM4) and trans-3-phenylacrylic acid (12.00 g, 80.99 mmol) were dissolved in PPA (60 g) and stirred at 95 °C for 0.75 h. The reaction was

quenched by pouring into ice-cold water and warmed to 80 °C and stirred for 2 h. The precipitate was filtered, dried under vacuum and recrystallised from ethanol. 5,6-Dimethoxy-3-phenyl-2,3-dihydro-1*H*-inden-1-one (**13**) was obtained as light yellow crystals (16.73 g, 77% yield); m.p. = 106-107 °C (lit.^[90]; = 107-108 °C) ; IR (film)/cm⁻¹: 3086, 3012, 2981, 2885, 2831, 1696, 1601, 1498, 1482, 1478, 1411, 1366, 1301, 1242, 1230, 1200, 1113, 1048, 1019, 1002, 958, 939, 852, 798, 731; ¹H NMR (400 MHz, CDCl₃): δ_H 7.25 (t, J_{fg} = 7.0 Hz, J_{gh} = 6.3 Hz, 2H, H_g), 7.18 (t, J_{gh} = 6.3 Hz, 1H, H_h), 7.16 (s, 1H, H_b), 7.05 (d, J_{fg} = 7.0 Hz, 2H, H_f), 6.57 (s, 1H, H_a), 4.42 (dd, J_{ce} = 7.7 Hz, J = 3.3 Hz, 1H, H_e), 3.87 (s, 3H, OMe), 3.77 (s, 3H, OMe), 3.13 (dd, J_{cd} = 19.0 Hz, J_{ce} = 7.7 Hz, 1H, H_c), 2.56 (dd, J_{cd} = 19.0 Hz, J_{de} = 3.3 Hz, 1H, H_d) ¹³C NMR (100 MHz, CDCl₃): δ_C 205.1 (C=O), 156.2, 153.6, 150.2, 144.3, 130.3, 129.3, 128.0, 127.4, 107.8, 104.0 (Aryl), 56.7, 56.6 (OMe), 47.6, 44.6 (Alkyl); LRMS, (EI⁺), m/z : 268 (M⁺, 100%).

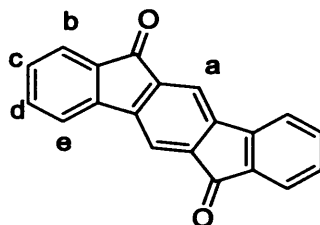
6.2.14 2,3-Dimethoxy-9*H*-fluoren-9-one (**14**)



A sample of 2-amino-4,5-dimethoxybenzophenone (6.00 g, 23.32 mmol) (**5**) was dissolved in a mixture of water (85 mL) and conc. HCl (30 mL) and cooled to 0 °C. NaNO₂ (1.87 g, 26.67 mmol) was added to the mixture and stirred for 1 h. The solution was filtered to remove excess NaNO₂ and the filtrate was added drop-wise to boiling water (85 mL) and stirred for 1 h. The precipitate was filtered and washed with water, dried in a vacuum oven and purified by flash chromatography. 2,3-Dimethoxy-9*H*-fluoren-9-one (**14**) was obtained as orange crystals (4.59 g, 82% yield); m.p. = 159-161 °C (lit.^[102]; m.p. = 160-161 °C); IR (film)/cm⁻¹: 3062, 3005, 2974, 2923, 2853, 2826, 1705, 1589, 1500, 1480, 1464, 1413, 1326, 1299, 1288, 1265, 1243, 1211, 1115, 1080, 1025, 1011, 989, 879, 859, 841, 798, 779, 764, 736, 714, 695, 664, 635, 612; ¹H NMR (500 MHz, CDCl₃): δ_H 7.49 (d, J_{ef} = 7.4 Hz, 1H, H_f), 7.33 (t, J_{ef} = 7.4 Hz, 1H, H_e), 7.29 (d, J = 7.4 Hz, 1H, H_c), 7.14 (s, 1H, H_b), 7.14 (t, J = 7.4 Hz, 1H, H_d), 6.97 (s, 1H, H_a), 3.97 (s, 1H, OMe), 3.87 (s, 1H, OMe); ¹³C NMR (125 MHz, CDCl₃): δ_C 154.6, 149.8, 144.0, 139.5, 134.2, 128.2, 126.9, 123.8, 119.1 (all aryl), 56.4, 56.3 (OMe); LRMS, (EI⁺), m/z : 240 (M⁺, 100%).

6.2.15 2,3,6,7-Tetramethoxy-9H-fluoren-9-one (15)

A sample of 9-(chloromethyl)-2,3,6,7-tetramethoxyfluorene (1.00 g, 2.98 mmol) (**7**) was dissolved in pyridine (19 mL) and water (0.90 mL), containing potassium permanganate (1.15 g). The mixture was refluxed and potassium permanganate (0.50 g) in water (1.50 mL) was added every half an hour for 2 h. After 5 h, water (20 mL) was added and the reaction was refluxed overnight. The mixture was then filtered and extracted with ethyl acetate (5 x 10 mL). The organic fractions were combined, dried over magnesium sulphate and reduced in volume under vacuum. The crude red solid was recrystallized from ethanol giving 2,3,6,7-tetramethoxy-9H-fluoren-9-one (**15**) as orange granular crystals (0.61 g, 68% yield); m.p. = 202 - 203 °C (lit.^[103]; m.p. = 202 - 203 °C); IR (film)/cm⁻¹: 3062, 3004, 2939, 2839, 1700, 1590, 1496, 1468, 1439, 1420, 1367, 1313, 1255, 1313, 1173, 1079, 1042, 1003, 978, 916, 876, 840, 780, 759, 728, 647, 593; ¹H NMR (500 MHz, CDCl₃): δ_H 7.08 (s, 2H, H_b), 6.84 (s, 2H, H_a) 3.95 (s, 6H, OMe) 3.84 (s 6H, OMe); ¹³C NMR (100 MHz, CDCl₃): δ_C 193.1 (C=O), 154.4, 149.3, 139.2, 127.6, 107.7, 103.4 (Aryl); 56.8, 56.7 (OMe); LRMS, (EI⁺), *m/z*: 300 (M⁺, 100%).

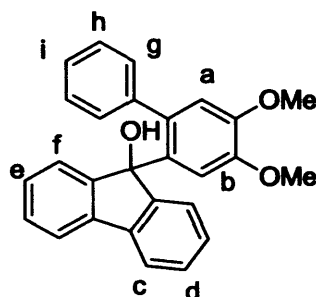
6.2.16 Indeno[1,2-*b*]fluorene-6,12-dione (16)

A sample of 2,5-diphenylterephthalic acid (2.00 g, 6.29 mmol) (**2**) was dissolved in small portions in conc. sulphuric acid (100 mL). The green mixture was stirred at room temperature

for 2 h. The mixture was then poured onto ice. The purple precipitate was filtered and washed with water. The precipitate was then stirred for 4 h in 3M potassium carbonate solution, filtered under pressure and dried in vacuum oven at 100 °C to afford (1.57 g, 88% yield) of indeno[1,2-*b*]fluorene-6,12-dione (**16**) as a purple solid; m.p. = 344–346 °C (lit.^[104], m.p. = 345–346 °C); IR (film)/cm⁻¹: 3045, 1714, 1602, 1470, 1429, 1289, 1269, 1179, 1123, 1086, 918; ¹H NMR (400 MHz, CDCl₃): δ_H 7.14 (s, 2H, H_a), 7.63 (d, *J* = 7.6 Hz, 2H, H_b), 7.52–7.48 (m, 4H, H_c, H_d), 7.31–7.28 (m, 2H, H_e); LRMS, (EI⁺), *m/z*: 282 (M⁺, 100%); in accordance with literature values^[91].

General procedure for organolithium initiated halo biaryl nucleophilic addition to a ketone.

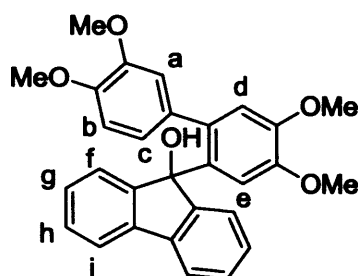
6.2.17 9-(4,5-Dimethoxybiphenyl-2-yl)-9H-fluoren-9-ol (**17**)



A mixture of 2-iodo-4,5-dimethoxybiphenyl (2.00 g, 5.88 mmol) (**11**) and 9H-fluoren-9-one (0.96 g, 5.35 mmol) (**SM1**) were added to a flame dried flask and dissolved in the minimum volume of THF (10 mL) and subjected to a nitrogen atmosphere. The mixture was cooled to -78 °C and *n*-butyl lithium dissolved in cyclohexane (3.24 mL, 2.0 M) was added drop-wise over a 10 min period. The mixture was allowed to react at -78 °C for 1 h and then allowed to reach room temperature for a further 2 h. The reaction was quenched by addition of NH₄Cl_(aq) (15 mL) and diluted with EtOAc. The organic layer was separated and washed with brine (10 mL) and water (10 mL). The organic layer was reduced in volume and purified by flash chromatography (elutant 3:7 EtOAc/hexane). 0.81 g of 9-(4,5-dimethoxybiphenyl-2-yl)-9H-fluoren-9-ol (**17**) was obtained as a white powder (2.05 mmol, 38% yield), m.p = 142 - 144 °C; IR (film)/cm⁻¹: 3286, 3065, 3000, 2942, 2936, 2928, 2835, 1605, 1594, 1512, 1488, 1453, 1449, 1392, 1338, 1260, 1211, 1129, 1100, 1046, 871, 793, 764, 748, 734, 701, 613; ¹H NMR (400 MHz, CDCl₃): δ_H 8.08 (s, 1H, OH), 7.17–6.91 (m, 9H, H_a, H_c, H_d, H_g, H_h), 6.78 (t, *J* = 7.4 Hz, 1H, H_i), 6.57 (t, *J*_{ef} = 7.8 Hz, 2H, H_e), 6.41 (s, 1H, H_b), 5.95 (d, *J*_{ef} = 7.8 Hz, 2H, H_f), 4.07 (s, 3H, OMe), 3.74 (s, 3H, OMe); ¹³C NMR (125 MHz, CDCl₃): δ_C 150.8, 147.9,

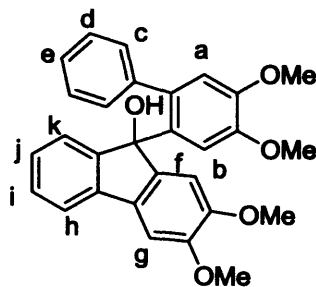
147.7, 147.5, 147.1, 140.2, 140.1, 133.7, 133.4, 132.0, 131.8, 129.3, 129.1, 128.6, 127.9, 127.7, 126.2, 125.9, 125.1, 124.3, 112.0, 115.1, 114.7, 110.0 (Aryl), 82.2 (R₃COH), 56.2, 55.9 (OMe); LRMS (EI) m/z (relative intensity): 394 (M⁺, 91%).

6.2.18 9-(3',4,4',5-Tetramethoxybiphenyl-2-yl)-9H-fluoren-9-ol (18)



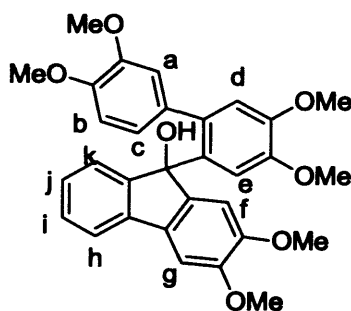
Following the general procedure described in the synthesis of 9-(4,5-dimethoxybiphenyl-2-yl)-9H-fluoren-9-ol (17), 2-bromo-3',4,4',5-tetramethoxybiphenyl (1.82 g, 5.14 mmol) (9), and 9-fluoren-9-one (0.84 g, 4.68 mmol) (SM1) were treated with *n*-butyl lithium in cyclohexane solution (2.83 mL, 2.0M) to give 9-(3',4,4',5-tetramethoxybiphenyl-2-yl)-9H-fluoren-9-ol (18) as a white powder (0.85 g, 40% yield), m.p = 168 - 170 °C; IR (film)/cm⁻¹: 3484, 3066, 3043, 3001, 2944, 2936, 2923, 2835, 1603, 1583, 1503, 1464, 1449, 1409, 1312, 1251, 1213, 1171, 1126, 1100, 1081, 1053, 1030, 913, 873, 835, 808, 784, 770, 749, 734, 682, 658, 647, 603; ¹H NMR (400 MHz, CDCl₃): δ_H 8.07 (s, 1H, OH), 7.29 - 7.20 (m, 8H, H_f, H_g, H_h, H_i), 7.20 (d, J_{ac} = 1.6 Hz, 1H, H_a) 6.49 (s, 1H, H_d), 6.14 (d, J_{bc} = 8.2 Hz, 1H, H_b), 5.59 (dd, J_{bc} = 8.2 Hz, J_{ac} = 1.6 Hz, 1H, H_c), 5.55 (s, 1H, H_e), 4.14 (s, 3H, OMe), 3.82 (s, 3H, OMe), 3.76 (s, 3H, OMe), 3.38 (s, 3H, OMe); ¹³C NMR (125 MHz, CDCl₃): δ_C 151.1, 149.4, 148.9, 147.9, 147.9, 147.4, 146.9, 142.0, 135.0, 133.3, 129.2, 129.0, 128.4, 128.3, 128.2, 128.0, 124.7, 122.4, 120.3, 115.1, 112.7, 110.3, 109.84, 107.3 (Aryl), 102.6 (R₃COH), 56.6, 56.5, 56.3, 56.2 (OMe); LRMS (EI) m/z (relative intensity): 454 (M⁺, 100%).

6.2.19 (±)9-(4,5-Dimethoxybiphenyl-2-yl)-2,3-dimethoxy-9H-fluoren-9-ol (19)



Following the general procedure described in the synthesis of 9-(4,5-dimethoxybiphenyl-2-yl)-9H-fluoren-9-ol (17), 2-iodo-3',4,4',5-tetramethoxybiphenyl (4.48 g, 13.17 mmol) (11), and 2,3-dimethoxy-9H-fluoren-9-one (2.88 g, 11.97 mmol) (14) were treated with *n*-butyl lithium in cyclohexane solution (7.24 mL, 2.0M) to give 9-(4,5-dimethoxybiphenyl-2-yl)-2,3-dimethoxy-9H-fluoren-9-ol (19) as a white powder (1.85 g, 34% yield), m.p = 158 - 161 °C; IR (film)/cm⁻¹: 3386, 3066, 3000, 2943, 2936, 2833, 1606, 1502, 1488, 1458, 1409, 1349, 1269, 1211, 1124, 1036, 853, 790, 776, 755, 734, 701, 611; ¹H NMR (400 MHz, CDCl₃): δ_H 7.95 (s, 1H, OH), 7.12 – 7.07 (m, 3H, H_d, H_e), 7.04 (d, *J* = 7.4 Hz, 1H, H_c), 6.96 (d, *J*_{hi} = 7.4 Hz, 1H, H_b), 6.76 (t, *J*_{hi} = 7.4 Hz, 1H, H_i), 6.67 (s, 2H, H_a, H_g), 6.62 (t, *J*_{jk} = 7.4 Hz, 1H, H_j), 6.56 (s, 1H, H_f), 6.36 (s, 1H, H_b), 6.04 (d, *J*_{jk} = 7.4 Hz, 1H, H_k), 4.05 (s, 3H, OMe), 3.83 (s, 3H, OMe), 3.79 (s, 3H, OMe), 3.72 (s, 3H, OMe); ¹³C NMR (125 MHz, CDCl₃): δ_C 151.1, 149.9, 149.7, 147.5, 147.1, 143.1, 140.4, 140.3, 133.4, 132.9, 131.9, 129.2, 128.6, 127.2, 126.8, 126.2, 125.2, 124.0, 123.8, 119.0, 114.8, 110.0, 107.5, 103.4 (Aryl), 82.2 (R₃COH), 56.4, 56.3, 56.2, 55.8 (OMe); LRMS (EI) *m/z* (relative intensity): 454 (M⁺, 75%).

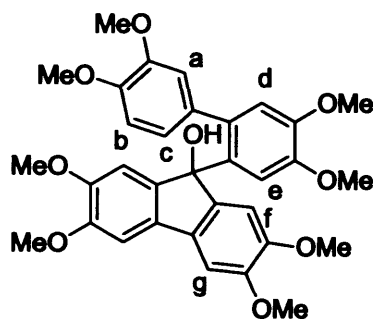
6.2.20 (±)2,3-Dimethoxy-9-(3',4,4',5-tetramethoxybiphenyl-2-yl)-9H-fluoren-9-ol (20)



Following the general procedure described in the synthesis of 9-(4,5-dimethoxybiphenyl-2-yl)-9H-fluoren-9-ol (17), 2-bromo-3',4,4',5-tetramethoxybiphenyl (9) (1.53 g, 4.32 mmol), and 2,3-dimethoxy-9H-fluoren-9-one (14) (0.94 g, 3.93 mmol) were treated with *n*-butyl

lithium in cyclohexane solution (2.38 mL 2.0M) to give 2,3-dimethoxy-9-(3',4,4',5-tetramethoxybiphenyl-2-yl)-9H-fluoren-9-ol (**20**) as a white powder (0.91 g, 45% yield), m.p = 179 - 181 °C; IR (film)/cm⁻¹: 3378, 3062, 2999, 2953, 2946, 2834, 1606, 1589, 1501, 1496, 1463, 1450, 1409, 1348, 1339, 1256, 1250, 1214, 1170, 1131, 1122, 1053, 1030, 856, 776, 760, 733; ¹H NMR (400 MHz, CDCl₃): δ_H 8.05 (s, 1H, OH), 7.74 (d, J = 7.6, 1H, H_b), 7.38 – 7.36 (m, 2H, H_j, H_a), 7.26 (s, 1H, H_d), 7.25 – 7.10 (m, 2H, H_b, H_c), 7.07 (t, J = 7.0 Hz, 1H, H_i), 6.69 (d, J = 7.5 Hz, 1H, H_k), 6.24 (s, 1H, H_g), 6.19 (s, 2H, H_f, H_e), 4.08 (s, 3H, OMe), 4.05 (s, 6H, OMe), 3.68 (s, 3H, OMe), 3.64 (s, 6H, OMe); ¹³C NMR (125 MHz, CDCl₃): δ_C 149.5, 149.3, 149.2, 149.1, 148.5, 141.9, 141.0, 134.5, 134.2, 127.5, 126.6, 123.7, 118.8, 114.8, 106.9, 106.8, 102.9, 102.2 (Aryl), 65.7 (R₃COH), 56.2, 56.1, 55.8 (OMe); LRMS (EI) m/z (relative intensity): 514 (M⁺, 100 %).

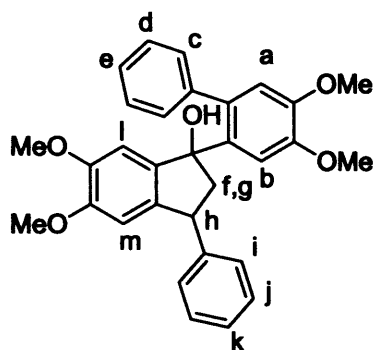
6.2.21 2,3,6,7-Tetramethoxy-9-(3',4,4',5-tetramethoxybiphenyl-2-yl)-9H-fluoren-9-ol (**21**)



Following the general procedure described in the synthesis of 9-(4,5-dimethoxybiphenyl-2-yl)-9H-fluoren-9-ol (**17**), 2-bromo-3',4,4',5-tetramethoxybiphenyl (1.80 g, 5.10 mmol) (**9**), and 2,3,6,7-tetramethoxy-9H-fluoren-9-one (1.39 g, 4.64 mmol) (**15**) were treated with *n*-butyl lithium in cyclohexane solution (2.81 mL 2.0M) to give 2,3,6,7-tetramethoxy-9-(3',4,4',5-tetramethoxybiphenyl-2-yl)-9H-fluoren-9-ol (**21**) was obtained as a white powder (1.12 g, 42% yield), m.p = 178 - 182 °C; IR (film)/cm⁻¹: 3466, 3066, 2999, 2937, 2920, 2835, 1686, 1597, 1577, 1500, 1464, 1412, 1310, 1256, 1215, 1171, 1137, 1111, 1052, 1028, 856, 831, 778, 751, 731; ¹H NMR (400 MHz, CDCl₃): δ_H 7.19 (d, J_{ac} = 1.4 Hz, 1H, H_a), 7.17 (s, 3H, H_d, H_g), 7.00 (dd, J_{bc} = 8.3 Hz, J_{ac} = 1.4 Hz, 1H, H_c), 6.87 (d, J_{bc} = 8.3 Hz, 1H, H_b), 6.11 (s, 3H, H_e, H_f), 3.97 (s, 9H, OMe), 3.88 (s, 3H, OMe), 3.86 (s, 3H, OMe), 3.57 (s, 9H, OMe); ¹³C NMR (125 MHz, CDCl₃): δ_C 149.5, 148.8, 148.7, 141.5, 134.8, 134.6, 119.5, 111.8,

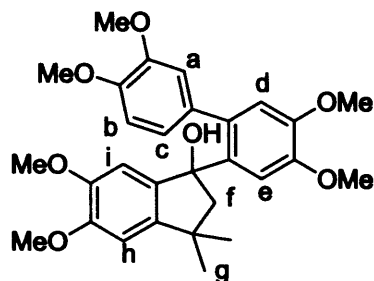
110.7, 107.3, 102.6 (Aryl), 65.9 (R_3COH) 56.7, 56.6, 56.5, 56.4, (OMe); LRMS (EI) m/z (relative intensity): 574 (M^+ , 100 %).

6.2.22 1-(4,5-Dimethoxybiphenyl-2-yl)-5,6-dimethoxy-3-phenyl-2,3-dihydro-1*H*-inden-1-ol (22)



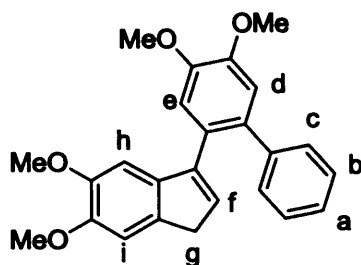
Following the general procedure described in the synthesis of 9-(4,5-dimethoxybiphenyl-2-yl)-9*H*-fluoren-9-ol (17), 2-iodo-3',4,4',5-tetramethoxybiphenyl (1.52 g, 4.47 mmol) (11), and 5,6-dimethoxy-3-phenyl-2,3-dihydro-1*H*-inden-1-one (1.09 g, 4.07 mmol) (13) were treated with *n*-butyl lithium in cyclohexane solution (2.46 mL, 2.0M) to give 1-(4,5-dimethoxybiphenyl-2-yl)-5,6-dimethoxy-3-phenyl-2,3-dihydro-1*H*-inden-1-ol (22) as a white powder (0.53 g, 1.10 mmol, 27% yield), m.p = 86 - 90 °C; IR (film)/cm⁻¹: 3507, 3071, 3012, 2999, 2948, 2935, 2886, 2821, 1604, 1599, 1503, 1490, 1464, 1461, 1459, 1411, 1389, 1350, 1311, 1279, 1256, 1209, 1191, 1181, 1144, 1094, 1085, 1045, 857, 768, 735, 701; ¹H NMR (400 MHz, CDCl₃): δ_H 7.29 (d, J = 7.6 Hz, 2H, H_i), 7.24 -7.10 (m, 5H, H_d, H_j, H_k), 7.07 (d, J = 7.5 Hz, 2H, H_c), 6.94 (t, J = 7.6 Hz, 1H, H_e), 6.78 (s, 1H, H_a) 6.68 (s, 1H, H_m), 6.59 (s, 1H, H_b), 6.25 (s, 1H, H_l), 4.42 (dd, J_{fh} = 7.7 Hz, J_{gh} = 3.4 Hz, 1H, H_h), 3.79 (s, 3H, OMe), 3.78 (s, 3H, OMe), 3.71 (s, 3H, OMe), 3.61 (s, 3H, OMe), 3.15 (dd, J_{fg} = 18.0 Hz, J_{fh} = 7.7 Hz, 1H, H_f), 2.53 (dd, J_{fg} = 18.0 Hz, J_{gh} = 3.4 Hz, 1H, H_g); ¹³C NMR (125 MHz, CDCl₃): δ_C 148.9, 148.4, 148.3, 147.7, 144.4, 142.0, 141.1, 140.4, 137.3, 137.2, 134.1, 129.6 129.3, 129.0, 128.4, 128.3, 127.2, 127.1, 127.0, 115.0, 113.8, 113.5, 107.9, 104.7 (Aryl) 63.5 (R₄C), 34.8, 21.1 (Alkyl); 56.5, 56.4, 56.3, 55.9 (OMe); LRMS (EI) m/z (relative intensity): 482 (M^+ , 100 %).

6.2.23 5,6-Dimethoxy-3,3-dimethyl-1-(3',4,4',5-tetramethoxybiphenyl-2-yl)-2,3-dihydro-1*H*-inden-1-ol (23)



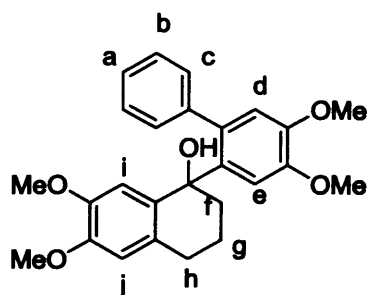
Following the general procedure described in the synthesis of 9-(4,5-dimethoxybiphenyl-2-yl)-9*H*-fluoren-9-ol (17), 2-bromo-3',4,4',5-tetramethoxybiphenyl (1.87 g, 5.29 mmol) (9), and 5,6-dimethoxy-3,3-dimethyl-2,3-dihydro-1*H*-inden-1-one (1.06 g, 4.81 mmol) (12) were treated with *n*-butyl lithium in cyclohexane solution (2.91 mL 2.0M) to give of 5,6-dimethoxy-3,3-dimethyl-1-(3',4,4',5-tetramethoxybiphenyl-2-yl)-2,3-dihydro-1*H*-inden-1-ol (23) as a white powder (0.88 g, 37% yield), m.p = 150 - 154 °C; IR (film)/cm⁻¹: 3432, 3111, 3065, 3002, 3000, 2999, 2934, 2931, 2902, 2834, 1602, 1574, 1500, 1443, 1405, 1308, 1261, 1230, 1208, 1176, 1167, 1144, 1059, 1023, 882, 852, 809, 764; ¹H NMR (400 MHz, CDCl₃): δ_H 7.18 (dd, $J_{cb} = 7.4$ Hz, $J = 1.4$ Hz, 1H, H_c), 7.08 (d, $J_{cb} = 7.4$ Hz, 1H, H_b), 6.68 (s, 1H, H_i), 6.57 (s, 2H, H_d, H_h), 5.78 (s, 1H, H_e), 5.72 (d, $J_{ac} = 1.4$ Hz, 1H, H_a), 3.95 (s, 6H, OMe), 3.87 (s, 3H, OMe), 3.74 (s, 6H, OMe), 3.48 (s, 3H, OMe), 2.45 (s, 2H, H_f), 1.26 (s, 6H, H_g); ¹³C NMR (125 MHz, CDCl₃): δ_C 148.2, 148.1, 147.9, 147.8, 146.0, 143.9, 140.4, 135.5, 133.5, 130.5, 127.7, 126.8, 113.4, 113.3, 113.0, 110.7, 105.3, 104.7 (Aryl), 56.3, 56.1, 56.1, 56.0, 55.9, 55.6 (OMe), 48.4, 48.3 (Alkyl) 24.52 (Me); LRMS (EI) m/z (relative intensity): 494 (M^+ , 100 %).

6.2.24 3-(4,5-Dimethoxybiphenyl-2-yl)-6,6'-dimethoxy-1*H*-indene (24)



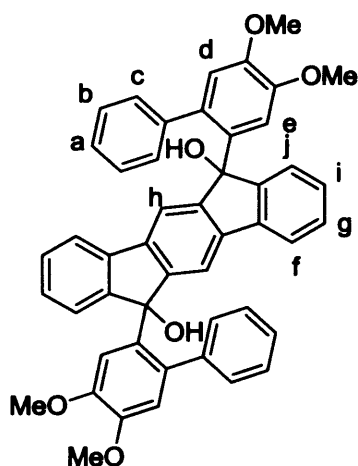
Following the general procedure described in the synthesis of 9-(4,5-dimethoxybiphenyl-2-yl)-9*H*-fluoren-9-ol (17), 2-iodo-3',4,4',5-tetramethoxybiphenyl (2.25 g, 6.61 mmol) (11), and 5,6-dimethoxy-1*H*-inden-1-one (1.15 g, 6.01 mmol) were treated with *n*-butyl lithium in cyclohexane solution (3.47 mL, 2.0M) to give 3-(4,5-dimethoxybiphenyl-2-yl)-6,6'-dimethoxy-1*H*-indene (24) as a white powder (0.63 g, 27% yield), m.p = 126 - 128 °C; IR (film)/cm⁻¹: 3413, 3051, 2999, 2951, 2940, 2901, 2825, 1602, 1559, 1521, 1496, 1460, 1451, 1446, 1421, 1396, 1351, 1324, 1275, 1251, 1232, 1206, 1163, 1147, 1078, 1024, 1021, 1016, 980, 898, 870, 826, 813, 797, 761, 734, 701; ¹H NMR (400 MHz, CDCl₃): δ_H 7.24 (d, J = 7.4 Hz, 2H, H_c), 7.08 (m, 3H, H_b, H_a), 6.95 (s, 1H, H_i), 6.94 (s, 1H, H_d), 6.93 (s, 1H, H_e), 6.43 (s, 1H, H_h), 6.11 (t, J = 1.8 Hz, 1H, H_f), 3.90 (s, 3H, OMe), 3.87 (s, 3H, OMe), 3.80 (s, 3H, OMe), 3.61 (s, 1H, OMe), 3.25 (d, J = 1.8 Hz, 2H, H_g); ¹³C NMR (100 MHz, CDCl₃): δ_C 148.9, 148.2, 148.0, 147.2, 145.3, 143.8, 142.5, 142.0, 138.2, 137.0, 133.8, 129.4, 128.3, 128.0, 127.0, 113.8, 113.6, 107.9, 104.6 (Aryl) 94.5 (R₂=CH), 56.5, 56.4, 56.3 (OMe), 39.0, (Alkyl); LRMS (EI) m/z (relative intensity): 388 (M⁺, 100 %).

6.2.25 (±)1-(4,5-Dimethoxybiphenyl-2-yl)-6,7-dimethoxy-1,2,3,4-tetrahydronaphthalen-1-ol (25)



Following the general procedure described in the synthesis of 9-(4,5-dimethoxybiphenyl-2-yl)-9*H*-fluoren-9-ol (**17**), 2-iodo-3',4,4',5-tetramethoxybiphenyl (1.46 g, 4.30 mmol) (**11**), and 6,7-dimethoxy-1-tetralone (0.81 g, 3.91 mmol) were treated with *n*-butyl lithium in cyclohexane solution (2.0M, 2.37 mL) to give 1-(4,5-dimethoxybiphenyl-2-yl)-6,7-dimethoxy-1,2,3,4-tetrahydronaphthalen-1-ol (**25**) as a white powder (0.51 g, 31% yield), m.p = 114 - 120 °C; IR (film)/cm⁻¹: 3361, 3061, 2998, 2934, 2861, 2831, 1603, 1565, 1511, 1490, 1463, 1460, 1458, 1366, 1357, 1354, 1350, 1266, 1237, 1207, 1151, 1105, 1039, 1036, 1034, 913, 866, 797, 768, 730, 701; ¹H NMR (400 MHz, CDCl₃): δ_H 7.23 (d, J_{cb} = 8.5 Hz, 2H, H_c), 7.10 (dt, J_{cb} = 8.5 Hz, J_{ab} = 7.3 Hz, 2H, H_b), 7.05 (t, J_{ab} = 7.3 Hz, 1H, H_a), 6.77 (s, 2H, H_d, H_j), 6.55 (s, 1H, H_e), 6.82 (s, 1H, H_i), 3.89 (s, 3H, OMe), 3.84 (s, 3H, OMe), 3.77 (s, 3H, OMe), 3.56 (s, 3H, OMe), 2.59 (t, J_{fg} = 8.2 Hz, 2H, H_f), 2.15 (dt, J_{fg} = 8.2 Hz, J_{gh} = 8.1 Hz, 2H, H_g), 1.18 (t, J_{gh} = 8.1 Hz, 2H, H_h); ¹³C NMR (125 MHz, CDCl₃): δ_C 148.8, 158.4, 158.0, 144.9, 147.2, 145.0, 142.0, 139.8, 137.8, 136.5, 133.9, 131.5, 129.4, 129.3, 128.3, 128.2, 128.3, 127.0 (Aryl), 113.8 (R₃COH) 113.7, 108.0, 104.6 (alkyl), 56.5, 56.3 (OMe); LRMS (EI) m/z (relative intensity): 420 (M⁺, 100 %).

6.2.26 6,12-Dihydroxy-6,12-bis(4,5-dimethoxybiphenyl-2-yl)-6,12-dihydroindeno[1,2-*b*]fluorene (**26**)

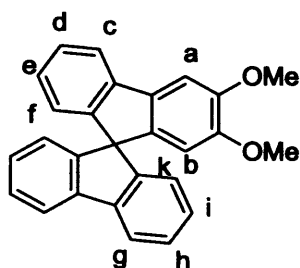


Following the general procedure described in the synthesis of 9-(4,5-dimethoxybiphenyl-2-yl)-9*H*-fluoren-9-ol (**17**), two equivalents of 2-iodo-3',4,4',5-tetramethoxybiphenyl (2.54 g, 7.46 mmol) (**11**), and indeno[1,2-*b*]fluorene-6,12-dione (0.96 g, 3.39 mmol) (**16**) were treated with *n*-butyl lithium in cyclohexane solution (4.10 mL, 2.0M) to give 6,12-dihydroxy-6,12-

bis(4,5-dimethoxybiphenyl-2-yl)-6,12-dihydroindeno[1,2-*b*]fluorene (**26**) as a white powder (0.41 g, 17% yield), m.p = 278 - 282 °C; IR (film)/cm⁻¹: 3431, 3066, 3041, 2999, 2937, 2931, 2861, 2853, 1709, 1605, 1506, 1486, 1464, 1441, 1397, 1353, 1305, 1265, 1236. 1206, 1127, 1048, 1034, 1006, 922, 892, 863, 783, 776, 755, 704; ¹H NMR (400 MHz, CDCl₃): δ_H 7.99 (s, 2H, OH), 7.20 (s, 2H, H_d), 7.19 – 7.05 (m, 8H, H_a, H_b, H_g), 6.87 (s, 2H, H_h), 6.74 (t, *J*_{ij} = 7.4 Hz, 2H, H_i), (d, *J* = 6.6 Hz, 2H, H_c), 6.34 (s, 2H, H_e), 6.02 (d, *J* = 7.2 Hz, 2H, H_f), 5.85 (d, *J*_{ij} = 7.4 Hz, 2H, H_j), 4.09 (s, 6H, OMe), 3.42 (s, 6H, OMe); ¹³C NMR (125 MHz, CDCl₃): δ_C 149.9, 148.8, 141.3, 141.1, 140.7, 137.5, 135.9, 130.1, 128.1, 127.4, 126.2, 124.4, 124.1, 121.1, 120.7, 119.1, 114.0, 110.1, 107.8, 100.2, 98.7 (Aryl), 66.1 (R3COH), 56.9, 56.8 (OMe); LRMS (EI) *m/z* (relative intensity): 710 (M⁺, 100 %).

General procedure for cyclization of an alcohol to form a spiro centre.

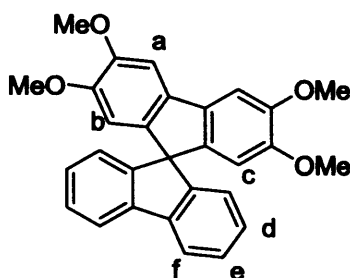
6.2.27 2,3-Dimethoxy-9,9'-spirobisfluorene (**27**)



9-(4,5-Dimethoxybiphenyl-2-yl)-9*H*-fluoren-9-ol (0.70 g, 1.77 mmol) (**17**) was dissolved in acetic acid (15 mL) and heated. When the solution reached reflux, five drops of conc. HCl were added and the solution was refluxed for a further 2 h. The solution was cooled and the reaction was quenched with ice-cold water. The precipitate was filtered and dried under vacuum and crystallized from ethanol to give 2,3-dimethoxy-9,9'-spirobisfluorene (**27**) as a white powder (0.61 g, 92% yield) m.p = 179 - 181 °C; IR (film)/cm⁻¹: 3061, 3002, 2952, 2934, 2856, 2831, 1605, 1580, 1500, 1475, 1463, 1446, 1440, 1407, 1344, 1332, 1311, 1284, 1273, 1253, 1240, 1205, 1176, 1155, 1130, 1084, 1034, 1005, 984, 852, 783, 773, 749, 733, 701, 690, 658, 626, 612; ¹H NMR (400 MHz, CDCl₃): δ_H 7.86 (d, *J*_{gh} = 7.6 Hz, 2H, H_g), 7.74 (d, *J*_{cd} = 7.6 Hz, 1H, H_c), 7.40 (t, *J*_{gh} = 7.6 Hz, 2H, H_h), 7.36 (s, 1H, H_a), 7.34 (t, *J*_{ef} = 7.5 Hz, 1H, H_e), 7.14 (t, *J*_{ik} = 7.5 Hz, 2H, H_i), 7.03 (t, *J*_{cd} = 7.6 Hz, 1H, H_d), 6.76 (d, *J*_{ik} = 7.5 Hz, 2H, H_k), 6.67 (d, *J*_{ef} = 7.5 Hz, 1H, H_f), 6.25 (s, 1H, H_b), 4.05 (s, 3H, OMe), 3.65 (s, 3H, OMe); ¹³C

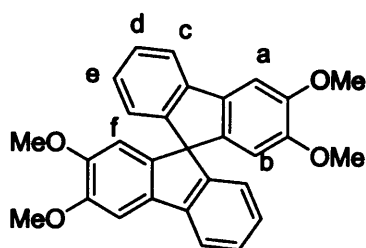
NMR (125 MHz, CDCl₃): δ 149.6, 149.4, 149.1, 148.9, 142.0, 141.7, 140.7, 134.4, 127.8, 127.7, 127.6, 126.5, 124.1, 123.6, 119.9, 118.8, 106.9, 103.0 (Aryl), 65.9 (R₄C), 56.2, 56.1 (OMe); LRMS (EI) m/z (relative intensity) 376 (M⁺, 98 %).

6.2.28 2,3,6,7-Tetramethoxy-9,9'-spirobisfluorene (28)



Following the general procedure described in the synthesis of 2,3-dimethoxy-9,9'-spirobisfluorene (27), 9-(3',4,4',5-tetramethoxybiphenyl-2-yl)-9*H*-fluoren-9-ol (0.65 g, 1.43 mmol) (18) was reacted in acetic acid (15 mL) to give 2,3,6,7-tetramethoxy-9,9'-spirobisfluorene (28) as a white powder (0.59 g, 95% yield) m.p = 120 - 123 °C; IR (film)/cm⁻¹: 3061, 2997, 2934, 2855, 2831, 1605, 1579, 1500, 1478, 1463, 1441, 1406, 1341, 1299, 1275, 1251, 1239, 1204, 1157, 1145, 1133, 1118, 1105, 1084, 1030, 1002, 952, 854, 820, 778, 751, 735, 701, 687, 632, 571; ¹H NMR (400 MHz, CDCl₃): δ_H 7.78 (d, J_{ef} = 7.6 Hz, 2H, H_f), 7.03 (t, J_{cd} = 7.5 Hz, 2H, H_c), 7.18 (s, 2H, H_a), 7.06 (t, J_{ef} = 7.6 Hz, 2H, H_e), 6.68 (d, J_{cd} = 7.5 Hz, 2H, H_d), 6.11 (s, 2H, H_b), 3.97 (s, 6H, OMe), 3.49 (s, 6H, OMe); ¹³C NMR (125 MHz, CDCl₃): δ_C 149.5, 149.3, 149.2, 149.0, 141.63, 134.6, 127.9, 127.6, 124.1, 119.9 (Aryl), 56.2, 56.1 (OMe), LRMS (EI) m/z (relative intensity): 436 (M⁺, 100 %).

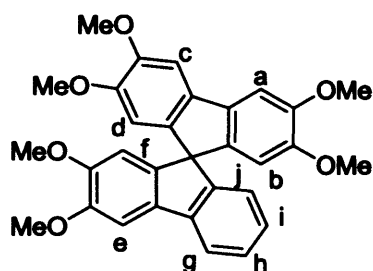
6.2.29 2,2',3,3'-Tetramethoxy-9,9'-spirobisfluorene (29)



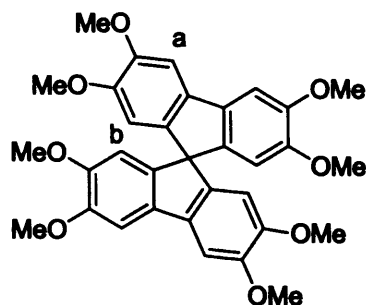
Following the general procedure described in the synthesis of 2,3-dimethoxy-9,9'-spirobisfluorene (27), 9-(4,5-dimethoxybiphenyl-2-yl)-2,3-dimethoxy-9*H*-fluoren-9-ol (1.25

g, 2.75 mmol) (**19**) was reacted in acetic acid (20 mL) to give 2,2',3,3'-tetramethoxy-9,9'-spirobisfluorene (**29**) as a white powder (1.09 g, 91% yield) m.p = 221 - 223 °C; IR (film)/cm⁻¹: 3061, 3000, 2935, 2908, 2856, 2831, 1606, 1579, 1558, 1500, 1479, 1456, 1447, 1440, 1406, 1345, 1309, 272, 1251, 1233, 1201, 1174, 1142, 1120, 1084, 1034, 1018, 993, 939, 891, 852, 785, 778, 766, 754, 741, 701, 687, 668, 656, 642, 623, 610; ¹H NMR (500 MHz, CDCl₃): δ_H 7.64 (d, J_{cd} = 7.4 Hz, 2H, H_c), 7.26 (s, 2H, H_a), 7.25 (t, J_{cd} = 7.4 Hz, 2H, H_d), 6.95 (t, J_{ef} = 7.6 Hz, 2H, H_e), 6.58 (d, J_{ef} = 7.6 Hz, 2H, H_f), 6.16 (s, 2H, H_b), 3.96 (s, 6H, OMe), 3.57 (s, 6H, OMe); ¹³C NMR (125 MHz, CDCl₃): δ 149.6, 149.4, 149.2, 141.9, 140.9, 134.31, 127.5, 126.6, 123.7, 118.8, 106.9, 103.0 (Aryl), 65.8 (R₄C), 56.2, 56.1 (OMe); LRMS (EI) m/z (relative intensity): 436 (M⁺, 100 %).

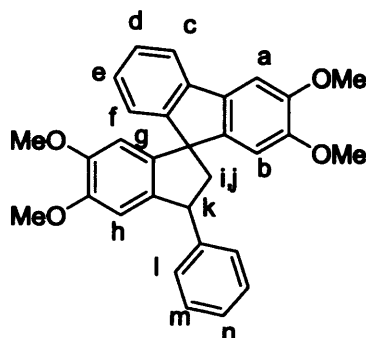
6.2.30 2,2',3,3',6,7-Hexamethoxy-9,9'-spirobisfluorene (**30**)



Following the general procedure described in the synthesis of 2,3-dimethoxy-9,9'-spirobisfluorene (**27**), 2,3-dimethoxy-9-(3',4,4',5-tetramethoxybiphenyl-2-yl)-9H-fluoren-9-ol (0.81 g, 1.57 mmol) (**20**) was reacted in acetic acid (15 mL) to give 2,2',3,3',6,7-hexamethoxy-9,9'-spirobisfluorene (**30**) as a white powder (0.73 g, 94% yield). m.p = 228 - 230 °C; IR (film)/cm⁻¹: 3063, 2996, 2936, 2831, 1607, 1495, 1464, 1439, 1407, 1344, 1311, 1283, 1257, 1230, 1199, 1171, 1140, 1110, 1081, 1035, 1004, 880, 852, 797, 775, 756, 737, 701, 685, 669, 640, 630, 597; ¹H NMR (400 MHz, CDCl₃): δ_H 7.73 (d, J = 7.5 Hz, 1H, H_g), 7.36 (s, 1H, H_f), 7.35 (t, J = 7.5 Hz, 1H, H_h), 7.26 (s, 2H, H_d, H_b), 7.06 (t, J = 7.5 Hz, 1H, H_i), 6.69 (d, J = 7.5 Hz, 1H, H_j), 6.24 (s, 1H, H_e), 6.20 (s, 2H, H_c, H_a), 4.06 (s, 9H, OMe), 3.68 (s, 9H, OMe); ¹³C NMR (125 MHz, CDCl₃): δ_C 150.2, 149.8, 147.9, 147.5, 146.9, 143.9, 143.1, 142.0, 141.1, 135.0, 144.4, 133.2, 129.0, 128.0, 126.6, 124.1, 122.4, 118.0, 112.3, 110.4, 109.4, 107.1, 103.2, 102.2 (Aryl), 66.0 (R₄C), 56.6, 56.5, 56.4, 56.3, 56.2, 56.1 (OMe); LRMS (EI) m/z (relative intensity): 496 (M⁺, 100 %).

6.2.31 2,2',3,3',6,6',7,7'-Octamethoxy-9,9'-spirobisfluorene (31)

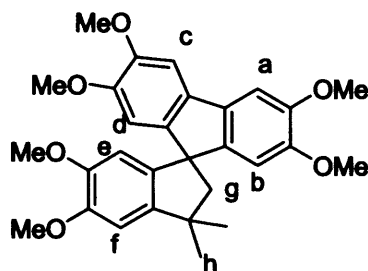
Following the general procedure described in the synthesis of 2,3-dimethoxy-9,9'-spirobisfluorene (27), 2,3,6,7-tetramethoxy-9-(3',4,4',5-tetramethoxybiphenyl-2-yl)-9*H*-fluoren-9-ol (0.90 g, 1.57 mmol) (21) was reacted in acetic acid (15 mL) to give 2,2',3,3',6,6',7,7'-octamethoxy-9,9'-spirobisfluorene (31) as a white powder (0.82 g 1.47 mmol, 94% yield). m.p = 232 - 235 °C; IR (film)/cm⁻¹: 3063, 2995, 2936, 2833, 1607, 1591, 1558, 1490, 1465, 1409, 1336, 1313, 1255, 1228, 1197, 1184, 1135, 1079, 1040, 1010, 974, 857, 833, 809, 787, 762, 734, 701, 679, 639, 576; ¹H NMR (400 MHz, CDCl₃): δ_H 7.17 (s, 4H, H_b), 6.11 (s, 4H, H_a), 3.97 (s, 12H, OMe), 3.57 (s, 12H, OMe); ¹³C NMR (125 MHz, CDCl₃): δ 149.2, 148.5, 141.1, 134.4, 107.0, 102.2 (Aryl), 56.2, 56.1 (OMe); LRMS (EI) *m/z* (relative intensity): 556 (M⁺, 100 %).

6.2.32 2,3,5',6'-Tetramethoxy-3'-phenyl-2',3'-dihydrospiro[fluorene-9,1'-indene] (32)

Following the general procedure described in the synthesis of 2,3-dimethoxy-9,9'-spirobisfluorene (27), 1-(4,5-dimethoxybiphenyl-2-yl)-5,6-dimethoxy-3-phenyl-2,3-dihydro-1*H*-inden-1-ol (0.45 g, 0.93 mmol) (22) was reacted in acetic acid (12 mL) to give 2,3,5',6'-tetramethoxy-3'-phenyl-2',3'-dihydrospiro[fluorene-9,1'-indene] (32) was obtained as a white

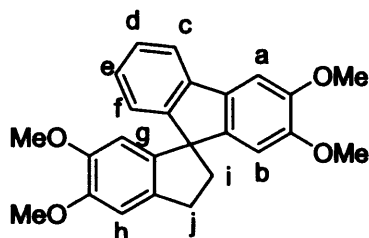
powder (0.39 g, 89% yield). m.p = 189 - 191 °C; IR (film)/cm⁻¹: 3056, 2983, 2934, 2855, 1603, 1505, 1451, 1301, 1190, 1128, 1029, 871, 791, 746; ¹H NMR (400 MHz, CDCl₃): δ_H 7.32 (d, J = 7.6 Hz, 1H, H_l), 7.22 (m, 3H, H_m, H_n), 7.12 (t, J_{ef} = 7.4 Hz, 1H, H_e), 7.10 (d, J_{ef} = 7.4 Hz, 1H, H_f), 7.13, (s, 2H, H_b, H_g), 7.15 (d, J_{cd} = 7.4 Hz, 1H, H_c), 6.87 (t, J_{cd} = 7.4 Hz, 1H, H_d), 6.30 (s, 1H, H_a), 5.78 (s, 1H, H_h), 4.48 (dd, J_{jk} = 7.6 Hz, J_{ik} = 3.4 Hz, 1H), 3.79 (s, 6H, OMe), 3.71 (s, 6H, OMe), 3.10 (dd, J_{ij} = 19.0 Hz, J_{jk} = 7.6 Hz, 1H, H_j), 2.58 (dd, J_{ij} = 19.0 Hz, J_{ik} = 3.4 Hz, 1H, H_i); ¹³C NMR (100 MHz, CDCl₃): δ_C 151.2, 147.5, 148.3, 148, 147.9, 147.8, 147.6, 141.8, 141.5, 140.6, 139.9, 138.8, 138.5, 138.3, 130.2, 129.2, 128.6, 128.0, 127.3, 120.5, 112.9, 112.3, 109.3, 108.5 (Aryl), 63.8 (R₄C), 56.8, 56.7 (OMe), 44.7, 44.3 (Alkyl); LRMS (EI) m/z (relative intensity): 464 (M⁺, 100 %).

6.2.33 2,3,5',6,6',7-Hexamethoxy-3',3'-dimethyl-2',3'-dihydrospiro[fluorene-9,1'-indene] (33)



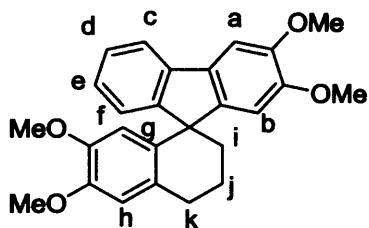
Following the general procedure described in the synthesis of 2,3-dimethoxy-9,9'-spirobisfluorene (27), 5,6-dimethoxy-3,3-dimethyl-1-(3',4,4',5-tetramethoxybiphenyl-2-yl)-2,3-dihydro-1*H*-inden-1-ol (0.75 g, 1.52 mmol) (23) was reacted in acetic acid (15 mL) to give of 2,3,5',6,6',7-hexamethoxy-3',3'-dimethyl-2',3'-dihydrospiro[fluorene-9,1'-indene] (33) was obtained as a white powder (0.66 g, 92% yield) m.p = 88 - 92 °C; IR (film)/cm⁻¹: 3060, 2995, 2953, 2862, 2832, 1695, 1605, 1496, 1465, 1409, 1361, 1341, 1315, 1265, 1253, 1225, 1213, 1158, 1142, 1117, 1072, 1039, 1008, 921.8, 852, 782, 766, 734, 698, 581; H NMR (400 MHz, CDCl₃): δ_H 7.01 (s, 1H, H_b), 6.98 (s, 1H, H_d), 6.85 (s, 1H, H_e), 6.79 (s, 1H, H_f), 6.51 (s, 1H, H_c), 6.01 (s, 1H, H_a), 3.99 (s, 3H, OMe), 3.96 (s, 3H, OMe), 3.92 (s, 3H, OMe), 3.85 (s, 3H, OMe), 3.72 (s, 3H, OMe), 3.58 (s, 3H, OMe), 2.53 (s, 2H, H_g), 1.26 (s, 6H, H_h); (125 MHz, CDCl₃): δ 148.2, 148.1, 147.9, 147.8, 146.0, 143.9, 140.4, 135.5, 133.5, 130.5, 127.7, 126.8, 113.4, 113.3, 113.0, 110.7, 105.3, 104.7 (Aryl), 56.3, 56.1, 56.1, 56.0, 55.9, 55.6 (OMe), 48.4, 36.5 (Alkyl), 24.52 (Me); LRMS (EI) m/z (relative intensity): 476 (M⁺, 100%).

6.2.34 2,3,5',6'-Tetramethoxy-2',3'-dihydrospiro[fluorene-9,1'-indene] (34)



Following the general procedure described in the synthesis of 2,3-dimethoxy-9,9'-spirobisfluorene (27), 1-(4,5-dimethoxybiphenyl-2-yl)-5,6-dimethoxy-2,3-dihydro-1*H*-inden-1-ol (0.50 g, 1.23 mmol) (24) was reacted in acetic acid (12 mL) to give 2,3,5',6'-tetramethoxy-2',3'-dihydrospiro[fluorene-9,1'-indene] (34) as a white powder (0.42 g 1.08 mmol, 88% yield). m.p = 239 - 241 °C IR (film)/cm⁻¹: 3053, 3001, 2961, 2934, 2832, 1608, 1592, 1408, 1337, 1312, 1283, 1257, 1213, 1200, 1172, 1155, 1140, 1115, 1080, 1038, 1020, 1000, 952, 842, 835, 819, 799, 769, 748, 721, 692, 681, 667, 620, 601; (400 MHz, CDCl₃): δ_H 7.57 (d, J = 7.5 Hz, 1H, H_e), 7.25 (t, J = 7.3 Hz, 1H, H_d), 7.19 (s, 1H, H_b), 7.07 (m, 2H, H_f, H_c), 6.86 (s, 1H, H_g), 6.66 (s, 1H, H_h), 5.88 (s, 1H, H_a), 3.94 (s, 3H, OMe), 3.84 (s, 3H, OMe), 3.77 (s, 3H, OMe), 3.49 (s, 3H, OMe), 3.24 (m, 2H, H_i), 2.49 (m, 1H, H_j); ¹³C NMR (125 MHz, CDCl₃): δ_C 153.2, 149.5, 149.1, 148.7, 148.6, 139.8, 139.3, 136.1, 132.5, 127.2, 1256.3, 123.4, 118.7, 107.6, 107.0, 106.3, 102.9 (Aryl), 63.3 (R₄C), 56.8, 56.2, 56.0, 55.9 (OMe), 40.8, 31.8 (Alkyl); LRMS (EI) m/z (relative intensity): 388.17 (M⁺, 100%).

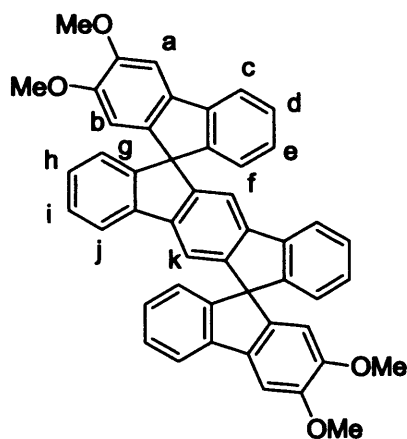
6.2.35 2,3,6',7'-Tetramethoxy-3',4'-dihydro-2'*H*-spiro[fluorene-9,1'-naphthalene] (35)



Following the general procedure described in the synthesis of 2,3-dimethoxy-9,9'-spirobisfluorene (27), 1-(4,5-dimethoxybiphenyl-2-yl)-6,7-dimethoxy-1,2,3,4-

tetrahydronaphthalen-1-ol (0.45 g, 1.07 mmol) (**25**) was reacted in acetic acid (12 mL) to give 2,3,6',7'-tetramethoxy-3',4C-dihydro-2'*H*-spiro[fluorene-9,1'-naphthalene] (**35**) as a white powder (0.38 g, 89% yield); m.p = 118 - 121 °C; IR (film)/cm⁻¹: 3062, 2996, 2932, 2852, 2828, 1603, 1565, 1511, 1491, 1463, 1393, 1357, 1344, 1327, 1264, 1237, 1206, 1151, 1105, 109, 1022, 1007, 866, 823, 798, 768, 701, 668; ¹H NMR (400 MHz, CDCl₃): δ_H 7.23 (d, J_{cd} = 8.5 Hz, 2H, H_c, H_f), 7.10 (t, J_{cd} = 8.5 Hz, 2H, H_d, H_e), 6.87 (s, 1H, H_h), 6.76 (s, 1H, H_a), 6.54 (s, 1H, H_g), 6.28 (s, 1H, H_b), 3.88 (s, 3H, OMe), 3.83 (s, 1H, OMe), 3.77 (s, 3H, OMe), 3.56 (s, 3H, OMe), 2.95 (t, J_{ij} = 4.6 Hz, 2H, H_i), 2.59 (tt, J_{jk} = 4.8 Hz, J_{ij} = 4.6 Hz, 2H, H_j), 2.14 (t, J_{jk} = 4.8 Hz, 2H, H_k); ¹³C NMR (125 MHz, CDCl₃): δ 148.1, 147.9, 147.6, 146.8, 138.7, 138.5, 133.8, 131.6, 128.8, 128.7, 128.5, 127.7, 127.2, 126.3, 113.7, 113.2, 110.0, 109.6 (Aryl), 56.1, 56.0, 55.9, 55.8 (OMe) 27.7, 23.7, 20.7 (Alkyl); LRMS (EI) *m/z* (relative intensity): 402 (M⁺, 100%).

6.2.36 2,2'',3,3''-Tetrahydroxydispiro[9*H*-fluorene-9,6'(12'*H*)-indeno[1,2-*b*]fluorene-12',9''-[9*H*]fluorene] (**36**)

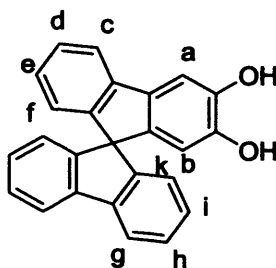


Following the general procedure described in the synthesis of 2,3-dimethoxy-9,9'-spirobisfluorene (**27**), 6,12-dihydroxy-6,12-bis(4,5-dimethoxybiphenyl-2-yl)-6,12-dihydroindeno[1,2-*b*]fluorene (0.50 g, 0.70 mmol) (**26**) was reacted in acetic acid (20 mL) to give 2,2'',3,3''-tetramethoxydispiro[9*H*-fluorene-9,6'(12'*H*)-indeno[1,2-*b*]fluorene-12',9''-[9*H*]fluorene] (**36**) as a white powder (0.43 g, 90% yield). m.p = 338 - 340 °C; IR (film)/cm⁻¹: 3062, 2993, 2933, 2854, 2801, 1604, 1501, 1474, 1462, 1444, 1408, 1347, 1328, 1286, 1275, 1256, 1233, 1207, 1178, 1154, 1120, 1090, 1038, 984, 918, 891, 870, 844, 777, 767, 751,

738, 723, 697, 682, 628, 606; ^1H NMR (400 MHz, CDCl_3): δ_{H} 7.71 (d, $J_{\text{cd}} = 7.6$ Hz, 2H, H_{c}), 7.47 (d, $J_{\text{ef}} = 7.5$ Hz, 2H, H_{f}), 7.35 (s, 2H, H_{a}), 7.31 (t, $J_{\text{cd}} = 7.6$ Hz, 2H, H_{d}), 7.16 (t, $J_{\text{gh}} = 7.6$ Hz, 2H, H_{h}), 7.08 (s, 2H, H_{b}), 6.99 (t, $J_{\text{ij}} = 7.6$ Hz, 2H, H_{i}), 6.96 (t, $J_{\text{ef}} = 7.5$ Hz, 2H, H_{e}), 6.66 (d, $J_{\text{gh}} = 7.5$ Hz, 2H, H_{g}), 6.62 (d, $J_{\text{ij}} = 7.5$ Hz, 2H, H_{j}), 6.23 (s, 2H, H_{k}) 4.00 (s, 6H, OMe), 3.59 (s, 6H, OMe); ^{13}C NMR (125 MHz, CDCl_3): δ_{C} 151.5, 150.8, 150.4, 146.0, 145.9, 144.3, 143.7, 143.5, 143.2, 142.6, 128.2, 127.5, 127.2, 121.8, 120.3, 120.1, 119.9, 117.7, 115.3, 108.8, 101.3 (Aryl), 65.6 (R_4C), 56.7, 56.3 (OMe); LRMS (EI) m/z (relative intensity): 674 (M^+ , 100%).

General procedure for protodemethylation of methoxylated spiro compounds.

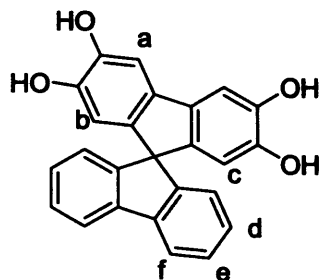
6.2.37 2,3-Tetrahydroxy-9,9'-spirobisfluorene (37)



2,3-dimethoxy-9,9'-spirobisfluorene (0.55 g, 1.46 mmol) (**27**) was dissolved in distilled DCM (20 mL) and placed under an inert atmosphere. The solution was cooled to 0 °C and boron tribromide (0.21 mL, 2.19 mmol) was added drop-wise over 5 mins. The reaction was monitored by TLC and allowed to react for 2 h. The solution was poured into ice-cold water and stirred for 0.5 h, extracted with diethyl ether (3 x 20 mL) and the collected organic washings were dried over MgSO_4 . The solution was filtered and reduced in volume under vacuum, washed with DCM and then dried under vacuum overnight. 2,3-Dihydroxy-9,9'-spirobisfluorene (**37**) was obtained as a light brown powder (0.47 g, 93% yield), m.p = 242 - 246 °C; IR (film)/ cm^{-1} : 3420, 3058, 2990, 2895, 2848, 1630, 1502, 1441, 1340, 1289, 1190, 1114, 1091, 995, 865, 749, 733, 669; ^1H NMR (400 MHz, $\text{MeOD}-d_4$): δ_{H} 7.89 (d, $J_{\text{gh}} = 7.6$ Hz, 2H, H_{g}), 7.69 (d, $J_{\text{cd}} = 7.5$ Hz, 1H, H_{c}), 7.36 (t, $J_{\text{ik}} = 7.5$ Hz, 2H, H_{i}), 7.29 (s, 1H, H_{a}), 7.29 (t, $J_{\text{ef}} = 7.6$ Hz, 1H, H_{e}), 7.13 (t, $J_{\text{cd}} = 7.5$ Hz, 1H, H_{d}), 6.96 (t, $J_{\text{gh}} = 7.6$ Hz, 2H, H_{h}) 6.67 (d, $J_{\text{ik}} = 7.5$ Hz, 2H, H_{k}), 6.52 (d, $J_{\text{ef}} = 7.5$ Hz, 1H, H_{f}), 5.52 (s, 1H, H_{b}); ^{13}C NMR (125 MHz, $\text{MeOD}-d_4$): δ 150.8, 150.2, 147.0, 146.8, 143.9, 141.5, 135.1, 128.8, 128.6, 127.1,

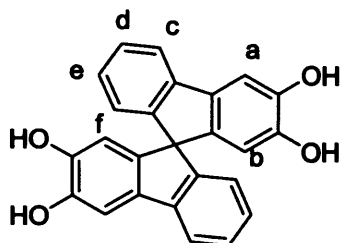
125.1, 124.9, 124.4, 120.9, 119.8, 111.48, 107.7 (Aryl), 66.9 (R_4C); HRMS (EI), calculated for $C_{25}H_{16}O_2$: 348.1150, found: 348.1160.

6.2.38 2,3,6,7-Tetrahydroxy-9,9'-spirobisfluorene (38)



Following the general procedure described for 2,3-dihydroxy-9,9'-spirobisfluorene (27), 2,3,6,7-tetramethoxy-9,9'-spirobisfluorene (0.50 g, 1.15 mmol) (28) was reacted with 3.5 equiv. of boron tribromide (0.38 mL, 4.03 mmol) to give 2,3,6,7-tetrahydroxy-9,9'-spirobisfluorene (38) as a light brown powder (0.37 g, 85% yield); m.p = 144 - 146 °C; IR (film)/ cm^{-1} : 3366, 3059, 2957, 2934, 2854, 1608, 1500, 1481, 1454, 1307, 1279, 1250, 1227, 1186, 1153, 1070, 1037, 1018, 980, 866, 825, 794, 780, 751, 733, 680, 625; 1H NMR (400 MHz, $MeOD-d_4$): δ_H 7.73 (d, J_{ef} = 7.6 Hz, 2H, H_f), 7.22 (t, J_{ef} = 7.5 Hz, 2H, H_e), 7.00 (s, 2H, H_a), 7.00 (t, J_{cd} = 7.5 Hz, 2H, H_c), 6.58 (d, J_{cd} = 7.6 Hz, 2H, H_d), 5.86 (s, 2H, H_b); ^{13}C NMR (125 MHz, $MeOD-d_4$): δ_C 147.0, 145.7, 142.1, 141.0, 133.4, 128.4, 127.3, 124.8, 119.7, 112.5, 112.0, 111.2 (Aryl), 64.3 (R_4C); HRMS (EI), calculated for $C_{25}H_{16}O_4$: 380.1049, found: 380.1051.

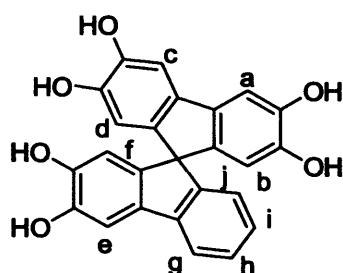
6.2.39 2,2',3,3'-Tetrahydroxy-9,9'-spirobisfluorene (39)



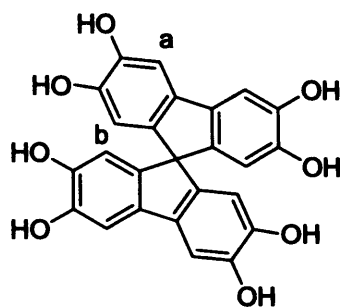
Following the general procedure described for 2,3-dihydroxy-9,9'-spirobisfluorene (37), 2,2',3,3'-tetramethoxy-9,9'-spirobisfluorene (1.00 g, 2.29 mmol) (29) was reacted with 3.5 equiv. of boron tribromide (0.76 mL, 8.02 mmol) to give 2,2',3,3'-tetrahydroxy-9,9'-

spirobisfluorene (**39**) as a light brown powder (0.77 g, 88% yield), m.p = 256 - 259 °C; IR (film)/cm⁻¹: 3385, 3061, 2936, 2891, 2806, 1606, 1498, 1477, 1442, 1339, 1291, 1242, 865, 790, 422; ¹H NMR (400 MHz, MeOD-*d*₄): δ_H 7.66 (d, J_{cd} = 7.6 Hz, 2H, H_c), 7.28 (s, 2H, H_a), 7.27 (t, J_{cd} = 7.6 Hz, 2H, H_d), 6.99 (t, J_{ef} = 7.6 Hz, 2H, H_e), 6.56 (d, J_{ef} = 7.6 Hz, 2H, H_f), 6.10 (s, 2H, H_b); ¹³C NMR (125 MHz, MeOD-*d*₄): δ_C 150.8, 146.8, 146.5, 143.6, 142.2, 134.9, 128.4, 127.0, 124.5, 119.6, 111.5, 107.6 (Aryl), 65.8 (R₄C); HRMS (EI), calculated for C₂₅H₁₆O₄: 380.1049, found: 380.1055.

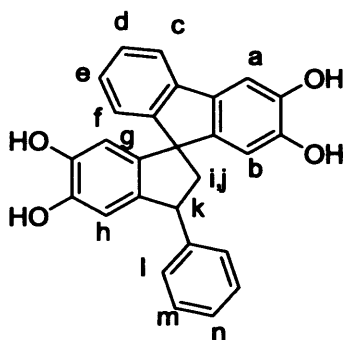
6.2.40 2,2',3,3',6,7-Hexahydroxy-9,9'-spirobisfluorene (**40**)



Following the general procedure described for 2,3-dihydroxy-9,9'-spirobisfluorene (**37**), 2,2',3,3',6,7-hexamethoxy-9,9'-spirobisfluorene (0.65 g, 1.31 mmol) (**30**) was reacted with 4.5 equiv. of boron tribromide (0.56 mL, 5.90 mmol) to give of 2,2',3,3',6,7-hexahydroxy-9,9'-spirobisfluorene (**40**) as a light brown powder (0.46 g, 86% yield); m.p = 170 - 174 °C; IR (film)/cm⁻¹: 3341, 3061, 2903, 2865, 2804, 1612, 1499, 1442, 1342, 1277, 1203, 1159, 1132, 1065, 862, 786, 759; ¹H NMR (400 MHz, MeOD-*d*₄): δ_H 7.50 (d, J_{gh} = 7.6 Hz, 1H, H_g), 7.14 (t, J_{gh} = 7.6 Hz, 1H, H_h), 7.13 (s, 1H, H_e), 6.97 (s, 2H, H_a, H_c), 6.87 (t, J_{ij} = 7.6 Hz, 1H, H_i), 6.48 (d, J_{ij} = 7.6 Hz, 1H, H_j), 6.02 (s, 1H, H_f), 5.91 (s, 2H, H_b, H_d); ¹³C NMR (125 MHz, MeOD-*d*₄): δ_C 151.9, 147.9, 147.3, 147.1, 146.6, 143.8, 143.3, 142.5, 136.0, 135.1, 128.6, 127.3, 137.4, 124.9, 119.9, 112.0, 107.8, 107.1 (Aryl), 66.5 (R₄C); HRMS (ES), calculated for C₂₅H₁₆O₆: 412.0947, found 847.1576 (2M+Na⁺, 13%), 863.1576 (2M+K⁺, 20%), 888.2089 (2M+MeCNNa⁺, 100%).

6.2.41 2,2',3,3',6,6',7,7'-Octahydroxy-9,9'-spirobisfluorene (41)

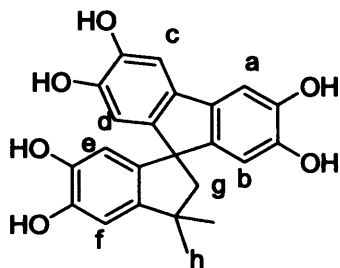
Following the general procedure described for 2,3-dihydroxy-9,9'-spirobisfluorene (37), 2,2',3,3',6,6',7,7'-octamethoxy-9,9'-spirobisfluorenes (0.75 g, 1.35 mmol) (31) was reacted with 6 equiv. of boron tribromide (0.77 mL, 8.10 mmol) to give 2,2',3,3',6,6',7,7'-octahydroxy-9,9'-spirobisfluorene (41) as a light brown powder (0.53 g, 89% yield), m.p = 252 - 255 °C; IR (film)/cm⁻¹: 3171, 3061, 2939, 2908, 2857 1611, 1502, 1448.76, 1353, 1283, 1205, 1123, 832, 801, 775; ¹H NMR (400 MHz, MeOD-*d*₄): δ_H 6.93 (s, 4H, H_a), 5.94 (s, 4H, H_b); ¹³C NMR (125 MHz, MeOD-*d*₄): δ_C 146.4, 145.5, 143.2, 135.8, 112.0, 107.0 (Aryl); HRMS (EI), calculated for C₂₅H₁₆O₈: 444.0845, found: 444.0849.

6.2.42 2,3,5',6'-Tetrahydroxy-3'-phenyl-2',3'-dihydrospiro[fluorene-9,1'-indene] (42)

Following the general procedure described for 2,3-dihydroxy-9,9'-spirobisfluorene (37), 2,3,5',6'-tetramethoxy-3'-phenyl-2',3'-dihydrospiro[fluorene-9,1'-indene] (0.35 g, 0.75 mmol) (32) was reacted with 3 equiv. of boron tribromide (0.21 mL, 2.25 mmol) to give of 2,3,5',6'-tetrahydroxy-3'-phenyl-2',3'-dihydrospiro[fluorene-9,1'-indene] (42) as a light brown powder (0.27 g, 88% yield), m.p = 104 - 108 °C; IR (film)/cm⁻¹: 3391, 3058, 2982, 2934, 2856, 1604, 1501, 1453, 1299, 1190, 1128, 1029, 871, 809, 787, 745, 701; ¹H NMR (400

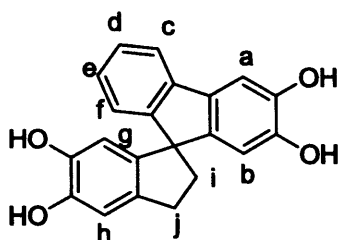
MHz, MeOD- d_4): δ_H 7.44 (d, $J = 7.6$ Hz, 1H, H_i), 7.22 (m, 3H, H_m , H_n), 7.12 (t, $J_{cd} = 7.4$ Hz, 1H, H_d), 7.11 (d, $J_{cd} = 7.4$ Hz, 1H, H_c), 7.08, (s, 2H, H_a , H_h), 7.05 (d, $J_{ef} = 7.4$ Hz, 1H, H_f), 6.97 (t, $J_{ef} = 7.4$ Hz, 1H, H_e), 6.29 (s, 1H, H_g), 5.77 (s, 1H, H_b), 4.27 (dd, $J_{ik} = 7.6$ Hz, $J_{jk} = 3.5$ Hz, 1H, H_k), 2.57 (dd, $J_{ij} = 18.8$ Hz, $J_{ik} = 7.6$ Hz, 1H, H_i), 2.48 (dd, $J_{ij} = 18.8$ Hz, $J_{jk} = 3.4$ Hz, 1H, H_j); ^{13}C NMR (100 MHz, MeOD- d_4): δ_C 150.0, 148.9, 148.7, 148.5, 148.4, 148.3, 148.2, 141.5, 141.4, 140.1, 139.8, 138.6, 138.4, 138.3, 129.9, 129.7, 128.6, 128.1, 127.0, 120.1, 112.9, 112.1, 110.0, 107.6 (Aryl), 63.5 (R_4C), 34.8, 21.1 (Alkyl); HRMS (EI), calculated for $C_{27}H_{20}O_4$: 408.1362, found: 408.1371.

6.2.43 2,3,5',6,6',7-Hexahydroxy-3',3'-dimethyl-2',3'-dihydrospiro[fluorene-9,1'-indene] (43)



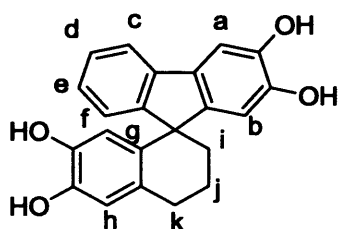
Following the general procedure described for 2,3-dihydroxy-9,9'-spirobisfluorene (37), 2,3,5',6,6',7-hexamethoxy-3',3'-dimethyl-2',3'-dihydrospiro[fluorene-9,1'-indene] (0.60 g, 1.26 mmol) (33) was reacted with 4.5 equiv. of boron tribromide (0.54 mL, 5.67 mmol) to give of 2,3,5',6,6',7-hexahydroxy-3',3'-dimethyl-2',3'-dihydrospiro[fluorene-9,1'-indene] (43) as a light brown powder (0.45 g, 91% yield), m.p = 144 - 147 °C; IR (film)/ cm^{-1} : 3246, 3064, 2951, 2823, 1611, 1506, 1447, 1387, 1282, 1241, 1204, 1183, 1133, 1106, 870, 836, 795, 774, 667; ^1H NMR (400 MHz, MeOD- d_4): δ_H 6.83 (s, 2H, H_a , H_c), 6.58 (s, 1H, H_f), 6.42 (s, 2H, H_b , H_d), 5.57 (s, 1H, H_e), 2.32 (s, 2H, H_g), 1.40 (s, 6H, H_h); ^{13}C NMR (125 MHz, MeOD- d_4): δ_C 150.9, 149.8, 145.8, 141.7, 138.1, 135.7, 130.9, 124.6, 124.0, 118.8, 117.2, 117.5, 116.8, 110.9, 109.9, 105.0, 104.3, 101.8 (Aryl), 44.4, 33.2 (Alkyl), 24.2 (Me); HRMS (EI), calculated for $C_{23}H_{20}O_6$: 392.1260, found: 392.1260.

6.2.44 2,3,5',6'-Tetrahydroxy-2',3'-dihydrospiro[fluorene-9,1'-indene] (44)



Following the general procedure described for 2,3-dihydroxy-9,9'-spirobisfluorene (39), 2,3,5',6'-tetramethoxy-2',3'-dihydrospiro[fluorene-9,1'-indene] (0.37 g, 0.95 mmol) (34) was reacted with 3 equiv. of boron tribromide (0.27 mL, 2.85 mmol) to give of 2,3,5',6'-tetrahydroxy-2',3'-dihydrospiro[fluorene-9,1'-indene] (44) as a light brown powder (0.28 g, 89% yield), m.p = 180–184 °C; IR (film)/cm⁻¹: 3324, 3060, 2951, 2941, 2844, 1604, 1495, 1441, 1344, 1274, 1209, 1153, 1130, 1107, 1068, 993, 857, 808, 778, 746, 620; ¹H NMR (400 MHz, MeOD-*d*₄): δ_H 7.54 (d, *J* = 6.8 Hz, 1H, H_c), 7.24 (t, *J* = 6.9 Hz, 1H, H_e), 7.16 (s, 1H, H_a), 7.09 (m, 2H, H_d, H_f), 6.81 (s, 1H, H_h), 6.62 (s, 1H, H_b), 5.81 (s, 1H, H_g), 3.32 (t, *J*_{ij} = 7.2 Hz, 2H, H_i), 3.20 (m, 2H, H_j); ¹³C NMR (125 MHz, MeOD-*d*₄): δ_C 154.6, 146.7, 146.4, 146.1, 145.8, 145.3, 141.7, 140.6, 136.6, 133.0, 128.0, 126.9, 124.4, 119.3, 112.1, 111.7, 110.9, 107.3 (Aryl), 63.9 (R₄C), 41.8, 32.3 (Alkyl); HRMS (EI), calculated for C₂₁H₁₆O₄: 332.1049, found: 332.1043.

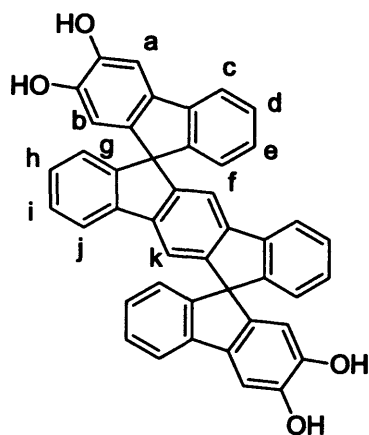
6.2.45 2,3,6',7'-Tetrahydroxy-3',4'-dihydro-2'*H*-spiro[fluorene-9,1'-naphthalene] (45)



Following the general procedure described for 2,3-dihydroxy-9,9'-spirobisfluorene (39), 2,3,6',7'-tetramethoxy-3',4'-dihydro-2'*H*-spiro[fluorene-9,1'-naphthalene] (0.32 g, 0.80 mmol) (35) was reacted with 3 equiv. of boron tribromide (0.23 mL, 2.40 mmol) to give of 2,3,6',7'-tetrahydroxy-3',4'-dihydro-2'*H*-spiro[fluorene-9,1'-naphthalene] (45) as a light brown powder (0.25 g, 92% yield), m.p = 120 - 123 °C; IR (film)/cm⁻¹: 3306, 3061, 2928, 2907, 2856, 1603,

1515, 1480, 1442, 1332, 1294, 1270, 1182, 900, 864, 831, 782, 750; ^1H NMR (400 MHz, MeOD- d_4): δ_{H} 7.56 (d, $J_{cd} = 7.6$ Hz, 1H, H_c), 7.24 (t, $J_{cd} = 7.6$ Hz, 1H, H_d), 7.17 (s, 1H, H_a), 7.13 (t, $J_{ef} = 7.6$ Hz, 1H, H_e), 7.10 (d, $J_{ef} = 7.6$ Hz, 1H, H_f), 6.65 (s, 1H, H_h), 6.57 (s, 1H, H_b), 5.66 (s, 1H, H_i), 2.91 (t, $J_{ij} = 6.3$ Hz, 2H, H_i), 2.14 (dt, $J_{jk} = 5.4$, $J_{ij} = 6.3$ Hz, 2H, H_j), 1.95 (t, $J_{jk} = 5.4$ Hz, 2H, H_k); ^{13}C NMR (125 MHz, MeOD- d_4): δ_{C} 150.3, 148.9, 147.1, 146.6, 139.7, 138.2, 133.9, 131.2, 128.6, 128.5, 128.4, 127.7, 127.1, 126.9, 113.8, 113.1, 111.1, 109.4 (Aryl), 27.5, 23.2, 21.4 (Alkyl); HRMS (EI), calculated for C₂₂H₁₈O₄: 346.1205, found: 346.1211.

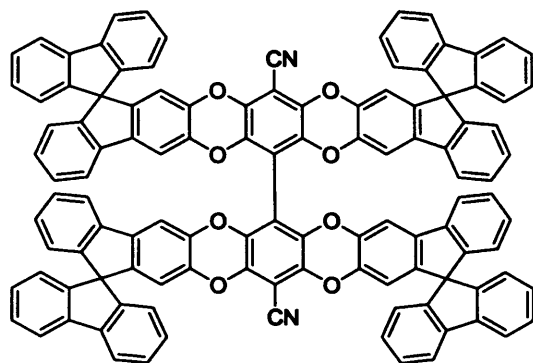
6.2.46 2,2'',3,3''-Tetrahydroxydispiro[9H-fluorene-9,6'(12'H)-indeno[1,2-b]fluorene-12',9''-[9H]fluorene] (46)



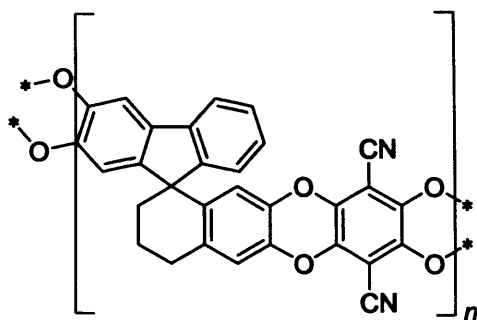
Following the general procedure described for 2,3-dihydroxy-9,9'-spirobisfluorene (39), 2,2'',3,3''-tetramethoxydispiro[9H-fluorene-9,6'(12'H)-indeno[1,2-b]fluorene-12',9''-[9H]fluorene] (0.48 g, 0.71 mmol) (36) was reacted with 3 equiv. of boron tribromide (0.20 mL, 2.13 mmol) to give of 2,2'',3,3''-tetrahydroxydispiro[9H-fluorene-9,6'(12'H)-indeno[1,2-b]fluorene-12',9''-[9H]fluorene] (46) as a light brown powder (0.38 g, 86% yield), m.p = 350 - 354 °C; IR (film)/cm⁻¹: 3434, 3059, 2901, 2958, 2880, 1603, 1477, 1442, 1341, 1293, 1192, 874, 756, 729, 669; ^1H NMR (400 MHz, MeOD- d_4): δ_{H} 7.84 (s, 2H, H_a), 7.65 (d, $J_{cd} = 7.6$ Hz, 2H, H_c), 7.50 (d, $J_{ef} = 7.6$ Hz, 2H, H_f), 7.26 (s, 2H, H_k), 7.24 (t, $J_{cd} = 7.6$ Hz, 2H, H_d), 7.12 (t, $J_{ef} = 7.6$ Hz, 2H, H_e), 7.04 (s, 2H, H_b), 6.96 – 6.90 (m, $J = 7.6$ Hz, 4H, H_h, H_i), 6.52 (d, $J = 7.6$ Hz, 2H, H_g), 6.04 (d, $J = 7.7$ Hz, 2H, H_j); ^{13}C NMR (125 MHz, MeOD- d_4): δ_{C} 150.9, 150.8, 150.3, 147.0, 144.9, 143.0, 143.3, 143.1, 142.9, 142.5, 128.7, 128.5, 127.3,

120.8, 119.9, 120.8, 119.9, 116.3, 111.7, 107.9, 101.3 (Aryl), 66.7 (R₄C); HRMS (EI), calculated for C₄₄H₂₆O₄: 618.1831, found: 618.1840.

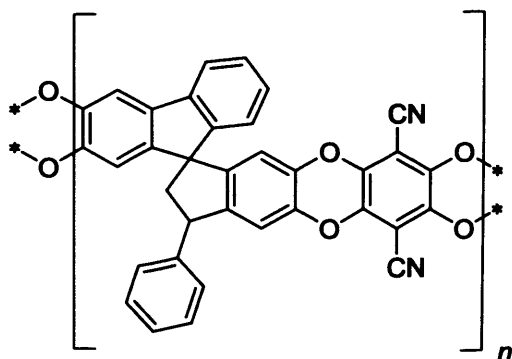
6.2.47 OMIM 1 (47)



Under a nitrogen atmosphere, 2,3-dihydroxy-9,9'-spirobisfluorene (**37**) (0.1557 g, 0.447 mmol), and 4,4'-dicyano-2,2',3,3',5,5',6,6'-octafluorobiphenyl (0.0371 g, 0.106 mmol) (OFPN) were added to anhydrous DMF (4 mL). The mixture was heated to 50 °C until the starting materials had dissolved, then dry potassium carbonate (0.15 g, 1.12 mmol) was added and the mixture stirred for 18 h at 70 °C. The solution was quenched with water (50 mL), the precipitate filtered and washed with copious amounts of water. The precipitate was dissolved in chloroform (40 mL) then washed with water and brine before being dried with magnesium sulphate. The crude material was subjected to flash chromatography with DCM and hexane as the solvent (6/4) to give the product (**48**) (0.091 g, 54%) as a fluorescent yellow solid. BET surface area = 0 m²/g; IR (nujol)/cm⁻¹: 2240, 1605, 1442, 1352, 1308, 1277, 1231, 1199, 1163, 1105, 1006, 984, 868, 816, 783, 772, 748, 738, 719; ¹H NMR (400 MHz, CDCl₃): δ_H 7.80 - 7.65 (m, 16H), 7.35 - 7.15 (m, 16H), 7.10 - 6.85 (m, 16H), 6.65 - 6.50 (m, 16H), 6.04 (s, 2H), 6.02 (s, 2H), 5.97 (s, 2H), 5.94 (s, 2H); MS (MALDI-TOF): cluster centred at m/z 1581.55 (MH⁺). Initial weight loss due to thermal degradation commences at ~ 403 °C (19% mass loss).

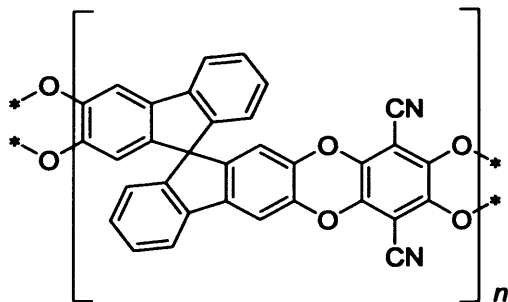
6.2.48 LADDER POLYMER 1 (48)

In a two-necked round bottom flask 2,3,6',7'-tetrahydroxy-3',4'-dihydro-2'*H*-spiro[fluorene-9,1'-naphthalene] (220 mg, 0.635 mmol) (**45**), 2,3,5,6-tetrafluoroterephthalonitrile (127 mg, 0.635 mmol) (TFPN), and dry dimethylformamide (20 mL) were added under a dry nitrogen atmosphere. The mixture was heated to 65 °C, until complete dissolution of the two starting materials was observed, then dry potassium carbonate (0.70 g, 5.08 mmol) was added and the mixture kept to stirring for 96 h. The reaction was quenched in water (100 mL) and excess base was neutralised with HCl (20 mL, 2.0M). The precipitate was filtered and washed with water (100 mL). The filtrate was washed in acetone, in which it fully dissolved. The acetone was removed under rotary evaporation and then dried in an oven at 100 °C. The solid material refluxed in methanol overnight and then filtered. The filtrate was dried overnight in a vacuum oven at 120 °C to give a light brown solid (242 mg, 82% based on the molecular weight of the repeat unit). IR (nujol)/cm⁻¹: 2239, 1599, 1351, 1323, 1201, 1159, 1016, 1015, 872, 750, 722 cm⁻¹; ¹H NMR (400 MHz, DMSO-*d*₆): δ_H 8.20 – 7.65 (br t, 2H), 7.50 – 7.20 (br d, 2H), 7.15 – 6.95 (br s, 2H), 5.70 – 5.50 (br s, 2H), 3.05 – 2.75 (br t, 2H), 2.25 – 1.75 (br m, 2H), 1.30 – 1.00 (br t, 2H); BET surface area = 0 m²/g; TGA analysis (nitrogen): Initial weight loss due to thermal degradation commences at ~ 417 °C (27% mass loss).

6.2.49 LADDER POLYMER 2 (49)

In a two-necked round bottom flask 2,3,5',6'-tetrahydroxy-3'-phenyl-2',3'-dihydrospiro[fluorene-9,1'-indene] (225 mg, 0.55 mmol) (**42**), 2,3,5,6-tetrafluoroterephthalonitrile (110 mg, 0.55 mmol) (**TFPN**), and dry dimethylformamide (20 mL) were added under a dry nitrogen atmosphere. The mixture was heated to 75 °C, until complete dissolution of the two starting materials was observed, then dry potassium carbonate (0.61 g, 4.40 mmol) was added and the mixture kept stirring for 96 h. The reaction was quenched in water (100 mL) and excess base was neutralised with HCl (20 mL, 2.0M). The precipitate was filtered and washed with water (100 mL). The filtrate was washed in acetone, in which it fully dissolved. The acetone was removed under rotary evaporation and then dried in an oven at 100 °C. The solid material refluxed in methanol overnight and then filtered. The filtrate was dried overnight in a vacuum oven at 120 °C to give a light brown solid (211 mg, 73% based on the molecular weight of the repeated unit). IR (film)/cm⁻¹: 3058, 2982, 2934, 2856, 2239, 1604, 1453, 1348, 1295, 1267, 1189, 1126, 1006, 875, 773, 742, 698, 666; ¹H NMR (400 MHz, DMSO-*d*₆): δ_H 8.70 – 8.50 (br s, 2H), 8.00 – 7.65 (br m, 9H), 7.75 – 7.55 (br s, 1H), 6.60– 6.25 (br s, 1H), 4.85 – 4.65 (br m, 1H), 2.90 – 2.45 (br m, 2H); BET surface area = 0 m²/g; TGA analysis (nitrogen): Initial weight loss due to thermal degradation commences at ~ 220 °C (32% mass loss).

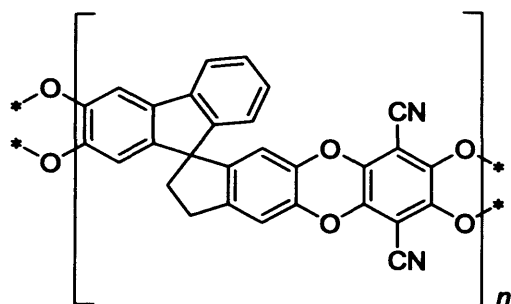
6.2.50 LADDER POLYMER 3 (**50**)



In a two-necked round bottom flask 2,2',3,3'-tetrahydroxy-9,9'-spirobisfluorene (494 mg, 1.30 mmol) (**39**), 2,3,5,6-tetrafluoroterephthalonitrile (260 mg, 1.30 mmol) (**TFPN**), and dry dimethylformamide (20 mL) were added under a dry nitrogen atmosphere. The mixture was heated to 75 °C, until complete dissolution of the two starting materials was observed, then dry potassium carbonate (1.43 g, 10.4 mmol) was added and the mixture kept to stirring for 96 h. The reaction was quenched in water (100 mL) and excess base was neutralised with HCl (20 mL, 2.0M). The precipitate was filtered and washed with water (100 mL). The filtrate was washed in acetone, in which it fully dissolved. The acetone was removed under rotary evaporation and then dried in an oven at 100 °C. The solid material refluxed in

methanol overnight and then filtered. The filtrate was dried overnight in a vacuum oven at 120 °C to give a light brown solid (568 mg, 87% based on the molecular weight of the repeat unit). IR (nujol)/cm⁻¹: 2240, 1611, 1301, 1273, 1209, 1155, 1008; ¹H NMR (400 MHz, DMSO-*d*₆): δ_H 7.90 – 7.80 (br d, 2H), 7.65 – 7.55 (br t, 2H), 7.32 – 7.25 (br s, 2H), 7.10 – 7.00 (br d, 2H), 6.63 – 6.55 (br t, 2H), 6.30 – 6.28 (br s, 2H); BET surface area = 0 m²/g; TGA analysis (nitrogen): Initial weight loss due to thermal degradation commences at ~ 200 °C (38% mass loss).

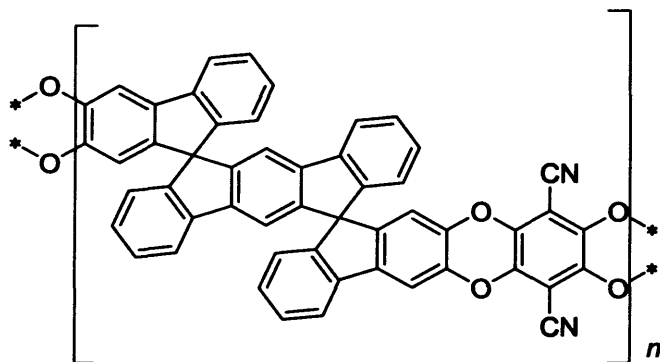
6.2.51 LADDER POLYMER 4 (51)



In a two-necked round bottom flask 2,3,5',6'-tetrahydroxy-2',3'-dihydrospiro[fluorene-9,1'-indene] (250 mg, 0.75 mmol) (**44**), 2,3,5,6-tetrafluoroterephthalonitrile (151 mg, 0.75 mmol) (TFPN), and dry dimethylformamide (20 mL) were added under a dry nitrogen atmosphere. The mixture was heated to 80 °C, until complete dissolution of the two starting material was observed, then dry potassium carbonate (0.83 g, 6.00 mmol) was added and the mixture kept to stirring for 96 h. The reaction was quenched in water (100 mL) and excess base was neutralised with HCl (20 mL, 2.0M). The precipitate was filtered and washed with water (100 mL). The filtrate was washed in acetone, in which it fully dissolved. The acetone was removed under rotary evaporation and then dried in an oven at 100 °C. The solid material refluxed in methanol overnight and then filtered. The filtrate was dried overnight in a vacuum oven at 120 °C to give a light brown solid (291 mg, 86% based on the molecular weight of

the repeat unit). IR (nujol)/ cm^{-1} : 2242, 1635, 1267, 1152, 1011, 951, 862, 742, 736; ^1H NMR (400 MHz, $\text{DMSO}-d_6$): δ_{H} 8.25 – 7.75 (br s, 2H), 7.55 – 7.25 (br m, 2H), 7.25 – 7.00 (br m, 2H), 6.80 – 6.60 (br s, 1H), 6.40 – 6.10 (br s, 1H), 1.40 – 1.30 (br t, 2H), 1.25 – 1.00 (br t, 2H); BET surface area = $20 \text{ m}^2/\text{g}$, pore volume of $0.24 \text{ cm}^3/\text{g}$ at (P/P_0) 0.98; TGA analysis (nitrogen): Initial weight loss due to thermal degradation commences at $\sim 345 \text{ }^\circ\text{C}$ (42% mass loss).

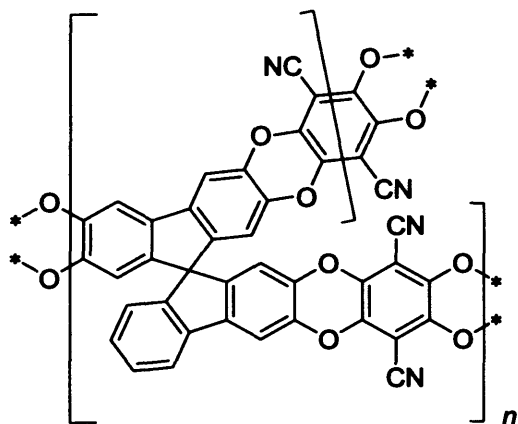
6.2.52 LADDER POLYMER 5 (52)



In a two-necked round bottom flask 2,2',3,3''-tetrahydroxydispiro[9H-fluorene-9,6'(12'H)-indeno[1,2-b]fluorene-12',9''-[9H]fluorene] (406 mg, 0.66 mmol) (**46**), 2,3,5,6-tetrafluoroterephthalonitrile (131 mg, 0.66 mmol) (TFPN), and dry dimethylformamide (20 mL) were added under a dry nitrogen atmosphere. The mixture was heated to $80 \text{ }^\circ\text{C}$, until complete dissolution of the two starting material was observed, then dry potassium carbonate (0.73 g, 5.28 mmol) was added and the mixture kept stirring for 96 h. The reaction was quenched in water (100 mL) and excess base was neutralised with HCl (20 mL, 2.0M). The precipitate was filtered and washed with water (100 mL). The filtrate was washed in acetone, in which it fully dissolved. The acetone was removed under rotary evaporation and then dried in an oven at $100 \text{ }^\circ\text{C}$. The solid material was refluxed in methanol overnight and then filtered.

The filtrate was dried overnight in a vacuum oven at 120 °C to give a light brown solid (384 mg, 79% based on the molecular weight of the repeat unit; IR (nujol)/cm⁻¹: 2248, 1602, 1498, 1443, 1406, 1298, 1259, 1086, 1014, 870, 795; ¹H NMR (400 MHz, DMSO-*d*₆): δ_H 8.20 – 8.15 (br s, 2H), 8.05 – 8.00 (br d, 2H), 7.95 – 7.80 (br t, 2H), 7.75 – 7.70 (br d, 2H), 7.52 – 7.46 (br s, 2H), 7.40 – 7.20 (br t, 2H), 7.15 – 7.05 (br s, 2H), 6.80 – 6.60 (br m, 4H), 6.38 – 6.28 (br d, 2H), 6.12 – 6.08 (br d, 2H) BET surface area = 0 m²/g; TGA analysis (nitrogen): Initial weight loss due to thermal degradation commences at ~ 258 °C (41% mass loss).

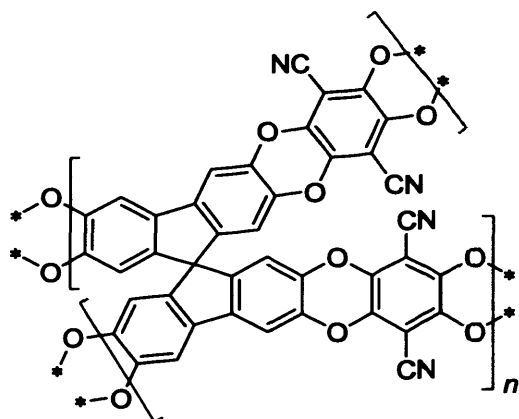
6.2.53 NETWORK POLYMER 1 (53)



In a two-necked round bottom flask 2,2',3,3',6,7-hexahydroxy-9,9'-spirobisfluorene (354 mg, 0.86 mmol) (**40**), 2,3,5,6-tetrafluoroterephthalonitrile (258 mg, 1.28 mmol) (TFPN), and dry dimethylformamide (20 mL) were added under a dry nitrogen atmosphere. The mixture was heated to 85 °C, until complete dissolution of the two starting material was observed, then dry potassium carbonate (1.42 g, 10.24 mmol) was added and the mixture kept stirring for 24 h. The reaction was quenched in water (100 mL) and excess base was neutralised with HCl (20 mL, 2.0M). The precipitate was filtered and washed with water (100 mL). The filtrate

was refluxed in acetone, chloroform, and methanol successively for 5 h in each solvent. The remaining solid material was dried overnight in a vacuum oven at 120 °C to give a light brown solid (469 mg, 92% based on the molecular weight of the repeat unit). IR (nujol)/cm⁻¹: 2241, 1601, 1350, 1267, 1011, 978, 862, 737; BET surface area = 1048 m²/g; total pore volume = 0.75 cm³/g at (P/P_0) 0.98, adsorption; TGA analysis (nitrogen): Initial weight loss due to thermal degradation commences at ~ 497 °C (36% mass loss); EA calc C 80.00, H 2.35, N 7.00, found C 67.69, H 1.89, N 6.05.

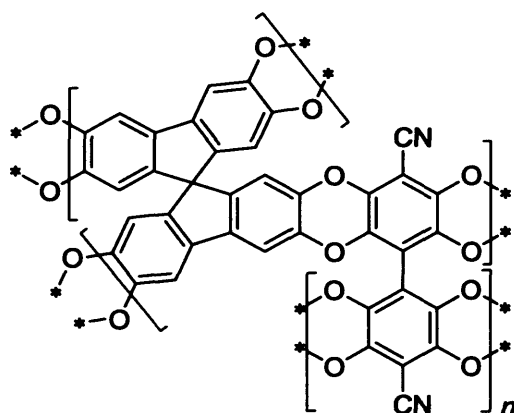
6.2.54 NETWORK POLYMER 2 (54)



In a two-necked round bottom 2,2',3,3',6,6',7,7'-octahydroxy-9,9'-spirobisfluorene (220 mg, 0.495 mmol) (**41**), 2,3,5,6-tetrafluoroterephthalonitrile (198 mg, 0.990 mmol) (TFPN), and dry dimethylformamide (20 mL) were added under a dry nitrogen atmosphere. The mixture was heated to 85 °C, until complete dissolution of the two starting materials was observed, then dry potassium carbonate (1.09 g, 7.92 mmol) was added and the mixture kept to stirring for 24 h. The reaction was quenched in water (100 mL) and excess base was neutralised with HCl (20 mL, 2.0M). The precipitate was filtered and washed with water (100 mL). The filtrate was refluxed in acetone, chloroform, and methanol successively for 5 h in each

solvent. The remaining solid material was dried overnight in a vacuum oven at 120 °C to give a light brown solid (305 mg, 90% based on the molecular weight of the repeat unit). IR (nujol)/cm⁻¹: 2242, 1601, 1350, 1268, 1058, 1011, 979, 945, 871, 769, 666; BET surface area = 550 m²/g; total pore volume = 0.32 cm³/g at (P/P_0) 0.98, adsorption; TGA analysis (nitrogen): 5% loss of weight occurred at ~ 320 °C. Initial weight loss due to thermal degradation commences at ~ 432 °C (36% mass loss); EA calc C 71.94, H 1.18, N 8.18, found C 61.86, H 2.21, N 7.23

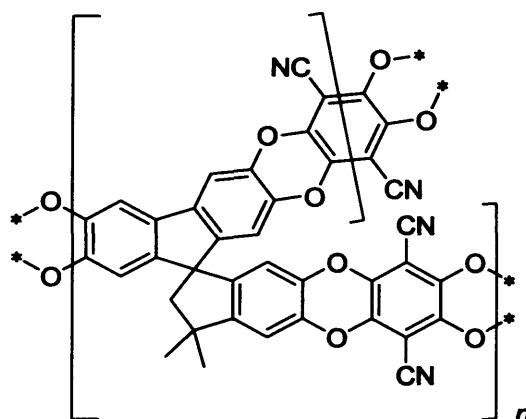
6.2.55 NETWORK POLYMER 3 (55)



In a two-necked round bottom flask 2,2',3,3',6,6',7,7'-octahydroxy-9,9'-spirobisfluorene (220 mg, 0.495 mmol) (**41**), 4,4'-dicyano-2,2',3,3',5,5',6,6'-octafluorobiphenyl (172 mg, 0.495 mmol) (**OFPN**), and dry dimethylformamide (20 mL) were added under a dry nitrogen atmosphere. The mixture was heated to 85 °C, until complete dissolution of the two starting materials was observed, then dry potassium carbonate (0.55 g, 3.96 mmol) was added and the mixture kept to stirring for 24 h. The reaction was quenched in water (100 mL) and excess

base was neutralised with HCl (20 mL, 2.0M). The precipitate was filtered and washed with water (100 mL). The filtrate was refluxed in acetone, chloroform, and methanol successively for 5 h in each solvent. The remaining solid material was dried overnight in a vacuum oven at 120 °C to give a light brown solid (284 mg, 91% based on the molecular weight of the repeat unit). IR (nujol)/cm⁻¹: 2242, 1601, 1350, 1270, 1011, 975, 858, 773, 722, 666; BET surface area = 1084 m²/g; total pore volume = 0.63 cm³/g at (*P*/*P*₀) 0.98, adsorption; TGA analysis (nitrogen): Initial weight loss due to thermal degradation commences at ~ 474 °C (51 % mass loss); EA calc C 74.06, H 1.27, N 4.43, found C 57.97, H 1.45, N 3.90.

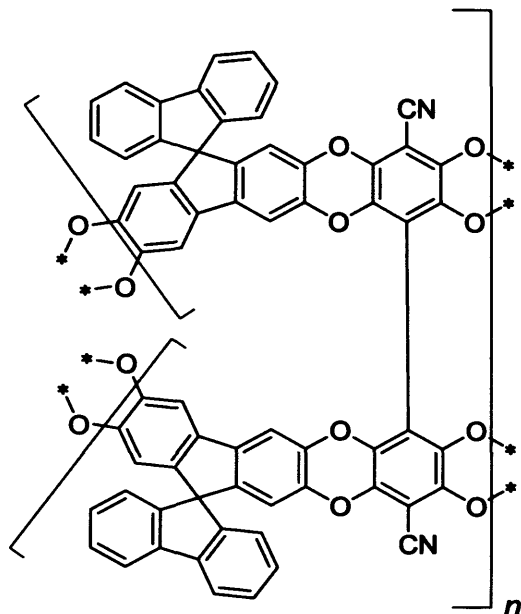
6.2.56 NETWORK POLYMER 4 (56)



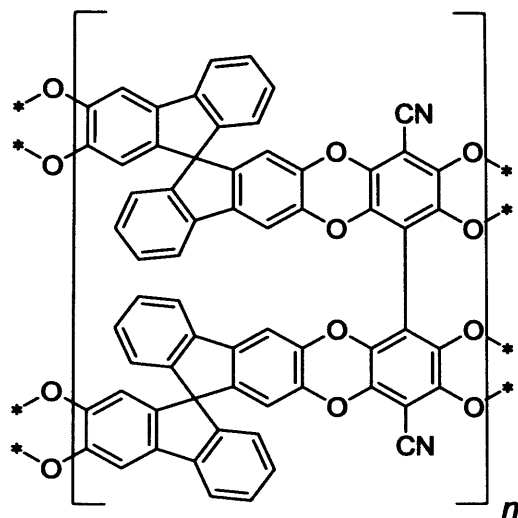
In a two-necked round bottom 2,3,5',6,6',7-hexahydroxy-3',3'-dimethyl-2',3'-dihydrospiro[fluorene-9,1'-indene] (361 mg, 0.92 mmol) (**43**), 2,3,5,6-tetrafluoroterephthalonitrile (276 mg, 1.38 mmol) (TFPN), and dry dimethylformamide (20 mL) were added under a dry nitrogen atmosphere. The mixture was heated to 85 °C, until complete dissolution of the two starting materials was observed, then dry potassium carbonate (1.02 g, 7.36 mmol) was added and the mixture kept stirring for 24 h. The reaction was quenched in water (100 mL) and excess base was neutralised with HCl (20 mL, 2.0M). The precipitate was filtered and washed with water (100 mL). The filtrate was refluxed in acetone, chloroform, and methanol successively for 5 h in each solvent. The remaining solid material was dried overnight in a vacuum oven at 120 °C to give a light brown solid (488 mg, 93 % based on the molecular weight of the repeated unit). IR (nujol)/cm⁻¹: 2241, 1603, 1267, 1070, 1118, 1093, 1008, 978, 870, 722, 666; BET surface area = 1054 m²/g; total pore volume = 0.78 cm³/g at (*P*/*P*₀) 0.98, adsorption; TGA analysis (nitrogen): Initial weight loss

due to thermal degradation commences at ~ 468 °C (37 % mass loss); EA calc C 78.61, H 3.13, N 7.24, found C 67.60, H 2.47, N 7.01.

6.2.57 NETWORK POLYMER 5 (57)



In a two-necked round bottom flask 2,3,6,7-tetrahydroxy-9,9'-spirobisfluorene (281 mg, 0.739 mmol) (**38**), 4,4'-dicyano-2,2',3,3',5,5',6,6'-octafluorobiphenyl (129 mg, 0.369 mmol) (TFPN), and dry dimethylformamide (20 mL) were added under a dry nitrogen atmosphere. The mixture was heated to 85 °C, until complete dissolution of the two starting materials was observed, then dry potassium carbonate (0.82 g, 5.91 mmol) was added and the mixture kept to stirring for 24 h. The reaction was quenched in water (100 mL) and excess base was neutralised with HCl (20 mL, 2.0M). The precipitate was filtered and washed with water (100 mL). The filtrate was refluxed in acetone, chloroform, and methanol successively for 5 h in each solvent. The remaining solid material was dried overnight in a vacuum oven at 120 °C to give a light brown solid (289 mg, 83% based on the molecular weight of the repeat unit). IR (nujol)/cm⁻¹: 2241, 1602, 1351, 1271, 1009, 996, 872, 775, 747; BET surface area = 593 m²/g; total pore volume = 0.38 cm³/g at (P/P_0) 0.98, adsorption; TGA analysis (nitrogen): 6% loss of weight occurred at ~ 95 °C. Initial weight loss due to thermal degradation commences at ~ 516 °C (31 % mass loss); EA calc C 81.01, H 2.55, N 2.95, found C 68.04, H 2.33, N 7.85.

6.2.58 NETWORK POLYMER 6 (58)

In a two-necked round bottom flask 2,2',3,3'-tetrahydroxy-9,9'-spirobisfluorene (273 mg, 0.718 mmol) (**39**), 4,4'-dicyano-2,2',3,3',5,5',6,6'-octafluorobiphenyl (125 mg, 0.359 mmol) (**TFPN**), and dry dimethylformamide (20 mL) were added under a dry nitrogen atmosphere. The mixture was heated to 85 °C, until complete dissolution of the two starting materials was observed, then dry potassium carbonate (0.79 g, 5.74 mmol) was added and the mixture kept to stirring for 24 hrs. The reaction was quenched in water (100 mL) and excess base was neutralised with HCl (20 mL, 2.0M). The precipitate was filtered and washed with water (100 mL). The filtrate was refluxed in acetone, chloroform, and methanol successively for 5 hours in each solvent. The remaining solid material was dried overnight in a vacuum oven at 120 °C to give a light yellow solid (258 mg, 76% based on the molecular weight of the repeated unit). IR (nujol)/cm⁻¹: 2239, 1598, 1352, 1306, 1274, 1199, 1155, 1002, 976, 890, 868; BET surface area = 20 m²/g; total pore volume = 0.07 cm³/g at (*P/P*₀) 0.98, adsorption; TGA analysis (nitrogen): Initial weight loss due to thermal degradation commences at ~ 277 °C (30% mass loss).

Bibliography

- [1] A. B. Arons and M. B. Peppard, *American Journal of Physics* **1965**, *33*, 367-374.
- [2] H. Hertz, *Annalen der Physik* **1887**, *267*, 421-448.
- [3] E. Rutherford, *Philosophical Magazine Series 6* **1911**, *21*, 669 - 688.
- [4] N. Bohr, *Nature* **1921**, *127*, 104-107.
- [5] H. Dingle, *The British Journal for the History of Science* **1963**, *1*, 199-216.
- [6] B. Coasne, K. Gubbins and R. M. Pellenq, *Particle & Particle Systems Characterization* **2004**, *21*, 149-160.
- [7] O. Shornikova, E. Kogan, N. Sorokina and V. Avdeev, *Russian Journal of Physical Chemistry A, Focus on Chemistry* **2009**, *83*, 1022-1025.
- [8] R. Drake, D. C. Sherrington and S. J. Thomson, *Journal of the Chemical Society, Perkin Transactions 1* **2002**, 1523-1534.
- [9] M. A. Harmer, W. E. Farneth and Q. Sun, *Journal of the American Chemical Society* **1996**, *118*, 7708-7715.
- [10] V. Aguilera, K. Kontturi, L. Murtomäki and P. Ramírez, *Journal of Controlled Release* **1994**, *32*, 249-257.
- [11] K. S. W. Sing, D. H. Everett, R. A. W. Haul, L. Moscou, R. A. Pierotti, J. Rouqueol and T. Siemieniewska, *Pure and Applied Chemistry* **1985**, *57*, 603-619.
- [12] D. V. Laciak and M. Langsam, *MEMBRANE SEPARATIONS | Gas Separations With Polymer Membranes*, Academic Press, Oxford, **2000**, 1725-1738.
- [13] N. B. McKeown, P. M. Budd, K. J. Msayib, B. S. Ghanem, H. J. Kingston, C. E. Tattershall, S. Makhseed, K. J. Reynolds and D. Fritsch, *Chemistry – A European Journal* **2005**, *11*, 2610-2620.

Bibliography

- [14] N. B. McKeown, P. M. Budd and D. Book, *Macromolecular Rapid Communications* **2007**, *28*, 995-1002.
- [15] C. D. Wood, B. Tan, A. Trewin, F. Su, M. J. Rosseinsky, D. Bradshaw, Y. Sun, L. Zhou and A. I. Cooper, *Advanced Materials* **2008**, *20*, 1916-1921.
- [16] M. Fischer, F. Hoffmann and M. Froba, *Chemphyschem : a European journal of chemical physics and physical chemistry* **2010**, *11*, 2220-2229.
- [17] C. J. Doonan, D. J. Tranchemontagne, T. G. Glover, J. R. Hunt and O. M. Yaghi, *Nat Chem* **2010**, *2*, 235-238.
- [18] H. G. Karge and J. Raskó, *Journal of Colloid and Interface Science* **1978**, *64*, 522-532.
- [19] H. Mahzoul, J. F. Brilhac and P. Gilot, *Applied Catalysis B: Environmental* **1999**, *20*, 47-55.
- [20] Y.-C. Chiang, P.-C. Chiang and C.-P. Huang, *Carbon* **2001**, *39*, 523-534.
- [21] B. Hammer, Y. Morikawa and J. K. Rskov, *Physical Review Letters* **1996**, *76*, 2141.
- [22] E. Zaremba and W. Kohn, *Physical Review B* **1976**, *13*, 2270.
- [23] I. Langmuir, *Journal of the American Chemical Society* **1916**, *38*, 2221-2295.
- [24] S. Brunauer, P. H. Emmett and E. Teller, *Journal of the American Chemical Society* **1938**, *60*, 309-319.
- [25] T. J. Barton, L. M. Bull, W. G. Klemperer, D. A. Loy, B. McEnaney, M. Misono, P. A. Monson, G. Pez, G. W. Scherer, J. C. Vartuli and O. M. Yaghi, *Chemistry of Materials* **1999**, *11*, 2633-2656.
- [26] H. Marsh and F. Rodríguez-Reinoso in *Activated carbon*, Elsevier Science Ltd, Oxford, **2006**, 1-12.
- [27] C. L. Mangun, Z. Yue, J. Economy, S. Maloney, P. Kemme and D. Cropek, *Chemistry of Materials* **2001**, *13*, 2356-2360.
- [28] V. Yakovlev and A. Fomkin, *Colloid Journal* **2009**, *71*, 877-881.

Bibliography

- [29] Y. K. Kalpakli and İ. Koyuncu, *Annali di Chimica* **2007**, *97*, 1291-1302.
- [30] H. Shimada, T. Akazawa, N. Ikenaga and T. Suzuki, *Applied Catalysis A: General* **1998**, *168*, 243-250.
- [31] S. G. J. Heijman and R. Hopman, *Colloids and Surfaces A: Physicochemical and Engineering Aspects* **1999**, *151*, 303-310.
- [32] Z. Shen, W. Wang, J. Jia, J. Ye, X. Feng and A. Peng, *Journal of Hazardous Materials* **2001**, *84*, 107-116.
- [33] S. E. Iyuke, W. R. W. Daud, A. B. Mohamad, A. A. H. Kadhum, Z. Fisal and A. M. Shariff, *Chemical Engineering Science* **2000**, *55*, 4745-4755.
- [34] H. Teng, T. S. Yeh and L. Y. Hsu, *Carbon* **1998**, *36*, 1387-1395.
- [35] M. Franz, H. A. Arafat and N. G. Pinto, *Carbon* **2000**, *38*, 1807-1819.
- [36] D. Lennon, D. T. Lundie, S. D. Jackson, G. J. Kelly and S. F. Parker, *Langmuir* **2002**, *18*, 4667-4673.
- [37] H. Z. Geng, T. H. Kim, S. C. Lim, H. K. Jeong, M. H. Jin, Y. W. Jo and Y. H. Lee, *International Journal of Hydrogen Energy* **2010**, *35*, 2073-2082.
- [38] D. W. Breck, W. G. Eversole, R. M. Milton, T. B. Reed and T. L. Thomas, *Journal of the American Chemical Society* **1956**, *78*, 5963-5972.
- [39] T. B. Reed and D. W. Breck, *Journal of the American Chemical Society* **1956**, *78*, 5972-5977.
- [40] Y. Okamoto, M. Ogawa, A. Maezawa and T. Imanaka, *Journal of Catalysis* **1988**, *112*, 427-436.
- [41] E. Lippmaa, M. Maegi, A. Samoson, M. Tarmak and G. Engelhardt, *Journal of the American Chemical Society* **1981**, *103*, 4992-4996.
- [42] K. S. Hui and C. Y. H. Chao, *Journal of Hazardous Materials* **2006**, *137*, 401-409.

Bibliography

- [43] N. Y. Chen, W. W. Kaeding and F. G. Dwyer, *Journal of the American Chemical Society* **1979**, *101*, 6783-6784.
- [44] J. C. van der Waal and V. B. H., *Journal of Porous Materials* **1998**, *5*, 289-303.
- [45] A. Corma, M. J. Diaz-Cabanas, J. Martinez-Triguero, F. Rey and J. Rius, *Nature* **2002**, *418*, 514-517.
- [46] C. Urban, E. F. McCord, O. W. Webster, L. Abrams, H. W. Long, H. Gaede, P. Tang and A. Pines, *Chemistry of Materials* **1995**, *7*, 1325-1332.
- [47] J. Huang, *Journal of Colloid and Interface Science* **2009**, *339*, 296-301.
- [48] M. P. Tsyurupa and V. A. Davankov, *Reactive and Functional Polymers* **2006**, *66*, 768-779.
- [49] C. D. Wood, B. Tan, A. Trewin, H. Niu, D. Bradshaw, M. J. Rosseinsky, Y. Z. Khimyak, N. L. Campbell, R. Kirk, E. Stöckel and A. I. Cooper, *Chemistry of Materials* **2007**, *19*, 2034-2048.
- [50] R. Dawson, A. Laybourn, R. Clowes, Y. Z. Khimyak, D. J. Adams and A. I. Cooper, *Macromolecules* **2009**, *42*, 8809-8816.
- [51] J. R. Holst, E. Stöckel, D. J. Adams and A. I. Cooper, *Macromolecules* **2010**, *43*, 8531-8538.
- [52] Y. Qi, F. Luo, Y. Che and J. Zheng, *Crystal Growth & Design* **2007**, *8*, 606-611.
- [53] T. Yildirim and M. R. Hartman, *Physical Review Letters* **2005**, *95*, 215504.
- [54] D. J. Tranchemontagne, J. R. Hunt and O. M. Yaghi, *Tetrahedron* **2008**, *64*, 8553-8557.
- [55] O. M. Yaghi, M. O'Keeffe, N. W. Ockwig, H. K. Chae, M. Eddaoudi and J. Kim, *Nature* **2003**, *423*, 705-714.
- [56] A. P. Côté, H. M. El-Kaderi, H. Furukawa, J. R. Hunt and O. M. Yaghi, *Journal of the American Chemical Society* **2007**, *129*, 12914-12915.

Bibliography

- [57] M. A. A. Musa, C.-Y. Yin and R. M. Savory, *Materials Chemistry and Physics* **2010**, *123*, 5-8.
- [58] P. Kuhn, M. Antonietti and A. Thomas, *Angewandte Chemie International Edition* **2008**, *47*, 3450-3453.
- [59] F. J. Uribe-Romo, J. R. Hunt, H. Furukawa, C. Klöck, M. O’Keeffe and O. M. Yaghi, *Journal of the American Chemical Society* **2009**, *131*, 4570-4571.
- [60] N. B. McKeown and P. M. Budd, *Chemical Society Reviews* **2006**, *35*, 675-683.
- [61] B. S. Ghanem, M. Hashem, K. D. M. Harris, K. J. Msayib, M. Xu, P. M. Budd, N. Chaukura, D. Book, S. Tedds, A. Walton and N. B. McKeown, *Macromolecules* **2010**, *43*, 5287-5294.
- [62] P. M. Budd, B. S. Ghanem, S. Makhseed, N. B. McKeown, K. J. Msayib and C. E. Tattershall, *Chemical communications* **2004**, 230-231.
- [63] P. M. Budd, N. B. McKeown and D. Fritsch, *Journal of Materials Chemistry* **2005**, *15*, 1977-1986.
- [64] N. B. McKeown, B. Gahnem, K. J. Msayib, P. M. Budd, C. E. Tattershall, K. Mahmood, S. Tan, D. Book, H. W. Langmi and A. Walton, *Angewandte Chemie International Edition* **2006**, *45*, 1804-1807.
- [65] P. M. Budd, K. J. Msayib, C. E. Tattershall, B. S. Ghanem, K. J. Reynolds, N. B. McKeown and D. Fritsch, *Journal of Membrane Science* **2005**, *251*, 263-269.
- [66] M. Carta, K. J. Msayib, P. M. Budd and N. B. McKeown, *Organic Letters* **2008**, *10*, 2641-2643.
- [67] Z. Wang, B. Zhang, H. Yu, L. Sun, C. Jiao and W. Liu, *Chemical Communications* **2010**, *46*, 7730-7732.
- [68] M. E. Brown and M. D. Hollingsworth, *Nature* **1995**, *376*, 323-327.

Bibliography

- [69] J. Bjork, M. Brostrom and D. Whitcomb, *Journal of Chemical Crystallography* **1997**, 27, 223-230.
- [70] E. Demers, T. Maris, J. Cabana, J.-H. Fournier and J. D. Wuest, *Crystal Growth & Design* **2005**, 5, 1237-1245.
- [71] J. H. Fournier, T. Maris and J. D. Wuest, *The Journal of Organic Chemistry* **2003**, 69, 1762-1775.
- [72] C. Song and T. M. Swager, *The Journal of Organic Chemistry* **2009**, 75, 999-1005.
- [73] M. S. Wong and X. L. Zhang, *Tetrahedron Letters* **2001**, 42, 4087-4089.
- [74] T. D. Nelson and R. D. Crouch, *Cu, Ni, and Pd Mediated Homocoupling Reactions in Biaryl Syntheses: The Ullmann Reaction*, John Wiley & Sons, Inc., **2004**
- [75] J. L. Schulte and S. Laschat, *Synthesis* **1999**, 475-478.
- [76] L. Deng, S. Sundriyal, V. Rubio, Z.-z. Shi and Y. Song, *Journal of Medicinal Chemistry* **2009**, 52, 6539-6542.
- [77] A. Sahoo, T. Oda, Y. Nakao and T. Hiyama, *Advanced Synthesis & Catalysis* **2004**, 346, 1715-1727.
- [78] T. Kang, Q. Feng and M. Luo, *Synlett* **2005**, 15, 2305-2308.
- [79] J. M. Blatchly, J. F. W. McOmie and M. L. Watts, *Journal of the Chemical Society* **1962**, 5085-5090.
- [80] M. M. V. Ramana and P. V. Potnis, *Synthesis* **1993**, 6, 575-576.
- [81] P. W. Rabideau and Z. Marcinow, *The Birch Reduction of Aromatic Compounds*, John Wiley & Sons, Inc., **2004**, p.
- [82] P. G. Gassman and J. J. Talley, *Tetrahedron Letters* **1978**, 19, 3773-3776.
- [83] L. Ciske, J. Fred, and W.D. Jones, *Synthesis* **1998**, 8, 1195-1198.
- [84] M. Prashad, Y. Liu, X. Y. Mak, D. Har, O. Repic and T. J. Blacklock, *Tetrahedron Letters* **2002**, 43, 8559-8562.

Bibliography

- [85] Y. Saikawa, K. Moriya, K. Hashimoto and M. Nakata, *Tetrahedron Letters* **2006**, *47*, 2535-2538.
- [86] A. V. Butin, S. K. Smirnov, T. A. Stroganova, W. Bender and G. D. Krapivin, *Tetrahedron* **2007**, *63*, 474-491.
- [87] F. Korte and O. Behner, *Justus Liebigs Annalen der Chemie* **1959**, *621*, 51-57.
- [88] R. Quelet and E. Matarasso-Tchiroukhine, *Comptes rendus de l'Académie des sciences* **1958**, 1127.
- [89] P. Kraft and W. Eichenberger, *European Journal of Organic Chemistry* **2003**, *2003*, 3735-3743.
- [90] F. H. Marquardt, *Helvetica Chimica Acta* **1965**, *48*, 1476-1485.
- [91] T. Hadizad, J. Zhang, Z. Y. Wang, T. C. Gorjanc and C. Py, *Organic Letters* **2005**, *7*, 795-797.
- [92] J. F. W. McOmie, M. L. Watts and D. E. West, *Tetrahedron* **1968**, *24*, 2289-2292.
- [93] P. M. Budd, B. S. Ghanem, S. Makhseed, N. B. McKeown, K. J. Msayib and C. E. Tattershall, *Chemical Communications* **2004**, 230-231.
- [94] C. A. Hunter and J. K. M. Sanders, *Journal of the American Chemical Society* **1990**, *112*, 5525-5534.
- [95] R. Guilhemat, M. Pereyre and M. Petraud, *Bulletin de la Societe Chimique de France* **1980**, *8*, 334-344.
- [96] X. Lin, I. Telepeni, A. J. Blake, A. Dailly, C. M. Brown, J. M. Simmons, M. Zoppi, G. S. Walker, K. M. Thomas, T. J. Mays, P. Hubberstey, N. R. Champness and M. Schröder, *Journal of the American Chemical Society* **2009**, *131*, 2159-2171.
- [97] W. Bandaranayake and N. Riggs, *Australian Journal of Chemistry* **1981**, *34*, 115-129.
- [98] C. Seer and E. Karl, *Monatshefte für Chemie / Chemical Monthly* **1913**, *34*, 631-648.

Bibliography

- [99] A. Fürstner and J. W. J. Kennedy, *Chemistry – A European Journal* **2006**, *12*, 7398-7410.
- [100] H. Hart, K. Harada and C. J. F. Du, *The Journal of Organic Chemistry* **1985**, *50*, 3104-3110.
- [101] E. Fillion, D. Fishlock, A. Wilsily and J. M. Goll, *The Journal of Organic Chemistry* **2005**, *70*, 1316-1327.
- [102] C. F. Koelsch and R. N. Flesch, *The Journal of Organic Chemistry* **1955**, *20*, 1270-1276.
- [103] P. Dreyfuss, *Gazzetta Chimica Italiana* **1938**, *68*, 92-95.
- [104] W. Deuschel, *Helvetica Chimica Acta* **1951**, *34*, 2403-2416.

